

Medium Access Control for Dynamic Spectrum Sharing in Cognitive Radio Networks



Le Thanh Tan

Centre Énergie Matériaux & Télécommunications

Institut National de la Recherche Scientifique

Université du Québec

A dissertation submitted to INRS-EMT in partial fulfillment of the
requirements for the degree of

Doctor of Philosophy

Montréal, Québec, Canada, August 2015

© All rights reserved to Le Thanh Tan, 2015.

1. External examiners: Prof. Wessam Ajib, Université du Québec à Montréal
Prof. Jean-François Frigon, École Polytechnique de Montréal

2. Internal examiners: Prof. André Girard, INRS-EMT

3. Supervisor: Prof. Long Le, INRS-EMT

Day of the defense:

Signature from head of PhD committee:

Declaration

I hereby declare that I am the sole author of this dissertation. This is a true copy of the dissertation, including any required final revisions, as accepted by my examiners.

I understand that my dissertation may be made electronically available to the public.

Montreal,

Abstract

The proliferation of wireless services and applications over the past decade has led to the rapidly increasing demand in wireless spectrum. Hence, we have been facing a critical spectrum shortage problem even though several measurements have indicated that most licensed radio spectrum is very underutilized. These facts have motivated the development of dynamic spectrum access (DSA) and cognitive radio techniques to enhance the efficiency and flexibility of spectrum utilization.

In this dissertation, we investigate design, analysis, and optimization issues for joint spectrum sensing and cognitive medium access control (CMAC) protocol engineering for cognitive radio networks (CRNs). The joint spectrum sensing and CMAC design is considered under the interweave spectrum sharing paradigm and different communications settings. Our research has resulted in four major research contributions, which are presented in four corresponding main chapters of this dissertation.

First, we consider the CMAC protocol design with parallel spectrum sensing for both single-channel and multi-channel scenarios, which is presented in Chapter 5. The considered setting captures the case where each secondary user (SU) is equipped with multiple transceivers to perform sensing and access of spectrum holes on several channels simultaneously.

Second, we study the single-transceiver-based CMAC protocol engineering for hardware-constrained CRNs, which is covered in Chapter 6. In this setting, each SU performs sequential sensing over the assigned channels and access one available channel for communication by using random access. We also investigate the channel assignment problem for SUs to maximize the network throughput.

Third, we design a distributed framework integrating our developed CMAC protocol and cooperative sensing for multi-channel and heterogeneous CRNs, which

is presented in details in Chapter 7. The MAC protocol is based on the p-persistent carrier sense multiple access (CSMA) mechanism and a general cooperative sensing adopting the a-out-of-b aggregation rule is employed. Moreover, impacts of reporting errors in the considered cooperative sensing scheme are also investigated.

Finally, we propose an asynchronous Full-Duplex cognitive MAC (FDC-MAC) exploiting the full-duplex (FD) capability of SUs' radios for simultaneous spectrum sensing and access. The research outcomes of this research are presented in Chapter 8. Our design enables to timely detect the PUs' activity during transmission and adaptive reconfigure the sensing time and SUs' transmit powers to achieve the best performance. Therefore, the proposed FDC-MAC protocol is more general and flexible compared with existing FD CMAC protocols proposed in the literature.

We develop various analytical models for throughput performance analysis of our proposed CMAC protocol designs. Based on these analytical models, we develop different efficient algorithms to configure the CMAC protocol including channel allocation, sensing time, transmit power, contention window to maximize the total throughput of the secondary network. Furthermore, extensive numerical results are presented to gain further insights and to evaluate the performance of our CMAC protocol designs. Both the numerical and simulation results confirm that our proposed CMAC protocols can achieve efficient spectrum utilization and significant performance gains compared to existing and unoptimized designs.

Acknowledgements

First of all, I wish to express my deepest thanks and gratitude to my Ph.D. advisor Prof. Long Le for his precious advices and encouragements throughout the years. I would like to thank him as well for the long inspiring discussions we had together, for all the confidence he put in me. My distinguished thanks should also go to all the jury members who have accepted to take time from their very busy schedule in order to evaluate this dissertation. It is quite an honor for me to have them peer review this work. I would like also to thank all the graduate students in INRS that have collaborated with me during the last five years. Special thanks should also go to my wife Ta Thi Huynh Nhu for her patience during all the time she spent alone in my homeland while I was doing research. Last but not the least, I would like to thank all my family members for their continued support, encouragement and sacrifice throughout the years, and I will be forever indebted to them for all what they have ever done for me.

To my parents

To my wife Ta Thi Huynh Nhu

To my cute daughters Le Thanh Van and Le Ha My

Contents

List of Figures	xi
List of Tables	xv
1 Introduction	1
1.1 Dynamic Spectrum Access	2
1.2 Hierarchical Access Model and Cognitive MAC Protocol	3
1.2.1 Hierarchical Access Model	3
1.2.2 Cognitive MAC Protocol	5
1.3 Research Challenges and Motivations	6
1.3.1 CMAC with Parallel Sensing	6
1.3.2 CMAC with Sequential Sensing	7
1.3.3 CMAC with Cooperative Sensing	7
1.3.4 Full-Duplex MAC Protocol for Cognitive Radio Networks	8
1.4 Research Contributions and Organization of the Dissertation	9
2 Background and Literature Review	12
2.1 Research Background	12
2.1.1 Spectrum Sensing	12
2.1.1.1 Individual Sensing	14
2.1.1.2 Cooperative Spectrum Sensing	15
2.1.2 MAC Protocol in Traditional Wireless Networks	18
2.1.2.1 Single-channel MAC Protocols	18
2.1.2.2 Multi-channel MAC Protocols	26
2.1.3 Cognitive MAC Protocol for CRNs	29
2.2 Literature Review	29
2.2.1 Spectrum Sensing	31

2.2.2	Cognitive MAC Protocol Design	31
2.2.2.1	CMAC with Parallel Sensing	32
2.2.2.2	CMAC with Sequential Sensing	32
2.2.2.3	CMAC with Cooperative Sensing	32
2.2.2.4	Full-Duplex CMAC Protocol for CRNs	33
3	Distributed MAC Protocol for Cognitive Radio Networks: Design, Analysis, and Optimization	34
3.1	Abstract	34
3.2	Introduction	35
3.3	Related Works	36
3.4	System and Spectrum Sensing Models	37
3.4.1	System Model	37
3.4.2	Spectrum Sensing	38
3.5	MAC Design, Analysis and Optimization: Single Channel Case	40
3.5.1	MAC Protocol Design	40
3.5.2	Throughput Maximization	42
3.5.3	Throughput Analysis and Optimization	42
3.5.3.1	Calculation of $\Pr(n = n_0)$	43
3.5.3.2	Calculation of Conditional Throughput	44
3.5.3.3	Optimal Sensing and MAC Protocol Design	46
3.5.4	Some Practical Implementation Issues	48
3.6	MAC Design, Analysis, and Optimization: Multiple Channel Case	48
3.6.1	MAC Protocol Design	48
3.6.2	Throughput Maximization	49
3.6.3	Throughput Analysis and Optimization	50
3.6.3.1	Calculation of $\Pr(n = n_0)$ and $\mathbf{E}[l]$	50
3.6.3.2	Optimal Sensing and MAC Protocol Design	51
3.7	Numerical Results	52
3.7.1	Performance of Single Channel MAC Protocol	53
3.7.2	Performance of Multi-Channel MAC Protocol	55
3.8	Conclusion	57
3.9	Appendices	57
3.9.1	Proof of Proposition 1	57
3.9.2	Proof of Proposition 2	62

4 Channel Assignment With Access Contention Resolution for Cognitive Radio Networks	67
4.1 Abstract	67
4.2 Introduction	68
4.3 Related Works	70
4.4 System Model and Problem Formulation	71
4.4.1 System Model	71
4.4.2 Problem Formulation	72
4.4.3 Optimal Algorithm and Its Complexity	73
4.5 Non-overlapping Channel Assignment Algorithm	73
4.6 Overlapping Channel Assignment	75
4.6.1 MAC Protocol	75
4.6.2 Overlapping Channel Assignment Algorithm	78
4.6.3 Calculation of Contention Window	80
4.6.4 Calculation of MAC Protocol Overhead	81
4.6.5 Update δ inside Alg. 3	81
4.6.6 Practical Implementation Issues	81
4.7 Performance Analysis	82
4.7.1 Throughput Analysis	82
4.7.2 Impacts of Contention Collision	85
4.7.3 Complexity Analysis	86
4.8 Further Extensions and Design Issues	87
4.8.1 Fair Channel Assignment	87
4.8.2 Throughput Analysis under Imperfect Sensing	89
4.8.3 Congestion of Control Channel	95
4.9 Numerical Results	96
4.9.1 MAC Protocol Configuration	99
4.9.2 Comparisons of Proposed Algorithms versus Optimal Algorithms	101
4.9.3 Throughput Performance of Proposed Algorithms	102
4.10 Conclusion	103

5	Joint Cooperative Spectrum Sensing and MAC Protocol Design for Multi-channel Cognitive Radio Networks	105
5.1	Abstract	105
5.2	Introduction	106
5.3	System Model and Spectrum Sensing Design	109
5.3.1	System Model	109
5.3.2	Semi-Distributed Cooperative Spectrum Sensing	111
5.4	Performance Analysis and Optimization for Cognitive MAC Protocol	115
5.4.1	Cognitive MAC Protocol Design	115
5.4.2	Saturation Throughput Analysis	116
5.4.3	Semi-Distributed Cooperative Spectrum Sensing and p -persistent CSMA Access Optimization	121
5.4.4	Optimization of Channel Sensing Sets	123
5.4.4.1	Brute-force Search Algorithm	124
5.4.4.2	Low-Complexity Greedy Algorithm	124
5.4.5	Complexity Analysis	125
5.4.5.1	Brute-force Search Algorithm	125
5.4.5.2	Low-complexity Greedy Algorithm	126
5.4.6	Practical Implementation Issues	127
5.5	Consideration of Reporting Errors	127
5.5.1	Cooperative Sensing with Reporting Errors	128
5.5.2	Throughput Analysis Considering Reporting Errors	128
5.5.3	Design Optimization with Reporting Errors	133
5.6	Numerical Results	134
5.7	Conclusion	140
6	Design and Optimal Configuration of Full-Duplex MAC Protocol for Cognitive Radio Networks Considering Self-Interference	141
6.1	Abstract	141
6.2	Introduction	142
6.2.1	Related Works	143
6.2.2	Our Contributions	144
6.3	System and PU Activity Models	145
6.3.1	System Model	145
6.3.2	Primary User Activity	146

6.4	Full-Duplex Cognitive MAC Protocol	146
6.4.1	FDC-MAC Protocol Design	146
6.4.2	Throughput Analysis	149
6.4.2.1	Derivation of T_{ove}	149
6.4.2.2	Derivation of \mathcal{B}	150
6.5	FDC-MAC Protocol Configuration for Throughput Maximization	151
6.5.1	Problem Formulation	151
6.5.2	Parameter Configuration for FDC-MAC Protocol	152
6.6	Numerical Results	153
6.7	Conclusion	160
6.8	Appendices	160
6.8.1	Derivation of \bar{T}_{cont}	160
6.8.2	Derivations of $\mathcal{B}_1, \mathcal{B}_2, \mathcal{B}_3$	162
6.8.3	False Alarm and Detection Probabilities	164
6.8.4	Proof of Proposition 1	165
6.8.5	Approximation of \mathcal{P}_f^{00} and Its First and Second Derivatives	170
7	Conclusions and Further Works	171
7.1	Major Research Contributions	171
7.2	Further Research Directions	173
7.2.1	Multi-channel MAC protocol design for FD CRNs	173
7.2.2	CMAC and routing design for multi-hop HD and FD CRNs	173
7.2.3	Applications of cognitive radio networking techniques for smartgrids	173
7.3	List of publication	174
8	Appendix	176
8.1	Channel Assignment for Throughput Maximization in Cognitive Radio Networks	176
8.2	Fair Channel Allocation and Access Design for Cognitive Ad Hoc Networks	177
8.3	General Analytical Framework for Cooperative Sensing and Access Trade-off Optimization	178
8.4	Distributed MAC Protocol Design for Full-Duplex Cognitive Radio Networks	179
	References	180

List of Figures

1.1	The broad landscape of Dynamic Spectrum Access (DSA) [2, 3].	2
1.2	Positioning our contributions within the broad CMAC landscape.	9
2.1	Cooperative sensing examples with (a) centralized processing, (b) distributed processing.	16
2.2	Example of basic access mechanism for window-based CSMA MAC protocol [85].	19
2.3	Example of RTS/CTS access mechanism for window-based CSMA MAC protocol [85].	19
2.4	Markov chain model for window-based CSMA MAC protocol [85].	20
2.5	Time diagram for p -persistent CSMA MAC protocol [70].	23
2.6	Dedicated control channel mechanism for multi-channel MAC protocols [31].	27
2.7	Common hopping mechanism for multi-channel MAC protocols [31].	27
2.8	Split phase mechanism for multi-channel MAC protocols [31].	27
2.9	The generic functionalities of the CMAC protocol [59].	30
3.1	Considered network and spectrum sharing model (PU: primary user, SU: secondary user).	38
3.2	Timing diagram of the proposed multi-channel MAC protocol.	41
3.3	Normalized throughput versus contention window W for $\tau = 1ms$, $m = 3$, different N and basic access mechanism.	53
3.4	Normalized throughput versus the sensing time τ for $W = 32$, $m = 3$, different N and basic access mechanism.	54
3.5	Normalized throughput versus sensing time τ and contention window W for $N = 15$, $m = 4$ and basic access mechanism.	54
3.6	Normalized throughput versus sensing time τ and contention window W for $N = 10$, $m = 4$, $M = 5$ and basic access mechanism.	55

LIST OF FIGURES

4.1	Timing diagram for the proposed multi-channel MAC protocol.	75
4.2	Collision probability versus the contention window (for $M = 15$).	96
4.3	Total throughput versus target collision probability under throughput maximization design (for $M = 10$)	96
4.4	Total throughput versus the number of channels under throughput maximization design (for $M = 2$, Theo: Theory, Sim: Simulation, Over: Overlapping, Non: Non-overlapping, Opt: Optimal assignment).	97
4.5	Total throughput versus the number of channels under throughput maximization design (for $M = 3$, Theo: Theory, Sim: Simulation, Over: Overlapping, Non: Non-overlapping, Opt: Optimal assignment).	97
4.6	Minimum throughput versus the number of channels under max-min fairness (for $M = 2$, Theo: Theory, Sim: Simulation, Over: Overlapping, Non: Non-overlapping, Opt: Optimal assignment).	98
4.7	Minimum throughput versus the number of channels under max-min fairness (for $M = 3$, Theo: Theory, Sim: Simulation, Over: Overlapping, Non: Non-overlapping, Opt: Optimal assignment).	98
4.8	Total throughput versus the number of channels under throughput maximization design (for $M = 15$, Theo: Theory, Sim: Simulation, Over: Overlapping, Non: Non-overlapping, 5-Over: 5-user sharing Overlapping)	99
4.9	Throughput gain between Alg. 3 and Alg. 2 versus the number of channels	99
4.10	Throughput gain between Alg. 3 and P-blind 5-user sharing versus the number of channels	100
4.11	Minimum throughput versus the number of channels under max-min fairness (for $M = 5$, Theo: Theory, Sim: Simulation, Over: Overlapping, Non: Non-overlapping).	100
4.12	Total throughput versus the number of channels under throughput maximization design (for $M = 5, \mathcal{P}_f^{ij} \in [0.1, 0.15], \mathcal{P}_d^{ij} = 0.9$, Theo: Theory, Sim: Simulation, Over: Overlapping, Non: Non-overlapping, Per: Perfect sensing, Imp: Imperfect sensing).	101
5.1	Considered network and spectrum sharing model (PU: primary user, SU: secondary user, and C_i is the channel i corresponding to PU_i)	111
5.2	Example for SDCSS on 1 channel.	113
5.3	Timing diagram of cognitive p -persistent CSMA protocol for one specific channel j	116

LIST OF FIGURES

5.4	Illustration of different sets in one combined scenario.	131
5.5	Convergence illustration for Alg. 8.	135
5.6	Normalized throughput versus transmission probability p and sensing time τ^{11} for $\Delta\gamma = -7$, $N = 10$ and $M = 4$	136
5.7	Normalized throughput versus SNR shift $\Delta\gamma$ for $N = 10$ and $M = 4$ under 4 aggregation rules.	136
5.8	Normalized throughput versus SNR shift $\Delta\gamma$ for $N = 10$ and $M = 4$ for optimized and non-optimized scenarios.	137
5.9	Normalized throughput versus SNR shift $\Delta\gamma$ for $N = 10$ and $M = 4$ for optimized and RR channel assignments.	138
5.10	Normalized throughput versus probability of having vacant channel $\mathcal{P}_j(\mathcal{H}_0)$ for $N = 10$ and $M = 4$ for optimized channel assignments and a-out-of-b aggregation rule.	139
5.11	Normalized throughput versus SNR shift $\Delta\gamma$ for $N = 4$ and $M = 3$ for optimized channel assignments and a-out-of-b aggregation rules.	139
6.1	Timing diagram of the proposed full-duplex cognitive MAC protocol.	147
6.2	Normalized throughput versus transmission probability p for $T = 18$ ms, $\bar{\tau}_{id} = 1000$ ms, $\bar{\tau}_{ac} = 100$ ms, and varying ξ	154
6.3	Normalized throughput versus the number of SUs n_0 for $T = 18$ ms, $p =$ 0.0022 , $\bar{\tau}_{id} = 1000$ ms, $\bar{\tau}_{ac} = 100$ ms, and varying ξ	154
6.4	Normalized throughput versus SU transmit power P_{sen} and sensing time T_S for $p = 0.0022$, $\bar{\tau}_{id} = 500$ ms, $\bar{\tau}_{ac} = 50$ ms, $n_0 = 40$, $\xi = 1$, $\zeta = 0.7$ and FDTx with $P_{dat} = 15$ dB.	155
6.5	Normalized throughput versus SU transmit power P_{sen} and sensing time T_S for $p = 0.0022$, $\bar{\tau}_{id} = 500$ ms, $\bar{\tau}_{ac} = 50$ ms, $n_0 = 40$, $\xi = 1$, $\zeta = 0.08$ and FDTx with $P_{dat} = 15$ dB.	156
6.6	Normalized throughput versus SU transmit power P_{sen} and sensing time T_S for $p = 0.0022$, $\bar{\tau}_{id} = 150$ ms, $\bar{\tau}_{ac} = 50$ ms, $n_0 = 40$, $\xi = 0.95$, $\zeta = 0.08$ and FDTx with $P_{dat} = 15$ dB.	156
6.7	Normalized throughput versus SU transmit power P_{sen} and sensing time T_S for $p = 0.0022$, $\bar{\tau}_{id} = 150$ ms, $\bar{\tau}_{ac} = 50$ ms, $n_0 = 40$, $\xi = 0.95$, $\zeta = 0.8$ and FDTx with $P_{dat} = 15$ dB.	157

LIST OF FIGURES

6.8	Normalized throughput versus SU transmit power P_{sen} and sensing time T_S for $p = 0.0022$, $\bar{\tau}_{\text{id}} = 150$ ms, $\bar{\tau}_{\text{ac}} = 50$ ms, $n_0 = 40$, $\xi = 0.95$, $\zeta = 0.08$ and HDTx.	158
6.9	Normalized throughput versus SU transmit power P_{sen} for $T_S = 2.2$ ms, $p = 0.0022$, $\bar{\tau}_{\text{id}} = 1000$ ms, $\bar{\tau}_{\text{ac}} = 50$ ms, $n_0 = 40$, $\xi = 0.95$, $\zeta = 0.08$, varying T , and FDTx with $P_{\text{dat}} = 15$ dB.	159
6.10	Normalized throughput versus P_{max} for $\bar{\tau}_{\text{id}} = 150$ ms, $\bar{\tau}_{\text{ac}} = 75$ ms, $n_0 = 40$, $\xi = 0.85$, $n_0 = 40$, $\zeta = \{0.2, 0.7\}$, and FDTx with $P_{\text{dat}} = P_{\text{max}}$ dB.	159

List of Tables

3.1	Comparison between the normalized throughputs of basic access and RTS/CTS access	56
4.1	Channel Assignment Example (M=3, N =6)	76
5.1	Summary of Key Variables	110
5.2	Channel Assignment Example for SUs (x denotes an assignment)	114
5.3	Throughput vs probability of vacant channel (MxN=4x4)	134
5.4	Round-robin Channel Assignment (x denotes an assignment)	138

GLOSSARY

AP	Access point
ACK	Acknowledgment
AWGN	Additive white Gaussian noise
CMAC	Cognitive MAC protocol
CRN	Cognitive radio network
CSCG	Circularly symmetric complex Gaussian
CSMA	Carrier sense multiple access
CSMA/CA	Carrier sense multiple access with collision avoidance
CTS	Clear-to-send
DCF	Distributed coordination function
DIFS	Distributed inter-frame space
DSA	Dynamic spectrum access
EGC	Equal gain combining
FCC	Federal Communication Committee
FD	Full-duplex
FDTx	Full-duplex transmission
FDC-MAC	Full-duplex cognitive MAC protocol
GSC	Generalized selection combining
HD	Half-duplex
HDTx	Half-duplex transmission
MAC	Medium Access Control

MC	Markov chain
McMAC	Multi-channel MAC protocol
MRC	Maximal ratio combining
NAV	Network allocation vector
NP-hard	Non-deterministic Polynomial-time hard
OFDM	Orthogonal frequency-division multiplexing
OSA	Opportunistic spectrum access
PD	Propagation delay
PDF	Probability density function
PMF	Probability mass function
PSK	Phase-shift keying
PU_s	Primary users
QoS	Quality of service
QSIC	Quality of self-interference cancellation
RR	Round-robin
RTS	Request-to-send
RV	Random variable
SC	Selection combining
SSCH	Slotted seeded channel hopping MAC protocol
SDCSS	Semi-distributed cooperative spectrum sensing
SIC	Self-interference cancellation
SINR	Signal-to-interference-plus-noise ratio
SLC	Square-law combining

SIFS	Short inter-frame space
SLS	Square-law selection
SNR	Signal-to-noise ratio
SSC	Switch and stay combining
SUs	Secondary users
WiFi	Wireless Fidelity
WRAN	Wireless regional area network

Chapter 1

Introduction

The proliferation of wireless services and applications over the past decade has led to the rapidly increasing demand in wireless spectrum. Hence, we have been facing a critical spectrum shortage problem. Several recent measurements have, however, reported that a large portion of licensed radio spectrum is very underutilized in spatial and temporal domains [1], [2]. These facts have motivated the development of dynamic spectrum access (DSA) techniques to enhance the efficiency and flexibility of spectrum utilization. DSA can be categorized into three major models, namely dynamic exclusive use, open sharing, and hierarchical access models [2]. The third model which is also referred to as opportunistic spectrum access (OSA), which provides fundamental ground for an extremely active research theme, i.e., the cognitive radio research. OSA in cognitive radio networks can be further divided into three access paradigms, namely underlay, overlay, and interweave [2–4].

The research in this dissertation considers the interweave paradigm where the licensed spectrum is shared between the primary and secondary networks whose users are referred to as primary and secondary users (PUs and SUs), respectively. In particular, SUs can opportunistically exploit spectrum holes (i.e., idle spectrum in time, frequency, and space) for their data transmission as long as they do not severely interfere the transmissions of PUs. This access principle implies that PUs have strictly higher priority than SUs in accessing the underlying spectrum; hence, SUs can only access the licensed spectrum if PUs do not occupy them. Toward this end, SUs can perform spectrum sensing to explore spectrum holes and adopt suitable spectrum access mechanisms to share the discovered available spectrum with one another [5].

Although the spectrum sensing and access functions are tightly coupled, they are usually not treated jointly in the existing multi-user cognitive radio literature. Moreover, it is desir-

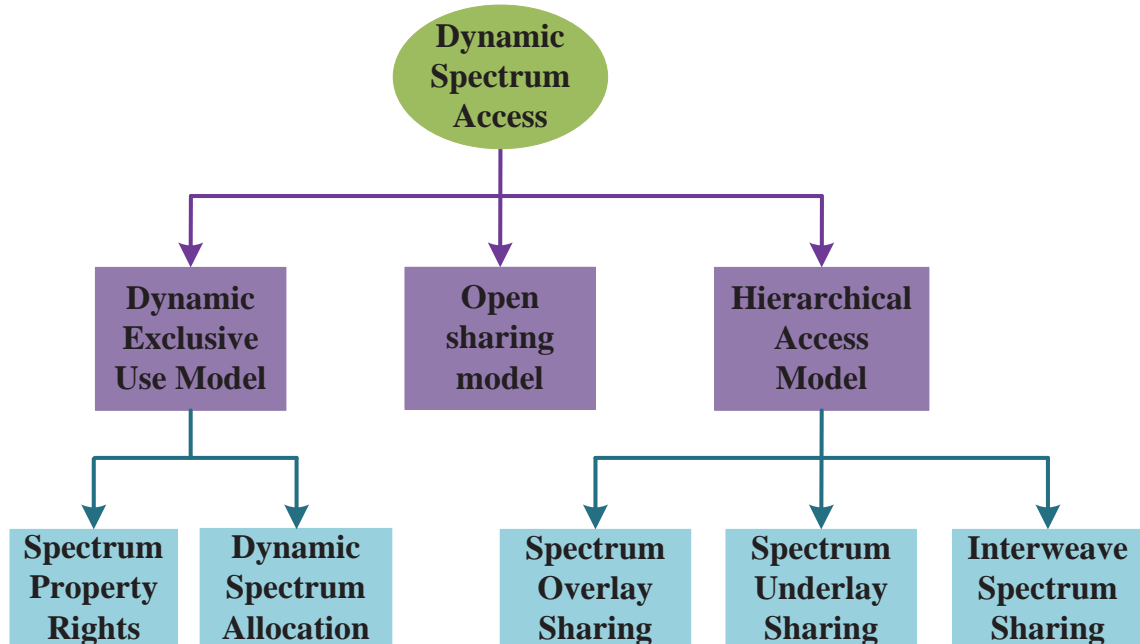


Figure 1.1: The broad landscape of Dynamic Spectrum Access (DSA) [2, 3].

able to employ a distributed cognitive MAC protocol for spectrum sharing in many wireless applications, which is usually more cost-efficient compared to the centralized cognitive MAC counterpart. An efficient cognitive MAC protocol should achieve good performance in certain performance measures such as throughput (spectrum utilization), delay, fairness, and energy consumption. This dissertation aims to engineer the distributed cognitive MAC protocol with extensive performance analysis and optimization for several practically relevant cognitive network settings.

1.1 Dynamic Spectrum Access

To resolve the under-utilization of wireless spectrum and support the increasing spectrum demand of the wireless sector, spectrum management authorities in many countries (e.g., Federal Communication Committee (FCC) in US) have recently adopted more flexible spectrum management policies for certain parts of the wireless spectrum such as TV bands compared to the rigid and non-dynamic policies employed in the past. In the following, we describe three different DSA models, namely, dynamic exclusive use, open sharing, and hierarchical access models [2] where the DSA taxonomy is illustrated in Fig. 1.1.

Dynamic exclusive use model: This model can be realized through two different

approaches, namely, the spectrum property right and dynamic spectrum allocation. In the spectrum property right approach [6], the unused spectrum of the licensees can be leased or traded, which can result in more flexibility in the spectrum management. Here, the market and economy play a critical role in achieving efficient use of the spectrum. The dynamic spectrum allocation approach was proposed by the European DRiVE project [7] where the spatio-temporal traffic statistics are exploited for dynamic spectrum assignment to different services, which use the assigned spectrum exclusively.

Open sharing model: This model is also called as *Spectrum Commons* in [8] where the spectrum can be shared by a number of peer users in a specific region under the open sharing basis. This spectrum sharing model is motivated by the very successful deployment of wireless services in the unlicensed spectrum band (e.g., WiFi). This spectrum sharing model can be realized in the centralized or distributed manner [9, 10].

Hierarchical access model: This model classifies the spectrum access users into PUs (i.e., licensed users) and SUs. Specifically, it adopts a hierarchical access structure where PUs must be protected from the interference created by SUs. There are three main approaches for opportunistic spectrum sharing under this model, namely underlay, overlay, and interweave [2–4].

This dissertation focuses on the cognitive MAC protocol design for cognitive radio networks under the hierarchical access model, which will be described in more details in the following section.

1.2 Hierarchical Access Model and Cognitive MAC Protocol

1.2.1 Hierarchical Access Model

Recent changes in spectrum regulation and management have motivated the development of the hierarchical spectrum access techniques for efficient spectrum sharing between the primary users/network and secondary users/network. In this spectrum sharing model, SUs are allowed to access the spectrum as long as transmissions from PUs can be satisfactorily protected from the interference caused by the SUs. As mentioned previously, one of the three approaches can be adopted for hierarchical spectrum access, i.e., the underlay, overlay, and interweave access paradigms [2–4], which are discussed in the following.

1.2 Hierarchical Access Model and Cognitive MAC Protocol

In the underlay paradigm, PUs' and SUs' transmissions can co-exist on the same frequency band at the same time; however, the interference created by SUs at each PU must remain below an allowable limit [11, 12]. Advanced communications and signal processing techniques can be employed for efficient interference management and mitigation to maintain this interference constraint. In particular, we can set the transmit power of the secondary signal to maintain the interference constraint at the PU's receiver by using power control techniques. Furthermore, the more advanced beamforming technique can be adopted in the multi-antenna secondary system to achieve good performance for SUs while nulling interference toward PUs. In general, SUs need to acquire suitable information related to PUs such as channel state information, PUs' locations to maintain the interference constraint. This is, however, difficult to achieve in practice.

For the overlay paradigm, PUs' and SUs' signals can also co-exist at the same frequency band simultaneously; however, the SU is assumed to have knowledge about the PUs' codebooks and messages, which can be achieved in different ways [3]. Knowledge about the PUs' codebooks and/or messages can be used to mitigate or cancel the interference seen at the PUs' and SUs' receivers. Also, SUs can use the knowledge about the PUs' messages to eliminate the interference generated by the PUs' transmissions seen at the SUs' receivers. Moreover, SUs can use part of their energy to enhance and assist the communications of PUs through cooperative communications [13–15] and use the remaining energy for their communications. With this cooperation, the interference due to the SUs' signals to the PUs' receivers can be compensated by the cooperation gain while the SUs can still exploit the spectrum for their transmissions [13–15]. Implementation of the overlay spectrum sharing paradigm requires SUs to acquire information about PUs' messages before the PUs begin their transmissions, which is not easy to achieve in practice.

Finally, in the interweave paradigm, SUs opportunistically exploit the idle spectrum in time and/or frequency domains, which are called spectrum holes or white spaces, for data communication [16–46]. To identify spectral holes, SUs must employ a suitable spectrum sensing strategy. Upon correctly discovering spectrum holes on the licensed spectrum, SUs can transmit at high power levels without subject to the interference constraints at SUs as in the underlay spectrum sharing paradigm. For the case where the SUs can synchronize their transmissions with PUs' idle time intervals and perfect sensing can be achieved, SUs will not create any interference to active PUs. However, half-duplex SUs cannot sense the spectrum and transmit simultaneously; therefore, SUs could not detect the event in which

1.2 Hierarchical Access Model and Cognitive MAC Protocol

an PU changes its status from idle to active during their transmissions. Consequently, SUs employing half-duplex radios may cause interference to active PUs.

In comparison with the underlay and overlay paradigms, the interweave approach requires to acquire less information about the PUs and it can also utilize the spectrum more efficiently since there is no transmit power constraint [3]. Moreover, PUs are not required to change or adapt their communication strategies or parameters to realize the spectrum sharing with SUs. Inspired by these advantages, we focus on the MAC protocol design issues for this interweave spectrum sharing paradigm in this dissertation.

1.2.2 Cognitive MAC Protocol

Different from conventional MAC protocols, a CMAC protocol must integrate the spectrum sensing function to identify spectrum holes before sharing the available spectrum through a spectrum access mechanism. In addition, a CMAC protocol must be designed appropriately considering the communication capability of SUs' radio, i.e., half-duplex (HD) or full-duplex (FD) radio. Most existing research works have considered the design and analysis of HD CMAC protocols (e.g., see [47, 48] and references therein) where SUs are synchronized with each other to perform periodic spectrum sensing and access. Due to the HD constraint, SUs typically employ a two-stage sensing/access procedure where they sense the spectrum in the first stage before accessing available channels for data transmission in the second stage [16–34, 37–46]. Some other works assume that the primary and secondary networks are synchronized with each other so exact idle intervals on the spectrum of interest are known to the SUs [17, 18, 30]. This assumption would, however, be difficult to achieve in practice.

In an HD CMAC protocol, if an PU changes from the idle to active status when the SUs are occupying the spectrum, then transmissions from SUs can cause strong interference to active PUs. With recent advances in the full-duplex technologies (e.g., see [49–54]), some recent works consider FD spectrum access design for cognitive radio networks (CRNs) [55, 56] where each SU can perform sensing and transmission simultaneously. This implies that SUs may be able to detect the PUs' active status while they are utilizing the licensed spectrum with the FD radio. However, self-interference due to simultaneous sensing and transmission of FD radios may lead to performance degradation of the SUs' spectrum sensing. Therefore, FD CMAC protocols must be designed appropriately to manage the FD self-interference by using suitable mechanisms such as power control.

1.3 Research Challenges and Motivations

Efficient design of CRNs imposes many new challenges that are not present in the conventional wireless networks [47, 57–60]. These design challenges are originated from the variations of white spaces in time and space as well as the time-varying wireless channel quality. SUs who have the lower priority than PUs in accessing the licensed spectrum must tune their operations and transmission parameters so as not to cause harmful interference to active PUs. We can highlight some major challenges in designing opportunistic cognitive MAC (CMAC) protocols for CRNs as follows: 1) Efficient joint spectrum sensing and access design; 2) The trade-off between spectrum utilization and interference to PUs; 3) Fair spectrum access among SUs; 4) Hardware limitations; 5) Multi-channel hidden/exposed terminal problem; 6) Control channel configuration; 7) Spectrum heterogeneity seen by SUs; 8) QoS provisioning; 9) Asynchronicity between SU and PU networks.

In this dissertation, we aim to design, analyze, and optimize CMAC protocols for CRNs under different practically relevant scenarios. Specifically, the first three contributions are related to the design of synchronous CMAC protocols for the HD CRNs in three different settings whilst the last contribution involves the engineering of an asynchronous CMAC protocol to FD CRNs. To motivate our research, we briefly discuss the existing CMAC literature and describe its limitations for different considered scenarios in the following.

1.3.1 CMAC with Parallel Sensing

In many existing works, the two-stage CMAC protocol with parallel sensing is considered where SUs are equipped with multiple HD transceivers; hence, they are able to sense or access multiple channels simultaneously. In this setting, the sensing time in the first sensing phase can be quite short, hence SUs can efficiently exploit the spectrum holes to transmit data in the second transmission phase. Existing works considering this scenario have the following limitations: they *i)* usually assume perfect spectrum sensing [61, 62]; *ii)* only analyze the network throughput performance but very few of them consider optimizing the network and protocol parameters to maximize the network performance [26].

Efficient CMAC design with parallel sensing presents the following challenges. The design must integrate both spectrum sensing and access functions in the CMAC protocol. For distributed implementation, contention-based MAC mechanism based on the popular carrier sense multiple access (CSMA) principle can be employed for contention resolution. Furthermore, protocol optimization, which adapts different protocol parameters such as contention

windows, back-off durations, and access probability to maximize the network performance (e.g., throughput) while appropriately protecting active PUs is an important issue to investigate. Toward this end, performance analysis for the developed CMAC protocol is needed. Our dissertation indeed makes some contributions along these lines.

1.3.2 CMAC with Sequential Sensing

Deploying multiple transceivers for each SU as in the previous case leads to high implementation complexity and cost. Therefore, the scenario in which each SU has a single transceiver would be preferred in many practical applications. A CMAC protocol in this setting, however, must employ sequential sensing where spectrum sensing for multiple channels is sensed by each SU one by one in a sequential manner. Moreover, each SU can access at most one idle channel for communications.

Spectrum sensing, which is integrated into the CMAC protocol, should be carefully designed to achieve efficient tradeoff between sensing time overhead and achieved performance. Different sensing designs have been proposed to deal with this scenario, i.e., sensing-period and optimal channel sensing order optimization [16], random- and negotiation-based spectrum-sensing schemes [17–19, 21, 63]. Moreover, each SU may only sense a subset of channels to reduce the spectrum sensing time. Furthermore, the channel assignment optimization for SUs to determine the optimal subset of channels allocated for each SU is important, which is, however, not well investigated in the literature.

Therefore, efficient MAC protocol engineering in this setting must consider the interactions between achieved sensing/network performance and channel assignments. Moreover, fairness among SUs could be considered in designing the CMAC and channel assignment. Our dissertation makes some important contributions in resolving some of these issues.

1.3.3 CMAC with Cooperative Sensing

In order to enhance the spectrum sensing performance, cooperative spectrum sensing can be employed where a fusion center can be installed (e.g., at an access point (AP)) to collect individual sensing data from SUs based on which it makes final sensing results and broadcasts them to the SUs [64, 65]. Detailed design of such cooperative spectrum sensing can vary depending on the underlying aggregation rules and hard- or soft-decision strategy [66, 67]. In addition, the distributed cooperative spectrum sensing would be preferred to the centralized one in most practical deployments. In distributed cooperative spectrum sensing, the sensing

tasks are shared among SUs (i.e., there is fusion center (AP)) and each SU performs sensing independently and then makes its own decision of sensing outcomes with some suitable exchanges of sensing data.

In [26, 34, 68, 69], different multi-channel CMAC protocols were proposed considering either parallel or sequential spectrum sensing method. In these existing works, design and optimization of the cooperative spectrum sensing parameters are pursued. However, they do not consider spectrum access issues or they assume the availability of multiple transceivers for simultaneously sensing all channels.

In addition, the MAC protocol in these works are non-optimized standard window-based CSMA MAC protocol, which is known to achieved smaller throughput than the optimized p -persistent CSMA MAC protocol [70]. Furthermore, either the single-channel setting or homogeneous network scenario (i.e., SUs experience the same channel condition and spectrum statistics for different channels) was assumed in these works. Finally, existing cooperative spectrum sensing schemes rely on a central controller to aggregate sensing results for white space detection (i.e., centralized design). We have developed a CMAC protocol employing distributed cooperative spectrum sensing in this dissertation, which overcomes several limitations of existing CMAC protocols mentioned above.

1.3.4 Full-Duplex MAC Protocol for Cognitive Radio Networks

As discussed earlier, SUs in the HD CRN must employ the two-stage sensing/access procedure due to the HD constraint. This constraint also requires SUs be synchronized during the spectrum sensing stage, which could be difficult to achieve in practice. In general, HD-MAC protocols may not exploit white spaces very efficiently since significant sensing time may be required, which would otherwise be utilized for data transmission. Moreover, SUs may not timely detect the PUs' activity during their transmissions, which can cause severe interference to active PUs.

Recent advances in FD technologies [49–51] has opened opportunities to develop FD cognitive MAC protocols that can overcome many aforementioned limitations of HD CMAC protocols. With FD radios, SUs can indeed perform spectrum sensing and access simultaneously. However, the presence of self-interference, which is caused by power leakage from the transmitter to the receiver of a FD transceiver, may indeed lead to sensing/transmission performance degradation.

Several FD CMAC protocols have been recently proposed. The authors in [55] investigate three operation modes for the FD cognitive radio network (i.e., transmission-only,

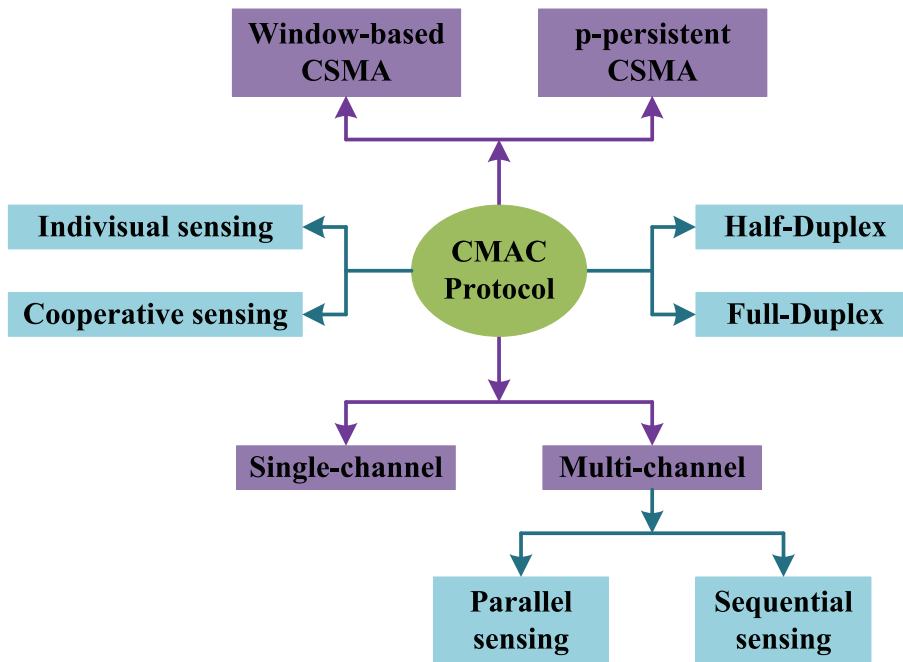


Figure 1.2: Positioning our contributions within the broad CMAC landscape.

transmission-sensing, and transmission-reception modes) and the optimal parameter configurations by solving three corresponding optimization problems. In [56], another FD CMAC protocol is developed where both PUs and SUs are assumed to employ the same p -persistent MAC protocol for channel contention resolution. This design is not applicable to CRNs where PUs should have higher spectrum access priority compared to SUs. In general, it is desirable to design a FD CMAC protocol with following characteristics: *i*) a distributed FD CMAC protocol can operate efficiently in an asynchronous manner where SUs are not required be synchronized with each other; *ii*) SUs must timely detect the PUs' reactivation during their transmissions to protect active PUs; *iii*) the FD CMAC protocol can be easily reconfigured where its parameters can be adapted to specific channel state and network conditions. Our developed FD CMAC protocol satisfactorily achieve these requirements.

1.4 Research Contributions and Organization of the Dissertation

The overall objective of this dissertation is to design, analyze, and optimize the cognitive MAC protocol for efficient dynamic spectrum sharing in CRNs. Our main contributions, which are highlighted in Fig. 1.2, are described in the following.

1.4 Research Contributions and Organization of the Dissertation

1. *CMAC protocol design with parallel sensing [22]*: We consider the setting where each SU can perform parallel sensing and exploit all available channels for data transmissions. We develop a synchronous CMAC protocol integrating the parallel spectrum sensing function. We then analyze the throughput performance and study the optimization of its access and sensing parameters for throughput maximization. This work fundamentally extends the throughput-sensing optimization framework in [5], which was proposed for the single-SU setting.
2. *CMAC protocol and channel assignment with sequential sensing [33, 39]*: This contribution covers the joint sensing and access design for the scenario where each SU performs sequential sensing over multiple channels and can access at most one idle channel for communications [33]. We devise and analyze the saturation throughput performance of the proposed CMAC protocol. Then, we develop efficient channel allocation for SUs to maximize the total throughput of the secondary network. Furthermore, we also investigate a fair channel allocation problem where each node is allocated a subset of channels which are sensed and accessed periodically by using a CMAC protocol.
3. *Distributed CMAC protocol and cooperative sensing design [37]*: We propose a distributed cooperative spectrum and p -persistent CMAC protocol for multi-channel and heterogeneous CRNs [37]. In particular, we develop the distributed cooperative spectrum sensing where we assume SUs directly exchange sensing results to make decisions on all channels' statuses by using the general a-out-of-b aggregation rule. We conduct the performance analysis and configuration optimization for the proposed CMAC protocol considering both perfect and imperfect exchanges of sensing results. We also propose a different joint cooperative spectrum and contention window-based MAC protocol for multi-channel and heterogeneous CRNs in [40].
4. *Asynchronous full-duplex MAC protocol for cognitive radio networks [36]*: We propose the FD cognitive MAC protocol (FDC-MAC) which employs the distributed p -persistent CSMA access mechanism and FD spectrum sensing [36]. Our design exploits the fact that FD SUs can perform spectrum sensing and access simultaneously, which enable them to detect the PUs' activity during transmission. Each data frame is divided into the sensing and access stages to timely detect the PUs' transmission and enable SUs' performance optimization. Furthermore, we develop a mathematical model to analyze the throughput performance of the proposed FDC-MAC protocol.

1.4 Research Contributions and Organization of the Dissertation

Then, we propose an algorithm to configure the CMAC protocol so that efficient self-interference management and sensing overhead control can be achieved. The proposed FDC-MAC protocol design is very flexible, which can be configured to operate in the HD mode or having simultaneous sensing and access for the whole data frame as in [35].

The remaining of this dissertation is organized as follows. In chapter 4, we present the research background and literature review. In chapter 5, we discuss the joint MAC and sensing design under parallel sensing. We describe the proposed protocol design framework under sequential sensing in chapter 6. The developed distributed cooperative sensing and MAC design are presented in chapter 7. Chapter 8 describes the distributed MAC protocol design for FD cognitive radio networks. Chapter 9 summarizes the contributions of the dissertation and point out some future research directions.

Chapter 2

Background and Literature Review

In this chapter, we present the research background and literature survey on different research issues studied in our dissertation. In particular, some background on spectrum sensing is presented where basics of spectrum sensing and more advanced spectrum sensing methods such as cooperative spectrum sensing are discussed. Then, we describe fundamentals of MAC protocols for conventional single- and multi-channel wireless networks. Finally, we provide a comprehensive review and taxonomy of the state-of-the-art CMAC protocols.

2.1 Research Background

2.1.1 Spectrum Sensing

Spectrum sensing and channel probing, which aim at acquiring real-time spectrum/channel information required by the cognitive MAC layer, are critical components of CRNs. In particular, spectrum sensing performs the following tasks [71]: *i)* detection of spectrum holes; *ii)* determination of spectral resolution of each spectrum hole; *iii)* estimation of the spatial directions of incoming interfering signal; *iv)* signal classification. Among these tasks, detection of spectrum holes, which is probably the most important one, boils down to a binary hypothesis-testing problem. Therefore, detection of spectrum holes on a narrow frequency band is usually referred to as spectrum sensing, which aims at deciding the presence or absence of PUs in the underlying band. Some extensive reviews of spectrum sensing techniques for CRNs can be found in [48, 71–73].

We now describe the spectrum sensing in some more details. Let B be the signal bandwidth, f_s be the sampling frequency, τ be the observation time over which signal samples are collected, then $N = \lceil \tau f_s \rceil$ is the number of samples (we assume $N = \tau f_s$ is an integer

for simplicity). Let $s(n)$ denote the PU's signal with zero mean and variance σ_s , $u(n)$ be the additive white Gaussian noise (AWGN) with zero mean and variance N_0 , $\gamma = \frac{\sigma_s}{N_0}$ be the received signal-to-noise ratio (SNR). Note that $s(n)$ could capture the fading and multi-path effects of the wireless channels.

Let \mathcal{H}_0 and \mathcal{H}_1 represent two events (hypotheses) corresponding to the cases where PUs are absent or present in the underlying spectrum, respectively. The sampled signal received at the SU, denoted as $y(n)$, corresponding to these two hypotheses can be written as

$$\begin{aligned}\mathcal{H}_0 : \quad & y(n) = u(n) \\ \mathcal{H}_1 : \quad & y(n) = s(n) + u(n).\end{aligned}\tag{2.1}$$

Let Y denote the test statistic and λ be the decision threshold. The objective of narrow-band spectrum sensing is to make a decision on presence or absence of the PUs' signals (i.e., choose hypothesis \mathcal{H}_0 or \mathcal{H}_1) based on the received signals (observations). Such decision can be made by comparing the test statistic with the threshold as follows:

$$\begin{aligned}\mathcal{H}_0 : \quad & Y < \lambda \\ \mathcal{H}_1 : \quad & Y > \lambda.\end{aligned}\tag{2.2}$$

To quantify the spectrum sensing performance, we usually employ two important performance measures, namely detection probability \mathcal{P}_d and false-alarm probability \mathcal{P}_f . In particular, \mathcal{P}_d captures the probability that a spectrum sensor successfully detects a busy channel and \mathcal{P}_f represents the event where a spectrum sensor returns a busy state for an idle channel (i.e., a transmission opportunity is overlooked). Therefore, the detection and false-alarm probabilities can be expressed as

$$\begin{aligned}\mathcal{P}_d &= \Pr(Y > \lambda | \mathcal{H}_1) \\ \mathcal{P}_f &= \Pr(Y > \lambda | \mathcal{H}_0).\end{aligned}\tag{2.3}$$

A spectrum sensing algorithm is more efficient if it achieves higher \mathcal{P}_d and lower \mathcal{P}_f . With higher \mathcal{P}_d , active PUs would be better protected and lower \mathcal{P}_f means that the white space is likely not overlooked by SUs (cognitive radios).

There are many different spectrum sensing strategies proposed in the literature, which can be categorized into the following three main groups, namely energy detection, matched-filter detection, and feature detection where the first one is non-coherent detection and the others belong to the coherent detection. In coherent detection, a spectrum sensor requires a

priori knowledge of PU's signal to coherently detect the presence of the PU. In contrast, a spectrum sensor in non-coherent detection does not require a priori knowledge of PU's signal for detection. Furthermore, SUs can perform spectrum sensing independently or several SUs can collaborate to perform detection, which are termed individual sensing and cooperative spectrum sensing, respectively in this dissertation.

2.1.1.1 Individual Sensing

1. *Energy Detection:*

We first discuss the energy detection which is one popular spectrum sensing method since it is simple and does not require a priori knowledge of PU's signal. As the name suggests, this sensing method detects the PUs' signal by using the energy of the received signal. Specifically, the test statistic is based on the energy of received signal, i.e.,

$$Y = \frac{1}{N} \sum_{i=1}^N |y(n)|^2 \quad (2.4)$$

Consider the scenario with a single antenna and a single sensor. Under \mathcal{H}_0 , Y involves the sum of the squares of N standard Gaussian variates with zero mean and variance N_0 . Therefore, Y follows a central chi-squared distribution with $2N$ degrees of freedom, i.e., $Y \sim \chi_{2B}^2$. Under \mathcal{H}_1 , the test statistic Y follows a non-central distribution χ^2 with $2N$ degrees of freedom and a non-centrality parameter 2γ [74]. Therefore, we can summarize the test statistic under the two hypotheses as

$$\begin{aligned} \mathcal{H}_0 : \quad & Y \sim \chi_{2B}^2 \\ \mathcal{H}_1 : \quad & Y \sim \chi_{2B}^2(2\gamma). \end{aligned} \quad (2.5)$$

We now derive the detection and false alarm probabilities where we assume that transmission signals from PUs are complex-valued phase-shift keying (PSK) signals, whereas the noise is independent and identically distributed (i.i.d.) circularly symmetric complex Gaussian $\mathcal{CN}(0, N_0)$. For large N , the probability density function (PDF) of Y under hypothesis \mathcal{H}_0 and \mathcal{H}_1 can be approximated by Gaussian distributions with mean $\mu_0 = N_0$, $\mu_1 = (\gamma + 1) N_0$ and variance $\sigma_0^2 = \frac{1}{N} N_0^2$, $\sigma_1^2 = \frac{1}{N} (\gamma + 1) N_0^2$, respectively. Therefore, the detection and false-alarm probabilities given in (2.3) can be rewritten as [5]

$$\mathcal{P}_d(\lambda, \tau) = \mathcal{Q} \left(\left(\frac{\lambda}{N_0} - \gamma - 1 \right) \sqrt{\frac{\tau f_s}{2\gamma + 1}} \right), \quad (2.6)$$

$$\mathcal{P}_f(\lambda, \tau) = \mathcal{Q}\left(\left(\frac{\lambda}{N_0} - 1\right)\sqrt{\tau f_s}\right). \quad (2.7)$$

Recall that λ is the detection threshold for an energy detector, γ is the SNR of the PU's signal at the SU, f_s is the sampling frequency, N_0 is the noise power, and τ is the sensing interval. Moreover, $\mathcal{Q}(\circ)$ is defined as $\mathcal{Q}(x) = (1/\sqrt{2\pi}) \int_x^\infty \exp(-t^2/2) dt$.

Similarly, for other kinds of noise and primary signals, we can derive the detection and false-alarm probabilities as presented in [5]. For the i.i.d. and correlated fading channels and multi-antenna setting, the probabilities of detection and false alarm can be found in [45, 46, 75, 76].

2. Other Sensing Mechanisms:

There are other spectrum sensing methods proposed for CRNs, e.g., waveform-based sensing [77–79], cyclostationarity-based sensing, radio identification based sensing, multi-taper spectral estimation [58, 80], matched-filtering [58], wavelet transform based estimation, Hough transform, and time-frequency analysis [57, 71]. In addition, the wavelet approach can be employed for detecting edges in the power spectral density of a wideband channel [81]. The wavelet-based sensing method proposed in [81] is extended in [42–44, 82, 83] by using sub-Nyquist sampling which is termed as the compressed spectrum sensing.

2.1.1.2 Cooperative Spectrum Sensing

Cooperative spectrum sensing has been proposed to improve the sensing performance where several SUs collaborate with each other to identify spectrum holes. The detection performances of cooperative spectrum sensing in terms of detection and false-alarm probabilities can be significantly better than those due to individual spectrum sensing thanks to the spatial diversity gain. However, it is required to collect, share, and combine individual sensing information to make final sensing decisions. In addition, spectrum sensors can make soft or hard decisions based on their measurements and then share their decisions to others [66].

When the number of spectrum sensors that collaborate to sense one particular channel increases, the sensing overhead is increased because more sensing information must be exchanged, which would consume more system resources. Therefore, optimized design of cooperative sensing is important, e.g., we can optimize the number of sensors assigned to sense each channel to achieve good balance between sensing performance and overhead. In the following, we describe cooperative spectrum sensing with hard and soft decisions.

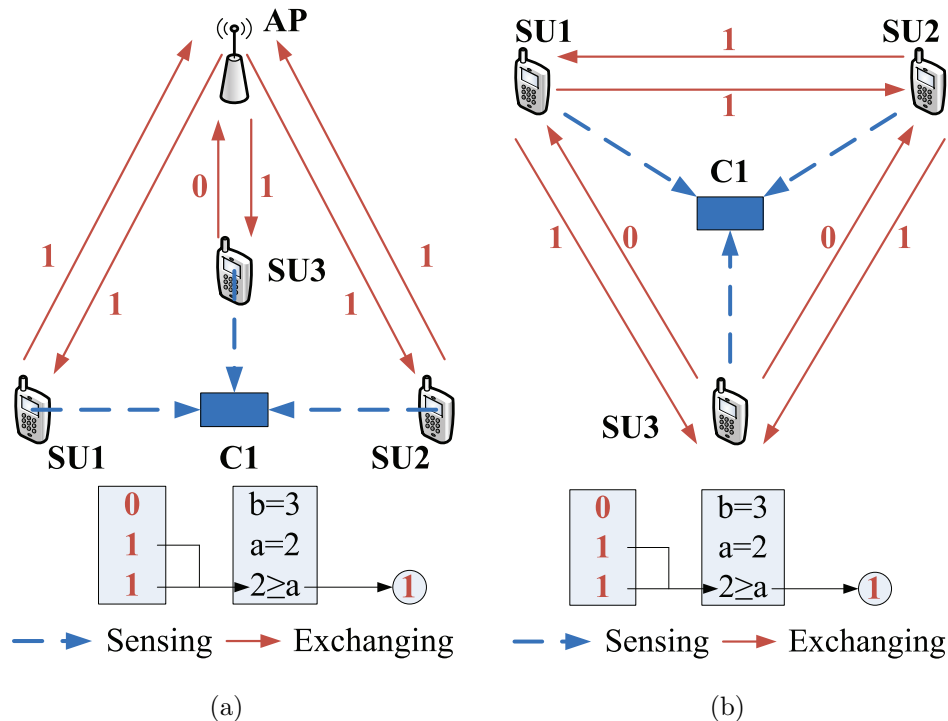


Figure 2.1: Cooperative sensing examples with (a) centralized processing, (b) distributed processing.

1. Cooperative spectrum sensing with hard decisions

Cooperative spectrum sensing can be realized via centralized and distributed implementations. In the centralized approach, a central unit (e.g., an AP) collects sensing information from SUs, makes sensing decisions then broadcasts them to all SUs. In the distributed sensing method, all SUs perform sensing on their assigned channels then exchange the sensing results with others. Finally, SUs make their sensing decisions independently by themselves.

We now study the centralized spectrum sensing algorithm. We assume that each SU i is assigned in advance a set of channels \mathcal{S}_i for sensing at the beginning of each sensing cycle. Upon completing the channel sensing, each SU i sends the idle/busy states of all channels in \mathcal{S}_i to the central unit for further processing. Suppose that the channel status of each channel can be represented by one bit (e.g., 1 for idle and 0 for busy status). Upon collecting sensing results from all SUs, the central unit decides the idle/busy status for all channels, then it broadcasts the list of available channels to all SUs for exploitation.

Consider a general cooperative sensing rule, namely a -out-of- b rule, which is employed by the central unit to determine the idle/busy status of each channel based on reported sensing

results from all SUs. In this scheme, the central unit declares that a channel is idle if a or more SUs out of b SUs report that the underlying channel is idle. The a -out-of- b rule covers different other rules including OR, AND and Majority rules as special cases. In particular, when $a = 1$, it is the OR rule; when $a = b$, it is the AND rule; and when $a = \lfloor b/2 \rfloor$, it is the Majority rule.

We now analyze the cooperative sensing performance for a particular channel j . Let \mathcal{S}_j^U denote the set of SUs that sense channel j and $b_j = |\mathcal{S}_j^U|$ be the number of SUs sensing channel j . Then, the detection and false alarm probabilities for this channel can be calculated respectively as [84]

$$\mathcal{P}_u^j(\bar{\varepsilon}^j, \bar{\tau}^j, a_j) = \sum_{l=a_j}^{b_j} \sum_{k=1}^{C_{b_j}^l} \prod_{i_1 \in \Phi_l^k} \mathcal{P}_u^{i_1 j} \prod_{i_2 \in \mathcal{S}_j^U \setminus \Phi_l^k} \bar{\mathcal{P}}_u^{i_2 j}, \quad (2.8)$$

where u represents d or f as we calculate the probability of detection \mathcal{P}_d^j or false alarm \mathcal{P}_f^j , respectively; \mathcal{P}_d^{ij} and \mathcal{P}_f^{ij} are the probabilities of detection and false alarm at SU i for channel j , respectively; $\bar{\mathcal{P}}$ is defined as $\bar{\mathcal{P}} = 1 - \mathcal{P}$; Φ_l^k in (2.8) denotes a particular set with l SUs whose sensing outcomes suggest that channel j is busy given that this channel is indeed busy and idle as u represents d and f , respectively. In this calculation, we generate all possible sets Φ_l^k where there are indeed $C_{b_j}^l$ combinations. Also, $\bar{\varepsilon}^j = \{\varepsilon^{ij}\}$, $\bar{\tau}^j = \{\tau^{ij}\}$, $i \in \mathcal{S}_j^U$ represent the set of detection thresholds and sensing times, respectively.

To illustrate the operations of the a -out-of- b rule, let us consider a simple example for the centralized cooperative spectrum sensing implementation shown in Fig. 2.1(a). Here, we assume that 3 SUs collaborate to sense channel one (C1) with $a = 2$ and $b = 3$. After sensing the channel, all SUs report their sensing outcomes to an AP. Here, the AP receives the reporting results comprising two “1s” and one “0” where “1” means that the channel is busy and “0” means channel is idle. Because the total number of “1s” is two which is larger than or equal to $a = 2$, the AP outputs the “1” in the final sensing result, i.e., the channel is busy. Then, the AP broadcast this final sensing result to all SUs.

Now we investigate the distributed cooperative spectrum sensing. Upon completing the channel sensing, each SU i exchanges the sensing results (i.e., idle/busy status of all channels in \mathcal{S}_i) with other SUs for further processing. After collecting the sensing results, each SU will decide the idle/busy status for each channel. Fig. 2.1(b) illustrates the distributed cooperative spectrum sensing using the a -out-of- b rule where 3 SUs collaborate to sense channel one with $a = 2$ and $b = 3$. After sensing the channel, all SUs exchange their sensing

outcomes. SU3 receives the reporting results comprising two “1s” and one “0”. Because the total number of “1s” is two which is larger than or equal to $a = 2$, SU3 outputs the “1” in the final sensing result, i.e., the channel is busy.

2. *Cooperative spectrum sensing with soft decisions*

In this sensing method, the SUs must send their measurements (not the decisions) to the central unit and then the central unit will make final sensing decisions and broadcast them to all SUs. Performance analysis of this method for the i.i.d., correlated fading channels, and multi-antenna settings is conducted in [45, 46, 75, 76]. Here, different combining techniques such as maximal ratio combining (MRC), selection combining (SC), equal gain combining (EGC), switch and stay combining (SSC), square-law selection (SLS), square-law combining (SLC), and generalized selection combining (GSC) schemes can be employed to exploit the spatial diversity for sensing performance enhancement.

2.1.2 MAC Protocol in Traditional Wireless Networks

2.1.2.1 Single-channel MAC Protocols

There are many random-access-based MAC protocols, which have been developed over the past decades and employed in different wireless systems and standards. Popular MAC protocols include ALOHA, Slotted ALOHA, p -persistent carrier sense multiple access (CSMA) [70] (including non-persistent, p -persistent, and 1-persistent) and CSMA/CA (CSMA with collision avoidance) [85] (or window-based CSMA) MAC protocols. In these MAC protocols, active stations (users) perform contention to capture the channel for data transmission in the distributed manner. Moreover, suitable mechanisms are adopted to mitigate the potential collisions among users (e.g., the well-known backoff mechanism for contention resolution in the CSMA/CA protocol). We provide more detailed discussions and performance analysis for some of these popular MAC protocols in the following where a single channel is shared by multiple users.

1. *Window-based CSMA MAC Protocol*

(a) *MAC protocol*

To capture the channel for data transmission, all active users employ the same contention resolution mechanism, which is described in the following [85]. To avoid collisions among contending users, each user takes a random waiting time before access, which is chosen based

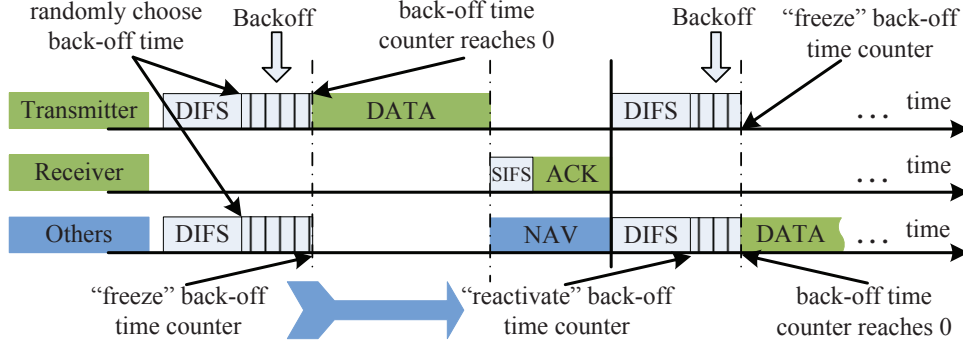


Figure 2.2: Example of basic access mechanism for window-based CSMA MAC protocol [85].

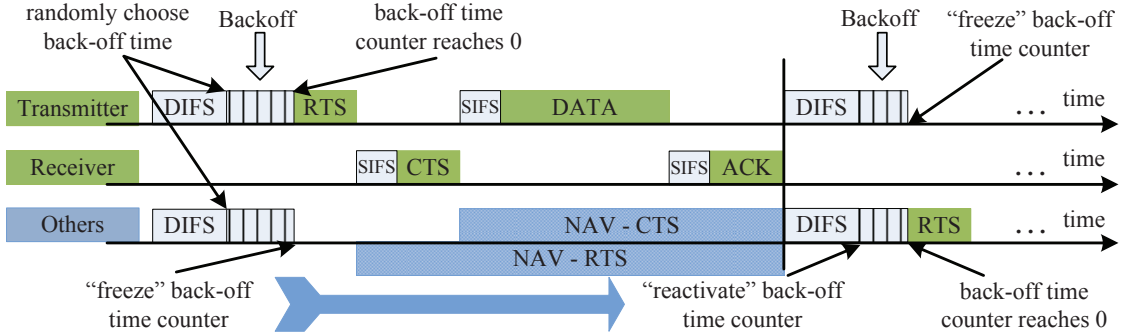


Figure 2.3: Example of RTS/CTS access mechanism for window-based CSMA MAC protocol [85].

on the so-called contention window W . Moreover, the value of this contention window W is doubled after each collision until the contention window reaches $2^m W_0$ where W_0 is the minimum value of contention window and m is called maximum back-off stage.

Suppose that the current back-off stage of a particular user is i then it starts the contention by choosing a random back-off time uniformly distributed in the range $[0, 2^i W_0 - 1]$, $0 \leq i \leq m$. This user then starts decrementing its back-off time counter while carrier sensing transmissions from other users. Let σ denote a mini-slot interval, each of which corresponds one unit of the back-off time counter. Upon hearing a transmission from any other users, the underlying user will “freeze” its back-off time counter and reactivate when the channel is sensed idle again. Otherwise, if the back-off time counter reaches zero, the underlying user wins the contention and transmits its data.

Either two-way or four-way handshake with Request-to-send/Clear-to-send (RTS/CTS) exchange can be employed. In the four-way handshake, the transmitter sends RTS to the receiver and waits until it successfully receives CTS from the receiver before sending a data

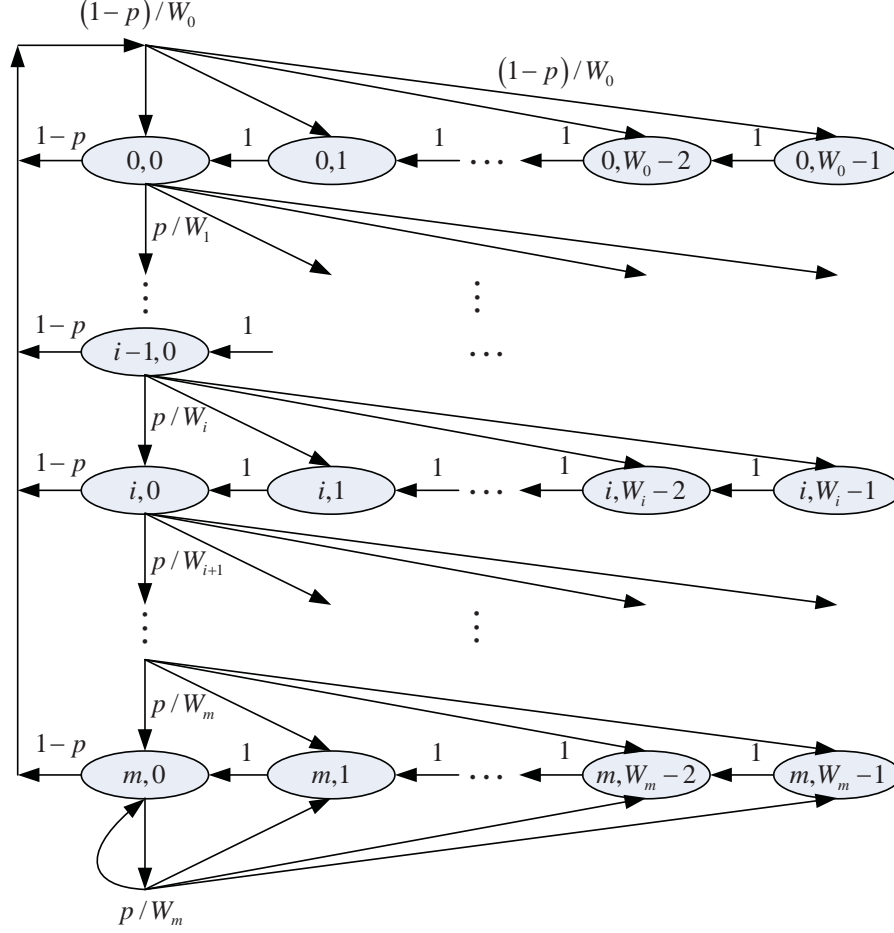


Figure 2.4: Markov chain model for window-based CSMA MAC protocol [85].

packet. Note that the RTS and CTS contain the information of the packet length, hence other users can obtain these information by listening to the channel. With these information, users can update the so-called network allocation vector (NAV) which indicates the period of a busy channel. In both handshake mechanisms, after sending each data packet the transmitter expects an acknowledgment (ACK) from the receiver to indicate a successful reception of the packet. Standard small intervals, namely short inter-frame space (SIFS) and distributed inter-frame space (DIFS), are used before the back-off countdown process and ACK packet transmission as described in [85]. We refer to the CSMA MAC protocol using the two-way handshaking technique as a basic access scheme in the following. Timing diagram for basic and RTS/CTS based CSMA MAC protocols are illustrated in Figs. 2.2 and 2.3, respectively.

(b) *Markov Chain Model for Throughput Analysis of CSMA Protocol*

In the following, we present the throughput analysis of the CSMA/CA protocol for a network with n_0 users [85]. We consider the 2D Markov chain (MC) for CSMA/CA MAC protocol $(s(t), c(t))$ where $s(t)$ represents the backoff stage of the station at time t where $s(t) = [0, m]$. Moreover, we have $c(t) = [0, W_i - 1]$ where $W_i = 2^i W_0$ describes the states of the backoff counter. Fig. 2.4 shows the state transition diagram of this MC.

Let $b_{i,k} = \lim_{t \rightarrow \infty} \Pr(s(t) = i, c(t) = k)$ ($i \in [0, m]$, $k \in [0, W_i - 1]$) denote the stationary probability of the Markov chain. For convenience, we define $W = W_0$ in the following derivations. Using the analysis as in [85], we can arrive at the following the relationship for the steady-state probabilities: $b_{i,0} = p^i b_{0,0}$ (for $i \in [0, m]$), $b_{m-1,0} p = (1-p)b_{m,0}$ or $b_{m,0} = \frac{p}{1-p} b_{0,0}$, and $b_{i,k} = \frac{W_i - k}{W_i} b_{i,0}$ (for $i \in [0, m]$, $k \in [0, W_i - 1]$). Since we have $\sum_{i,k} b_{i,k} = 1$, substitute the above results for all $b_{i,k}$ and perform some manipulations, we can obtain

$$1 = \frac{b_{0,0}}{2} \left\{ W \left[\sum_{i=0}^{m-1} (2p)^i + \frac{(2p)^m}{1-p} \right] + \frac{1}{1-p} \right\}. \quad (2.9)$$

From these results, we can find the relationship among $b_{0,0}$, p , W as follows [85]:

$$b_{0,0} = \frac{2(1-2p)(1-p)}{(1-2p)(W+1) + pW[1-(2p)^m]}. \quad (2.10)$$

The throughput can be calculated by using the technique developed by Bianchi in [85] where we approximately assume a fixed transmission probability ϕ in a generic slot time. Specifically, Bianchi shows that this transmission probability can be calculated from the following two equations [85]

$$\phi = \frac{2(1-2p)}{(1-2p)(W+1) + pW(1-(2p)^m)}, \quad (2.11)$$

$$p = 1 - (1-\phi)^{n_0-1}, \quad (2.12)$$

where m is the maximum back-off stage, p is the conditional collision probability (i.e., the probability that a collision occurs given that there is one user transmitting its data).

The probability that at least one user transmits its data packet can be written as

$$\mathcal{P}_t = 1 - (1-\phi)^{n_0}. \quad (2.13)$$

However, the probability that a transmission on the channel is successful given there is at least one user transmitting can be written as

$$\mathcal{P}_s = \frac{n_0 \phi (1-\phi)^{n_0-1}}{\mathcal{P}_t}. \quad (2.14)$$

The average duration of a generic slot time can be calculated as

$$\bar{T}_{sd} = (1 - \mathcal{P}_t) T_e + \mathcal{P}_t \mathcal{P}_s T_s + \mathcal{P}_t (1 - \mathcal{P}_s) T_c, \quad (2.15)$$

where $T_e = \sigma$, T_s and T_c represent the duration of an empty slot, the average time the channel is sensed busy due to a successful transmission, and the average time the channel is sensed busy due to a collision, respectively. These quantities can be calculated as [85]

For basic mechanism:

$$\begin{cases} T_s = T_s^1 = H + PS + SIFS + 2PD + ACK + DIFS \\ T_c = T_c^1 = H + PS + DIFS + PD \\ H = H_{PHY} + H_{MAC} \end{cases}, \quad (2.16)$$

where H_{PHY} and H_{MAC} are the packet headers for physical and MAC layers, PS is the average packet size, PD is the propagation delay, $SIFS$ is the length of a short inter-frame space, $DIFS$ is the length of a distributed inter-frame space, ACK is the length of an acknowledgment.

For RTS/CTS mechanism:

$$\begin{cases} T_s = T_s^2 = H + PS + 3SIFS + 2PD + RTS + CTS + ACK + DIFS \\ T_c = T_c^2 = H + DIFS + RTS + PD \end{cases}, \quad (2.17)$$

where RTS and CTS represent the length of RTS and CTS control packets, respectively.

Based on these quantities, we can express the normalized throughput as follows:

$$\mathcal{T} = \frac{\mathcal{P}_s \mathcal{P}_t PS}{\bar{T}_{sd}}. \quad (2.18)$$

2. The p -persistent CSMA MAC Protocol

(a) MAC protocol

We briefly describe the p -persistent CSMA MAC protocol and then present the saturation throughput analysis for this protocol. In this protocol, each user attempts to transmit on the chosen channel with a probability of p if it senses an available channel (i.e., no other users transmit data) [70]. In case the user decides not to transmit (with probability of $1 - p$), it will carrier sense the channel and attempt to transmit again in the next slot with probability

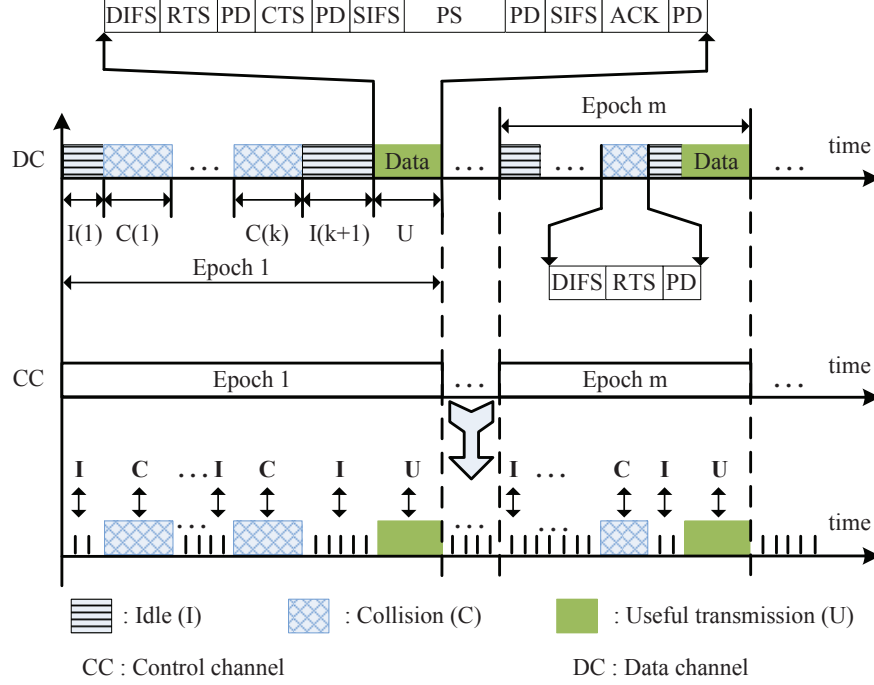


Figure 2.5: Time diagram for p -persistent CSMA MAC protocol [70].

p . If there is a collision, the user will wait until the channel is available and attempt to transmit with probability p as before.

The basic 2-way or 4-way handshake with RTS/CTS [85] can be employed to reserve a channel for data transmission. An ACK from the receiver is transmitted to the transmitter to indicate the successful reception of a packet. The timing diagram of this MAC protocol is presented in Fig. 2.5 which will be further clarified later. In this MAC protocol, transmission time is divided into time slot (we call time slot or slot size interchangeably). The average packet size is assumed to be PS time slots.

(b) *Saturation Throughput Analysis*

In the following, we will derive the saturation throughput \mathcal{T} where each user always has data packets ready to transmit. As shown in Fig. 2.5, each contention and access cycle (called epoch in this figure) between two consecutive successful packet transmissions comprises several idle and busy periods denoted as I and B , respectively. In particular, an epoch starts with an idle period $I(1)$ and then followed by several collisions ($C(i)$) and idle periods ($I(i + 1)$) and finally ends with a successful transmission (U). Note that an idle period is the time interval between two consecutive packet transmissions (a collision or a successful transmission).

Let us define \bar{T}_{cont} as the average time due to contention, collisions, and RTS/CTS exchanges before a successful packet transmission; T_S is the total time due to data packet transmission, ACK control packet, and overhead between these data and ACK packets. Then, the saturation throughput \mathcal{T} can be written as

$$\mathcal{T} = \frac{T_S}{\bar{T}_{\text{cont}} + T_S}. \quad (2.19)$$

To calculate \bar{T}_{cont} , we define some further parameters as follows. Let denote T_C as the duration of a collision; T_S as the duration required for a successful data transmission (including the overhead); \bar{T}_S is the required time for successful RTS/CTS transmission. These quantities can be calculated under the 4-way handshake as

$$\begin{cases} T_S = PS + 2SIFS + 2PD + ACK \\ \bar{T}_S = DIFS + RTS + CTS + 2PD \\ T_C = RTS + DIFS + PD \end{cases}, \quad (2.20)$$

where PS is the packet size, ACK is the length of an ACK packet, $SIFS$ is the length of a short interframe space, $DIFS$ is the length of a distributed interframe space, PD is the propagation delay where PD is usually relatively small compared to the slot time σ .

Let T_I^i be the i -th idle duration between two consecutive RTS/CTS transmissions (they can be collisions or successes). Then, T_I^{i,j_2} can be calculated based on its probability mass function (pmf), which is derived as follows. Recall that all quantities are defined in terms of number of time slots. Now, suppose there are n_0 users contending to capture the channel, let \mathcal{P}_S , \mathcal{P}_C and \mathcal{P}_I denote the probabilities that a generic slot corresponds to a successful transmission, a collision, and an idle slot, respectively. These quantities can be calculated as follows:

$$\mathcal{P}_S = n_0 p (1 - p)^{n_0 - 1} \quad (2.21)$$

$$\mathcal{P}_I = (1 - p)^{n_0} \quad (2.22)$$

$$\mathcal{P}_C = 1 - \mathcal{P}_S - \mathcal{P}_I, \quad (2.23)$$

where p is the transmission probability of any user in a generic slot. Note that \bar{T}_{cont} is a random variable (RV) consisting of several intervals corresponding to idle periods, collisions, and one successful RTS/CTS transmission. Hence, this quantity can be calculated as

$$\bar{T}_{\text{cont}} = \sum_{i=1}^{N_c} (T_C + T_I^i) + T_I^{N_c+1} + \bar{T}_S, \quad (2.24)$$

where N_c is the number of collisions before the first successful RTS/CTS exchange, which is a geometric RV with parameter $1 - \mathcal{P}_C/\bar{\mathcal{P}}_I$ (where $\bar{\mathcal{P}}_I = 1 - \mathcal{P}_I$). Its pmf can be expressed as

$$f_X^{N_c}(x) = \left(\frac{\mathcal{P}_C}{\bar{\mathcal{P}}_I}\right)^x \left(1 - \frac{\mathcal{P}_C}{\bar{\mathcal{P}}_I}\right), \quad x = 0, 1, 2, \dots \quad (2.25)$$

Also, T_I^i represents the number of consecutive idle slots, which is also a geometric RV with parameter $1 - \mathcal{P}_I$ with the following pmf

$$f_X^I(x) = (\mathcal{P}_I)^x (1 - \mathcal{P}_I), \quad x = 0, 1, 2, \dots \quad (2.26)$$

Therefore, \bar{T}_{cont} can be written as follows [70]:

$$\bar{T}_{\text{cont}} = \bar{N}_c T_C + \bar{T}_I (\bar{N}_c + 1) + \bar{T}_S, \quad (2.27)$$

where \bar{T}_I and \bar{N}_c can be calculated as

$$\bar{T}_I = \frac{(1-p)^{n_0}}{1 - (1-p)^{n_0}} \quad (2.28)$$

$$\bar{N}_c = \frac{1 - (1-p)^{n_0}}{n_0 p (1-p)^{n_0-1}} - 1. \quad (2.29)$$

These expressions are obtained by using the pmfs of the corresponding RVs given in (2.25) and (2.26), respectively [70].

3. Other MAC Protocols

(a) ALOHA protocol

The ALOHA protocol was initially developed for satellite communication [86], which has been then employed for other wireless networks such as wireless sensor networks [87, 88]. The original design objective of the ALOHA protocol is to provide a random access mechanism to multiplex a large number of users that communicate with a satellite using a single communication channel [86]. Whenever the satellite correctly receives a frame, it will broadcast an ACK including the addresses of the source user to all users. Hence, the source user can recognize a possible collision and re-transmit the frame in the case that it does not receive the ACK of the transmitted frame.

There is also another method without ACK where the satellite will rebroadcast the received data frame from a source user. Therefore, the source user can listen to the channel and decode the received broadcast frame from the satellite to know the outcome of its transmitted

data frame. In this method, the satellite ignores all corrupted frames due to collisions or interference, and hence the source users must re-send their frames. Different from the CSMA/CA MAC protocol, a user with data backlogs in the ALOHA protocol will transmit its data with a certain probability without carrier sensing the channel. There are two basic types of ALOHA protocols, namely pure ALOHA and slotted ALOHA. In the pure ALOHA, a user can start transmission at any time whereas in the slotted ALOHA, all users have to be synchronized and perform data transmissions in fixed-size time slots.

(b) *Other persistent CSMA protocols*

There are different kinds of persistent CSMA protocols, namely 1-persistent CSMA, non-persistent CSMA beside the p -persistent CSMA [70, 89, 90]. The 1-persistent CSMA protocol operates as follows. Whenever a user senses the idle channel, it will transmit the data packet immediately (i.e., it transmits packet data with a probability of 1). If the channel is sensed to be busy, a user keeps listening the channel and transmits immediately when the channel becomes idle. In the case of collisions, each user will wait and start over again.

We now discuss the main difference between non-persistent and 1-persistent CSMA protocols. In the non-persistent CSMA protocol, if a user senses the busy channel, it waits for a period of time, and senses the channels again. Hence, the non-persistent CSMA protocol can reduce the collision probability and the efficiency as well while the 1-persistent CSMA protocol increases the efficiency and also the collision probability. The p -persistent CSMA protocol can result in more efficient trade-off between transmission efficiency and the collision probability, which can, therefore, achieve better performance than the other two counterparts.

2.1.2.2 Multi-channel MAC Protocols

When there are multiple channels for data transmissions, the overall network throughput and communication delay can be improved because of the increasing spectrum resources. The critical design issues here are how to efficiently arrange simultaneous transmissions on multiple channels by using distributed contention resolution. In this section, we present some important multi-channel MAC protocols which are categorized accordingly four different approaches employed to perform data channel arrangement for the users [31]. The first three approaches are the dedicated control channel, common hopping, and split phase approaches which result in the so-called single rendezvous protocols, while the last approach leads to the multiple rendezvous MAC protocol.

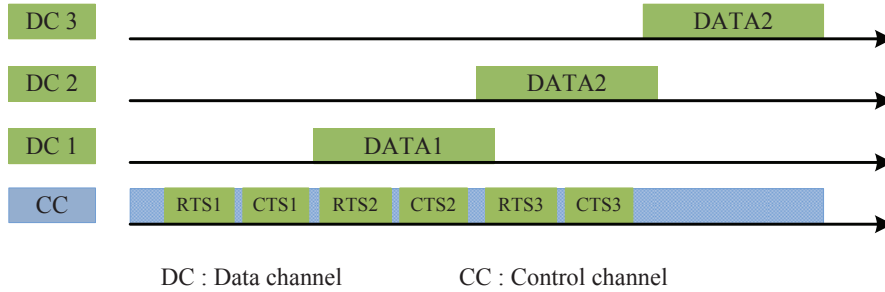


Figure 2.6: Dedicated control channel mechanism for multi-channel MAC protocols [31].

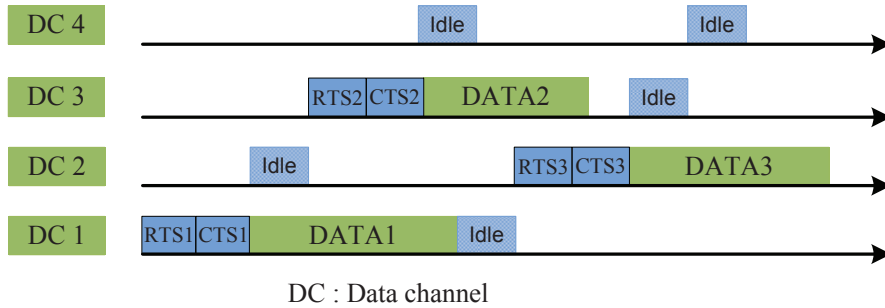


Figure 2.7: Common hopping mechanism for multi-channel MAC protocols [31].

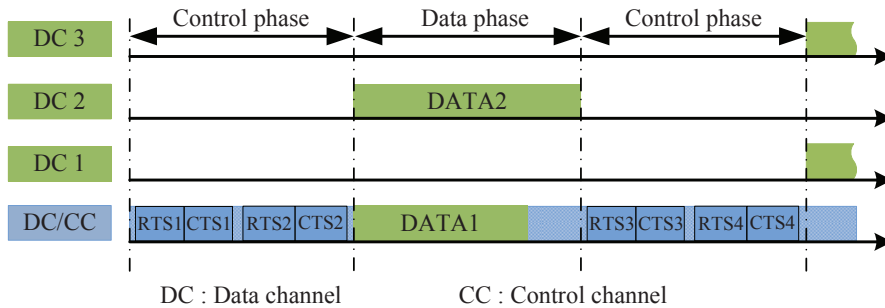


Figure 2.8: Split phase mechanism for multi-channel MAC protocols [31].

1. *Dedicated Control Channel Approach*

In this approach, each user is equipped with two transceivers where the first transceiver is used for channel agreement operating on the control channel while the second transceiver is used for data transmission on a data channel. MAC protocol design in this case is quite simple since every user can always have the knowledge of other users' channel agreements and network state by listening to the control channel. Moreover, we can efficiently reduce loads for busy channels with large number of sharing users during the channel selection process.

Operations of a multi-channel MAC protocol using the dedicated control channel approach

and RTS/CTS handshake is illustrated in Fig. 2.6. Here, RTS and CTS exchanges are performed on the control channel and the RTS and CTS packets can include information of channel agreements obtained by using certain channel selection criteria. Moreover, the RTS and CTS packets can also carry a NAV to inform the duration of busy time on the selected channel. After the successful RTS/CTS exchange, the user transmits data on the selected channel.

2. *Common Hopping Approach*

Users are required to have only one transceiver in the common hopping approach; hence, they perform a channel agreement on one common channel [31, 91]. To achieve this goal, all users follow the same hopping pattern and they can negotiate to choose one data channel through exchanging the RTS/CTS control messages. After the channel selection, the involved pair of users stops the hopping and jumps to the chosen channel for data transmission. After the transmission is completed, the users return to the hopping pattern with other users. Detailed operations of this approach is illustrated in Fig. 2.7.

3. *Split Phase Mechanism*

In this approach, the user is equipped with only one transceiver, which alternatively performs channel selection and data transmission in the control and data phases. A control channel is needed for channel agreement in the control phase; however, the control channel can be used for data transmission in the data phase. Active users again exchange RTS/CTS control packets on the control channel containing the chosen data channel (e.g., the idle channel with the lowest channel index). In the second data phase, all users start their data transmissions on the chosen channels. Note that one channel may be chosen by multiple users. If it is the case, further scheduling or contention would be performed in the data phase. Detailed operation of the split phase mechanism is illustrated in Fig. 2.8.

4. *Parallel Rendezvous Approach*

Different from the previous approaches, the parallel rendezvous approach allows multiple pairs of users to make simultaneously channel agreements on different channels. Therefore, we can resolve the congestion problem due to the single control channel. However, a sophisticated coordination is required to make successful channel agreements in this design. Toward this end, each transmitter can be assigned a hopping sequence and it then finds the intended receiver based on its hopping sequence. When both transmitter and receiver hops to the same channel, they can negotiate to choose the data channel for data communications.

Further information for this approach can be found in the descriptions of the SSCH protocol [92] and McMAC protocol [93].

2.1.3 Cognitive MAC Protocol for CRNs

Different from the conventional wireless networks, a CMAC protocol must perform both exploration and exploitation of the spectrum holes in a dynamic manner because the spectrum holes are opportunistic resources [47, 59, 94]. In addition, various practical constraints must be carefully considered in the CMAC design including the availability of a control channel for channel agreements and the number of available transceivers to perform contention, sensing, and transmission. In general, a good CMAC protocol should well balance between spectrum sensing and access times to achieve high spectrum utilization and network performance.

Specifically, spectrum sensing should be designed so that minimum sensing time is required while maintaining the target sensing performance (in terms of detection and/or false-alarm probabilities). Furthermore, spectrum sensing operations should be scheduled repeated to timely detect PUs' active status and avoid creating intolerable interference to PUs' transmissions.

Basic functions of the CMAC protocol include spectrum sensing, spectrum sharing, and control channel management [59], which are tightly coupled as illustrated in Fig. 2.9. While spectrum sensing is a physical layer functionality providing information about spectrum holes for the MAC layer, spectrum access aims at improving the spectrum utilization efficiency whilst assuring transparency and protection for PUs. Moreover, the spectrum sharing function aims at coordinating the medium access, allocation, and sharing of spectrum holes for SUs, which can be implemented in either centralized or distributed manner (see [47, 59, 94]). Finally, the control channel management provides mechanisms for coordination and collaboration between the SUs and the spectrum sensing and sharing processes. In addition, the control channel management is responsible for many tasks in CRNs, e.g., allocation, establishment, and monitoring of available channels via broadcasting relevant control information [59].

2.2 Literature Review

Hierarchical spectrum sharing between the primary and secondary networks is one of the most important research topics in cognitive radio literature. For this spectrum sharing paradigm, PUs have strictly higher priority than SUs in accessing the underlying spectrum.

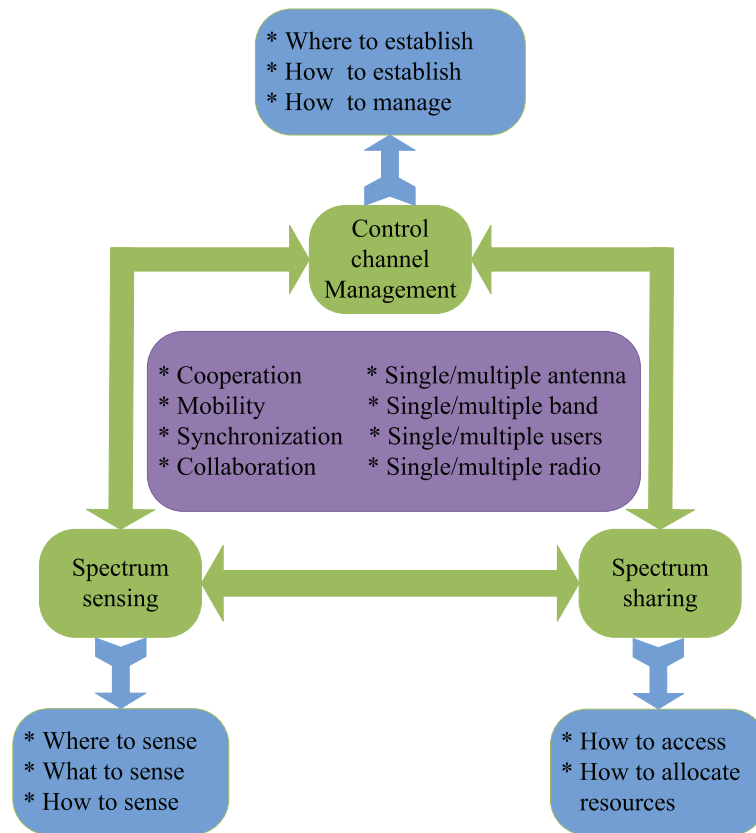


Figure 2.9: The generic functionalities of the CMAC protocol [59].

Here, primary and secondary networks can transmit simultaneously on the same spectrum with appropriate interference control to protect the primary network [12], [11]. In particular, it is typically required that a certain interference constraint due to SUs' transmissions must be maintained at each primary receiver.

Instead of imposing interference constraints, spectrum sensing can be employed by SUs to seek and exploit spectrum holes over space and time [5]. There are several challenging issues related to this spectrum exploration and exploitation problem. On one hand, SUs should spend sufficient time for spectrum sensing so that they can correctly identify spectrum holes, which avoid creating undesirable interference for PUs. On the other hand, SUs wish to spend more time for data transmission for better utilization of spectrum holes. In what follows, we will provide the comprehensive survey of the state-of-the-art spectrum sensing and CMAC protocol designs.

2.2.1 Spectrum Sensing

There is a rich literature on spectrum sensing for cognitive radio networks (e.g., see [48] and references therein). Spectrum sensing literature is very diverse ranging from the popular energy detection scheme to advanced cooperative sensing strategies [95] where multiple SUs collaborate to achieve more reliable sensing performance [64, 69, 84, 96–98]. In a typical cooperative sensing strategy, each SU performs sensing independently and then sends its sensing results to a control center, which then makes sensing decisions on the idle/busy status of each channel using certain aggregation rule.

Cooperative spectrum sensing has been proposed to improve the sensing performance via collaborations among SUs [64–66, 69, 84, 96–99]. To combine individual sensing results from different SUs, a central controller (e.g., an AP) can employ various aggregation rules to decide whether or not a particular frequency band is available for secondary access. In [66], the authors studied the performance of hard decisions and soft decisions at a central controller (fusion center). They also investigated the impact of reporting errors on the cooperative sensing performance. Recently, the authors of [67] proposed a novel cooperative spectrum sensing scheme using hard decision combining considering feedback errors. In [96], weighted data based fusion is proposed to improve sensing performance.

In [84, 97–99], optimization of cooperative sensing under the a-out-of-b aggregation rule was studied. In [84], the game-theoretic based method was proposed for cooperative spectrum sensing. In [69], the authors investigated the multi-channel scenario where the central controller collects statistics from SUs to decide whether it should stop at the current time slot. In [100, 101], two different optimization problems for cooperative sensing were studied. The first one focuses on throughput maximization where throughput depends on the false alarm probability and the second one attempts to perform interference management where the objective function is related to the detection probability.

2.2.2 Cognitive MAC Protocol Design

There is the rich literature on CMAC protocol design and analysis for CRNs [16–34, 47, 62, 63, 68, 85, 102–107] (see [47, 59, 60, 94] for a survey of recent works). In the following, we provide survey of existing works in this topic according to four main scenarios considered in our dissertation, i.e., CMAC with parallel sensing, CMAC with sequential sensing, CMAC with cooperative sensing, and FD CMAC protocols.

2.2.2.1 CMAC with Parallel Sensing

In [16], sensing-time optimization and optimal channel sequencing algorithms were proposed to efficiently discover spectrum holes and to minimize the exploration delay. Another work along this line was conducted in [17], where a control-channel-based MAC protocol was proposed for SUs to exploit white spaces in the cognitive ad hoc network. In particular, the authors of this paper developed both random- and negotiation-based spectrum-sensing schemes and performed throughput analysis for both saturation and non-saturation scenarios. There are several other proposed synchronous CMAC protocols that rely on a control channel for spectrum negotiation and access [18, 19, 21, 63]. Since in these existing works, the spectrum sensing and access aspects are addressed separately; development of a concrete CMAC framework considering both aspects and optimized configuration for the sensing and access parameters would be important research issues to tackle.

2.2.2.2 CMAC with Sequential Sensing

The above CMAC protocols use parallel sensing with the requirement that each SU is equipped by multiple transceivers. However, having multiple transceivers at the SUs will increase the complexity and deployment cost; therefore, the MAC protocol with a single transceiver would be preferred in many CRN deployments [16–21, 63, 105]. There have been many existing works that propose different CMAC protocols with sequential sensing where each SU must perform sequential sensing over multiple channels and can access at most one idle channel for communications. Here, the channel assignment is an important design task since it would reduce the sensing time while efficiently exploring spectrum holes if each SU is assigned a “best” subset of channels for sensing. Reduction of sensing time through effective channel assignment for sensing can then result in improving cognitive network throughput.

2.2.2.3 CMAC with Cooperative Sensing

In [68], a multi-channel MAC protocol was proposed considering location-dependent detection performance of SUs on different channels so that white spaces can be efficiently exploited while satisfactorily protecting PUs. In [26, 34], the authors conducted design and analysis for a CMAC protocol using cooperative spectrum sensing where parallel spectrum sensing on different channels was assumed at each SU.

Most existing works focused on designing and optimizing parameters for the cooperative spectrum sensing algorithm; however, they did not consider spectrum access issues. Fur-

thermore, either the single channel setting or multi-channel scenario with parallel sensing was assumed. Moreover, existing cooperative spectrum sensing schemes rely on a central controller to aggregate sensing results for white space detection (i.e., centralized design). Finally, homogeneous environments (i.e., SUs experience the same channel condition and spectrum statistics for different channels) have been commonly assumed in the literature, which would not be very realistic.

2.2.2.4 Full-Duplex CMAC Protocol for CRNs

Despite recent advances on self-interference cancellation (SIC) techniques for FD radios [49–51] (e.g., propagation SIC, analog-circuit SIC, and digital baseband SIC), self-interference still exists due to various reasons such as the limitation of hardware and channel estimation errors. The FD technology has been employed for more efficient spectrum access design in CRNs [35, 55, 56, 108–110] where SUs can perform sensing and transmission simultaneously.

In [55], the authors considered the cognitive FD-MAC design assuming that SUs perform sensing in multiple small time slots to detect the PU’s activity during their transmissions, which may not be very efficient. Furthermore, they proposed three operation modes for the SU network, i.e., transmission-only, transmission-sensing, and transmission-reception modes. Then, they study the optimal parameter configurations for these modes by solving three corresponding optimization problems. In practice, it would be desirable to design a single adaptable MAC protocol, which can be configured to operate in an optimal fashion depending on specific channel and network conditions.

In [56], a FD-MAC protocol which allows simultaneous spectrum access of the SU and PU networks was developed. In addition, both PUs and SUs are assumed to employ the same p -persistent MAC protocol for channel contention resolution. This design is, however, not applicable to the hierarchical spectrum access in the CRNs where PUs should have higher spectrum access priority compared to SUs. Moreover, engineering of a cognitive FD relaying network was considered in [108–110] where various resource allocation algorithms to improve the outage probability are proposed. In addition, the authors in [111] developed the joint routing and distributed resource allocation for FD wireless networks. In [112], Choi et al. studied the distributed power allocation for a hybrid FD/HD system where all network nodes operate in the HD mode but the AP communicates using the FD mode.

Chapter 3

Distributed MAC Protocol for Cognitive Radio Networks: Design, Analysis, and Optimization

The content of this chapter was published in IEEE Transactions on Vehicular Technology in the following paper:

L. T. Tan, and L. B. Le, “Distributed MAC Protocol for Cognitive Radio Networks: Design, Analysis, and Optimization,” *IEEE Trans. Veh. Tech.*, vol. 60, no. 8, pp. 3990–4003, 2011.

3.1 Abstract

In this paper, we investigate the joint optimal sensing and distributed MAC protocol design problem for cognitive radio networks. We consider both scenarios with single and multiple channels. For each scenario, we design a synchronized MAC protocol for dynamic spectrum sharing among multiple secondary users (SUs), which incorporates spectrum sensing for protecting active primary users. We perform saturation throughput analysis for the corresponding proposed MAC protocols that explicitly capture spectrum sensing performance. Then, we find their optimal configuration by formulating throughput maximization problems subject to detection probability constraints for primary users. In particular, the optimal solution of the optimization problem returns the required sensing time for primary users’ protection and optimal contention window for maximizing total throughput of the secondary network.

Finally, numerical results are presented to illustrate developed theoretical findings in the paper and significant performance gains of the optimal sensing and protocol configuration.

3.2 Introduction

Emerging broadband wireless applications have been demanding unprecedented increase in radio spectrum resources. As a result, we have been facing a serious spectrum shortage problem. However, several recent measurements reveal very low spectrum utilization in most useful frequency bands [2]. To resolve this spectrum shortage problem, the Federal Communications Commission (FCC) has opened licensed bands for unlicensed users' access. This important change in spectrum regulation has resulted in growing research interests on dynamic spectrum sharing and cognitive radio in both industry and academia. In particular, IEEE has established an IEEE 802.22 workgroup to build the standard for WRAN based on CR techniques [113].

Hierarchical spectrum sharing between primary networks and secondary networks is one of the most widely studied dynamic spectrum sharing paradigms. For this spectrum sharing paradigm, primary users (PUs) typically have strictly higher priority than SUs (SUs) in accessing the underlying spectrum. One potential approach for dynamic spectrum sharing is to allow both primary and secondary networks to transmit simultaneously on the same frequency with appropriate interference control to protect the primary network [11, 12]. In particular, it is typically required that a certain interference temperature limit due to SUs' transmissions must be maintained at each primary receiver. Therefore, power allocation for SUs should be carefully performed to meet stringent interference requirements in this spectrum sharing model.

Instead of imposing interference constraints for PUs, spectrum sensing can be adopted by SUs to search for and exploit spectrum holes (i.e., available frequency bands) [5, 97]. Several challenging technical issues are related to this spectrum discovery and exploitation problem. On one hand, SUs should spend sufficient time for spectrum sensing so that they do not interfere with active PUs. On the other hand, SUs should efficiently exploit spectrum holes to transmit their data by using an appropriate spectrum sharing mechanism. Even though these aspects are tightly coupled with each other, they have not been treated thoroughly in the existing literature.

In this paper, we make a further bold step in designing, analyzing, and optimizing Medium Access Control (MAC) protocols for cognitive radio networks, considering sensing

performance captured in detection and false alarm probabilities. In particular, the contributions of this paper can be summarized as follows.

1. We design distributed synchronized MAC protocols for cognitive radio networks incorporating spectrum sensing operation for both single and multiple channel scenarios.
2. We analyze saturation throughput of the proposed MAC protocols.
3. We perform throughput maximization of the proposed MAC protocols against their key parameters, namely sensing time and minimum contention window.
4. We present numerical results to illustrate performance of the proposed MAC protocols and the throughput gains due to optimal protocol configuration.

The remaining of this paper is organized as follows. In Section 3.3, we discuss some important related works in the literature. Section 3.4 describes system and sensing models. MAC protocol design, throughput analysis, and optimization for the single channel case are performed in Section 3.5. The multiple channel case is considered in Section 3.6. Section 3.7 presents numerical results followed by concluding remarks in Section 3.8.

3.3 Related Works

Various research problems and solution approaches have been considered for a dynamic spectrum sharing problem in the literature. In [12], [11], a dynamic power allocation problem for cognitive radio networks was investigated considering fairness among SUs and interference constraints for primary users. When only mean channel gains averaged over short term fading can be estimated, the authors proposed more relaxed protection constraints in terms of interference violation probabilities for the underlying fair power allocation problem. In [114], information theory limits of cognitive radio channels were derived. Game theoretic approach for dynamic spectrum sharing was considered in [115], [116].

There is a rich literature on spectrum sensing for cognitive radio networks (e.g., see [48] and references therein). Classical sensing schemes based on, for example, energy detection techniques or advanced cooperative sensing strategies [95] where multiple SUs collaborate with one another to improve the sensing performance have been investigated in the literature. There are a large number of papers considering MAC protocol design and analysis for cognitive radio networks [16–21, 47, 62] (see [47] for a survey of recent works in this topic). However, these existing works either assumed perfect spectrum sensing or did not

explicitly model the sensing imperfection in their design and analysis. In [5], optimization of sensing and throughput tradeoff under a detection probability constraint was investigated. It was shown that the detection constraint is met with equality at optimality. However, this optimization tradeoff was only investigated for a simple scenario with one pair of SUs. The extension of this sensing and throughput tradeoff to wireless fading channels was considered in [15].

There are also some recent works that propose to exploit cooperative relays to improve sensing and throughput performance of cognitive radio networks. In particular, a novel selective fusion spectrum sensing and best relay data transmission scheme was proposed in [14]. A closed-form expression for the spectrum hole utilization efficiency of the proposed scheme was derived and significant performance improvement compared with other sensing and transmission schemes was demonstrated through extensive numerical studies. In [117], a selective relay based cooperative spectrum sensing scheme was proposed that does not require a separate channel for reporting sensing results. In addition, the proposed scheme can achieve excellent sensing performance with controllable interference to primary users. These existing works, however, only consider a simple setting with one pair of SUs.

3.4 System and Spectrum Sensing Models

In this section, we describe the system and spectrum sensing models. Specifically, sensing performance in terms of detection and false alarm probabilities are explicitly described.

3.4.1 System Model

We consider a network setting where N pairs of SUs opportunistically exploit available frequency bands, which belong to a primary network, for their data transmission. Note that the optimization model in [5] is a special case of our model with only one pair of SUs. In particular, we will consider both scenarios in which one or multiple radio channels are exploited by these SUs. We will design synchronized MAC protocols for both scenarios assuming that each channel can be in idle or busy state for a predetermined periodic interval, which is referred to as a cycle in this paper.

We further assume that each pair of SUs can overhear transmissions from other pairs of SUs (i.e., collocated networks). In addition, it is assumed that transmission from each individual pair of SUs affects one different primary receiver. It is straightforward to relax this assumption to the scenario where each pair of SUs affects more than one primary receiver

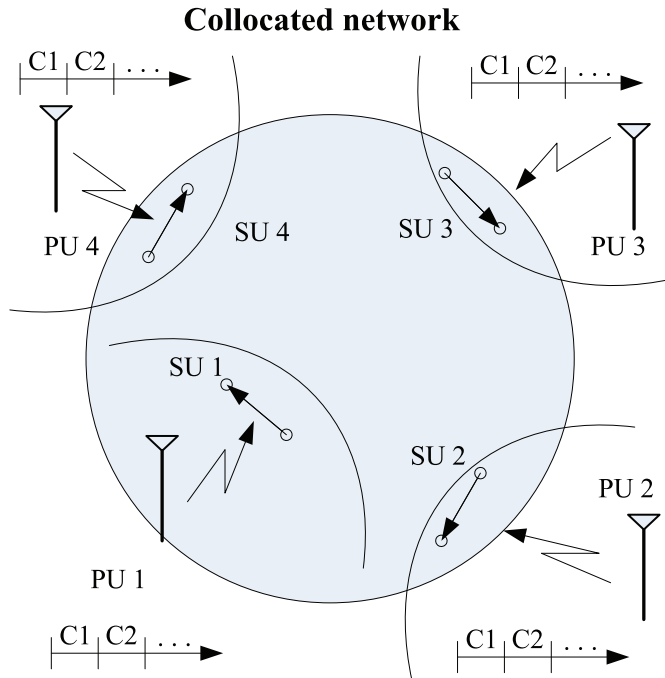


Figure 3.1: Considered network and spectrum sharing model (PU: primary user, SU: secondary user).

and/or each primary receiver is affected by more than one pair of SUs. The network setting under investigation is shown in Fig. 3.1. In the following, we will refer to pair i of SUs as secondary link i or flow i interchangeably.

Remark 1: In practice, SUs can change their idle/busy status any time (i.e., status changes can occur in the middle of any cycle). Our assumption on synchronous channel status changes is only needed to estimate the system throughput. In general, imposing this assumption would not sacrifice the accuracy of our network throughput calculation if primary users maintain their idle/busy status for sufficiently long time on average. This is actually the case for many practical scenarios such as in TV bands as reported by several recent studies (see [113] and references therein). In addition, our MAC protocols developed under this assumption would result in very few collisions with primary users because the cycle time is quite small compared to typical active/idle periods of PUs.

3.4.2 Spectrum Sensing

We assume that secondary links rely on a distributed synchronized MAC protocol to share available frequency channels. Specifically, time is divided into fixed-size cycles and it is

3.4 System and Spectrum Sensing Models

assumed that secondary links can perfectly synchronize with each other (i.e., there is no synchronization error) [62], [103]. It is assumed that each secondary link performs spectrum sensing at the beginning of each cycle and only proceeds to contention with other links to transmit on available channels if its sensing outcomes indicate at least one available channel (i.e., channels not being used by nearby PUs). For the multiple channel case, we assume that there are M channels and each secondary transmitter is equipped with M sensors to sense all channels simultaneously. Detailed MAC protocol design will be elaborated in the following sections.

Let \mathcal{H}_0 and \mathcal{H}_1 denote the events that a particular PU is idle and active, respectively (i.e., the underlying channel is available and busy, respectively) in any cycle. In addition, let $\mathcal{P}^{ij}(\mathcal{H}_0)$ and $\mathcal{P}^{ij}(\mathcal{H}_1) = 1 - \mathcal{P}^{ij}(\mathcal{H}_0)$ be the probabilities that channel j is available and not available at secondary link i , respectively. We assume that SUs employ an energy detection scheme and let f_s be the sampling frequency used in the sensing period whose length is τ for all secondary links. There are two important performance measures, which are used to quantify the sensing performance, namely detection and false alarm probabilities. In particular, detection event occurs when a secondary link successfully senses a busy channel and false alarm represents the situation when a spectrum sensor returns a busy state for an idle channel (i.e., a transmission opportunity is overlooked).

Assume that transmission signals from PUs are complex-valued PSK signals while the noise at the secondary links is independent and identically distributed circularly symmetric complex Gaussian $\mathcal{CN}(0, N_0)$ [5]. Then, the detection and false alarm probability for the channel j at secondary link i can be calculated as [5]

$$\mathcal{P}_d^{ij}(\varepsilon^{ij}, \tau) = \mathcal{Q} \left(\left(\frac{\varepsilon^{ij}}{N_0} - \gamma^{ij} - 1 \right) \sqrt{\frac{\tau f_s}{2\gamma^{ij} + 1}} \right), \quad (3.1)$$

$$\mathcal{P}_f^{ij}(\varepsilon^{ij}, \tau) = \mathcal{Q} \left(\left(\frac{\varepsilon^{ij}}{N_0} - 1 \right) \sqrt{\tau f_s} \right) = \mathcal{Q} \left(\sqrt{2\gamma^{ij} + 1} \mathcal{Q}^{-1}(\mathcal{P}_d^{ij}(\varepsilon^{ij}, \tau)) + \sqrt{\tau f_s} \gamma^{ij} \right), \quad (3.2)$$

where $i \in [1, N]$ is the index of a SU link, $j \in [1, M]$ is the index of a channel, ε^{ij} is the detection threshold for an energy detector, γ^{ij} is the signal-to-noise ratio (SNR) of the PU's signal at the secondary link, f_s is the sampling frequency, N_0 is the noise power, τ is the sensing interval, and $\mathcal{Q}(\cdot)$ is defined as $\mathcal{Q}(x) = (1/\sqrt{2\pi}) \int_x^\infty \exp(-t^2/2) dt$. In the analysis performed in the following sections, we assume a homogeneous scenario where sensing performance on different channels is the same for each SU. In this case, we denote these probabilities for SU i as \mathcal{P}_f^i and \mathcal{P}_d^i for brevity.

Remark 2: For simplicity, we do not consider the impact of wireless channel fading in modeling the sensing performance in (3.1), (3.2). This enables us to gain insight into the investigated spectrum sensing and access problem while keeping the problem sufficiently tractable. Extension of the model to capture wireless fading will be considered in our future works. Relevant results published in some recent works such as those in [15] would be useful for these further studies.

Remark 3: The analysis performed in the following sections can be easily extended to the case where each secondary transmitter is equipped with only one spectrum sensor or each secondary transmitter only senses a subset of all channels in each cycle. Specifically, we will need to adjust the sensing time for some spectrum sensing performance requirements. In particular, if only one spectrum sensor is available at each secondary transmitter, then the required sensing time should be M times larger than the case in which each transmitter has M spectrum sensors.

3.5 MAC Design, Analysis and Optimization: Single Channel Case

We consider the MAC protocol design, its throughput analysis and optimization for the single channel case in this section.

3.5.1 MAC Protocol Design

We now describe our proposed synchronized MAC for dynamic spectrum sharing among secondary flows. We assume that each fixed-size cycle of length T is divided into 3 phases, namely sensing phase, synchronization phase, and data transmission phase. During the sensing phase of length τ , all SUs perform spectrum sensing on the underlying channel. Then, only secondary links whose sensing outcomes indicate an available channel proceed to the next phase (they will be called active SUs/links in the following). In the synchronization phase, active SUs broadcast beacon signals for synchronization purposes. Finally, active SUs perform contention and transmit data in the data transmission phase. The timing diagram of one particular cycle is illustrated in Fig. 3.2. For this single channel scenario, synchronization, contention, and data transmission occur on the same channel.

We assume that the length of each cycle is sufficiently large so that SUs can transmit several packets during the data transmission phase. Indeed, the current 802.22 standard

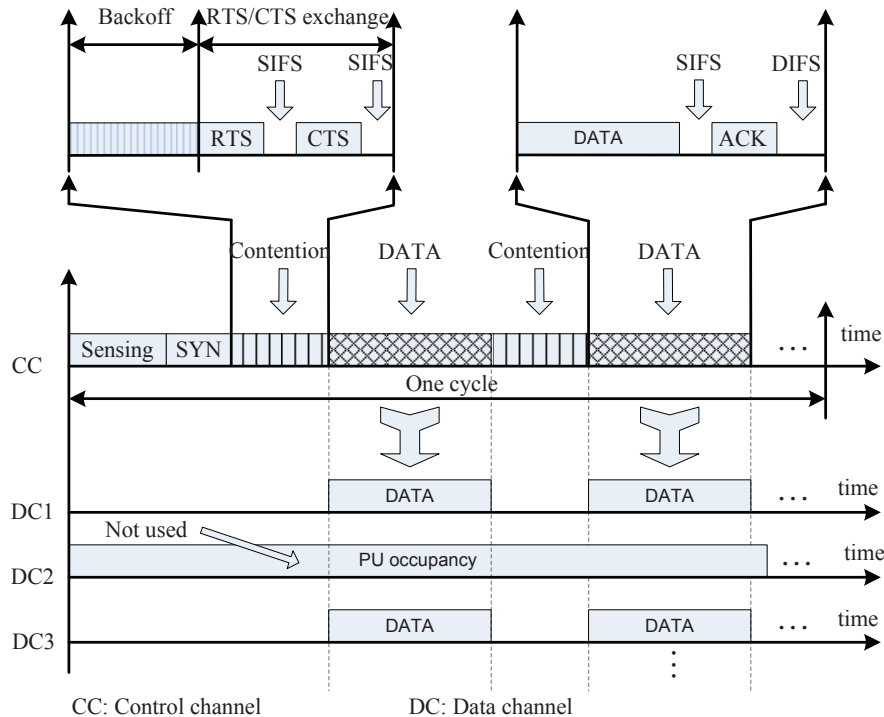


Figure 3.2: Timing diagram of the proposed multi-channel MAC protocol.

specifies the spectrum evacuation time upon the return of PUs is 2 seconds, which is a relatively large interval. Therefore, our assumption would be valid for most practical cognitive systems. During the data transmission phase, we assume that active SUs employ a standard contention technique to capture the channel similar to that in the CSMA/CA protocol. Exponential back-off with minimum contention window W and maximum back-off stage m [85] is employed in the contention phase. For brevity, we refer to W simply as contention window in the following. Specifically, suppose that the current back-off stage of a particular SU is i then it starts the contention by choosing a random back-off time uniformly distributed in the range $[0, 2^i W - 1]$, $0 \leq i \leq m$. This user then starts decrementing its back-off time counter while carrier sensing transmissions from other secondary links.

Let σ denote a mini-slot interval, each of which corresponds one unit of the back-off time counter. Upon hearing a transmission from any secondary link, each secondary link will “freeze” its back-off time counter and reactivate when the channel is sensed idle again. Otherwise, if the back-off time counter reaches zero, the underlying secondary link wins the contention. Here, either two-way or four-way handshake with RTS/CTS will be employed to transmit one data packet on the available channel. In the four-way handshake, the trans-

mitter sends RTS to the receiver and waits until it successfully receives CTS before sending a data packet. In both handshake schemes, after sending the data packet the transmitter expects an acknowledgment (ACK) from the receiver to indicate a successful reception of the packet. Standard small intervals, namely DIFS and SIFS, are used before back-off time decrements and ACK packet transmission as described in [85]. We refer to this two-way handshaking technique as a basic access scheme in the following analysis.

3.5.2 Throughput Maximization

Given the sensing model and proposed MAC protocol, we are interested in finding its optimal configuration to achieve the maximum throughput subject to protection constraints for primary receivers. Specifically, let $\mathcal{NJ}(\tau, W)$ be the normalized total throughput, which is a function of sensing time τ and contention window W . Suppose that each primary receiver requires that detection probability achieved by its conflicting primary link i be at least \bar{P}_d^i . Then, the throughput maximization problem can be stated as follows:

Problem 1:

$$\begin{aligned} \max_{\tau, W} \quad & \mathcal{NJ}(\tau, W) \\ \text{s.t.} \quad & \mathcal{P}_d^i(\varepsilon^i, \tau) \geq \bar{\mathcal{P}}_d^i, \quad i = 1, 2, \dots, N \\ & 0 < \tau \leq T, \quad 0 < W \leq W_{\max}, \end{aligned} \tag{3.3}$$

where W_{\max} is the maximum contention window and recall that T is the cycle interval. In fact, optimal sensing τ would allocate sufficient time to protect primary receivers and optimal contention window would balance between reducing collisions among active secondary links and limiting protocol overhead.

3.5.3 Throughput Analysis and Optimization

We perform saturation throughput analysis and solve the optimization problem (3.3) in this subsection. Throughput analysis for the cognitive radio setting under investigation is more involved compared to standard MAC protocol throughput analysis (e.g., see [103], [85]) because the number of active secondary links participating in the contention in each cycle varies depending on the sensing outcomes. Suppose that all secondary links have same packet length. Let $\Pr(n = n_0)$ and $\mathcal{J}(\tau, \phi | n = n_0)$ be the probability that n_0 secondary links participating in the contention and the conditional normalized throughput when n_0

3.5 MAC Design, Analysis and Optimization: Single Channel Case

secondary links join the channel contention, respectively. Then, the normalized throughput can be calculated as

$$\mathcal{NT} = \sum_{n_0=1}^N \mathcal{T}(\tau, W | n = n_0) \Pr(n = n_0), \quad (3.4)$$

where recall that N is the number of secondary links, τ is the sensing time, W is the contention window. In the following, we show how to calculate $\Pr(n = n_0)$ and $\mathcal{T}(\tau, \phi | n = n_0)$.

3.5.3.1 Calculation of $\Pr(n = n_0)$

Note that only secondary links whose sensing outcomes in the sensing phase indicate an available channel proceed to contention in the data transmission phase. This case can happen for a particular secondary link i in the following two scenarios:

- The PU is not active, and no false alarm is generated by the underlying secondary link.
- The PU is active, and secondary link i mis-detects its presence.

Therefore, secondary link i joins contention in the data transmission phase with probability

$$\mathcal{P}_{\text{idle}}^i = [1 - \mathcal{P}_f^i(\varepsilon^i, \tau)] \mathcal{P}^i(\mathcal{H}_0) + \mathcal{P}_m^i(\varepsilon^i, \tau) \mathcal{P}^i(\mathcal{H}_1), \quad (3.5)$$

where $\mathcal{P}_m^i(\varepsilon^i, \tau) = 1 - \mathcal{P}_d^i(\varepsilon^i, \tau)$ is the mis-detection probability. Otherwise, it will be silent for the whole cycle and waits until the next cycle. This occurs with probability

$$\mathcal{P}_{\text{busy}}^i = 1 - \mathcal{P}_{\text{idle}}^i = \mathcal{P}_f^i(\varepsilon^i, \tau) \mathcal{P}^i(\mathcal{H}_0) + \mathcal{P}_d^i(\varepsilon^i, \tau) \mathcal{P}^i(\mathcal{H}_1). \quad (3.6)$$

We assume that interference of active PUs to the SU is negligible; therefore, a transmission from any secondary link only fails when it collides with transmissions from other secondary links. Now, let \mathcal{S}_k denote one particular subset of all secondary links having exactly n_0 secondary links. There are $C_N^{n_0} = \frac{N!}{n_0!(N-n_0)!}$ such sets \mathcal{S}_k . The probability of the event that n_0 secondary links join contention in the data transmission phase can be calculated as

$$\Pr(n = n_0) = \sum_{k=1}^{C_N^{n_0}} \prod_{i \in \mathcal{S}_k} \mathcal{P}_{\text{idle}}^i \prod_{j \in \mathcal{S} \setminus \mathcal{S}_k} \mathcal{P}_{\text{busy}}^j, \quad (3.7)$$

where \mathcal{S} denotes the set of all N secondary links, and $\mathcal{S} \setminus \mathcal{S}_k$ is the complement of \mathcal{S}_k with $N - n_0$ secondary links. If all secondary links have the same SNR_p and the same probabilities

3.5 MAC Design, Analysis and Optimization: Single Channel Case

$\mathcal{P}^i(\mathcal{H}_0)$ and $\mathcal{P}^i(\mathcal{H}_1)$, then we have $\mathcal{P}_{\text{idle}}^i = \mathcal{P}_{\text{idle}}$ and $\mathcal{P}_{\text{busy}}^i = \mathcal{P}_{\text{busy}} = 1 - \mathcal{P}_{\text{idle}}$ for all i . In this case, (3.7) becomes

$$\Pr(n = n_0) = C_N^{n_0} (1 - \mathcal{P}_{\text{busy}})^{n_0} (\mathcal{P}_{\text{busy}})^{N - n_0}, \quad (3.8)$$

where all terms in the sum of (3.7) become the same.

Remark 4: In general, interference from active PUs will impact transmissions of SUs. However, strong interference from PUs would imply high SNR of sensing signals collected at PUs. In this high SNR regime, we typically require small sensing time while still satisfactorily protecting PUs. Therefore, for the case in which interference from active PUs to SUs is small, sensing time will have the most significant impact on the investigated sensing-throughput tradeoff. Therefore, consideration of this setting enables us to gain better insight into the underlying problem. Extension to the more general case is possible by explicitly calculating transmission rates achieved by SUs as a function of SINR. Due to the space constraint, we will not explore this issue further in this paper.

3.5.3.2 Calculation of Conditional Throughput

The conditional throughput can be calculated by using the technique developed by Bianchi in [85] where we approximately assume a fixed transmission probability ϕ in a generic slot time. Specifically, Bianchi shows that this transmission probability can be calculated from the following two equations [85]

$$\phi = \frac{2(1 - 2p)}{(1 - 2p)(W + 1) + Wp(1 - (2p)^m)}, \quad (3.9)$$

$$p = 1 - (1 - \phi)^{n-1}, \quad (3.10)$$

where m is the maximum back-off stage, p is the conditional collision probability (i.e., the probability that a collision is observed when a data packet is transmitted on the channel).

Suppose there are n_0 secondary links participating in contention in the third phase, the probability of the event that at least one secondary link transmits its data packet can be written as

$$\mathcal{P}_t = 1 - (1 - \phi)^{n_0}. \quad (3.11)$$

However, the probability that a transmission occurring on the channel is successful given there is at least one secondary link transmitting can be written as

$$\mathcal{P}_s = \frac{n_0 \phi (1 - \phi)^{n_0 - 1}}{\mathcal{P}_t}. \quad (3.12)$$

3.5 MAC Design, Analysis and Optimization: Single Channel Case

The average duration of a generic slot time can be calculated as

$$\bar{T}_{sd} = (1 - \mathcal{P}_t) T_e + \mathcal{P}_t \mathcal{P}_s T_s + \mathcal{P}_t (1 - \mathcal{P}_s) T_c, \quad (3.13)$$

where $T_e = \sigma$, T_s and T_c represent the duration of an empty slot, the average time the channel is sensed busy due to a successful transmission, and the average time the channel is sensed busy due to a collision, respectively. These quantities can be calculated as [85]

For basic mechanism:

$$\begin{cases} T_s = T_s^1 = H + PS + SIFS + 2PD + ACK + DIFS \\ T_c = T_c^1 = H + PS + DIFS + PD \\ H = H_{PHY} + H_{MAC} \end{cases}, \quad (3.14)$$

where H_{PHY} and H_{MAC} are the packet headers for physical and MAC layers, PS is the packet size, which is assumed to be fixed in this chapter, PD is the propagation delay, $SIFS$ is the length of a short inter-frame space, $DIFS$ is the length of a distributed inter-frame space, ACK is the length of an acknowledgment.

For RTS/CTS mechanism:

$$\begin{cases} T_s = T_s^2 = H + PS + 3SIFS + 2PD + RTS + CTS + ACK + DIFS \\ T_c = T_c^2 = H + DIFS + RTS + PD \end{cases}, \quad (3.15)$$

where we abuse notations by letting RTS and CTS represent the length of RTS and CTS control packets, respectively.

Based on these quantities, we can express the conditional normalized throughput as follows:

$$\mathcal{J}(\tau, \phi | n = n_0) = \left\lfloor \frac{T - \tau}{\bar{T}_{sd}} \right\rfloor \frac{\mathcal{P}_s \mathcal{P}_t PS}{T}, \quad (3.16)$$

where $\lfloor \cdot \rfloor$ denotes the floor function and recall that T is the duration of a cycle. Note that $\left\lfloor \frac{T - \tau}{\bar{T}_{sd}} \right\rfloor$ denotes the average number of generic slot times in one particular cycle excluding the sensing phase. Here, we omit the length of the synchronization phase, which is assumed to be negligible.

3.5.3.3 Optimal Sensing and MAC Protocol Design

Now, we turn to solve the throughput maximization problem formulated in (3.3). Note that we can calculate the normalized throughput given by (3.4) by using $\Pr(n = n_0)$ calculated from (3.7) and the conditional throughput calculated from (3.16). It can be observed that the detection probability $\mathcal{P}_d^i(\varepsilon^i, \tau)$ in the primary protection constraints $\mathcal{P}_d^i(\varepsilon^i, \tau) \geq \bar{\mathcal{P}}_d^i$ depends on both detection threshold ε^i and the optimization variable τ .

We can show that by optimizing the normalized throughput over τ and W while fixing detection thresholds $\varepsilon^i = \varepsilon_0^i$ where $\mathcal{P}_d^i(\varepsilon_0^i, \tau) = \bar{\mathcal{P}}_d^i, i = 1, 2, \dots, N$, we can achieve almost the maximum throughput gain. The intuition behind this observation can be interpreted as follows. If we choose $\varepsilon^i < \varepsilon_0^i$ for a given τ , then both $\mathcal{P}_d^i(\varepsilon^i, \tau)$ and $\mathcal{P}_f^i(\varepsilon^i, \tau)$ increase compared to the case $\varepsilon^i = \varepsilon_0^i$. As a result, $\mathcal{P}_{\text{busy}}^i$ given in (3.6) increases. Moreover, it can be verified that the increase in $\mathcal{P}_{\text{busy}}^i$ will lead to the shift of the probability distribution $\Pr(n = n_0)$ to the left. Specifically, $\Pr(n = n_0)$ given in (3.7) increases for small n_0 and decreases for large n_0 as $\mathcal{P}_{\text{busy}}^i$ increases. Fortunately, with appropriate choice of contention window W the conditional throughput $\mathcal{T}(\tau, W | n = n_0)$ given in (3.16) is quite flat for different n_0 (i.e., it only decreases slightly when n_0 increases). Therefore, the normalized throughput given by (3.4) is almost a constant when we choose $\varepsilon^i < \varepsilon_0^i$.

In the following, we will optimize the normalized throughput over τ and W while choosing detection thresholds such that $\mathcal{P}_d^i(\varepsilon_0^i, \tau) = \bar{\mathcal{P}}_d^i, i = 1, 2, \dots, N$. From these equality constraints and (3.2) we have

$$\mathcal{P}_f^i = \mathcal{Q}\left(\alpha^i + \sqrt{\tau f_s \gamma^i}\right) \quad (3.17)$$

where $\alpha^i = \sqrt{2\gamma^i + 1} \mathcal{Q}^{-1}(\bar{\mathcal{P}}_d^i)$. Hence, the optimization problem (3.3) becomes independent of all detection thresholds $\varepsilon^i, i = 1, 2, \dots, N$. Unfortunately, this optimization problem is still a mixed integer program (note that W takes integer values), which is difficult to solve. In fact, it can be verified even if we allow W to be a real number, the resulting optimization problem is still not convex because the objective function is not concave [118]. Therefore, standard convex optimization techniques cannot be employed to find the optimal solution for the optimization problem under investigation. Therefore, we have to rely on numerical optimization [119] to find the optimal configuration for the proposed MAC protocol. Specifically, for a given contention window W we can find the corresponding optimal sensing time τ as follows:

Problem 2:

$$\max_{0 < \tau \leq T} \mathcal{NJ}(\tau, W) = \sum_{n_0=1}^N \mathcal{J}(\tau, W | n = n_0) \Pr(n = n_0). \quad (3.18)$$

This optimization problem is not convex because its objective function is not concave in general. However, we will prove that $\mathcal{NJ}(\tau)$ is an unimodal function in the range of $[0, T]$. Specifically, $\mathcal{NJ}(\tau)$ is monotonically increasing in $[0, \bar{\tau}]$ while it is monotonically decreasing in $(\bar{\tau}, T]$ for some $0 < \bar{\tau} \leq T$. Hence, $\mathcal{NJ}(\bar{\tau})$ is the only global maximum in the entire range of $[0, T]$. This property is formally stated in the following proposition.

Proposition 1: The objective function $\mathcal{NJ}(\tau)$ of (3.18) satisfies the following properties

1. $\lim_{\tau \rightarrow T} \frac{\partial \mathcal{NJ}}{\partial \tau} < 0$,
2. $\lim_{\tau \rightarrow 0} \frac{\partial \mathcal{NJ}}{\partial \tau} = +\infty$,
3. there is an unique $\bar{\tau}$ where $\bar{\tau}$ is in the range of $[0, T]$ such that $\frac{\partial \mathcal{NJ}(\bar{\tau})}{\partial \tau} = 0$,
4. the objective function $\mathcal{NJ}(\tau)$ is bounded from above.

Proof. The proof is provided in Appendix 3.9.1. □

We would like to discuss the properties stated in Proposition 1. Properties 1, 2, and 4 imply that there must be at least one τ in $[0, T]$ that maximizes $\mathcal{NJ}(\tau)$. The third property implies that indeed such an optimal solution is unique. Therefore, one can find the globally optimal (W^*, τ^*) by finding optimal τ for each W in its feasible range $[1, W_{\max}]$. The procedure to find (W^*, τ^*) can be described in Alg. 1. Numerical studies reveal that this algorithm has quite low computation time for practical values of W_{\max} and T .

Algorithm 1 OPTIMIZATION OF COGNITIVE MAC PROTOCOL

- 1: For each integer value of $W \in [1, W_{\max}]$, find the optimal τ according to (3.18), i.e.,

$$\bar{\tau}(W) = \operatorname{argmax}_{0 < \tau \leq T} \mathcal{NJ}(\tau, W) \quad (3.19)$$

- 2: The globally optimal (W^*, τ^*) can then be found as

$$(W^*, \tau^*) = \operatorname{argmax}_{W, \bar{\tau}(W)} \mathcal{NJ}(\bar{\tau}(W), W). \quad (3.20)$$

3.5.4 Some Practical Implementation Issues

Implementation for the proposed optimal MAC protocol configuration can be done as follows. Each SU will need to spend some time to estimate the channel availability probabilities, channel SNRs, and the number of SUs sharing the underlying spectrum. When these system parameters have been estimated, each SU can independently calculate the optimal sensing time and minimum contention window and implement them. Therefore, implementation for optimal MAC protocol can be performed in a completely distributed manner, which would be very desirable.

3.6 MAC Design, Analysis, and Optimization: Multiple Channel Case

We consider the MAC protocol design, analysis and optimization for the multi-channel case in this section.

3.6.1 MAC Protocol Design

We propose a synchronized multi-channel MAC protocol for dynamic spectrum sharing in this subsection. To exploit spectrum holes in this case, we assume that there is one control channel which belongs to the secondary network (i.e., it is always available) and M data channels which can be exploited by SUs. We further assume that each transmitting SU employ a reconfigurable transceiver which can be tuned to the control channel or vacant channels for data transmission easily. In addition, we assume that this transceiver can turn on and off the carriers on the available or busy channels, respectively (e.g., this can be achieved by the OFDM technology).

There are still three phases for each cycle as in the single-channel case. However, in the first phase, namely the sensing phase of length τ , all SUs simultaneously perform spectrum sensing on all M underlying channels. Because the control channel is always available, all SUs exchange beacon signals to achieve synchronization in the second phase. Moreover, only active secondary links whose sensing outcomes indicate at least one vacant channel participate in the third phase (i.e., data transmission phase). As a result, the transmitter of the winning link in the contention phase will need to inform its receiver about the available channels. Finally, the winning secondary link will transmit data on all vacant channels in

the data transmission phase. The timing diagram of one particular cycle is illustrated in Fig. 3.2.

Again, we also assume that the length of each cycle is sufficiently large such that secondary links can transmit several packets on each available channel during the data transmission phase. In the data transmission phase, we assume that active secondary links adopt the standard contention technique to capture the channels similar to that employed by the CSMA/CA protocol using exponential back-off and either two-way or four-way handshake as described in Section 3.5. For the case with two-way handshake, both secondary transmitters and receivers need to perform spectrum sensing. With four-way handshake, only secondary transmitters need to perform spectrum sensing and the RTS message will contain additional information about the available channels on which the receiver will receive data packets. Also, multiple packets (i.e., one on each available channel) are transmitted by the winning secondary transmitter. Finally, the ACK message will be sent by the receiver to indicate successfully received packets on the vacant channels.

3.6.2 Throughput Maximization

In this subsection, we discuss how to find the optimal configuration to maximize the normalized throughput under sensing constraints for PUs. Suppose that each primary receiver requires that detection probability achieved by its conflicting primary link i on channel j be at least \bar{P}_d^{ij} . Then, the throughput maximization problem can be stated as follows:

Problem 3:

$$\begin{aligned}
 & \max_{\tau, W} \quad \mathcal{N}\mathcal{T}(\tau, W) \\
 & \text{s.t.} \quad \mathcal{P}_d^{ij}(\varepsilon^{ij}, \tau) \geq \bar{\mathcal{P}}_d^{ij}, i \in [1, N], j \in [1, M] \\
 & \quad \quad 0 < \tau \leq T, \quad 0 < W \leq W_{\max},
 \end{aligned} \tag{3.21}$$

where \mathcal{P}_d^{ij} is the detection probability for SU i on channel j , W_{\max} is the maximum contention window and recall that T is the cycle interval. We will assume that for each SU i , $\mathcal{P}_d(\varepsilon^{ij}, \tau)$ and $\bar{\mathcal{P}}_d^{ij}$ are the same for all channel j , respectively. This would be valid because sensing performance (i.e., captured in $\mathcal{P}_d(\varepsilon^{ij}, \tau)$ and $\mathcal{P}_f(\varepsilon^{ij}, \tau)$) depends on detection thresholds ε^{ij} and the SNR γ^{ij} , which would be the same for different channels j . In this case, the optimization problem reduces to that of the same form as (3.3) although the normalized throughput $\mathcal{N}\mathcal{T}(\tau, W)$ will need to be derived for this multi-channel case. For brevity, we will drop all channel index j in these quantities whenever possible.

3.6.3 Throughput Analysis and Optimization

We analyze the saturation throughput and show how to obtain an optimal solution for **Problem 3**. Again we assume that all secondary links transmit data packets of the same length. Let $\Pr(n = n_0)$, $\mathbf{E}[l]$ and $\mathcal{T}(\tau, \phi | n = n_0)$ denote the probability that n_0 secondary links participating in the contention phase, the average number of vacant channels at the winning SU link, and the conditional normalized throughput when n_0 secondary links join the contention, respectively. Then, the normalized throughput can be calculated as

$$\mathcal{N}\mathcal{T} = \sum_{n_0=1}^N \mathcal{T}(\tau, W | n = n_0) \Pr(n = n_0) \frac{\mathbf{E}[l]}{M}, \quad (3.22)$$

where recall that N is the number of secondary links, M is the number of channels, τ is the sensing time, W is the contention window. Note that this is the average system throughput per channel. We will calculate $\mathcal{T}(\tau, \phi | n = n_0)$ using (3.16) for the proposed MAC protocol with four-way handshake and exponential random back-off. In addition, we also show how to calculate $\Pr(n = n_0)$.

3.6.3.1 Calculation of $\Pr(n = n_0)$ and $\mathbf{E}[l]$

Recall that only secondary links whose sensing outcomes indicate at least one available channel participate in contention in the data transmission phase. Again, as in the single channel case derived in Section 3.5.3.1 the sensing outcome at SU i indicates that channel j is available or busy with probabilities $\mathcal{P}_{\text{idle}}^i$ and $\mathcal{P}_{\text{busy}}^i$, which are in the same forms with (3.6) and (3.5), respectively (recall that we have dropped the channel index j in these quantities). Now, $\Pr(n = n_0)$ can be calculated from these probabilities. Recall that secondary link i only joins the contention if its sensing outcomes indicate at least one vacant channel. Otherwise, it will be silent for the whole cycle and waits until the next cycle. This occurs if its sensing outcomes indicate that all channels are busy.

To gain insight into the optimal structure of the optimal solution while keeping mathematical details sufficiently tractable, we will consider the homogeneous case in the following where \mathcal{P}_f^i , \mathcal{P}_d^i (therefore, $\mathcal{P}_{\text{idle}}^i$ and $\mathcal{P}_{\text{busy}}^i$) are the same for all SUs i . The obtained results, however, can be extended to the general case even though the corresponding expressions will be more lengthy and tedious. For the homogeneous system, we will simplify $\mathcal{P}_{\text{SUidle}}^i$ and $\mathcal{P}_{\text{SUbusy}}^i$ to $\mathcal{P}_{\text{SUidle}}$ and $\mathcal{P}_{\text{SUbusy}}$, respectively for brevity. Therefore, the probability that a particular channel is indicated as busy or idle by the corresponding spectrum sensor can be written as

$$\mathcal{P}_{\text{busy}} = \mathcal{P}_f \mathcal{P}(\mathcal{H}_0) + \mathcal{P}_d \mathcal{P}(\mathcal{H}_1), \quad (3.23)$$

3.6 MAC Design, Analysis, and Optimization: Multiple Channel Case

$$\mathcal{P}_{\text{idle}} = 1 - \mathcal{P}_{\text{busy}}. \quad (3.24)$$

Let $\Pr(l = l_0)$ denote the probability that l_0 out of M channels are indicated as available by the spectrum sensors. Then, this probability can be calculated as

$$\Pr(l = l_0) = C_M^{l_0} \mathcal{P}_{\text{idle}}^{l_0} \mathcal{P}_{\text{busy}}^{M-l_0}. \quad (3.25)$$

Now, let $\mathcal{P}_{\text{SUidle}}$ be the probability that a particular secondary link i participates in the contention (i.e., its spectrum sensors indicate at least one available channel) and $\mathcal{P}_{\text{SUbusy}}$ be the probability that secondary link i is silent (i.e., its spectrum sensors indicate that all channels are busy). Then, these probabilities can be calculated as

$$\mathcal{P}_{\text{SUbusy}} = \Pr(l = 0) = \mathcal{P}_{\text{busy}}^M, \quad (3.26)$$

$$\mathcal{P}_{\text{SUidle}} = \sum_{l_0=1}^M \Pr(l = l_0) = 1 - \mathcal{P}_{\text{SUbusy}}. \quad (3.27)$$

Again we assume that a transmission from a particular secondary link only fails if it collides with transmissions from other secondary links. The probability that n_0 secondary links join the contention can be calculated by using (3.27) and (3.26) as follows:

$$\Pr(n = n_0) = C_N^{n_0} \mathcal{P}_{\text{SUidle}}^{n_0} \mathcal{P}_{\text{SUbusy}}^{N-n_0} = C_N^{n_0} (1 - \mathcal{P}_{\text{busy}}^M)^{n_0} \mathcal{P}_{\text{busy}}^{M(N-n_0)}. \quad (3.28)$$

From (3.25), we can calculate the average number of available channels, denoted by the expectation $\mathbf{E}[l]$, at one particular secondary link as

$$\mathbf{E}[l] = \sum_{l_0=0}^M l_0 \Pr(l = l_0) = \sum_{l_0=0}^M l_0 C_M^{l_0} \mathcal{P}_{\text{idle}}^{l_0} \mathcal{P}_{\text{busy}}^{M-l_0} = M \mathcal{P}_{\text{idle}} = M(1 - \mathcal{P}_{\text{busy}}). \quad (3.29)$$

3.6.3.2 Optimal Sensing and MAC Protocol Design

We now tackle the throughput maximization problem formulated in (3.21). In this case, the normalized throughput given by (3.22) can be calculated by using $\Pr(n = n_0)$ in (3.28), the conditional throughput in (3.16), and the average number of available channels in (3.29). Similar to the single-channel case, we will optimize the normalized throughput over τ and W while choosing a detection threshold such that $\mathcal{P}_d(\varepsilon_0, \tau) = \bar{\mathcal{P}}_d$. Under these equality constraints, the false alarm probability can be written as

$$\mathcal{P}_f = \mathcal{Q}\left(\alpha + \sqrt{\tau f_s \gamma}\right) \quad (3.30)$$

where $\alpha = \sqrt{2\gamma + 1}Q^{-1}(\bar{\mathcal{P}}_d)$. Hence, **Problem 3** is independent of detection thresholds. Again, for a given contention window W we can find the corresponding optimal sensing time τ in the following optimization problem

Problem 4:

$$\begin{aligned} \max_{\tau} \quad & \widetilde{\mathcal{N}}\mathcal{J}(\tau) \triangleq NT(\tau, W) |_{W=\bar{W}} \\ \text{s.t.} \quad & 0 \leq \tau \leq T \end{aligned} \quad (3.31)$$

Similar to the single-channel case, we will prove that $\widetilde{\mathcal{N}}\mathcal{J}(\tau)$ is a unimodal function in the range of $[0, T]$. Therefore, there is a unique global maximum in the entire range of $[0, T]$. This is indeed the result of several properties stated in the following proposition.

Proposition 2: The function $\widetilde{\mathcal{N}}\mathcal{J}(\tau)$ satisfies the following properties

1. $\lim_{\tau \rightarrow 0} \frac{\partial \widetilde{\mathcal{N}}\mathcal{J}(\tau)}{\partial \tau} > 0$,
2. $\lim_{\tau \rightarrow T} \frac{\partial \widetilde{\mathcal{N}}\mathcal{J}(\tau)}{\partial \tau} < 0$,
3. there is a unique $\bar{\tau}$ where $\bar{\tau}$ is in the range of $[0, T]$ such that $\frac{\partial \widetilde{\mathcal{N}}\mathcal{J}(\bar{\tau})}{\partial \tau} = 0$,
4. and the objective function $\widetilde{\mathcal{N}}\mathcal{J}(\tau)$ is bounded from above.

Therefore, it is a unimodal function in the range of $[0, T]$.

Proof. The proof is provided in Appendix 3.9.2. □

Therefore, given one particular value of W we can find a unique optimal $\bar{\tau}(W)$ for the optimization problem (3.31). Then, we can find the globally optimal (W^*, τ^*) by finding optimal τ for each W in its feasible range $[1, W_{\max}]$. The procedure to find (W^*, τ^*) is the same as that described in Alg. 1.

3.7 Numerical Results

We present numerical results to illustrate throughput performance of the proposed cognitive MAC protocols. We take key parameters for the MAC protocols from Table II in [85]. Other parameters are chosen as follows: cycle time is $T = 100ms$; mini-slot (i.e., generic empty slot time) is $\sigma = 20\mu s$; sampling frequency for spectrum sensing is $f_s = 6MHz$; bandwidth of PUs' QPSK signals is $6MHz$. In addition, the exponential back-off mechanism with the maximum back-off stage m is employed to reduce collisions.

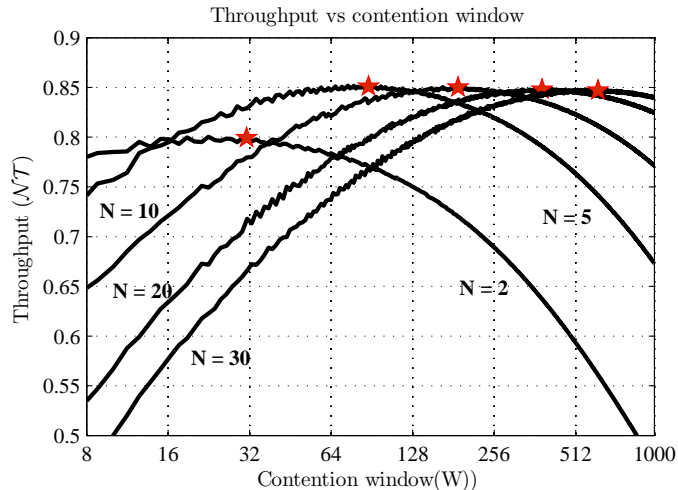


Figure 3.3: Normalized throughput versus contention window W for $\tau = 1ms$, $m = 3$, different N and basic access mechanism.

3.7.1 Performance of Single Channel MAC Protocol

For the results in this section, we choose other parameters of the cognitive network as follows. The signal-to-noise ratio of PU signals at secondary links SNR_p^i are chosen randomly in the range $[-15, -20]dB$. The target detection probability for secondary links and the probabilities $\mathcal{P}^i(\mathcal{H}_0)$ are chosen randomly in the intervals $[0.7, 0.9]$ and $[0.7, 0.8]$, respectively. The basic scheme is used as a handshaking mechanism for the MAC protocol.

In Fig. 3.3, we show the normalized throughput $\mathcal{N}\mathcal{T}$ versus contention window W for different values of N when the sensing time is fixed at $\tau = 1ms$ and the maximum backoff stage is chosen at $m = 3$ for one particular realization of system parameters. The maximum throughput on each curve is indicated by a star symbol. This figure indicates that the maximum throughput is achieved at larger W for larger N . This is expected because larger contention window can alleviate collisions among active secondary for larger number of secondary links. It is interesting to observe that the maximum throughput can be larger than 0.8 although $\mathcal{P}^i(\mathcal{H}_0)$ are chosen in the range $[0.7, 0.8]$. This is due to a multiuser gain because secondary links are in conflict with different primary receivers.

In Fig. 3.4 we present the normalized throughput $\mathcal{N}\mathcal{T}$ versus sensing time τ for a fixed contention window $W = 32$, maximum backoff stage $m = 3$, and different number of secondary links N . The maximum throughput is indicated by a star symbol on each curve. This figure confirms that the normalized throughput $\mathcal{N}\mathcal{T}$ increases when τ is small and decreases with large τ as being proved in Proposition 1. Moreover, for a fixed contention window the

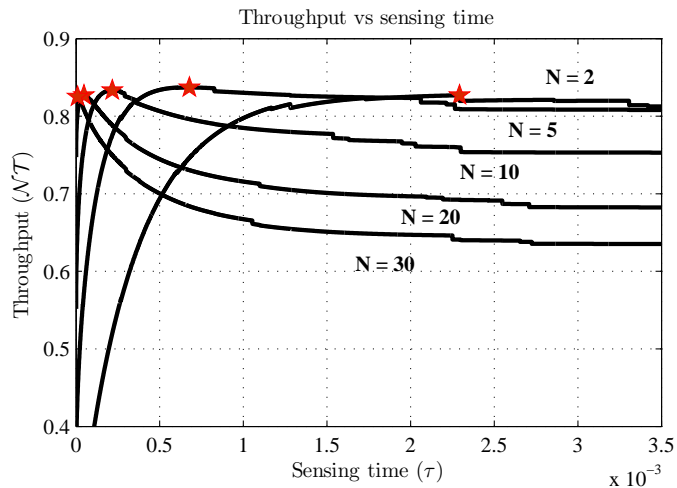


Figure 3.4: Normalized throughput versus the sensing time τ for $W = 32$, $m = 3$, different N and basic access mechanism.

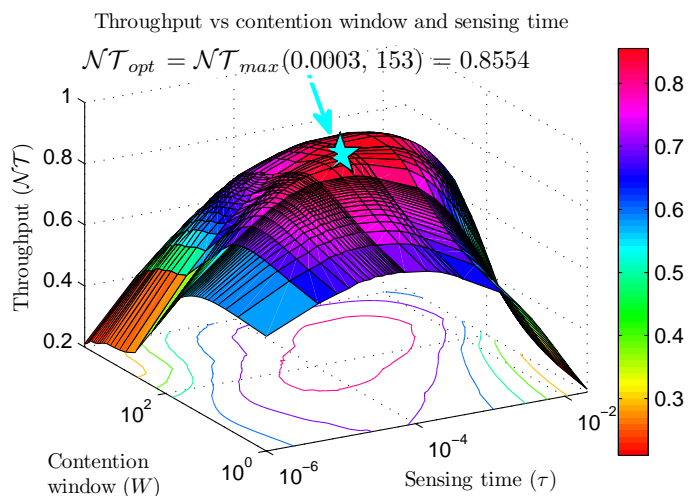


Figure 3.5: Normalized throughput versus sensing time τ and contention window W for $N = 15$, $m = 4$ and basic access mechanism.

optimal sensing time indeed decreases with the number of secondary links N . Finally, the multi-user diversity gain can also be observed in this figure.

To illustrate the joint effects of contention window W and sensing time τ , we show the normalized throughput \mathcal{NT} versus τ and contention window W for $N = 15$ and $m = 4$ in Fig. 3.5. We show the globally optimal parameters (ϕ^*, τ^*) which maximize the normalized throughput \mathcal{NT} of the proposed cognitive MAC protocol by a star symbol in this figure. This figure reveals that the performance gain due to optimal configuration of the proposed MAC

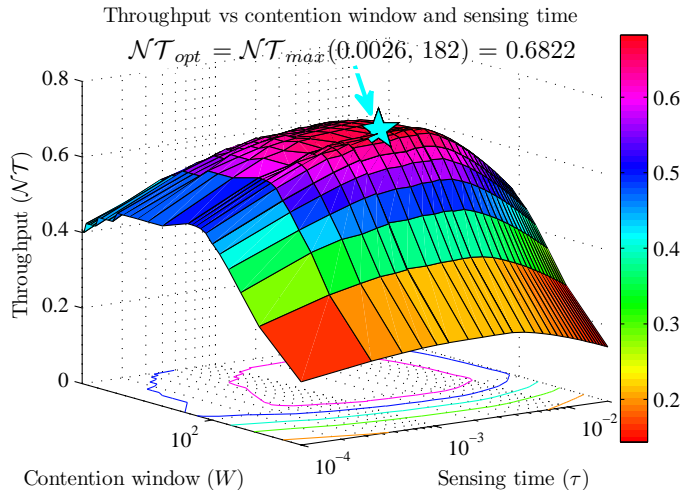


Figure 3.6: Normalized throughput versus sensing time τ and contention window W for $N = 10$, $m = 4$, $M = 5$ and basic access mechanism.

protocol is very significant. Specifically, while the normalized throughput \mathcal{NT} tends to be less sensitive to the contention window W , it decreases significantly when the sensing time τ deviates from the optimal value τ^* . Therefore, the proposed optimization approach would be very useful in achieving the largest throughput performance for the secondary network.

3.7.2 Performance of Multi-Channel MAC Protocol

In this section, we present numerical results for the proposed multi-channel MAC protocol. Although, we analyze the homogeneous scenario in Section 3.6 for brevity, we present simulation results for the heterogeneous settings in this subsection. The same parameters for the MAC protocol as in Section 3.7 are used. However, this model covers for the case in which each secondary link has multiple channels. In addition, some key parameters are chosen as follows. The SNRs of the signals from the primary user to secondary link i (i.e., SNR_p^{ij}) are randomly chosen in the range of $[-15, -20]$ dB. The target detection probabilities $\bar{\mathcal{P}}_d^{ij}$ and the probabilities $\mathcal{P}^{ij}(\mathcal{H}_0)$ for channel j at secondary link i are randomly chosen in the intervals $[0.7, 0.9]$ and $[0.7, 0.8]$, respectively. Again the exponential backoff mechanism with the maximum backoff stage m is employed to reduce collisions.

In Fig. 3.6, we illustrate the normalized throughput \mathcal{NT} versus sensing times τ and contention windows W for $N = 10$, $M = 5$ and $m = 4$ and the basic access mechanism. We show the optimal configuration (τ^*, W^*) , which maximizes the normalized throughput \mathcal{NT} of the proposed multichannel MAC protocol. Again it can be observed that the normalized

3.7 Numerical Results

Table 3.1: Comparison between the normalized throughputs of basic access and RTS/CTS access

BASIC ACCESS $(N, M, m) = (10, 5, 4)$						RTS/CTS ACCESS $(N, M, m) = (10, 5, 4)$					
$\mathcal{N}\mathcal{T}$		$\tau(ms)$				$\mathcal{N}\mathcal{T}$		$\tau(ms)$			
		1	2.6	10	20			1	2.6	10	20
W	16	0.4865	0.5545	0.5123	0.4677	W	16	0.6029	0.6654	0.6236	0.5568
	64	0.5803	0.6488	0.6004	0.5366		60	0.6022	0.6733	0.6231	0.5568
	182	0.6053	0.6822	0.6323	0.5594		128	0.5954	0.6707	0.6175	0.5533
	512	0.6014	0.6736	0.6251	0.5567		512	0.5737	0.6444	0.5982	0.5323
	1024	0.5744	0.6449	0.5982	0.5312		1024	0.5468	0.6134	0.5692	0.5059
BASIC ACCESS $(N, M, m) = (5, 3, 4)$						RTS/CTS ACCESS $(N, M, m) = (5, 3, 4)$					
$\mathcal{N}\mathcal{T}$		$\tau(ms)$				$\mathcal{N}\mathcal{T}$		$\tau(ms)$			
		1	2.3	10	20			1	2.5	10	20
W	16	0.5442	0.6172	0.5647	0.5079	W	22	0.5972	0.6789	0.6177	0.5529
	64	0.6015	0.6757	0.6302	0.5565		64	0.5931	0.6674	0.6217	0.5483
	100	0.6094	0.6841	0.6345	0.5665		128	0.5876	0.6604	0.6131	0.5441
	512	0.5735	0.6443	0.5983	0.5324		512	0.5458	0.6128	0.5691	0.5057
	1024	0.5210	0.5866	0.5447	0.4842		1024	0.4965	0.5591	0.5189	0.4610

throughput $\mathcal{N}\mathcal{T}$ tends to be less sensitive to the contention window W while it significantly decreases when the sensing time τ deviates from the optimal sensing time τ^* .

In order to study the joint effect of contention window W and sensing time τ in greater details, we show the normalized throughput $\mathcal{N}\mathcal{T}$ versus W and τ in Table 3.1. In this table, we consider both handshaking mechanisms, namely basic access and RTS/CTS access schemes. Each set of results applies to a particular setting with certain number of secondary links N , number of channels M and maximum backoff stage m . In particular, we will consider two settings, namely $(N, M, m) = (10, 5, 4)$ and $(N, M, m) = (5, 3, 4)$. Optimal normalized throughput is indicated by a bold number. It can be confirmed from this table that as (τ, W) deviate from the optimal (τ^*, W^*) , the normalized throughput decreases significantly.

This table also demonstrates potential effects of the number of secondary links N on the network throughput and optimal configuration for the MAC protocols. In particular, for secondary networks with the small number of secondary links, the probability of collision is lower than that for networks with the large number of secondary links. We consider the two scenarios corresponding to different combinations (N, M, m) . The first one which has a smaller number of secondary links N indeed requires smaller contention window W and maximum back-off stage m to achieve the maximum throughput. Finally, it can be observed

that for the same configuration of (N, M, m) , the basic access mechanism slightly outperforms the RTS/CTS access mechanism, while the RTS/CTS access mechanism can achieve the optimal normalized throughput at lower W compared to the basic access mechanism.

3.8 Conclusion

In this paper, we have proposed MAC protocols for cognitive radio networks that explicitly take into account spectrum sensing performance. Specifically, we have derived normalized throughput of the proposed MAC protocols and determined their optimal configuration for throughput maximization. These studies have been performed for both single and multiple channel scenarios subject to protection constraints for primary receivers. Finally, we have presented numerical results to confirm important theoretical findings in the paper and to show significant performance gains achieved by the optimal configuration for proposed MAC protocols.

3.9 Appendices

3.9.1 Proof of Proposition 1

We start the proof by defining the following quantities: $\varphi^j := -\frac{(\alpha^j + \sqrt{\tau f_s} \gamma^j)^2}{2}$ and $c_{n_0} := \frac{\mathcal{P}_s \mathcal{P}_t PS}{T}$. Taking the derivative of $\mathcal{N}\mathcal{T}$ versus τ , we have

$$\frac{\partial \mathcal{N}\mathcal{T}}{\partial \tau} = \sum_{n_0=1}^N c_{n_0} \sum_{k=1}^{C_N^{n_0}} \left\{ \begin{aligned} & \left(\frac{-1}{T_{sd}} \prod_{i \in \mathcal{S}_k} \mathcal{P}_{idle}^i \prod_{j \in \mathcal{S} \setminus \mathcal{S}_k} \mathcal{P}_{busy}^j + \left\lfloor \frac{T-\tau}{T_{sd}} \right\rfloor \sqrt{\frac{f_s}{8\pi\tau}} \times \right. \\ & \left. \left[\begin{aligned} & \sum_{i \in \mathcal{S}_k} \gamma^i \exp(\varphi^i) \mathcal{P}^i(\mathcal{H}_0) \prod_{l \in \mathcal{S}_k \setminus i} \mathcal{P}_{idle}^l \prod_{j \in \mathcal{S} \setminus \mathcal{S}_k} \mathcal{P}_{busy}^j \right] \right. \\ & \left. \left[- \sum_{j \in \mathcal{S} \setminus \mathcal{S}_k} \gamma^j \exp(\varphi^j) \mathcal{P}^j(\mathcal{H}_0) \prod_{l \in \mathcal{S} \setminus \mathcal{S}_k \setminus j} \mathcal{P}_{busy}^l \prod_{i \in \mathcal{S}_k} \mathcal{P}_{idle}^i \right] \right] \end{aligned} \right\}. \quad (3.32)$$

From this we have

$$\lim_{\tau \rightarrow T} \frac{\partial \mathcal{N}\mathcal{T}}{\partial \tau} = \sum_{n_0=1}^N c_{n_0} \sum_{k=1}^{C_N^{n_0}} \left(\frac{-1}{T_{sd}} \right) \prod_{i \in \mathcal{S}_k} \mathcal{P}_{idle}^i \prod_{j \in \mathcal{S} \setminus \mathcal{S}_k} \mathcal{P}_{busy}^j < 0. \quad (3.33)$$

Now, let us define the following quantity

$$\mathcal{K}_\tau \triangleq \sum_{n_0=1}^N c_{n_0} \sum_{k=1}^N C_N^{n_0} \left[\begin{array}{l} \sum_{i \in \mathcal{S}_k} \gamma^i \exp(\varphi^i) \mathcal{P}^i(\mathcal{H}_0) \prod_{l \in \mathcal{S}_k \setminus i} \mathcal{P}_{idle}^l \prod_{j \in \mathcal{S} \setminus \mathcal{S}_k} \mathcal{P}_{busy}^j \\ - \sum_{j \in \mathcal{S} \setminus \mathcal{S}_k} \gamma^j \exp(\varphi^j) \mathcal{P}^j(\mathcal{H}_0) \prod_{l \in \mathcal{S} \setminus \mathcal{S}_k \setminus j} \mathcal{P}_{busy}^l \prod_{i \in \mathcal{S}_k} \mathcal{P}_{idle}^i \end{array} \right]. \quad (3.34)$$

Then, it can be shown that $\mathcal{K}_\tau > 0$ as being explained in the following. First, it can be verified that the term c_{n_0} is almost a constant for different n_0 . Therefore, to highlight intuition behind the underlying property (i.e., $\mathcal{K}_\tau > 0$), we substitute $\mathcal{K} = c_{n_0}$ into the above equation. Then, \mathcal{K}_τ in (3.34) reduces to

$$\mathcal{K}_\tau = \mathcal{K}_a \sum_{n_0=1}^N C_N^{n_0} (n_0 \mathcal{P}_{idle}^{n_0-1} \mathcal{P}_{busy}^{N-n_0} - (N-n_0) \mathcal{P}_{busy}^{N-n_0-1}), \quad (3.35)$$

where $\mathcal{K}_a = \mathcal{K} \gamma \exp(\varphi) \mathcal{P}(\mathcal{H}_0)$. Let define the following quantities $x = \mathcal{P}_{busy}$, $x \in \mathbb{R}_x \triangleq [\mathcal{P}_d \mathcal{P}(\mathcal{H}_1), \mathcal{P}(\mathcal{H}_0) + \mathcal{P}_d \mathcal{P}(\mathcal{H}_1)]$. After some manipulations, we have

$$\mathcal{K}_\tau = \mathcal{K}_a \sum_{n_0=1}^N f(x) \left(\frac{n_0}{x(1-x)} - \frac{N}{x} \right), \quad (3.36)$$

where $f(x) = C_N^{n_0} (1-x)^{n_0} x^{N-n_0}$ is the binomial mass function [120] with $p = 1-x$ and $q = x$. Because the total probabilities and the mean of this binomial distribution are 1 and $Np = N(1-x)$, respectively, we have

$$\sum_{n_0=0}^N f(x) = 1, \quad (3.37)$$

$$\sum_{n_0=0}^N n_0 f(x) = N(1-x). \quad (3.38)$$

It can be observed that in (3.36), the element corresponding to $n_0 = 0$ is missing. Apply the results in (3.37) and (3.38) to (3.36) we have

$$\mathcal{K}_\tau = \mathcal{K}_a N x^{N-1} > 0, \quad \forall x. \quad (3.39)$$

Therefore, we have

$$\lim_{\tau \rightarrow 0} \frac{\partial \mathcal{N}\mathcal{T}}{\partial \tau} = +\infty. \quad (3.40)$$

Hence, we have completed the proof for first two properties of Proposition 1.

In order to prove the third property, let us find the solution of $\frac{\partial N\mathcal{I}}{\partial \tau} = 0$. After some simple manipulations and using the properties of the binomial distribution, this equation reduces to

$$h(\tau) = g(\tau), \quad (3.41)$$

where

$$g(\tau) = \left(\alpha + \gamma \sqrt{f_s \tau} \right)^2, \quad (3.42)$$

and

$$h(\tau) = 2 \log \left(\mathcal{P}(\mathcal{H}_0) \gamma \sqrt{\frac{f_s}{8\pi} \frac{T - \tau}{\sqrt{\tau}}} \right) + h_1(x) \quad (3.43)$$

where $h_1(x) = 2 \log \frac{\mathcal{K}_\tau / \mathcal{K}_\alpha}{\sum_{n_0=1}^N C_N^{n_0} f(x)} = 2 \log \frac{Nx^{N-1}}{1-x^N}$.

To prove the third property, we will show that $h(\tau)$ intersects $g(\tau)$ only once. We first state one important property of $h(\tau)$ in the following lemma.

Lemma 1: $h(\tau)$ is an decreasing function.

Proof. Taking the first derivative of $h(\cdot)$, we have

$$\frac{\partial h}{\partial \tau} = \frac{-1}{\tau} - \frac{2}{T - \tau} + \frac{\partial h_1}{\partial x} \frac{\partial x}{\partial \tau}. \quad (3.44)$$

We now derive $\frac{\partial x}{\partial \tau}$ and $\frac{\partial h_1}{\partial x}$ as follows:

$$\frac{\partial x}{\partial \tau} = -\mathcal{P}(\mathcal{H}_0) \gamma \sqrt{\frac{f_s}{8\pi\tau}} \exp \left(-\frac{(\alpha + \gamma \sqrt{f_s \tau})^2}{2} \right) < 0, \quad (3.45)$$

$$\frac{\partial h_1}{\partial x} = 2 \frac{N - 1 + x^N}{x(1 - x^N)} > 0. \quad (3.46)$$

Hence, $\frac{\partial h_1}{\partial x} \frac{\partial x}{\partial \tau} < 0$. Using this result in (3.44), we have $\frac{\partial h}{\partial \tau} < 0$. Therefore, we can conclude that $h(\tau)$ is monotonically decreasing. \square

We now consider function $g(\tau)$. Take the derivative of $g(\tau)$, we have

$$\frac{\partial g}{\partial \tau} = \left(\alpha + \gamma \sqrt{f_s \tau} \right) \frac{\gamma \sqrt{f_s}}{\sqrt{\tau}}. \quad (3.47)$$

Therefore, the monotonicity property of $g(\tau)$ only depends on $y = \alpha + \gamma\sqrt{f_s\tau}$. Properties 1 and 2 imply that there must be at least one intersection between $h(\tau)$ and $g(\tau)$. We now prove that there is indeed a unique intersection. To proceed, we consider two different regions for τ as follows:

$$\Omega_1 = \left\{ \tau \mid \alpha + \gamma\sqrt{f_s\tau} < 0, \tau \leq T \right\} = \left\{ 0 < \tau < \frac{\alpha^2}{\gamma^2 f_s} \right\}$$

and

$$\Omega_2 = \left\{ \tau \mid \alpha + \gamma\sqrt{f_s\tau} \geq 0, \tau \leq T \right\} = \left\{ \frac{\alpha^2}{\gamma^2 f_s} \leq \tau \leq T \right\}.$$

From the definitions of these two regions, we have $g(\tau)$ decreases in Ω_1 and increases in Ω_2 . To show that there is a unique intersection between $h(\tau)$ and $g(\tau)$, we prove the following.

Lemma 2: The following statements are correct:

1. If there is an intersection between $h(\tau)$ and $g(\tau)$ in Ω_2 then it is the only intersection in this region and there is no intersection in Ω_1 .
2. If there is an intersection between $h(\tau)$ and $g(\tau)$ in Ω_1 then it is the only intersection in this region and there is no intersection in Ω_2 .

Proof. We now prove the first statement. Recall that $g(\tau)$ monotonically increases in Ω_2 ; therefore, $g(\tau)$ and $h(\tau)$ can intersect at most once in this region (because $h(\tau)$ decreases). In addition, $g(\tau)$ and $h(\tau)$ cannot intersect in Ω_1 for this case if we can prove that $\frac{\partial h}{\partial \tau} < \frac{\partial g}{\partial \tau}$. This is because both functions decrease in Ω_1 . We will prove that $\frac{\partial h}{\partial \tau} < \frac{\partial g}{\partial \tau}$ in lemma 3 after this proof.

We now prove the second statement of lemma 2. Recall that we have $\frac{\partial h}{\partial \tau} < \frac{\partial g}{\partial \tau}$. Therefore, there is at most one intersection between $g(\tau)$ and $h(\tau)$ in Ω_1 . In addition, it is clear that there cannot be any intersection between these two functions in Ω_2 for this case. \square

Lemma 3: We have $\frac{\partial h}{\partial \tau} < \frac{\partial g}{\partial \tau}$.

Proof. From (3.44), we can see that lemma 3 holds if we can prove the following stronger result

$$-\frac{1}{\tau} + \frac{\partial h_1}{\partial \tau} < \frac{\partial g}{\partial \tau}, \tag{3.48}$$

where $\frac{\partial h_1}{\partial \tau} = \frac{\partial h_1}{\partial x} \frac{\partial x}{\partial \tau}$, $\frac{\partial x}{\partial \tau}$ is derived in (3.45), $\frac{\partial h_1}{\partial x}$ is derived in (3.46) and $\frac{\partial g}{\partial \tau}$ is given in (3.47).

To prove (3.48), we will prove the following

$$-\frac{1}{\tau} + \frac{y\mathcal{P}(\mathcal{H}_0)\gamma\sqrt{\frac{f_s}{\tau}}}{\mathcal{P}(\mathcal{H}_0) + \sqrt{2\pi}\mathcal{P}(\mathcal{H}_1)(1 - \bar{\mathcal{P}}_d)(-y)\exp\left(\frac{y^2}{2}\right)} < \frac{\partial g}{\partial \tau}, \quad (3.49)$$

where $y = (\alpha + \gamma\sqrt{f_s\tau} < 0)$. Then, we show that

$$\frac{\partial h_1}{\partial \tau} < \frac{y\mathcal{P}(\mathcal{H}_0)\gamma\sqrt{\frac{f_s}{\tau}}}{\mathcal{P}(\mathcal{H}_0) + \sqrt{2\pi}\mathcal{P}(\mathcal{H}_1)(1 - \bar{\mathcal{P}}_d)(-y)\exp\left(\frac{y^2}{2}\right)}. \quad (3.50)$$

Therefore, the result in (3.48) will hold. Let us prove (3.50) first. First, let us prove the following

$$\frac{\partial h_1}{\partial x} > \frac{2}{1-x}. \quad (3.51)$$

Using the result in $\frac{\partial h_1}{\partial x}$ from (3.46), (3.51) is equivalent to

$$2\frac{N-1+x^N}{x(1-x^N)} > \frac{2}{1-x}, \quad (3.52)$$

After some manipulations, we get

$$(1-x)(N-1-(x+x^2+\dots+x^{N-1})) > 0. \quad (3.53)$$

It can be observed that $0 < x < 1$ and $0 < x^i < 1$, $i \in [1, N-1]$. So $N-1-(x+x^2+\dots+x^{N-1}) > 0$; hence (3.53) holds. Therefore, we have completed the proof for (3.51).

We now show that the following inequality holds

$$\frac{2}{1-x} > \frac{2\sqrt{2\pi}(-y)\exp\left(\frac{y^2}{2}\right)}{\mathcal{P}(\mathcal{H}_0) + \sqrt{2\pi}\mathcal{P}(\mathcal{H}_1)(1 - \bar{\mathcal{P}}_d)(-y)\exp\left(\frac{y^2}{2}\right)}. \quad (3.54)$$

This can be proved as follows. In [121], it has been shown that $\mathcal{Q}(t)$ with $t > 0$ satisfies

$$\frac{1}{\mathcal{Q}(t)} > \sqrt{2\pi}t\exp\left(\frac{t^2}{2}\right). \quad (3.55)$$

Apply this result to $\mathcal{P}_f = \mathcal{Q}(y) = 1 - \mathcal{Q}(-y)$ with $y = (\alpha + \gamma\sqrt{f_s\tau}) < 0$ we have

$$\frac{1}{1-P_f} > \sqrt{2\pi}(-y)\exp\left(\frac{y^2}{2}\right). \quad (3.56)$$

After some manipulations, we obtain

$$\mathcal{P}_f > 1 - \frac{1}{\sqrt{2\pi}(-y) \exp\left(\frac{y^2}{2}\right)}. \quad (3.57)$$

Recall that we have defined $x = \mathcal{P}_f \mathcal{P}(\mathcal{H}_0) + \bar{\mathcal{P}}_d \mathcal{P}(\mathcal{H}_1)$. Using the result in (3.57), we can obtain the lower bound of $\frac{2}{1-x}$ given in (3.54). Using the results in (3.51) and (3.54), and the fact that $\frac{\partial x}{\partial \tau} < 0$, we finally complete the proof for (3.50).

To complete the proof of the lemma, we need to prove that (3.49) holds. Substitute $\frac{\partial g}{\partial \tau}$ from (3.47) to (3.49) and make some further manipulations, we have

$$\frac{-1}{y(y-\alpha)} > 1 - \frac{y \mathcal{P}(\mathcal{H}_0) \gamma \sqrt{\frac{f_s}{\tau}}}{\mathcal{P}(\mathcal{H}_0) + \sqrt{2\pi} \mathcal{P}(\mathcal{H}_1) (1 - \bar{\mathcal{P}}_d) (-y) \exp\left(\frac{y^2}{2}\right)}. \quad (3.58)$$

Let us consider the LHS of (3.58). We have $0 < y - \alpha = \gamma \sqrt{f_s \tau} < -\alpha$; therefore, we have $0 < -y < -\alpha$. Apply the Cauchy-Schwarz inequality to $-y$ and $y - \alpha$, we have the following

$$0 < -y(y - \alpha) \leq \left(\frac{-y + y - \alpha}{2}\right)^2 = \frac{\alpha^2}{4}. \quad (3.59)$$

Hence

$$\frac{1}{-y(y - \alpha)} \geq \frac{4}{\alpha^2} = \frac{4}{(2\gamma + 1)(\mathcal{Q}^{-1}(\bar{\mathcal{P}}_d))^2} > 1. \quad (3.60)$$

It can be observed that the RHS of (3.58) is less than 1. Therefore, (3.58) holds, which implies that (3.49) and (3.48) also hold. \square

Finally, the last property holds because because $\Pr(n = n_0) < 1$ and conditional throughput are all bounded from above. Therefore, we have completed the proof of Proposition 1.

3.9.2 Proof of Proposition 2

To prove the properties stated in Proposition 2, we first find the derivative of $\widetilde{\mathcal{N}}\mathcal{J}(\tau)$. Again, it can be verified that $\frac{\mathcal{P}_i \mathcal{P}_s PS}{T}$ is almost a constant for different n_0 . To demonstrate the proof for the proposition, we substitute this term as a constant value, denoted as \mathcal{K} , in the throughput formula. In addition, for large T , $\left\lfloor \frac{T-\tau}{T_{sd}} \right\rfloor$ is very close to $\frac{T-\tau}{T_{sd}}$. Therefore, $\widetilde{\mathcal{N}}\mathcal{J}$ can be accurately approximated as

$$\widetilde{\mathcal{N}}\mathcal{J}(\tau) = \sum_{n_0=1}^N \mathcal{K} C_N^{n_0} (T - \tau) (1 - x^M)^{n_0} x^{M(N-n_0)} (1 - x), \quad (3.61)$$

where $\mathcal{K} = \frac{P_t P_s P S}{T}$, and $x = P_{busy}$. Now, let us define the following function

$$f'(x) = (1 - x^M)^{n_0} x^{M(N-n_0)} (1 - x). \quad (3.62)$$

Then, we have

$$\frac{\partial f'}{\partial x} = f'(x) \left[\frac{-1}{1-x} - \frac{Mn_0}{1-x^M} x^{M-1} + \frac{M(N-n_0)}{x} \right], \quad (3.63)$$

and $\frac{\partial x}{\partial \tau}$ is the same as (3.45). Hence, the first derivation of $\widetilde{\mathcal{N}\mathcal{J}}(\tau)$ can be written as

$$\begin{aligned} \frac{\partial \widetilde{\mathcal{N}\mathcal{J}}(\tau)}{\partial \tau} &= \sum_{n_0=1}^N \mathcal{K} C_N^{n_0} \left[-f'(x) + (T - \tau) \frac{\partial f'}{\partial x} \frac{\partial x}{\partial \tau} \right] \\ &= \sum_{n_0=1}^N \mathcal{K} C_N^{n_0} f'(x) \times \\ &\quad \left[(T - \tau) \left[\frac{1}{1-x} + \frac{Mn_0}{1-x^M} x^{M-1} - \frac{M(N-n_0)}{x} \right] \right. \\ &\quad \left. \times \mathcal{P}(\mathcal{H}_0) \gamma \sqrt{\frac{f_s}{8\pi\tau}} \exp\left(-\frac{(\alpha + \gamma \sqrt{f_s \tau})^2}{2}\right) - 1 \right]. \end{aligned} \quad (3.64)$$

From (3.23), the range of x , namely \mathbb{R}_x can be expressed as $[\mathcal{P}_d \mathcal{P}(\mathcal{H}_1), \mathcal{P}(\mathcal{H}_0) + \mathcal{P}_d \mathcal{P}(\mathcal{H}_1)]$. Now, it can be observed that

$$\lim_{\tau \rightarrow T} \frac{\partial \widetilde{\mathcal{N}\mathcal{J}}(\tau)}{\partial \tau} = - \sum_{n_0=1}^N \mathcal{K} C_N^{n_0} f'(x) < 0. \quad (3.65)$$

Therefore, the second property of Proposition 2 holds.

Now, let us define the following quantity

$$\mathcal{K}'_\tau = \sum_{n_0=1}^N C_N^{n_0} f'(x) \left[\frac{1}{1-x} + \frac{Mn_0 x^{M-1}}{1-x^M} - \frac{M(N-n_0)}{x} \right]. \quad (3.66)$$

Then, it can be seen that $\lim_{\tau \rightarrow 0} \frac{\partial \widetilde{\mathcal{N}\mathcal{J}}(\tau)}{\partial \tau} = +\infty > 0$ if $\mathcal{K}'_\tau > 0, \forall M, N, x \in \mathbb{R}_x$. This last property is stated and proved in the following lemma.

Lemma 4: $\mathcal{K}'_\tau > 0, \forall M, N, x \in \mathbb{R}_x$.

Proof. Making some manipulations to (3.66), we have

$$\begin{aligned} \mathcal{K}'_\tau &= \left(1 - \frac{(1-x)M}{x}\right) \sum_{n_0=1}^N C_N^{n_0} (1-x^M)^{n_0} x^{M(N-n_0)} \\ &\quad + \frac{M(1-x)}{x(1-x^M)} \sum_{n_0=1}^N C_N^{n_0} n_0 (1-x^M)^{n_0} x^{M(N-n_0)}. \end{aligned} \quad (3.67)$$

It can be observed that $\sum_{n_0=1}^N C_N^{n_0} (1-x^M)^{n_0} x^{M(N-n_0)}$ and $\sum_{n_0=1}^N C_N^{n_0} n_0 (1-x^M)^{n_0} x^{M(N-n_0)}$ represent a cumulative distribution function (CDF) and the mean of a binomial distribution [120] with parameter p , respectively missing the term corresponding to $n_0 = 0$ where $p = 1 - x^M$. Note that the CDF and mean of such a distribution are 1 and $Np = N(1 - x^M)$, respectively. Hence, (3.67) can be rewritten as

$$\mathcal{K}'_{\tau} = \left(1 - \frac{(1-x)M}{x}\right) (1-x^{MN}) + \frac{M(1-x)}{x(1-x^M)} N(1-x^M). \quad (3.68)$$

After some manipulations, we have

$$\mathcal{K}'_{\tau} = 1 - x^{MN} + MNx^{MN-1}(1-x) > 0, \quad \forall x. \quad (3.69)$$

Therefore, we have completed the proof. □

Hence, the first property of Proposition 1 also holds.

To prove the third property, let us consider the following equation $\frac{\partial \tilde{\mathcal{N}}(\tau)}{\partial \tau} = 0$. After some manipulations, we have the following equivalent equation

$$g(\tau) = h'(\tau), \quad (3.70)$$

where

$$g(\tau) = \left(\alpha + \gamma\sqrt{f_s\tau}\right)^2, \quad (3.71)$$

$$h'(\tau) = 2 \log \left(\mathcal{P}(\mathcal{H}_0) \gamma \sqrt{\frac{f_s}{8\pi} \frac{T-\tau}{\sqrt{\tau}}} \right) + h'_1(x), \quad (3.72)$$

$$h'_1(x) = 2 \log \frac{\mathcal{K}'_{\tau}}{\sum_{n_0=1}^N C_N^{n_0} f'(x)}, \quad (3.73)$$

K'_{τ} is given in (3.66). We have the following result for $h'(\tau)$.

Lemma 5: $h'(\tau)$ monotonically decreases in τ .

Proof. The derivative of $h'(\tau)$ can be written as

$$\frac{\partial h'}{\partial \tau} = \frac{-1}{\tau} - \frac{2}{T-\tau} + \frac{\partial h'_1}{\partial \tau}. \quad (3.74)$$

In the following, we will show that $\frac{\partial h'_1}{\partial x} > 0$ for all $x \in \mathbb{R}_x$, all M and N , and $\frac{\partial x}{\partial \tau} < 0$. Hence $\frac{\partial h'_1}{\partial \tau} = \frac{\partial h'_1}{\partial x} \frac{\partial x}{\partial \tau} < 0$. From this, we have $\frac{\partial h'_1}{\partial \tau} < 0$; therefore, the property stated in lemma 5 holds.

We now show that $\frac{\partial h'_1}{\partial x} > 0$ for all $x \in \mathbb{R}_x$, all M and N . Substitute \mathcal{K}'_τ in (3.69) to (3.73) and exploit the property of the CDF of the binomial distribution function, we have

$$\begin{aligned} h'_1(x) &= 2 \log \frac{1-x^{MN} + MNx^{MN-1}(1-x)}{(1-x) \sum_{n_0=1}^N C_N^{n_0} (1-x^M)^{n_0} x^{M(N-n_0)}} \\ &= 2 \log \frac{1-x^{MN} + MNx^{MN-1}(1-x)}{(1-x)(1-x^{MN})}. \end{aligned} \quad (3.75)$$

Taking the first derivative of $h'_1(x)$ and performing some manipulations, we obtain

$$\frac{\partial h'_1}{\partial x} = 2 \frac{\left(\begin{array}{l} r(r-1)x^{r-2}(1-x)^2(1-x^r) \\ +(1-x^r)^2 + r^2x^{2(r-1)}(1-x)^2 \end{array} \right)}{(1-x^r + rx^{(r-1)}(1-x))(1-x)(1-x^r)}, \quad (3.76)$$

where $r = MN$. It can be observed that there is no negative term in (3.76); hence, $\frac{\partial h'_1}{\partial x} > 0$ for all $x \in \mathbb{R}_x$, all M and N . Therefore, we have proved the lemma. \square

To prove the third property, we show that $g(\tau)$ and $h'(\tau)$ intersect only once in the range of $[0, T]$. This will be done using the same approach as that in Appendix A. Specifically, we will consider two regions Ω_1 and Ω_2 and prove two properties stated in Lemma 2 for this case. As in Appendix A, the third property holds if we can prove $-\frac{1}{\tau} + \frac{\partial h'_1}{\partial \tau} < \frac{\partial g}{\partial \tau}$. It can be observed that all steps used to prove this inequality are the same as those in the proof of (3.48) for Proposition 1. Hence, we need to prove

$$\frac{\partial h'_1}{\partial x} > \frac{2}{1-x}. \quad (3.77)$$

Substitute $\frac{\partial h'_1}{\partial x}$ from (3.76) to (3.77), this inequality reduces to

$$2 \frac{\left(\begin{array}{l} r(r-1)x^{r-2}(1-x)^2(1-x^r) \\ +(1-x^r)^2 + r^2x^{2(r-1)}(1-x)^2 \end{array} \right)}{(1-x^r + rx^{(r-1)}(1-x))(1-x)(1-x^r)} > \frac{2}{1-x}. \quad (3.78)$$

After some manipulations, this inequality becomes equivalent to

$$rx^{(r-2)}(1-x)^2 [r - (1+x+x^2+\dots+x^{(r-1)})] > 0. \quad (3.79)$$

It can be observed that $0 < x < 1$ and $0 < x^i < 1$, $i \in [0, r - 1]$. Hence, we have $r - (1 + x + x^2 + \cdots + x^{(r-1)}) > 0$ which shows that (3.79) indeed holds. Therefore, (3.77) holds and we have completed the proof of the third property. Finally, the last property of the Proposition is obviously correct. Hence, we have completed the proof of Proposition 2.

Chapter 4

Channel Assignment With Access Contention Resolution for Cognitive Radio Networks

The content of this chapter was published in IEEE Transactions on Vehicular Technology in the following paper:

L. T. Tan, and L. B. Le, “Channel Assignment With Access Contention Resolution for Cognitive Radio Networks,” *IEEE Trans. Veh. Tech.*, vol. 61, no. 6, pp. 2808–2823, 2012.

4.1 Abstract

In this paper, we consider the channel allocation problem for throughput maximization in cognitive radio networks with hardware-constrained secondary users. In particular, we assume that secondary users (SUs) exploit spectrum holes on a set of channels where each SU can use at most one available channel for communication. We present the optimal brute-force search algorithm and its complexity for this non-linear integer optimization problem. Because the optimal solution has exponential complexity with the numbers of channels and SUs, we develop two low-complexity channel assignment algorithms that can efficiently utilize spectrum opportunities on these channels. In the first algorithm, SUs are assigned distinct sets of channels. We show that this algorithm achieves the maximum throughput limit if the number of channels is sufficiently large. In addition, we propose an overlapping channel assignment algorithm, that can improve the throughput performance compared to the non-overlapping channel assignment counterpart. Moreover, we design a distributed

MAC protocol for access contention resolution and integrate it into the overlapping channel assignment algorithm. We then analyze the saturation throughput and the complexity of the proposed channel assignment algorithms. We also present several potential extensions, including the development of greedy channel assignment algorithms under max-min fairness criterion and throughput analysis, considering sensing errors. Finally, numerical results are presented to validate the developed theoretical results and illustrate the performance gains due to the proposed channel assignment algorithms.

4.2 Introduction

Emerging broadband wireless applications have been demanding unprecedented increase in radio spectrum resources. As a result, we have been facing a serious spectrum shortage problem. However, several recent measurements reveal very low spectrum utilization in most useful frequency bands [2]. Cognitive radio technology is a promising technology that can fundamentally improve the spectrum utilization of licensed frequency bands through secondary spectrum access. However, transmissions from primary users (PUs) should be satisfactorily protected from secondary spectrum access due to their strictly higher access priority.

Protection of primary communications can be achieved through interference avoidance or interference control approach (i.e., spectrum overlay or spectrum underlay) [2]. For the interference control approach, transmission powers of SUs should be carefully controlled so that the aggregated interference they create at primary receivers does not severely affect ongoing primary communications [11]. In most practical scenarios where direct coordination between PUs and SUs is not possible and/or if distributed communications strategies are desired, it would be very difficult to maintain these interference constraints. The interference avoidance approach instead protects primary transmissions by requiring SUs to perform spectrum sensing to discover spectrum holes over which they can transmit data [5], [48]. This paper focuses on developing efficient channel assignment algorithms for a cognitive radio network with hardware-constrained secondary nodes using the interference avoidance spectrum sharing approach.

In particular, we consider the scenario where each SU can exploit at most one available channel for communications. This can be the case if SUs are equipped with only one radio employing a narrow-band RF front end [104]. In addition, it is assumed that white spaces are so dynamic that it is not affordable for each SU to sense all channels to discover available ones

and/or to exchange sensing results with one another. Under this setting, we are interested in determining a set of channels allocated to each SU in advance so that maximum network throughput can be achieved in a distributed manner. To the best of our knowledge, this important problem has not been considered before. The contributions of this paper can be summarized as follows.

- We formulate the channel assignment problem for throughput maximization as an integer optimization problem. We then derive user and total network throughput for the case SUs are assigned distinct sets of channels. We present the optimal brute-force search algorithm and analyze its complexity.
- We develop two greedy non-overlapping and overlapping channel assignment algorithms to solve the underlying NP-hard problem. We prove that the proposed non-overlapping channel assignment algorithm achieves the maximum throughput as the number of channels is sufficiently large. For the overlapping channel assignment algorithm, we design a medium access control (MAC) protocol for access contention resolution and we integrate the MAC protocol overhead analysis into the channel assignment algorithm.
- We analyze the saturation throughput and complexity of the proposed channel assignment algorithms. Moreover, we investigate the impact of contention collisions on the developed throughput analytical framework.
- We show how to extend the proposed channel assignment algorithms when max-min fairness is considered. We also extend the throughput analytical model to consider sensing errors and propose an alternative MAC protocol that can relieve congestion on the control channel.
- We demonstrate through numerical studies the interactions among various MAC protocol parameters and suggest its configuration. We show that the overlapping channel assignment algorithm can achieve noticeable network throughput improvement compared to the non-overlapping counterpart. In addition, we present the throughput gains due to both proposed channel assignment algorithms compared to the round-robin algorithms, which do not exploit the heterogeneity in the channel availability probabilities.

The remaining of this paper is organized as follows. In Section 4.3, we discuss important related works on spectrum sharing algorithms and MAC protocols. Section 4.4 describes the

system model and problem formulation. We present the non-overlapping channel assignment algorithm and describe its performance in Section 4.5. The overlapping channel assignment and the corresponding MAC protocol are developed in Section 4.6. Performance analysis of the overlapping channel assignment algorithm and the MAC protocol is presented in Section 4.7. Several potential extensions are discussed in Section 4.8. Section 4.9 demonstrates numerical results followed by concluding remarks in Section 4.10.

4.3 Related Works

Developing efficient spectrum sensing and access mechanisms for cognitive radio networks has been a very active research topic in the last several years [5, 16–22, 47, 62, 63, 102, 122–124]. A great survey of recent works on MAC protocol design and analysis is given in [47]. In [5], it was shown that by optimizing the sensing time, a significant throughput gain can be achieved for a SU. In [22], we extended the result in [5] to the multi-user setting where we design, analyze, and optimize a MAC protocol to achieve optimal tradeoff between sensing time and contention overhead. In fact, in [22], we assumed that each SU can use all available channels simultaneously. Therefore, the channel assignment problem and the exploitation of multi-user diversity do not exist in this setting, which is the topic of our current paper. Another related effort along this line was conducted in [16] where sensing-period optimization and optimal channel-sequencing algorithms were proposed to efficiently discover spectrum holes and to minimize the exploration delay.

In [17], a control-channel-based MAC protocol was proposed for secondary users to exploit white spaces in the cognitive ad hoc network setting. In particular, the authors of this paper developed both random and negotiation-based spectrum sensing schemes and performed throughput analysis for both saturation and non-saturation scenarios. There exists several other synchronous cognitive MAC protocols, which rely on a control channel for spectrum negotiation and access including those in [18–21, 63]. A synchronous MAC protocols without using a control channel was proposed and studied in [62]. In [102], a MAC layer framework was developed to dynamically reconfigure MAC and physical layer protocols. Here, by monitoring current network metrics the proposed framework can achieve great performance by selecting the best MAC protocol and its corresponding configuration.

In [122], a power-controlled MAC protocol was developed to efficiently exploit spectrum access opportunities while satisfactorily protecting PUs by respecting interference constraints. Another power control framework was described in [123], which aims to meet the

rate requirements of SUs and interference constraints of PUs. A novel clustering algorithm was devised in [124] for network formation, topology control, and exploitation of spectrum holes in a cognitive mesh network. It was shown that the proposed clustering mechanism can efficiently adapt to the changes in the network and radio transmission environment.

Optimal sensing and access design for cognitive radio networks were designed by using optimal stopping theory in [105]. In [68], a multichannel medium access control (McMAC) protocol was proposed taking into account the distance among users so that the white spaces can be efficiently exploited while satisfactorily protecting PUs. Different power and spectrum allocation algorithms were devised to maximize the secondary network throughput in [23, 24, 106]. Optimization of spectrum sensing and access in which either cellular or TV bands can be employed was performed in [25].

In [26], cooperative sequential spectrum sensing and packet scheduling were designed for cognitive radios which are equipped with multiple spectrum sensors. An energy-efficient MAC protocol was proposed for cognitive radio networks in [27]. Spectrum sensing, access, and power control algorithms were developed considering QoS protection for PUs and QoS provisioning for SUs in [28, 29]. Finally, a channel hopping based MAC protocol was proposed in [30] for cognitive radio networks to alleviate the congestion problem in the fixed control channel design. All these existing works, however, did not consider the scenario where cognitive radios have hardware constraints which allows them to access at most one channel at any time. Moreover, exploiting the multichannel diversity through efficient channel assignment is very critical to optimize the throughput performance of the secondary network for this problem. We will investigate this problem considering its unique design issues in this paper.

4.4 System Model and Problem Formulation

4.4.1 System Model

We consider a collocated cognitive radio network in which M SUs exploit spectrum opportunities in N channels. We assume that any SU can hear the transmissions of other SUs. In addition, each SU can use at most one channel for its data transmission. In addition, time is divided fixed-size cycle where SUs perform sensing on assigned channels at the beginning of each cycle to explore available channels for communications. We assume that perfect sensing can be achieved with no sensing error. Extension to the imperfect spectrum sensing

will be discussed in Section 4.8.2. It is assumed that SUs transmit at a constant rate with the normalized value of one.

4.4.2 Problem Formulation

We are interested in performing channel assignment to maximize the system throughput. Let T_i denote the throughput achieved by SU i . Let x_{ij} describe the channel assignment decision where $x_{ij} = 1$ if channel j is assigned to SU i and $x_{ij} = 0$, otherwise. The throughput maximization problem can be formally written as follows:

$$\max_{\mathbf{x}} \sum_{i=1}^M T_i. \quad (4.1)$$

For non-overlapping channel assignments, we have following constraints

$$\sum_{i=1}^M x_{ij} = 1, \quad \text{for all } j. \quad (4.2)$$

We can derive the throughput achieved by SU i for non-overlapping channel assignment as follows. Let S_i be the set of channels solely assigned to SU i . Let p_{ij} be the probability that channel j is available at SU i . For simplicity, we assume that p_{ij} are independent from one another. This assumption holds when each SU impacts different set of PUs on each channel. This can indeed be the case because spectrum holes depend on space. Note, however, that this assumption can be relaxed if the dependence structure of these probabilities is available. Under this assumption, T_i can be calculated as

$$T_i = 1 - \prod_{j \in S_i} \bar{p}_{ij} = 1 - \prod_{j=1}^N (\bar{p}_{ij})^{x_{ij}} \quad (4.3)$$

where $\bar{p}_{ij} = 1 - p_{ij}$ is the probability that channel j is not available for SU i . In fact, $1 - \prod_{j \in S_i} \bar{p}_{ij}$ is the probability that there is at least one channel available for SU i . Because each SU can use at most one available channel, its maximum throughput is 1. In the overlapping channel assignment scheme, constraints in (4.2) are not needed. From this calculation, it can be observed that the optimization problem (4.1)-(4.2) is a non-linear integer program, which is a NP-hard problem (interest readers can refer to Part VIII of reference [125] for detailed treatment of this hardness result).

4.4.3 Optimal Algorithm and Its Complexity

Due to the non-linear and combinatorial structure of the formulated channel assignment problem, it would be impossible to explicitly determine its optimal closed form solution. However, we can employ the brute-force search (i.e., exhaustive search) to determine the best channel assignment that results in the maximum total throughput. In particular, we can enumerate all possible channel assignment solutions then determine the best one by comparing their achieved throughput. This solution method requires a throughput analytical model that calculates the throughput for any particular channel assignment solution. We will develop such a model in Section 4.7.1 of this paper.

We now quantify the complexity of the optimal brute-force search algorithm. Let us consider SU i (i.e., $i \in \{1, \dots, M\}$). Suppose we assign k channels to this SU i where $k \in \{1, \dots, N\}$. Then, there are C_N^k ways to do so. Since k can take any values in $k \in \{1, \dots, N\}$, the total number of ways to assign channels to SU i is $\sum_{k=1}^N C_N^k \approx 2^N$. Hence, the total number of ways to assign channels to all SUs is asymptotically equal to $(2^N)^M = 2^{NM}$. Recall that we need to calculate the throughputs achieved by M SUs for each potential assignment to determine the best one. Therefore, the complexity of the optimal brute-force search algorithm is $\mathcal{O}(2^{NM})$. Given the exponentially large complexity required to find the optimal channel assignment solution, we will develop sub-optimal and low-complexity channel assignment algorithms in the following sections. In particular, we consider two different channel assignment schemes: 1) non-overlapping channel assignment and 2) overlapping channel assignment.

4.5 Non-overlapping Channel Assignment Algorithm

We develop a low-complexity algorithm for non-overlapping channel assignment in this section. Recall that \mathcal{S}_i is the set of channels solely assigned for SU i (i.e., $\mathcal{S}_i \cap \mathcal{S}_j = \emptyset$, $i \neq j$). The greedy channel assignment algorithm iteratively allocates channels to SUs that achieves the maximum increase in the throughput. A detailed description of the proposed algorithm is presented in Alg. 2. In each channel allocation iteration, each SU i calculates its increase in throughput if the best available channel (i.e., channel $j_i^* = \arg \max_{j \in \mathcal{S}_a} p_{ij}$) is allocated. This increase in throughput can be calculated as follows:

$$\Delta T_i = T_i^a - T_i^b = \left[1 - (1 - p_{ij_i^*}) \prod_{j \in \mathcal{S}_i} (1 - p_{ij}) \right] - \left[1 - \prod_{j \in \mathcal{S}_i} (1 - p_{ij}) \right] = p_{ij_i^*} \prod_{j \in \mathcal{S}_i} (1 - p_{ij}) \quad (4.4)$$

4.5 Non-overlapping Channel Assignment Algorithm

Based on (4.4), it can be observed that ΔT_i will quickly decrease over allocation iterations because $\prod_{j \in \mathcal{S}_i} (1 - p_{ij})$ tends to zero as the set \mathcal{S}_i is expanded. We have the following property for the resulting channel assignment due to Alg. 2.

Algorithm 2 NON-OVERLAPPING CHANNEL ASSIGNMENT

- 1: Initialize the set of available channels $\mathcal{S}_a := \{1, 2, \dots, N\}$ and $\mathcal{S}_i := \emptyset$ for $i = 1, 2, \dots, M$
 - 2: **for** $i = 1$ to M **do**
 - 3: $j_i^* = \underset{j \in \mathcal{S}_a}{\operatorname{argmax}} p_{ij}$
 - 4: **if** $\mathcal{S}_i \neq \emptyset$ **then**
 - 5: Find $\Delta T_i = T_i^a - T_i^b$, where T_i^a and T_i^b is the throughputs after and before assigning channel j_i^* .
 - 6: **else**
 - 7: Find $\Delta T_i = p_{ij_i^*}$,
 - 8: **end if**
 - 9: **end for**
 - 10: $i^* = \operatorname{argmax}_i \Delta T_i$.
 - 11: Assign channel $j_{i^*}^*$ to user i^* .
 - 12: Update $\mathcal{S}_a = \mathcal{S}_a \setminus j_{i^*}^*$.
 - 13: If \mathcal{S}_a is empty, terminate the algorithm. Otherwise, return to step 2.
-

Proposition 1: If we have $N \gg M$, then the throughput achieved by any SU i due to Alg. 2 is very close to the maximum value of 1.

Proof. This proposition can be proved by showing that if the number of channels is much larger than the number of SUs (i.e., $N \gg M$) then each SU will be assigned a large number of channels. Recall that Alg. 2 assigns channels to a particular SU i based on the increase-in-throughput metric ΔT_i . This property can be proved by observing that if a particular SU i has been assigned a large number of channels, its ΔT_i is very close to zero. Therefore, other SUs who have been assigned a small number of channels will have a good chance to receive more channels. As a result, all SUs are assigned a large number of channels if $N \gg M$. According to (4.3), throughput achieved by SU i will reach its maximum value of 1 if its number of assigned channels is sufficiently large. Hence, we have proved the proposition. \square

In practice, we do not need a very large number of channels to achieve the close-to-maximum throughput. In particular, if each channel is available for secondary spectrum access with probability at least 0.8 then the throughput achieved by a SU assigned three channels is not smaller than $1 - (1 - 0.8)^3 = 0.992$, which is less than 1% below the maximum throughput. Note that after running Alg. 2, we can establish the set of channels allocated to each SU, from which we calculate its throughput by using (4.3). Then, the total throughput of the secondary network can be calculated by summing the throughputs of all SUs. When the number of channel is not sufficiently large, we can potentially improve the system

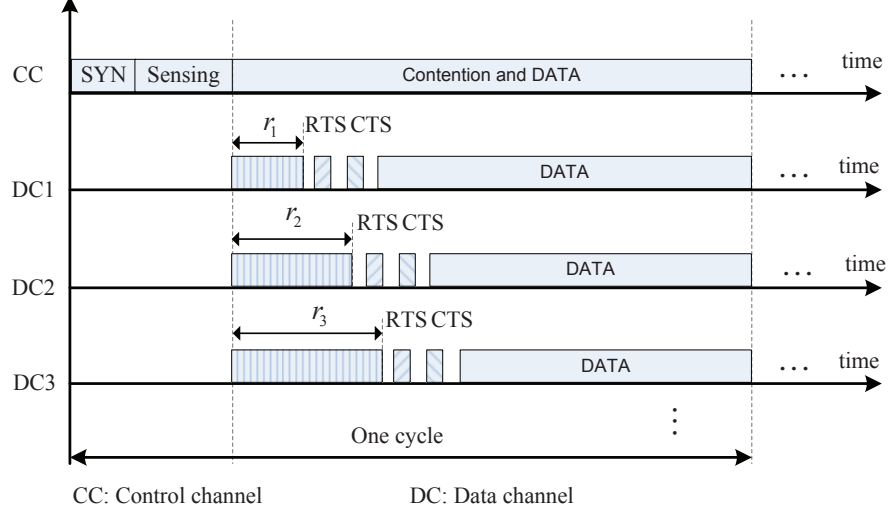


Figure 4.1: Timing diagram for the proposed multi-channel MAC protocol.

throughput by allowing overlapping channel assignment. We develop such an overlapping channel assignment algorithm in the next section.

4.6 Overlapping Channel Assignment

Overlapping channel assignment can improve the network throughput by exploiting the multiuser diversity gain. However, a MAC protocol is needed to resolve the access contention under the overlapping channel assignments. The MAC protocol incurs overhead that offsets the throughput gain due to the multiuser diversity. Hence, a sophisticated channel assignment algorithm is needed to balance the protocol overhead and throughput gain.

4.6.1 MAC Protocol

Let \mathcal{S}_i be the set of channels solely assigned for SU i and $\mathcal{S}_i^{\text{com}}$ be the set of channels assigned for SU i and some other SUs. Let denote $\mathcal{S}_i^{\text{tot}} = \mathcal{S}_i \cup \mathcal{S}_i^{\text{com}}$, which is the set of all channels assigned to SU i . Assume that there is one control channel, which is always available and used for access contention resolution. We consider the following MAC protocol run by any particular SU i , which belongs the class of synchronized MAC protocol [103]. The MAC protocol is illustrated in Fig. 4.1 where synchronization and sensing phases are employed before the channel contention and transmission phase in each cycle. A synchronization message is exchanged among SUs during the synchronization phase to establish the same

4.6 Overlapping Channel Assignment

starting epoch of each cycle. After sensing the assigned channels in the sensing phase, each SU i proceeds as follows. If there is at least one channel in \mathcal{S}_i available, then SU i chooses one of these available channels randomly for communication. If this is not the case, SU i will choose one available channel in $\mathcal{S}_i^{\text{com}}$ randomly (if there is any channel in this set available). For brevity, we simply call *users* instead of *SUs* when there is no confusion. Then, it chooses a random backoff value which is uniformly distributed in the interval $[0, W - 1]$ (i.e., W is the contention window) and starts decreasing its backoff counter while listening on the control channel.

Table 4.1: Channel Assignment Example (M=3, N =6)

	\mathcal{S}_1	\mathcal{S}_2	\mathcal{S}_3	$\mathcal{S}_1^{\text{com}}$	$\mathcal{S}_2^{\text{com}}$	$\mathcal{S}_3^{\text{com}}$
C1	x					
C2		x				
C3			x			
C4				x	x	
C5					x	x
C6				x	x	x

If it overhears transmissions of RTS/CTS from any other users, it will freeze from decreasing its backoff counter until the control channel is free again. As soon as a user's backoff counter reaches zero, its transmitter transmits an RTS message containing a chosen channel to its receiver. If the receiver successfully receives the RTS, it will reply with CTS and user i starts its communication on the chosen channel for the remaining of the cycle. If the RTS/CTS message exchange fails due to collisions, the corresponding user will quit the contention and wait until the next cycle. In addition, by overhearing RTS/CTS messages of neighboring users, which convey information about the channels chosen for communications, other users compared these channels with their chosen ones.

Any user who has its chosen channel coincides with the overheard channels quits the contention and waits until the next cycle. Otherwise, it will continue to decrease its backoff counter before exchanging RTS/CTS messages. Note that the fundamental aspect that makes this MAC protocol different from that proposed in [22] is that in [22] we assumed each winning user can use all available channels for communications while at most one available channel can be exploited by hardware-constrained secondary users in the current paper. Therefore, the channel assignment problem does not exist for the setting considered

in [22]. One example of overlapping channel assignment for three users and six channels is illustrated in Table 4.1. where channel assignments are indicated by an “x”.

Algorithm 3 OVERLAPPING CHANNEL ASSIGNMENT

```

1: Initialize the sets of allocated channels for all users  $\mathcal{S}_i := \emptyset$  for  $i = 1, 2, \dots, M$  and  $\delta_0$ 
2: Run Alg. 2 to obtain non-overlapping channel assignment solution.
3: Let the group of channels shared by  $l$  users be  $\mathcal{G}_l$  and  $\mathcal{U}_j$  be the set of users sharing channel  $j$  and set  $\mathcal{U}_j^{\text{temp}} := \mathcal{U}_j, \forall j = 1, 2, \dots, N$ .
4: continue := 1;  $h = 1$ ; updooverhead := 0
5: while continue = 1 do
6:   Find the group of channels shared by  $h$  users,  $\mathcal{G}_h$ 
7:   for  $j = 1$  to  $|\mathcal{G}_h|$  do
8:     for  $l = 1$  to  $M$  do
9:       if  $l \in \mathcal{U}_j$  then
10:         $\Delta T_l^{h,\text{est}}(j) = 0$ 
11:       else
12:        User  $l$  calculates  $\Delta T_l^{h,\text{est}}(j)$  assuming channel  $j$  is allocated to user  $l$ 
13:       end if
14:     end for
15:      $l_j^* = \text{argmax}_l \Delta T_l^{h,\text{est}}(j)$ .
16:   end for
17:    $j_{l^*}^* = \text{argmax}_j \Delta T_{l^*}^{h,\text{est}}(j)$ .
18:   if  $\Delta T_{l^*}^{h,\text{est}}(j_{l^*}^*) \leq \epsilon$  and updooverhead = 1 then
19:     Set: continue := 0
20:     Go to step 35
21:   end if
22:   if  $\Delta T_{l^*}^{h,\text{est}}(j_{l^*}^*) > \epsilon$  then
23:     Temporarily assign channel  $j_{l^*}^*$  to user  $l^*$ , i.e., update  $\mathcal{U}_{j_{l^*}^*}^{\text{temp}} = \mathcal{U}_{j_{l^*}^*} \cup \{l^*\}$ ;
24:     Calculate  $W$  and  $\delta$  with  $\mathcal{U}_{j_{l^*}^*}^{\text{temp}}$  by using methods in Sections 4.6.3 and 4.6.4, respectively.
25:     if  $|\delta - \delta_0| > \epsilon_\delta$  then
26:       Set: updooverhead := 1
27:       Return Step 7 using the updated  $\delta_0 = \delta$ 
28:     else
29:       Update  $\mathcal{U}_{j_{l^*}^*} := \mathcal{U}_{j_{l^*}^*}^{\text{temp}}$  (i.e., assign channel  $j_{l^*}^*$  to user  $l^*$ ), calculate  $W$  and  $\delta_0$  with  $\mathcal{U}_{j_{l^*}^*}$ , and update  $\mathcal{G}_h$ 
30:       Update: updooverhead := 0
31:     end if
32:   end if
33:   Return Step 7
34:    $h = h + 1$ 
35: end while

```

Remark 1: We focus on the saturation-buffer scenario in this paper. In practice, cognitive radios may have low backlog or, sometimes, even empty buffers. In addition, because the data transmission phase is quite large compared to a typical packet size, we should allow users to transmit several packets to completely fill the transmission phase in our MAC design. This condition can be realized by allowing only sufficiently backlogged users to participate in the sensing and access contention processes.

4.6.2 Overlapping Channel Assignment Algorithm

We develop an overlapping channel assignment algorithm that possesses two phases as follows. We run Alg. 2 to obtain the non-overlapping channel assignment solution in the first phase. Then, we perform overlapping channel assignment by allocating channels that have been assigned to some users to other users in the second phase. We devise a greedy overlapping channel assignment algorithm using the increase-of-throughput metric similar to that employed in Alg. 2. However, calculation of this metric exactly turns out to be a complicated task. Hence, we employ an estimate of the increase-of-throughput, which is derived as follows to perform channel assignment assuming that the MAC protocol overhead is $\delta < 1$. In fact, δ depends on the outcome of the channel assignment algorithm (i.e., sets of channels assigned to different users). We will show how to calculate δ and integrate it into this channel assignment algorithm later.

Consider a case where channel j is the common channel of users $i_1, i_2, \dots, i_{\mathcal{MS}}$. Here, \mathcal{MS} is the number of users sharing this channel. We are interested in estimating the increase in throughput for a particular user i if channel j is assigned to this user. Indeed, this increase of throughput can be achieved because user i may be able to exploit channel j if this channel is not available or not used by other users $i_1, i_2, \dots, i_{\mathcal{MS}}$. To estimate the increase of throughput, in the remaining of this paper we are only interested in a practical scenario where all p_{ij} are close to 1 (e.g., at least 0.8). This assumption would be reasonable, given several recent measurements reveal that spectrum utilization of useful frequency bands is very low (e.g., less than 15%). Under this assumption, we will show that the increase-of-throughput for user i can be estimated as

$$\Delta T_i^{\mathcal{MS}, \text{est}}(j) = (1 - 1/\mathcal{MS})(1 - \delta)p_{ij} \left(\prod_{h \in \mathcal{S}_i} \bar{p}_{ih} \right) \left(1 - \prod_{h \in \mathcal{S}_i^{\text{com}}} \bar{p}_{ih} \right) \sum_{k=1}^{\mathcal{MS}} \left[\bar{p}_{i_k j} \left(\prod_{q=1, q \neq k}^{\mathcal{MS}} p_{i_q j} \right) \right] \quad (4.5)$$

$$+ (1 - \delta)p_{ij} \prod_{h \in \mathcal{S}_i} \bar{p}_{ih} \prod_{h \in \mathcal{S}_i^{\text{com}}} \bar{p}_{ih} \prod_{q=1}^{\mathcal{MS}} p_{i_q j} \prod_{q=1}^{\mathcal{MS}} \left(1 - \prod_{h \in \mathcal{S}_{i_q}} \bar{p}_{i_q h} \right) \quad (4.6)$$

$$+ (1 - 1/\mathcal{MS})(1 - \delta)p_{ij} \prod_{h \in \mathcal{S}_i} \bar{p}_{ih} \left(1 - \prod_{h \in \mathcal{S}_i^{\text{com}}} \bar{p}_{ih} \right) \prod_{q=1}^{\mathcal{MS}} p_{i_q j} \prod_{q=1}^{\mathcal{MS}} \left(1 - \prod_{h \in \mathcal{S}_{i_q}} \bar{p}_{i_q h} \right) \quad (4.7)$$

This estimation is obtained by listing all possible scenarios/events in which user i can exploit channel j to increase its throughput. Because the user throughput is bounded by 1, we only count events that occur with non-negligible probabilities. In particular, under the assumption that p_{ij} are high (or \bar{p}_{ij} are small) we only count events whose probabilities have

4.6 Overlapping Channel Assignment

at most two such elements \bar{p}_{ij} in the product. In addition, we can determine the increase of throughput for user i by comparing its achievable throughput before and after channel j is assigned to it. It can be verified we have the following events for which the average increases of throughput are significant.

- Channel j is available for all users i and i_q , $q = 1, 2, \dots, \mathcal{MS}$ except i_k where $k = 1, 2, \dots, \mathcal{MS}$. In addition, all channels in S_i are not available and there is at least one channel in $\mathcal{S}_i^{\text{com}}$ available for user i . User i can achieve a maximum average throughput of $1 - \delta$ by exploiting channel j , while its minimum average throughput before being assigned channel i is at least $(1 - \delta)/\mathcal{MS}$ (when user i needs to share the available channel in $\mathcal{S}_i^{\text{com}}$ with \mathcal{MS} other users). The increase of throughput for this case is at most $(1 - 1/\mathcal{MS})(1 - \delta)$ and the upper-bound for the increase of throughput of user i is written in (4.5).
- Channel j is available for user i and all users i_q , $q = 1, 2, \dots, \mathcal{MS}$ but each user i_q uses other available channel in \mathcal{S}_{i_q} for his/her transmission. Moreover, there is no channel in $\mathcal{S}_i^{\text{tot}}$ available. In this case, the increase of throughput for user i is $1 - \delta$ and the average increase of throughput of user i is written in (4.6).
- Channel j is available for user i and all users i_q , $q = 1, 2, \dots, \mathcal{MS}$ but each user i_q uses other available channel in \mathcal{S}_{i_q} for transmission. Moreover, there is at least one channel in $\mathcal{S}_i^{\text{com}}$ available. In this case, the increase of throughput for user i is upper-bounded by $(1 - 1/\mathcal{MS})(1 - \delta)$ and the average increase of throughput of user i is written in (4.7).

The detailed description of the algorithm is given in Alg. 3. This algorithm has outer and inner loops where the outer loop increases the parameter h , which represents the maximum of users allowed to share any particular channel (i.e., \mathcal{MS} in the above estimation of the increase of throughput) and the inner loop performs channel allocation for one particular value of $h = \mathcal{MS}$. In each assignment iteration of the inner loop, we assign one “best” channel j to user i that achieves maximum $\Delta T_i^{h, \text{est}}(j)$. This assignment continues until the maximum $\Delta T_i^{h, \text{est}}(j)$ is less than a pre-determined number $\epsilon > 0$. As will be clear in the throughput analysis developed later, it is beneficial to maintain at least one channel in each set S_i . This case is because the throughput contributed by channels in S_i constitutes a significant fraction of the total throughput. Therefore, we will maintain this constraint when running Alg. 3.

4.6.3 Calculation of Contention Window

We show how to calculate contention window W so that collision probabilities among contending secondary users are sufficiently small. In fact, there is a trade-off between collision probabilities and the average overhead of the MAC protocol, which depends on W . In particular, larger values of W reduce collision probabilities at the cost of higher protocol overhead and vice versa. Because there can be several collisions during the contention phase each of which occurs if two or more users randomly choose the same value of backoff time. In addition, the probability of the first collision is largest because the number of contending users decreases for successive potential collisions.

Let \mathcal{P}_c be the probability of the first collision. In the following, we determine contention window W by imposing a constraint $\mathcal{P}_c \leq \epsilon_P$ where ϵ_P controls the collision probability and overhead tradeoff. Let us calculate \mathcal{P}_c as a function of W assuming that there are m secondary users in the contention phase. Without loss of generality, assume that the random backoff times of m users are ordered as $r_1 \leq r_2 \leq \dots \leq r_m$. The conditional probability of the first collision if there are m users in the contention stage can be written as

$$\begin{aligned} \mathcal{P}_c^{(m)} &= \sum_{j=2}^m \Pr(j \text{ users collide}) \\ &= \sum_{j=2}^m \sum_{i=0}^{W-2} C_m^j \left(\frac{1}{W}\right)^j \left(\frac{W-i-1}{W}\right)^{m-j} \end{aligned} \quad (4.8)$$

where each term in the double-sum represents the probability that j users collide when they choose the same backoff value equal to i . Hence, the probability of the first collision can be calculated as

$$\mathcal{P}_c = \sum_{m=2}^M \mathcal{P}_c^{(m)} \times \Pr\{m \text{ users contend}\}, \quad (4.9)$$

where $\mathcal{P}_c^{(m)}$ is given in (4.8) and $\Pr\{m \text{ users contend}\}$ is the probability that m users join the contention phase. To compute \mathcal{P}_c , we now derive $\Pr\{m \text{ users contend}\}$. It can be verified that user i joins contention if all channels in \mathcal{S}_i are busy and there is at least one channel in $\mathcal{S}_i^{\text{com}}$ available. The probability of this event can be written as

$$\begin{aligned} \mathcal{P}_{\text{con}}^{(i)} &= \Pr\{\text{all channels in } \mathcal{S}_i \text{ are busy, } \exists! \text{ some channels in } \mathcal{S}_i^{\text{com}} \text{ are available}\} \\ &= \left(\prod_{j \in \mathcal{S}_i} \bar{p}_{ij}\right) \left(1 - \prod_{j \in \mathcal{S}_i^{\text{com}}} \bar{p}_{ij}\right). \end{aligned} \quad (4.10)$$

The probability of the event that m users join the contention phase is

$$\Pr \{m \text{ users contend}\} = \sum_{n=1}^{C_M^m} \left(\prod_{i \in \Lambda_n} \mathcal{P}_{\text{con}}^{(i)} \right) \left(\prod_{j \in \Lambda_M \setminus \Lambda_n} \overline{\mathcal{P}}_{\text{con}}^{(j)} \right) \quad (4.11)$$

where Λ_n is one particular set of m users, Λ_M is the set of all M users ($\{1, 2, \dots, M\}$). Substitute the result in (4.11) into (4.9), we can calculate \mathcal{P}_c . Finally, we can determine W as

$$W = \min \{W \text{ such that } \mathcal{P}_c(W) \leq \epsilon_P\} \quad (4.12)$$

where for clarity we denote $\mathcal{P}_c(W)$, which is given in (4.9) as a function of W .

4.6.4 Calculation of MAC Protocol Overhead

Using the contention window calculated in (4.12), we can quantify the average overhead of the proposed MAC protocol. Toward this end, let r be the average value of the backoff value chosen by any SU. Then, we have $r = (W - 1)/2$ because the backoff counter value is uniformly chosen in the interval $[0, W - 1]$. As a result, average overhead can be calculated as follows:

$$\delta(W) = \frac{[W - 1]\theta/2 + t_{\text{RTS}} + t_{\text{CTS}} + 3t_{\text{SIFS}} + t_{\text{SEN}} + t_{\text{SYN}}}{T_{\text{cycle}}} \quad (4.13)$$

where θ is the time corresponding to one backoff unit; t_{RTS} , t_{CTS} , t_{SIFS} are the corresponding time of RTS, CTS and SIFS messages; t_{SEN} is the sensing time; t_{SYN} is the length of the synchronization message; and T_{cycle} is the cycle time.

4.6.5 Update δ inside Alg. 3

The overhead δ depends on the channel assignment outcome, which is not known when we are running Alg. 3. Therefore, in each allocation step we update δ based on the current channel assignment outcome. Because δ does not change much in two consecutive allocation decisions, Alg. 3 runs smoothly in practice.

4.6.6 Practical Implementation Issues

To perform channel assignment, we need to know p_{ij} for all users and channels. Fortunately, we only need to perform estimation of p_{ij} once these values change, which would be

infrequent in practice. These estimation and channel assignment tasks can be performed by one secondary node or collaboratively performed by several of them. For example, for the secondary network supporting communications between M secondary nodes and a single secondary base station (BS), the BS can take the responsibility of estimating p_{ij} and performing channel assignment. Once the channel assignment solution has been determined and forwarded to all SUs, each SU will perform spectrum sensing and run the underlying MAC protocol to access the spectrum in each cycle.

It is emphasized again that although sensing and MAC protocol are performed and run in every cycle, estimating p_{ij} and performing channel assignment (given these p_{ij}) are only performed if the values of p_{ij} change, which should be infrequent. Therefore, it would be affordable to estimate p_{ij} accurately by employing sufficiently long sensing time. This is because for most spectrum sensing schemes, including an energy detection scheme, mis-detection and false alarm probabilities tend to zero when the sensing time increases for a given sampling frequency [5, 48].

4.7 Performance Analysis

Suppose we have run Alg. 3 and obtained the set of users U_j associated with each allocated channel j . From this, we have the corresponding sets \mathcal{S}_i and $\mathcal{S}_i^{\text{com}}$ for each user i . Given this channel assignment outcome, we derive the throughput in the following assuming that there is no collision due to MAC protocol access contention. We will show that by appropriately choosing contention parameters for the MAC protocol, the throughput analysis under this assumption achieves accurate results.

4.7.1 Throughput Analysis

Because the total throughput is the sum of throughput of all users, it is sufficient to analyze the throughput of one particular user i . We will perform the throughput analysis by considering all possible sensing outcomes performed by the considered user i for its assigned channels. We will have the following cases, which correspond to different achievable throughput for the considered user.

- Case 1: If there is at least one channel in \mathcal{S}_i available, then user i will exploit this available channel and achieve the throughput of one. Here, we have

$$T_i \{\text{Case 1}\} = \Pr \{\text{Case 1}\} = 1 - \prod_{j \in \mathcal{S}_i} \bar{p}_{ij}. \quad (4.14)$$

- Case 2: In this case, we consider scenarios where all channels in \mathcal{S}_i are not available, at least one channel in $\mathcal{S}_i^{\text{com}}$ is available, and user i chooses the available channel j for transmission. Suppose that channel j is shared by \mathcal{MS}_j secondary users including user i (i.e., $\mathcal{MS}_j = |\mathcal{U}_j|$). The following four possible groups of users i_k , $k = 1, \dots, \mathcal{MS}_j$ share channel j .
 - **Group I:** channel j is available for user i_k and user i_k has at least 1 channel in \mathcal{S}_{i_k} available.
 - **Group II:** channel j is not available for user i_k .
 - **Group III:** channel j is available for user i_k , all channels in \mathcal{S}_{i_k} are not available and another channel j' in $\mathcal{S}_{i_k}^{\text{com}}$ is available for user i_k . In addition, user i_k chooses channel j' for transmission in the contention stage.
 - **Group IV:** channel j is available for user i_k , all channels in \mathcal{S}_{i_k} are not available. In addition, user i_k chooses channel j for transmission in the contention stage. Hence, user i_k competes with user i for channel j .

The throughput achieved by user i in this case can be written as

$$T_i(\text{Case 3}) = (1 - \delta)\Theta_i \sum_{A_1=0}^{\mathcal{MS}_j} \sum_{A_2=0}^{\mathcal{MS}_j - A_1} \sum_{A_3=0}^{\mathcal{MS}_j - A_1 - A_2} \Phi_1(A_1)\Phi_2(A_2)\Phi_3(A_3)\Phi_4(A_4) \quad (4.15)$$

where the following conditions hold.

- Θ_i is the probability that all channels in \mathcal{S}_i are not available and user i chooses some available channel j in $\mathcal{S}_i^{\text{com}}$ for transmission.
- $\Phi_1(A_1)$ denotes the probability that there are A_1 users belonging to Group I described above among \mathcal{MS}_j users sharing channel j .
- $\Phi_2(A_2)$ represents the probability that there are A_2 users belonging to Group II among \mathcal{MS}_j users sharing channel j .
- $\Phi_3(A_3)$ describes the probability that there are A_3 users belonging to Group III among \mathcal{MS}_j users sharing channel j .
- $\Phi_4(A_4)$ denotes the probability that there are $A_4 = \mathcal{MS}_j - A_1 - A_2 - A_3$ remaining users belonging to Group IV scaled by $1/(1 + A_4)$ where A_4 is the number of users excluding user i competing with user i for channel j .

We now proceed to calculate these quantities. We have

$$\Theta_i = \prod_{k \in \mathcal{S}_i} \bar{p}_{ik} \sum_{B_i=1}^{H_i} \sum_{h=1}^{C_{H_i}^{B_i}} \sum_{j \in \Psi_i^h} \frac{1}{B_i} \prod_{j_1 \in \Psi_i^h} p_{ij_1} \prod_{j_2 \in \mathcal{S}_i^{\text{com}} \setminus \Psi_i^h} \bar{p}_{ij_2} \quad (4.16)$$

where H_i denotes the number of channels in $\mathcal{S}_i^{\text{com}}$. The first product term in (4.16) represents the probability that all channels in \mathcal{S}_i are not available for user i . The second term in (4.16) describes the probability that user i chooses an available channel j among B_i available channels in $\mathcal{S}_i^{\text{com}}$ for transmission. Here, we consider all possible subsets of B_i available channels and for one such particular case Ψ_i^h describes the corresponding set of B_i available channels, i.e.,

$$\Phi_1(A_1) = \sum_{c_1=1}^{C_{\mathcal{MS}_j}^{A_1}} \prod_{m_1 \in \Omega_{c_1}^{(1)}} \left(p_{m_1 j} \left(1 - \prod_{l \in \mathcal{S}_{m_1}} \bar{p}_{m_1 l} \right) \right). \quad (4.17)$$

In (4.17), we consider all possible subsets of size A_1 belonging to Group I (there are $C_{\mathcal{MS}_j}^{A_1}$ such subsets). Each term inside the sum represents the probability for the corresponding event whose set of A_1 users is denoted by $\Omega_{c_1}^{(1)}$, i.e.,

$$\Phi_2(A_2) = \sum_{c_2=1}^{C_{\mathcal{MS}_j - A_1}^{A_2}} \prod_{m_2 \in \Omega_{c_2}^{(2)}} \bar{p}_{m_2 j}. \quad (4.18)$$

In (4.18), we capture the probability that channel j is not available for A_2 users in group II whose possible sets are denoted by $\Omega_{c_2}^{(2)}$, i.e.,

$$\Phi_3(A_3) = \sum_{c_3=1}^{C_{\mathcal{MS}_j - A_1 - A_2}^{A_3}} \prod_{m_3 \in \Omega_{c_3}^{(3)}} \left(p_{m_3 j} \prod_{l_3 \in \mathcal{S}_{m_3}} \bar{p}_{m_3 l_3} \right) \quad (4.19)$$

$$\times \left[\sum_{n=0}^{\beta} \sum_{q=1}^{C_{\beta}^n} \prod_{h_1 \in \mathcal{S}_{j, m_3}^{\text{com}, q}} p_{m_3 h_1} \prod_{h_2 \in \bar{\mathcal{S}}_{j, m_3}^{\text{com}, q}} \bar{p}_{m_3 h_2} \left(1 - \frac{1}{n+1} \right) \right]. \quad (4.20)$$

For each term in (4.19) we consider different possible subsets of A_3 users, which are denoted by $\Omega_{c_3}^{(3)}$. Then, each term in (4.19) represents the probability that channel j is available for each user $m_3 \in \Omega_{c_3}^{(3)}$ while all channels in \mathcal{S}_{m_3} for the user m_3 are not available. In (4.20), we consider all possible sensing outcomes for channels in $\mathcal{S}_{m_3}^{\text{com}}$ performed by user

$m_3 \in \Omega_{c_3}^{(3)}$. In addition, let $\mathcal{S}_{j,m_3}^{\text{com}} = \mathcal{S}_{m_3}^{\text{com}} \setminus \{j\}$ and $\beta = |\mathcal{S}_{j,m_3}^{\text{com}}|$. Then, in (4.20) we consider all possible scenarios in which there are n channels in $\mathcal{S}_{j,m_3}^{\text{com}}$ available; and user m_3 chooses a channel different from channel j for transmission (with probability $(1 - \frac{1}{n+1})$) where $\mathcal{S}_{j,m_3}^{\text{com}} = \mathcal{S}_{j,m_3}^{\text{com},q} \cup \bar{\mathcal{S}}_{j,m_3}^{\text{com},q}$ and $\mathcal{S}_{j,m_3}^{\text{com},q} \cap \bar{\mathcal{S}}_{j,m_3}^{\text{com},q} = \emptyset$. We have

$$\Phi_4(A_4) = \left(\frac{1}{1 + A_4} \right) \prod_{m_4 \in \Omega^{(4)}} \left(p_{m_4 j} \prod_{l_4 \in \mathcal{S}_{m_4}} \bar{p}_{m_4 l_4} \right) \quad (4.21)$$

$$\times \left[\sum_{m=0}^{\gamma} \sum_{q=1}^{C_{\gamma}^m} \prod_{h_1 \in \mathcal{S}_{j,m_4}^{\text{com},q}} p_{m_4 h_1} \prod_{h_2 \in \bar{\mathcal{S}}_{j,m_4}^{\text{com},q}} \bar{p}_{m_4 h_2} \left(\frac{1}{m+1} \right) \right]. \quad (4.22)$$

The sensing outcomes captured in (4.21) and (4.22) are similar to those in (4.19) and (4.20). However, given three sets of A_1 , A_2 , and A_3 users, the set $\Omega^{(4)}$ can be determined whose size is $|\Omega^{(4)}| = A_4$. Here, γ denotes cardinality of the set $\mathcal{S}_{j,m_4}^{\text{com}} = \mathcal{S}_{m_4}^{\text{com}} \setminus \{j\}$. Other sets are similar to those in (4.19) and (4.20). However, all users in $\Omega^{(4)}$ choose channel j for transmission in this case. Therefore, user i wins the contention with probability $1/(1 + A_4)$ and its achievable throughput is $(1 - \delta)/(1 + A_4)$.

Summarizing all considered cases, the throughput achieved by user i is given as

$$T_i = T_i \{\text{Case 1}\} + T_i \{\text{Case 3}\}. \quad (4.23)$$

In addition, the total throughput of the secondary network \mathcal{T} is the sum of throughputs achieved by all SUs.

4.7.2 Impacts of Contention Collision

We have presented the saturation throughput analysis assuming that there is no contention collision. Intuitively, if the MAC protocol is designed such that collision probability is sufficiently small then the impact of collision on the throughput performance would be negligible. For our MAC protocol, users perform contention resolution in case 2 considered in the previous throughput analysis, which occurs with a small probability. Therefore, if the contention window in (4.12) is chosen for a sufficiently small ϵ_P , then contention collisions would have negligible impacts on the network throughput. We formally state this intuitive result in the following proposition.

Proposition 2: The throughput \mathcal{T} derived in the previous sub-section has an error, which can be upper-bounded as

$$E_t \leq \epsilon_P \sum_{i=1}^M \prod_{j \in \mathcal{S}_i} \bar{p}_{ij} \left(1 - \prod_{j \in \mathcal{S}_i^{\text{com}}} \bar{p}_{ij} \right) \quad (4.24)$$

where ϵ_P is the target collision probability that is used to determine the contention window in (4.12).

Proof. As aforementioned, contention collision can only occur in case 2 of the previous throughput analysis. The probability covering all possible events for user i in this case is $\prod_{j \in \mathcal{S}_i} \bar{p}_{ij} \left(1 - \prod_{j \in \mathcal{S}_i^{\text{com}}} \bar{p}_{ij} \right)$. In addition, the maximum average throughput that a particular user i can achieve is $1 - \delta < 1$ (because no other users contend with user i to exploit a chosen channel). In addition, if contention collision happens then user i will quit the contention and may experience a maximum average throughput loss of $1 - \delta$ compared to the ideal case with no contention collision. In addition, the collision probabilities of all potential collisions is bounded above by ϵ_P . Therefore, the average error due to the proposed throughput analysis can be upper-bounded as in (4.24). \square

To illustrate the throughput error bound presented in this proposition, let us consider an example where $\bar{p}_{ij} \leq 0.2$ and $\epsilon_P \leq 0.03$. Because the sets \mathcal{S}_i returned by Alg. 3 contain at least one channel, the throughput error can be bounded by $M \times 0.2 \times 0.03 = 0.006M$. In addition, the total throughput will be at least $\sum_{i=1}^M \left(1 - \prod_{j \in \mathcal{S}_i} \bar{p}_{ij} \right) \geq 0.8M$ if we only consider throughput contribution from case 1. Therefore, the relative throughput error can be upper-bounded by $0.006M/0.8M \approx 0.75\%$, which is quite negligible. This example shows that the proposed throughput analytical model is very accurate in most practical settings.

4.7.3 Complexity Analysis

We analyze the complexity of Alg. 2 and Alg. 3 in this subsection. Let us proceed by analyzing the steps taken in each iteration in Alg. 2. To determine the best assignment for the first channel, we have to search over M SUs and N channels, which involves MN cases. Similarly, to assign the second channel, we need to perform searching over secondary users and $N - 1$ channels (one channel is already assigned in the first iteration). Hence, the second assignment involves $M(N - 1)$ cases. Similar analysis can be applied for other assignments

in later iterations. In summary, the total number of cases involved in assigning all channels to M SUs is $M(N + \dots + 2 + 1) = MN(N + 1)/2$, which is $O(MN^2)$. In Alg. 2, the increase of throughput used in the search is calculated by using (4.4).

In Alg. 3, we run Alg. 2 in the first phase then perform further overlapping channel assignments using Alg. 3 in the second phase. Hence, we need to analyze the complexity involved in the second phase (i.e., Alg. 3). In Alg. 3, we increase the parameter h from 1 to $M - 1$ over iterations of the *while loop* (to increase the number of users who share one channel). For a particular value of h , we search over the channels that have been shared by h users and over all M users. Therefore, we have NM cases to consider for each value of h each of which requires to calculate the corresponding increase of throughput using (4.5). Therefore, the worst case complexity of the second phase is $NM(M - 1)$, which is $O(NM^2)$. Considering the complexity of both phases, the complexity of Alg. 3 is $O(MN^2 + NM^2) = O(MN(M + N))$, which is much lower than that of the optimal brute-force search algorithm ($O(2^{NM})$).

4.8 Further Extensions and Design Issues

4.8.1 Fair Channel Assignment

We extend the channel assignment problem to consider the max-min fairness objective, which maximizes the minimum throughput achieved by all SUs [107]. In particular, the max-min channel assignment problem can be stated as follows:

$$\max_{\mathbf{x}} \min_i T_i. \quad (4.25)$$

Intuitively, the max-min fairness criterion tends to allocate more radio resources for “weak” users to balance the throughput performance among all users. Thanks to the exact throughput analytical model developed in Section 4.7.1, the optimal solution of the optimization problem (4.25) can be found by the exhaustive search, which, however, has extremely high computational complexity.

To resolve this complexity issue, we devise greedy fair non-overlapping and overlapping channel assignment algorithms, which are described in Alg. 4 and Alg. 5, respectively. In Section 4.9, we compare the performance of these algorithms with that of the optimal exhaustive search algorithm. These algorithms are different from Alg. 2 and Alg. 3 mainly in the way we choose the user to allocate one “best” channel in each iteration. In Alg. 4, we find the set of users who achieve a minimum throughput in each iteration. For each user

in this set, we find one available channel that results in the highest increase of throughput. Then, we assign the “best” channel that achieves the maximum increase of throughput considering all throughput-minimum users. Therefore, this assignment attempts to increase the throughput of a weak user while exploiting the multiuser diversity.

Algorithm 4 FAIR NON-OVERLAPPING CHANNEL ASSIGNMENT

- 1: Initialize SU i 's set of available channels, $\mathcal{S}_i^a := \{1, 2, \dots, N\}$ and $\mathcal{S}_i := \emptyset$ for $i = 1, 2, \dots, M$ where \mathcal{S}_i denotes the set of channels assigned for SU i .
 - 2: continue := 1
 - 3: **while** continue = 1 **do**
 - 4: Find the set of users who currently have minimum throughput $\mathcal{S}^{\min} = \underset{i}{\operatorname{argmin}} T_i^b$ where $\mathcal{S}^{\min} = \{i_1, \dots, i_m\} \subset \{1, \dots, M\}$ is the set of minimum-throughput SUs.
 - 5: **if** $\bigcap_{i_l \in \mathcal{S}^{\min}} (\mathcal{S}_{i_l}^a \neq \emptyset)$ **then**
 - 6: For each SU $i_l \in \mathcal{S}^{\min}$ and channel $j_{i_l} \in \mathcal{S}_{i_l}^a$, find $\Delta T_{i_l}(j_{i_l}) = T_{i_l}^a - T_{i_l}^b$ where $T_{i_l}^a$ and $T_{i_l}^b$ are the throughputs after and before assigning channel j_{i_l} ; and we set $\Delta T_{i_l} = 0$ if $\mathcal{S}_{i_l}^a = \emptyset$.
 - 7: $\{i_l^*, j_{i_l}^*\} = \underset{i_l \in \mathcal{S}^{\min}, j_{i_l} \in \mathcal{S}_{i_l}^a}{\operatorname{argmax}} \Delta T_{i_l}(j_{i_l})$
 - 8: Assign channel $j_{i_l}^*$ to SU i_l^* .
 - 9: Update $\mathcal{S}_{i_l^*} = \mathcal{S}_{i_l^*} \cup j_{i_l^*}^*$ and $\mathcal{S}_k^a = \mathcal{S}_k^a \setminus j_{i_l^*}^*$ for all $k \in \{1, \dots, M\}$.
 - 10: **else**
 - 11: Set continue := 0
 - 12: **end if**
 - 13: **end while**
-

In Alg. 5, we first run Alg. 4 to obtain non-overlapping sets of channels for all users. Then, we seek to improve the minimum throughput by performing overlapping channel assignments. In particular, we find the minimum-throughput user and an overlapping channel assignment that results in the largest increase in its throughput. The algorithm terminates when there is no such overlapping channel assignment. The search of an overlapping channel assignment in each iteration of Alg. 5 is performed in Alg. 6. Specifically, we sequentially search over channels which have already been allocated for a single user or shared by several users (i.e., channels in separate and common sets, respectively). Then, we update the current temporary assignment with a better one (if any) during the search. This search requires throughput calculations for which we use the analytical model developed in Section 4.7.1 with the MAC protocol overhead, $\delta < 1$ derived in Section 4.6.4. It can be observed that the proposed

Algorithm 5 FAIR OVERLAPPING CHANNEL ASSIGNMENT

```

1: Run Alg. 4 and obtain the sets  $\mathcal{S}_i$  for all SU  $i$ . Initialize  $\mathcal{S}_i^{\text{com}} = \emptyset$  for  $i$ .
2: continue := 1.
3: while continue = 1 do
4:   Find  $i^* = \underset{i \in \{1, \dots, M\}}{\text{argmin}} T_i^b$  and  $T_{\min} = T_{i^*}^b$  where ties are broken randomly.
5:    $\mathcal{S}_{i^*}^{\text{Sep}} = \bigcup_{i, i \neq i^*} \mathcal{S}_i$ ,  $\mathcal{S}_{i^*}^{\text{Uni}} = \bigcup_i \mathcal{S}_i^{\text{com}} \setminus \mathcal{S}_{i^*}^{\text{com}}$ .
6:   Run Alg. 6.
7:   if  $\bigcup_i \mathcal{R} \mathcal{S}_i^{\text{com, temp}} \neq \emptyset$  then
8:     Assign  $\mathcal{S}_i^{\text{com}} = \mathcal{S}_i^{\text{com, temp}}$  and  $\mathcal{S}_i = \mathcal{S}_i^{\text{temp}}$ .
9:   else
10:    Set continue := 0.
11:   end if
12: end while

```

throughput analysis is very useful since it can be used to evaluate the performance of any channel assignment solution and to perform channel assignments in greedy algorithms.

4.8.2 Throughput Analysis under Imperfect Sensing

We extend the throughput analysis considering imperfect sensing. The following two important performance measures are used to quantify the sensing performance: 1) detection probabilities and 2) false-alarm probabilities. Let \mathcal{P}_d^{ij} and \mathcal{P}_f^{ij} be detection and false alarm probabilities, respectively, of SU i on channel j . In particular, detection event occurs when a secondary link successfully senses a busy channel and false alarm represents the situation when a spectrum sensor returns a busy state for an idle channel (i.e., a transmission opportunity is overlooked). Also, let us define $\overline{\mathcal{P}}_d^{ij} = 1 - \mathcal{P}_d^{ij}$ and $\overline{\mathcal{P}}_f^{ij} = 1 - \mathcal{P}_f^{ij}$. Under imperfect sensing, the following four scenarios are possible for channel j and SU i .

- Scenario I: A spectrum sensor indicates that channel j is available and the nearby PU is not using channel j (i.e., correct sensing). This scenario occurs with the probability $\overline{\mathcal{P}}_f^{ij} p_{ij}$.
- Scenario II: A spectrum sensor indicates that channel j is available and the nearby PU is using channel j (i.e., mis-detection). This scenario occurs with the probability $\overline{\mathcal{P}}_d^{ij} \overline{p}_{ij}$. In this case, potential transmission of secondary user i will collide with that

Algorithm 6 SEARCHING POTENTIAL CHANNEL ASSIGNMENT

```

1: — Search potential channel assignment from separate sets —
2: for  $j \in \mathcal{S}_{i^*}^{\text{Sep}}$  do
3:   Find SU  $i'$  where  $j \in \mathcal{S}_{i'}$ . Let  $n_c = M - 2$ .
4:   for  $l = 0$  to  $n_c$  do
5:     for  $k = 1$  to  $C_{n_c}^l$  do
6:       Find  $T_{i^*}^a, T_{i'}^a$ , and  $T_m^a \Big|_{m \in \mathcal{U}_j^l}$ , where  $\mathcal{U}_j^l$  is the set of  $l$  new SUs sharing channel  $j$ .
7:       if  $\min \left( T_{i^*}^a, T_m^a \Big|_{m \in \mathcal{U}_j^l}, T_{i'}^a \right) > T_{\min}$  then
8:         - Temporarily assign channel  $j$  to SUs  $i^*, i'$  and all SUs  $m$ :  $\mathcal{S}_{i^*}^{\text{com,temp}} = \mathcal{S}_{i^*}^{\text{com}} \cup j$ ,  $\mathcal{S}_{i'}^{\text{com,temp}} = \mathcal{S}_{i'}^{\text{com}} \cup j$ ,
            $\mathcal{S}_{i'}^{\text{temp}} = \mathcal{S}_{i'} \setminus j$  and  $\mathcal{S}_m^{\text{com,temp}} = \mathcal{S}_m^{\text{com}} \cup j$ .
9:         - Update  $T_{\min} = \min \left( T_{i^*}^a, T_m^a \Big|_{m \in \mathcal{U}_j^l}, T_{i'}^a \right)$ .
10:        - Reset all temporary sets of other SUs to be empty.
11:       end if
12:     end for
13:   end for
14: end for

15: — Search potential channel assignment from common sets —
16: for  $j \in \mathcal{S}_{i^*}^{\text{Uni}}$  do
17:   Find the subset of SUs except SU  $i^*, \mathcal{S}^{\text{Use}}$  who use channel  $j$  as an overlapping channel.
18:   for  $l = 0$  to  $M - 1 - |\mathcal{S}^{\text{Use}}|$  do
19:     for  $k = 1$  to  $C_{M-1-|\mathcal{S}^{\text{Use}}|}^l$  do
20:       Find  $T_{i^*}^a, T_{i'}^a \Big|_{i' \in \mathcal{S}^{\text{Use}}}, T_m^a \Big|_{m \in \mathcal{U}_j^l}$ , where  $\mathcal{U}_j^l$  is the set of  $l$  new SUs sharing channel  $j$ .
21:       if  $\min \left( T_{i^*}^a, T_{i'}^a \Big|_{i' \in \mathcal{S}^{\text{Use}}}, T_m^a \Big|_{m \in \mathcal{U}_j^l} \right) > T_{\min}$  then
22:         - Temporarily assign channel  $j$  to SU  $i^*$ , all SUs  $i'$  and all SUs  $m$ :  $\mathcal{S}_{i^*}^{\text{com,temp}} = \mathcal{S}_{i^*}^{\text{com}} \cup j$ ,  $\mathcal{S}_m^{\text{com,temp}} = \mathcal{S}_m^{\text{com}} \cup j$ .
23:         - Update  $T_{\min} = \min \left( T_{i^*}^a, T_{i'}^a \Big|_{i' \in \mathcal{S}^{\text{Use}}}, T_m^a \Big|_{m \in \mathcal{U}_j^l} \right)$ .
24:         - Reset all temporary sets of other SUs to be empty.
25:       end if
26:     end for
27:   end for
28: end for
    
```

of the nearby primary user. We assume that both transmissions from SU i and the nearby PU fail.

- Scenario III: A spectrum sensor indicates that channel j is not available and the nearby PU is using channel j (i.e., correct detection). This scenario occurs with the probability $\mathcal{P}_d^{ij} \bar{p}_{ij}$.
- Scenario IV: A spectrum sensor indicates that channel j is not available and the nearby PU is not using channel j (i.e., false alarm). This scenario occurs with the probability $\mathcal{P}_f^{ij} p_{ij}$ and the channel opportunity is overlooked.

Because SUs make channel access decisions based on their sensing outcomes, the first two scenarios can result in spectrum access on channel j by SU i . Moreover, spectrum access in scenario one actually lead to successful data transmission. Let us define $\mathcal{P}_{\text{idle}}^{ij} = \bar{\mathcal{P}}_f^{ij} p_{ij} + \bar{\mathcal{P}}_d^{ij} \bar{p}_{ij}$ and $\mathcal{P}_{\text{busy}}^{ij} = 1 - \mathcal{P}_{\text{idle}}^{ij}$ as the probabilities under which SU i may and may not access channel j , respectively. The same synchronized MAC protocol described in Section 4.6.1 is assumed here. In addition, the MAC protocol overhead can be calculated as presented in Section 4.6.4 where the contention window W is determined as described in Section 4.6.3. However, p_{ij} and \bar{p}_{ij} are substituted by $\mathcal{P}_{\text{idle}}^{ij}$ and $\mathcal{P}_{\text{busy}}^{ij}$, respectively in the calculation of contention window in Section 4.6.3 for this case. This is because $\mathcal{P}_{\text{idle}}^{ij}$ and $\mathcal{P}_{\text{busy}}^{ij}$ capture the probabilities that channel j is available and busy for user i as indicated by sensing, respectively considering potential sensing errors. Because the total throughput is the sum of throughput of all users, it is sufficient to analyze the throughput of one particular user i . To analyze the throughput of user i , we consider the following cases.

- Case 1: At least one channel in \mathcal{S}_i is available and user i chooses one of these available channels for its transmission. User i can achieve throughput of one in such a successful access, which occurs with the following probability:

$$T_i \{\text{Case 1}\} = \Pr \{\text{Case 1}\} = \sum_{k_1=1}^{|\mathcal{S}_i|} \sum_{l_1=1}^{C_{|\mathcal{S}_i|}^{k_1}} \prod_{j_1 \in \mathcal{S}_i^{l_1}} p_{ij_1} \prod_{j_2 \in \mathcal{S}_i \setminus \mathcal{S}_i^{l_1}} \bar{p}_{ij_2} \quad (4.26)$$

$$\sum_{k_2=1}^{k_1} \sum_{l_2=1}^{C_{k_1}^{k_2}} \prod_{j_3 \in \mathcal{S}_i^{l_2}} \bar{\mathcal{P}}_f^{ij_3} \prod_{j_4 \in \mathcal{S}_i^{l_1} \setminus \mathcal{S}_i^{l_2}} \mathcal{P}_f^{ij_4} \quad (4.27)$$

$$\sum_{k_3=0}^{|\mathcal{S}_i| - k_1} \sum_{l_3=1}^{C_{|\mathcal{S}_i| - k_1}^{k_3}} \frac{k_2}{k_2 + k_3} \prod_{j_5 \in \mathcal{S}_i^{l_3}} \bar{\mathcal{P}}_d^{ij_5} \prod_{j_6 \in \mathcal{S}_i \setminus \mathcal{S}_i^{l_1} \setminus \mathcal{S}_i^{l_3}} \mathcal{P}_d^{ij_6}. \quad (4.28)$$

where we have $T_i \{\text{Case 1}\} = \Pr \{\text{Case 1}\}$. The quantity (4.26) represents the probability that there are k_1 actually available channels in \mathcal{S}_i (which may or may not be correctly sensed by SU i). Here, $\mathcal{S}_i^{l_1}$ denotes a particular set of k_1 actually available channels whose index is l_1 . In addition, the quantity (4.27) describes the probability that there are k_2 available channels as indicated by sensing (the remaining available channels are overlooked due to sensing errors) where $\mathcal{S}_i^{l_2}$ denotes the l_2 -th set with k_2 available channels. For the quantity in (4.28), k_3 denotes the number of channels that are not actually available but the sensing outcomes indicate they are available (i.e., due to mis-detection). Moreover, $k_2/(k_2 + k_3)$

represents the probability that SU i chooses the actually available channel for transmission given its sensing outcomes indicate $k_2 + k_3$ available channels. The remaining quantity in (4.28) describes the probability that the sensing outcomes due to SU i incorrectly indicates k_3 available channels.

- **Case 2:** All channels in \mathcal{S}_i are indicated as not available by sensing; there is at least one channel in $\mathcal{S}_i^{\text{com}}$ indicated as available by sensing, and user i chooses an actually available channel j for transmission. Suppose that channel j is shared by \mathcal{MS}_j secondary users including user i (i.e., $\mathcal{MS}_j = |\mathcal{U}_j|$). There are four possible groups of users i_k , $k = 1, \dots, \mathcal{MS}_j$ sharing channel j , which are described in the following
 - **Group I:** channel j is available for user i_k and user i_k has at least 1 channel in \mathcal{S}_{i_k} available as indicated by sensing.
 - **Group II:** channel j is indicated as not available for user i_k by sensing.
 - **Group III:** channel j is available for user i_k , all channels in \mathcal{S}_{i_k} are not available and there is another channel j' in $\mathcal{S}_{i_k}^{\text{com}}$ available for user i_k as indicated by sensing. In addition, user i_k chooses channel j' for transmission in the contention stage.
 - **Group IV:** channel j is available for user i_k , all channels in \mathcal{S}_{i_k} are not available as indicated by sensing. In addition, user i_k chooses channel j for transmission in the contention stage. Hence, user i_k competes with user i for channel j .

The throughput that was achieved by user i in this case can be written as

$$T_i(\text{Case 3}) = (1 - \delta)\Theta_i \sum_{A_1=0}^{\mathcal{MS}_j} \sum_{A_2=0}^{\mathcal{MS}_j - A_1} \sum_{A_3=0}^{\mathcal{MS}_j - A_1 - A_2} \Phi_1(A_1)\Phi_2(A_2)\Phi_3(A_3)\Phi_4(A_4). \quad (4.29)$$

Here, we use the same notations as in the perfect sensing scenario investigated in Section 4.7.1 where the following conditions hold.

- Θ_i is the probability that all channels in \mathcal{S}_i are indicated as not available by sensing and user i chooses some available channel j in $\mathcal{S}_i^{\text{com}}$ as indicated by sensing for transmission.
- $\Phi_1(A_1)$ denotes the probability that there are A_1 users belonging to Group I described above among \mathcal{MS}_j users sharing channel j .
- $\Phi_2(A_2)$ represents the probability that there are A_2 users belonging to Group II among \mathcal{MS}_j users sharing channel j .

- $\Phi_3(A_3)$ describes the probability that there are A_3 users belonging to Group III among \mathcal{MS}_j users sharing channel j .
- $\Phi_4(A_4)$ denotes the probability that there are $A_4 = \mathcal{MS}_j - A_1 - A_2 - A_3$ remaining users belonging to Group IV scaled by $1/(1 + A_4)$ where A_4 is the number of users excluding user i competing with user i for channel j .

We now proceed to calculate these quantities. We have

$$\Theta_i = \sum_{k_1=0}^{|\mathcal{S}_i|} \sum_{l_1=1}^{C_{|\mathcal{S}_i|}^{k_1}} \prod_{j_1 \in \mathcal{S}_i^{l_1}} \mathcal{P}_f^{ij_1} p_{ij_1} \prod_{j_2 \in \mathcal{S}_i \setminus \mathcal{S}_i^{l_1}} \bar{p}_{ij_2} \quad (4.30)$$

$$\sum_{k_2=1}^{H_i} \sum_{l_2=1}^{C_{H_i}^{k_2}} \prod_{j_3 \in \Psi_i^{l_2}} p_{ij_3} \prod_{j_4 \in \mathcal{S}_i^{\text{com}} \setminus \Psi_i^{l_2}} \bar{p}_{ij_4} \quad (4.31)$$

$$\sum_{k_3=1}^{k_2} \sum_{l_3=1}^{C_{k_2}^{k_3}} \sum_{j \in \Gamma_1^k} \prod_{j_5 \in \Gamma_1^{l_3}} \bar{\mathcal{P}}_f^{ij_5} \prod_{j_6 \in \Psi_i^{l_2} \setminus \Gamma_1^{l_3}} \mathcal{P}_f^{ij_6} \quad (4.32)$$

$$\sum_{k_4=0}^{H_i - k_2} \sum_{l_4=1}^{C_{H_i - k_2}^{k_4}} \frac{1}{k_3 + k_4} \prod_{j_7 \in \Gamma_2^{l_4}} \bar{\mathcal{P}}_d^{ij_7} \prod_{j_8 \in \mathcal{S}_i^{\text{com}} \setminus \Psi_i^{l_2} \setminus \Gamma_2^{l_4}} \mathcal{P}_d^{ij_8} \quad (4.33)$$

where H_i denotes the number of channels in $\mathcal{S}_i^{\text{com}}$. The quantity in (4.30) is the probability that all available channels in \mathcal{S}_i (if any) are overlooked by user i due to false alarms. Therefore, user i does not access any channels in \mathcal{S}_i . The quantity in (4.31) describes the probability that there are k_2 actually available channels in $\mathcal{S}_i^{\text{com}}$ and $\Psi_i^{l_2}$ denotes such a typical set with k_2 available channels. The quantity in (4.32) describes the probability that user i correctly detects k_3 channels out of k_2 available channels. The last quantity in (4.33) excluding the factor $1/(k_3 + k_4)$ denotes the probability that user i mis-detects k_4 channels among the remaining $H_i - k_2$ busy channels in $\mathcal{S}_i^{\text{com}}$. Finally, the factor $1/(k_3 + k_4)$ is the probability that user i correctly chooses one available channels in $\mathcal{S}_i^{\text{com}}$ for transmission out of $k_3 + k_4$ channels which are indicated as being available by sensing, i.e.,

$$\Phi_1(A_1) = \sum_{c_1=1}^{C_{\mathcal{MS}_j}^{A_1}} \prod_{m_1 \in \Omega_{c_1}^{(1)}} \left(\mathcal{P}_{\text{idle}}^{m_1 j} \left(1 - \prod_{l \in \mathcal{S}_{m_1}} \mathcal{P}_{\text{busy}}^{m_1 l} \right) \right). \quad (4.34)$$

In (4.34), we consider all possible subsets of users of size A_1 that belongs to Group I (there are $C_{\mathcal{MS}_j}^{A_1}$ such subsets). Each term inside the sum represents the probability of the corresponding

event whose set of A_1 users is denoted by $\Omega_{c_1}^{(1)}$, i.e.,

$$\Phi_2(A_2) = \sum_{c_2=1}^{C_{\mathcal{M}\mathcal{S}_j-A_1}^{A_2}} \prod_{m_2 \in \Omega_{c_2}^{(2)}} \mathcal{P}_{\text{busy}}^{m_2 j}. \quad (4.35)$$

In (4.35), we capture the probability that channel j is indicated as not being available by sensing for A_2 users in group II. Possible sets of these users are denoted by $\Omega_{c_2}^{(2)}$, i.e.,

$$\Phi_3(A_3) = \sum_{c_3=1}^{C_{\mathcal{M}\mathcal{S}_j-A_1-A_2}^{A_3}} \prod_{m_3 \in \Omega_{c_3}^{(3)}} \left(\mathcal{P}_{\text{idle}}^{m_3 j} \prod_{l_3 \in \mathcal{S}_{m_3}} \mathcal{P}_{\text{busy}}^{m_3 l_3} \right) \quad (4.36)$$

$$\times \left[\sum_{n=0}^{\beta} \sum_{q=1}^{C_{\beta}^n} \prod_{h_1 \in \mathcal{S}_{j,m_3}^{\text{com},q}} \mathcal{P}_{\text{idle}}^{m_3 h_1} \prod_{h_2 \in \bar{\mathcal{S}}_{j,m_3}^{\text{com},q}} \mathcal{P}_{\text{busy}}^{m_3 h_2} \left(1 - \frac{1}{n+1} \right) \right]. \quad (4.37)$$

For each term in (4.36) we consider different possible subsets of A_3 users, which are denoted by $\Omega_{c_3}^{(3)}$. Then, each term in (4.36) represents the probability that channel j is indicated as available by sensing for each user $m_3 \in \Omega_{c_3}^{(3)}$ while all channels in \mathcal{S}_{m_3} are indicated as not available by sensing. In (4.37), we consider all possible sensing outcomes for channels in $\mathcal{S}_{m_3}^{\text{com}}$ performed by user $m_3 \in \Omega_{c_3}^{(3)}$. In addition, let $\mathcal{S}_{j,m_3}^{\text{com}} = \mathcal{S}_{m_3}^{\text{com}} \setminus \{j\}$ and $\beta = |\mathcal{S}_{j,m_3}^{\text{com}}|$. Then, in (4.37) we consider all possible scenarios in which n channels in $\mathcal{S}_{j,m_3}^{\text{com}}$ are indicated as available by sensing; and user m_3 chooses a channel different from channel j for transmission (with probability $(1 - \frac{1}{n+1})$) where $\mathcal{S}_{j,m_3}^{\text{com}} = \mathcal{S}_{j,m_3}^{\text{com},q} \cup \bar{\mathcal{S}}_{j,m_3}^{\text{com},q}$ and $\mathcal{S}_{j,m_3}^{\text{com},q} \cap \bar{\mathcal{S}}_{j,m_3}^{\text{com},q} = \emptyset$. We have

$$\Phi_4(A_4) = \left(\frac{1}{1+A_4} \right) \prod_{m_4 \in \Omega^{(4)}} \left(\mathcal{P}_{\text{idle}}^{m_4 j} \prod_{l_4 \in \mathcal{S}_{m_4}} \mathcal{P}_{\text{busy}}^{m_4 l_4} \right) \quad (4.38)$$

$$\times \left[\sum_{m=0}^{\gamma} \sum_{q=1}^{C_{\gamma}^m} \prod_{h_1 \in \mathcal{S}_{j,m_4}^{\text{com},q}} \mathcal{P}_{\text{idle}}^{m_4 h_1} \prod_{h_2 \in \bar{\mathcal{S}}_{j,m_4}^{\text{com},q}} \mathcal{P}_{\text{busy}}^{m_4 h_2} \left(\frac{1}{m+1} \right) \right]. \quad (4.39)$$

The sensing outcomes captured in (4.38) and (4.39) are similar to those in (4.36) and (4.37). However, given three sets of A_1 , A_2 , and A_3 users, the set $\Omega^{(4)}$ can be determined whose size is $|\Omega^{(4)}| = A_4$. Here, γ denotes cardinality of the set $\mathcal{S}_{j,m_4}^{\text{com}} = \mathcal{S}_{m_4}^{\text{com}} \setminus \{j\}$. Other sets are similar to those in (4.36) and (4.37). However, all users in $\Omega^{(4)}$ choose channel j for transmission in this case. Therefore, user i wins the contention with probability $1/(1+A_4)$ and its achievable throughput is $(1-\delta)/(1+A_4)$.

Summarize all considered cases, the throughput achieved by user i is written as

$$T_i = T_i \{\text{Case 1}\} + T_i \{\text{Case 3}\}. \quad (4.40)$$

In addition, the total throughput \mathcal{T} can be calculated by summing the throughputs of all SUs.

4.8.3 Congestion of Control Channel

Under our design, contention on the control channel is mild if the number of channels N is relatively large compared to the number of SUs M . In particular, there is no need to employ a MAC protocol if we have $N \gg M$ since distinct sets of channels can be allocated for SUs by using Alg. 2. In contrast, if the number of channels N is small compared to the number of SUs M then the control channel may experience congestion due to excessive control message exchanges. The congestion of the control channel in such scenarios can be alleviated if we allow RTS/CTS messages to be exchanged in parallel on several channels (i.e., multiple rendezvous [31]).

We describe potential design of a multiple-rendezvous MAC protocol in the following using similar ideas of a multi-channel MAC protocol (McMAC) in [30, 31]. We assume that each SU hops through all channels by following a particular hopping pattern, which corresponds to a unique seed [31]. In addition, each SU puts its seed in every packets so that neighboring SUs can learn its hopping pattern. The same cycle structure as being described in Section 4.6.1 is employed here. Suppose SU A wishes to transmit data SU B in a particular cycle. Then, SU A turns to the current channel of B and senses this channel as well as its assigned channels in $\mathcal{S}_{AB}^{\text{tot}}$, which is the set of allocated channels for link AB . If SU A's sensing outcomes indicate that the current channel of SU B is available then SU A sends RTS/CTS messages with SU B containing a chosen available communication channel. Otherwise, SU A waits until the next cycle to perform sensing and contention again. If the handshake is successful, SU A transmits data to SU B on the chosen channel in the data phase. Upon completing data transmission, both SUs A and B return to their home hopping patterns. In general, collisions among SUs are less frequent under a multiple-rendezvous MAC protocol since contentions can occur in parallel on different channels.

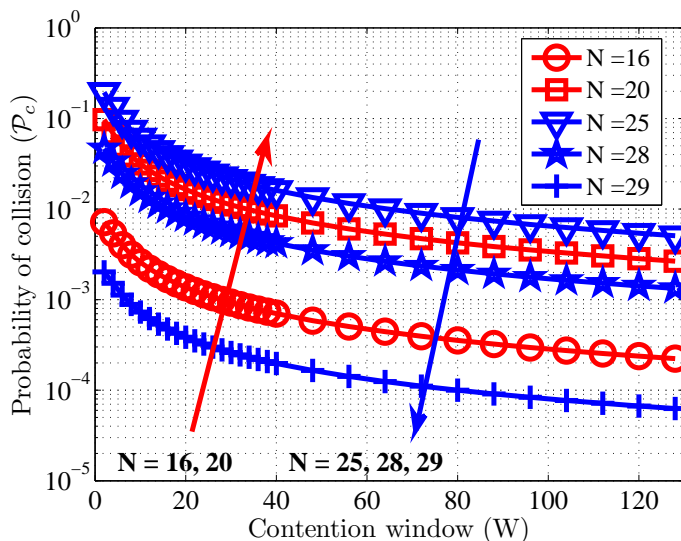


Figure 4.2: Collision probability versus the contention window (for $M = 15$).

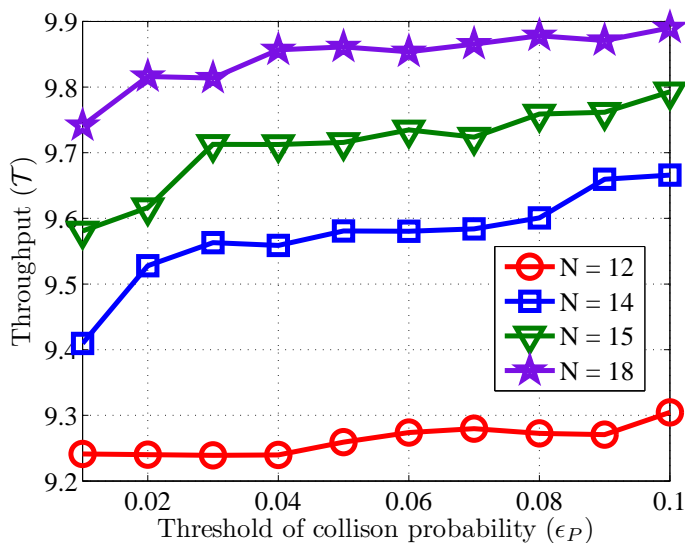


Figure 4.3: Total throughput versus target collision probability under throughput maximization design (for $M = 10$)

4.9 Numerical Results

We present numerical results to illustrate the throughput performance of the proposed channel assignment algorithms. To obtain the results, the probabilities $p_{i,j}$ are randomly realized in the interval $[0.7, 0.9]$ unless stated otherwise. We choose the length of control packets as follows: RTS including PHY header 288 bits, CTS including PHY header 240 bits, which correspond to $t_{\text{RTS}} = 48\mu\text{s}$, $t_{\text{CTS}} = 40\mu\text{s}$ for transmission rate of 6Mbps, which is the ba-

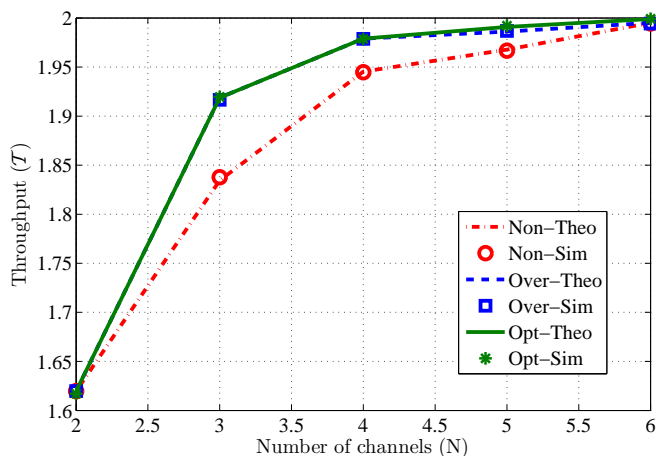


Figure 4.4: Total throughput versus the number of channels under throughput maximization design (for $M = 2$, Theo: Theory, Sim: Simulation, Over: Overlapping, Non: Non-overlapping, Opt: Optimal assignment).

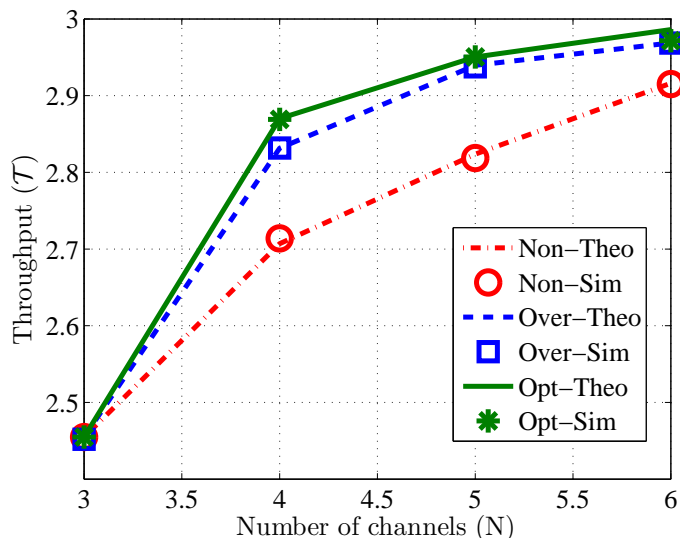


Figure 4.5: Total throughput versus the number of channels under throughput maximization design (for $M = 3$, Theo: Theory, Sim: Simulation, Over: Overlapping, Non: Non-overlapping, Opt: Optimal assignment).

sic rate of 802.11a/g standards [126]. Other parameters are chosen as follows: cycle time $T_{\text{cycle}} = 3\text{ms}$; $\theta = 20\mu\text{s}$, $t_{\text{SIFS}} = 28\mu\text{s}$, target collision probability $\epsilon_P = 0.03$; t_{SEN} and t_{SYN} are assumed to be negligible so they are ignored. Note that these values of θ and t_{SIFS} are typical (interested readers can refer to Tables I and II in the well-cited reference [85] for related information). The value of cycle time T_{cycle} is relatively small given the fact that practi-

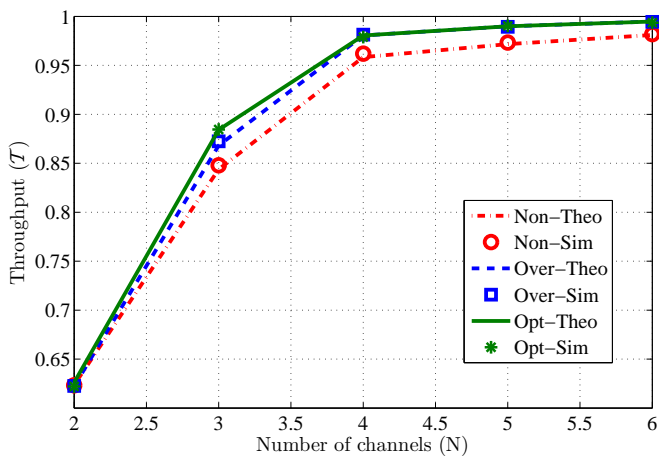


Figure 4.6: Minimum throughput versus the number of channels under max-min fairness (for $M = 2$, Theo: Theory, Sim: Simulation, Over: Overlapping, Non: Non-overlapping, Opt: Optimal assignment).

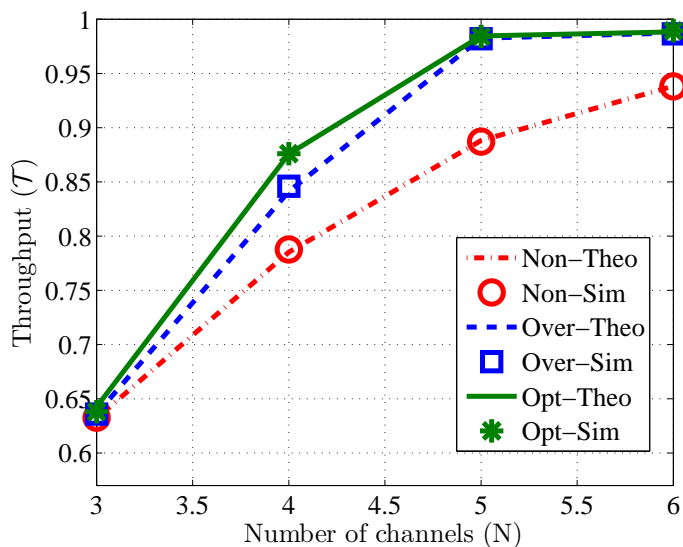


Figure 4.7: Minimum throughput versus the number of channels under max-min fairness (for $M = 3$, Theo: Theory, Sim: Simulation, Over: Overlapping, Non: Non-overlapping, Opt: Optimal assignment).

cal cognitive systems such as those operating on the TV bands standardized in the 802.22 standard requires the spectrum evacuation time of a few seconds [32]. We will present the total throughput under throughput maximization design and the minimum throughput under max-min fairness design in all numerical results. All throughput curves are obtained by averaging over 30 random realizations of $p_{i,j}$.

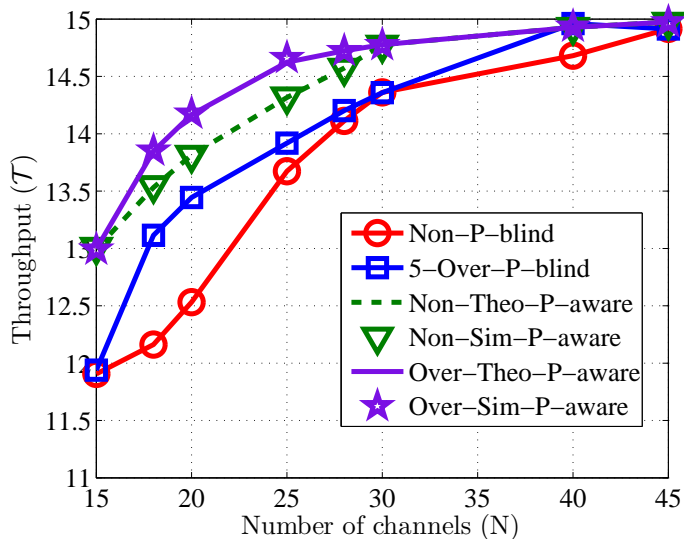


Figure 4.8: Total throughput versus the number of channels under throughput maximization design (for $M = 15$, Theo: Theory, Sim: Simulation, Over: Overlapping, Non: Non-overlapping, 5-Over: 5-user sharing Overlapping)

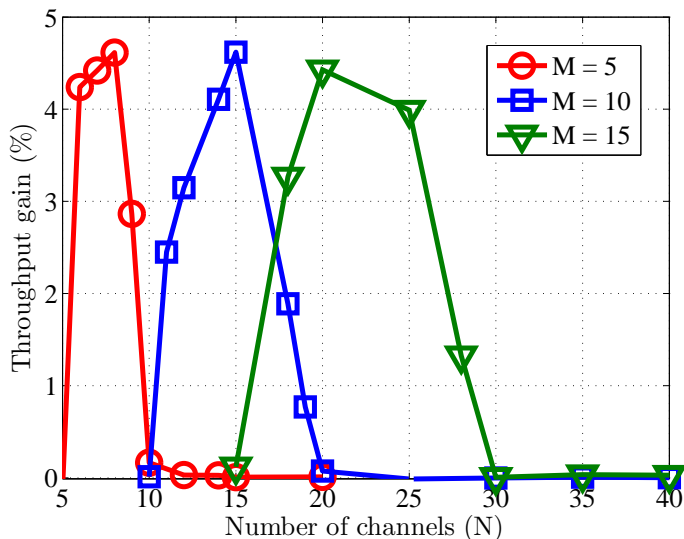


Figure 4.9: Throughput gain between Alg. 3 and Alg. 2 versus the number of channels

4.9.1 MAC Protocol Configuration

We first investigate interactions between MAC protocol parameters and the achievable throughput performance. In particular, we plot the average probability of the first collision, which is derived in Section 4.6.3 versus contention window in Fig. 4.2 when Alg. 3 is used for channel assignment. This figure shows that the collision probability first increases

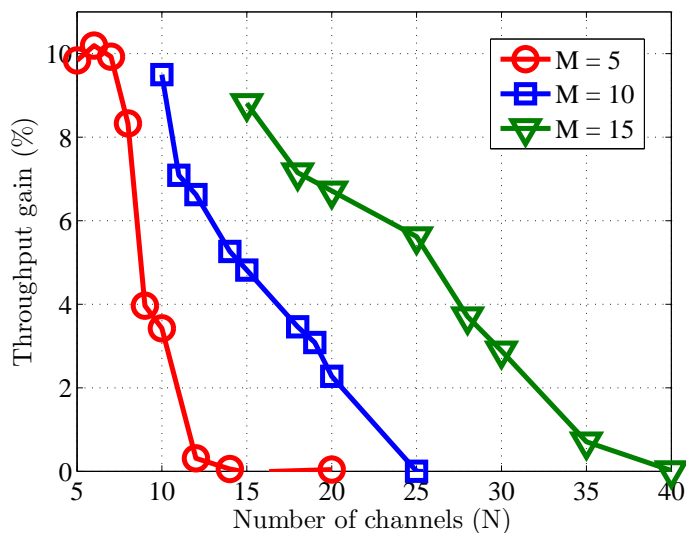


Figure 4.10: Throughput gain between Alg. 3 and P-blind 5-user sharing versus the number of channels

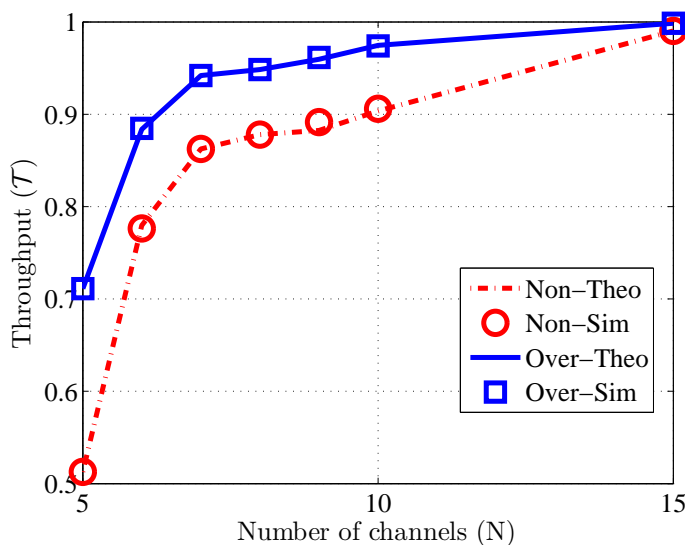


Figure 4.11: Minimum throughput versus the number of channels under max-min fairness (for $M = 5$, Theo: Theory, Sim: Simulation, Over: Overlapping, Non: Non-overlapping).

then decreases with N . This can be interpreted as follows. When N is relatively small, Alg. 3 tends to allow more overlapping channel assignments for increasing number of channels. However, more overlapping channel assignments increase the contention level because more users may want to exploit same channels, which results in larger collision probability. As N is sufficiently large, a few overlapping channel assignments is needed to achieve the

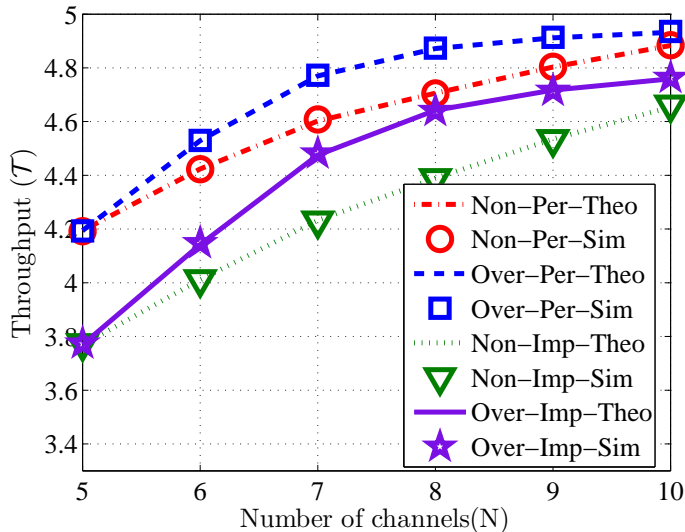


Figure 4.12: Total throughput versus the number of channels under throughput maximization design (for $M = 5$, $\mathcal{P}_f^{ij} \in [0.1, 0.15]$, $\mathcal{P}_d^{ij} = 0.9$, Theo: Theory, Sim: Simulation, Over: Overlapping, Non: Non-overlapping, Per: Perfect sensing, Imp: Imperfect sensing).

maximum throughput. Therefore, collision probability decreases with N .

We now consider the impact of target collision probability ϵ_P on the total network throughput, which is derived in Section 4.7.1. Recall that in this analysis collision probability is not taken into account, which is shown to have negligible errors in Proposition 2. Specifically, we plot the total network throughput versus ϵ_P for $M = 10$ and different values of N in Fig. 4.3. This figure shows that the total throughput slightly increases with ϵ_P . However, the increase is quite marginal as $\epsilon_P \geq 0.03$. In fact, the required contention window W given in (4.12) decreases with increasing ϵ_P (as can be observed from Fig. 4.2), which leads to decreasing MAC protocol overhead $\delta(W)$ as confirmed by (4.13) and therefore the increase in the total network throughput. Moreover, the total throughput may degrade with increasing ϵ_P because of the increasing number of collisions. Therefore, we will choose $\epsilon_P = 0.03$ to present the following results, which would be reasonable to balance between throughput gain due to moderate MAC protocol overhead and throughput loss due to contention collision.

4.9.2 Comparisons of Proposed Algorithms versus Optimal Algorithms

We demonstrate the efficacy of the proposed algorithms by comparing their throughput performances with those obtained by the optimal brute-force search algorithms for small

values of M and N . Numerical results are presented for both throughput-maximization and max-min fair objectives. In Figs. 4.4 and 4.5, we compare the throughputs of the proposed and optimal algorithms for $M = 2$ and $M = 3$ under the throughput-maximization objective. These figures confirm that Alg. 3 achieves throughput very close to that attained by the optimal solution for both values of M .

In Figs. 4.6, and 4.7, we plot the throughputs achieved by our proposed algorithm and the optimal algorithm for $M = 2$ and $M = 3$ under the max-min fair objective. Again, Alg. 5 achieves throughput very close to the optimal throughput under this design. In addition, analytical results match simulation results very well and non-overlapping channel assignment algorithms achieve noticeably lower throughputs than those attained by their overlapping counterparts if the number of channels is small. It can also be observed that the average throughput per user under the throughput maximization design is higher than the minimum throughput attained under max-min fair design. This is quite expected since the max-min fairness trades throughput for fairness.

4.9.3 Throughput Performance of Proposed Algorithms

We illustrate the total throughput \mathcal{T} versus the number of channels obtained by both Alg. 2 and Alg. 3 where each point is obtained by averaging the throughput over 30 different realizations of $p_{i,j}$ in Fig. 4.8. Throughput curves due to Alg. 2 and Alg. 3 are indicated as “P-ware” in this figure. In addition, for the comparison purposes, we also show the throughput performance achieved by “P-blind” algorithms, which simply allocate channels to users in a round-robin manner without exploiting the heterogeneity of $p_{i,j}$ (i.e., multiuser diversity gain). For P-blind algorithms, we show the performance of both non-overlapping and overlapping channel assignment algorithms. Here, the overlapping P-blind algorithm allows at most five users to share one particular channel. We have observed through numerical studies that allowing more users sharing one channel cannot achieve better throughput performance because of the excessive MAC protocol overhead.

As shown in Fig. 4.8, the analytical and simulation results achieved by both proposed algorithms match each other very well. This validates the accuracy of our throughput analytical model developed in Section 4.7.1. It also indicates that the total throughput reaches the maximum value, which is equal to $M = 15$ as the number of channels becomes sufficiently large for both Alg. 2 and Alg. 3. This confirms the result stated in Proposition 1. In addition, Alg. 3 achieves significantly larger throughput than Alg. 2 for low or moderate values of N . This performance gain comes from the multiuser diversity gain, which arises due to the

spatial dependence of white spaces. For large N (i.e., more than twice the number of users M), the negative impact of MAC protocol overhead prevents Alg. 3 from performing overlapped channel assignments. Therefore, both Alg. 2 and Alg. 3 achieve similar throughput performance.

Fig. 4.8 also indicates that both proposed algorithms outperform the round-robin channel assignment counterparts. In particular, Alg. 2 improves the total throughput significantly compared to the round-robin algorithm under non-overlapping channel assignments. For the overlapping channel assignment schemes, we show the throughput performance of the round-robin assignment algorithms when 5 users are allowed to share one channel (denoted as 5-user sharing in the figure). Although this achieves larger throughput for the round-robin algorithm, it still performs worse compared to the proposed algorithms. Moreover, we demonstrate the throughput gain due to Alg. 3 compared to Alg. 2 for different values of N and M in Fig. 4.9. This figure shows that performance gains up to 5% can be achieved when the number of channels is small or moderate. In addition, Fig. 4.10 presents the throughput gain due to Alg. 3 versus the P-blind algorithm with 5-user sharing. It can be observed that a significant throughput gain of up to 10% can be achieved for these investigated scenarios.

Fig. 4.11 illustrates the throughput of Alg. 4 and Alg. 5 where p_{ij} are chosen in the range of $[0.5, 0.9]$. It can be observed that the overlapping channel algorithm also improves the minimum throughput performance compared to the non-overlapping counterpart significantly. Finally, we plot the throughputs achieved by Alg. 2 and Alg. 3 under perfect and imperfect spectrum sensing for $M = 5$ in Fig. 4.12 where the detection probabilities are set as $\mathcal{P}_d^{ij} = 0.9$ while false alarm probabilities are randomly realized as $\mathcal{P}_f^{ij} \in [0.1, 0.15]$. This figure shows that sensing errors can significantly degrade the throughput performance of SUs. In addition, the presented results validate the throughput analytical model described in Section 4.8.2.

4.10 Conclusion

We have investigated the channel assignment problem for cognitive radio networks with hardware-constrained SUs. We have first presented the optimal brute-force search algorithm and analyzed its complexity. Then, we have developed the following two channel assignment algorithms for throughput maximization: 1) the non-overlapping overlapping channel assignment algorithm and 2) the overlapping channel assignment algorithm. In addition, we have developed an analytical model to analyze the saturation throughput that was achieved

by the overlapping channel assignment algorithm. We have also presented several potential extensions, including the design of max-min fair channel assignment algorithms and throughput analysis, considering imperfect spectrum sensing. We have validated our results through numerical studies and demonstrated significant throughput gains of the overlapping channel assignment algorithm compared with its non-overlapping and round-robin channel assignment counterparts in different network settings.

Chapter 5

Joint Cooperative Spectrum Sensing and MAC Protocol Design for Multi-channel Cognitive Radio Networks

The content of this chapter was published in EURASIP Journal on Wireless Communications and Networking in the following paper:

L. T. Tan, and L. B. Le, “Joint Cooperative Spectrum Sensing and MAC Protocol Design for Multi-channel Cognitive Radio Networks,” *EURASIP Journal on Wireless Communications and Networking*, 2014 (101), June 2014.

5.1 Abstract

In this paper, we propose a semi-distributed cooperative spectrum sensing (SDCSS) and channel access framework for multi-channel cognitive radio networks (CRNs). In particular, we consider a SDCSS scheme where secondary users (SUs) perform sensing and exchange sensing outcomes with each other to locate spectrum holes. In addition, we devise the p -persistent CSMA-based cognitive MAC protocol integrating the SDCSS to enable efficient spectrum sharing among SUs. We then perform throughput analysis and develop an algorithm to determine the spectrum sensing and access parameters to maximize the throughput for a given allocation of channel sensing sets. Moreover, we consider the spectrum sensing set optimization problem for SUs to maximize the overall system throughput. We present

both exhaustive search and low-complexity greedy algorithms to determine the sensing sets for SUs and analyze their complexity. We also show how our design and analysis can be extended to consider reporting errors. Finally, extensive numerical results are presented to demonstrate the significant performance gain of our optimized design framework with respect to non-optimized designs as well as the impacts of different protocol parameters on the throughput performance.

5.2 Introduction

It has been well recognized that cognitive radio is one of the most important technologies that would enable us to meet exponentially growing spectrum demand via fundamentally improving the utilization of our precious spectral resources [2]. Development of efficient spectrum sensing and access algorithms for cognitive radios are among the key research issues for successful deployment of this promising technology. There is indeed a growing literature on MAC protocol design and analysis for CRNs [5, 16–19, 22, 33, 47, 62, 63, 102] (see [47] for a survey of recent works in this topic). In [5], it was shown that a significant throughput gain can be achieved by optimizing the sensing time under the single-SU setting. Another related effort along this line was conducted in [16] where sensing-period optimization and optimal channel-sequencing algorithms were proposed to efficiently discover spectrum holes and to minimize the exploration delay.

In [17], a control-channel based MAC protocol was proposed for SUs to exploit white spaces in the cognitive ad hoc network. In particular, the authors of this paper developed both random and negotiation-based spectrum sensing schemes and performed throughput analysis for both saturation and non-saturation scenarios. There exists several other synchronous cognitive MAC protocols, which rely on a control channel for spectrum negotiation and access [18, 19, 62, 63, 102]. In [22] and [33], we designed, analyzed, and optimized a window-based MAC protocol to achieve efficient tradeoff between sensing time and contention overhead. However, these works considered the conventional single-user-energy-detection-based spectrum sensing scheme, which would only work well if the signal to noise ratio (SNR) is sufficiently high. In addition, the MAC protocol in these works was the standard window-based CSMA MAC protocol, which is known to be outperformed by the p-persistent CSMA MAC protocol [70].

Optimal sensing and access design for CRNs were designed by using optimal stopping theory in [105]. In [68], a multi-channel MAC protocol was proposed considering the distance

among users so that white spaces can be efficiently exploited while satisfactorily protecting primary users (PUs). Different power and spectrum allocation algorithms were devised to maximize the secondary network throughput in [23, 24, 106]. Optimization of spectrum sensing and access in which either cellular or TV bands can be employed was performed in [25]. These existing works either assumed perfect spectrum sensing or did not consider the cooperative spectrum sensing in their design and analysis.

Cooperative spectrum sensing has been proposed to improve the sensing performance where several SUs collaborate with each other to identify spectrum holes [64–66, 69, 84, 96–99]. In a typical cooperative sensing scheme, each SU performs sensing independently and then sends its sensing result to a central controller (e.g., an access point (AP)). Here, various aggregation rules can be employed to combine these sensing results at the central controller to decide whether or not a particular spectrum band is available for secondary access. In [66], the authors studied the performance of hard decisions and soft decisions at a fusion center. They also investigated the impact of reporting channel errors on the cooperative sensing performance. Recently, the authors of [67] proposed a novel cooperative spectrum sensing scheme using hard decision combining considering feedback errors.

In [84, 97–99], optimization of cooperative sensing under the a-out-of-b rule was studied. In [84], the game-theoretic based method was proposed for cooperative spectrum sensing. In [69], the authors investigated the multi-channel scenario where the AP collects statistics from SUs to decide whether it should stop at the current time slot. In [100, 101], two different optimization problems for cooperative sensing were studied. The first one focuses on throughput maximization where the objective is the probability of false alarm. The second one attempts to perform interference management where the objective is the probability of detection. These existing works focused on designing and optimizing parameters for the cooperative spectrum sensing algorithm; however, they did not consider spectrum access issues. Furthermore, either the single channel setting or homogeneous network scenario (i.e., SUs experience the same channel condition and spectrum statistics for different channels) was assumed in these works.

In [26] and [34], the authors conducted design and analysis for cooperative spectrum sensing and MAC protocol design for cognitive radios where parallel spectrum sensing on different channels was assumed to be performed by multiple spectrum sensors at each SU. In CRNs with parallel-sensing, there is no need to optimize spectrum sensing sets for SUs. These works again considered the homogeneous network and each SU simply senses all channels. To the best of our knowledge, existing cooperative spectrum sensing schemes rely on a central

controller to aggregate sensing results for white space detection (i.e., centralized design). In addition, homogeneous environments and parallel sensing have been commonly assumed in the literature, which would not be very realistic.

In this work, we consider a general SDCSS and access framework under the heterogeneous environment where statistics of wireless channels, and spectrum holes can be arbitrary and there is no central controller to collect sensing results and make spectrum status decisions. In addition, we assume that each SU is equipped with only one spectrum sensor so that SUs have to sense channels sequentially. This assumption would be applied to real-world hardware-constrained cognitive radios. The considered SDCSS scheme requires SUs to perform sensing on their assigned sets of channels and then exchange spectrum sensing results with other SUs, which can be subject to errors. After the sensing and reporting phases, SUs employ the p -persistent CSMA MAC protocol [70] to access one available channel. In this MAC protocol, parameter p denotes the access probability to the chosen channel if the carrier sensing indicates an available channel (i.e., no other SUs transmit on the chosen channel). It is of interest to determine the access parameter p that can mitigate the collisions and hence enhance the system throughput [70]. Also, optimization of the spectrum sensing set for each SU (i.e., the set of channels sensed by the SU) is very critical to achieve good system throughput. Moreover, analysis and optimization of the joint spectrum sensing and access design become much more challenging in the heterogeneous environment, which, however, can significantly improve the system performance. Our current paper aims to resolve these challenges whose contributions can be summarized as follows:

- We propose the distributed p -persistent CSMA protocol incorporating SDCSS for multi-channel CRNs. Then we analyze the saturation throughput and optimize the spectrum sensing time and access parameters to achieve maximum throughput for a given allocation of channel sensing sets. This analysis and optimization are performed in the general heterogeneous scenario assuming that spectrum sensing sets for SUs have been predetermined.
- We study the channel sensing set optimization (i.e., channel assignment) for throughput maximization and devise both exhaustive search and low-complexity greedy algorithms to solve the underlying NP-hard optimization problem. Specifically, an efficient solution for the considered problem would only allocate a subset of “good” SUs to sense each channel so that accurate sensing can be achieved with minimal sensing time. We also analyze the complexity of the brute-force search and the greedy algorithms.

5.3 System Model and Spectrum Sensing Design

- We extend the design and analysis to consider reporting errors as SUs exchange their spectrum sensing results. In particular, we describe cooperative spectrum sensing model, derive the saturation throughput considering reporting errors. Moreover, we discuss how the proposed algorithms to optimize the sensing/access parameters and sensing sets can be adapted to consider reporting errors. Again, all the analysis is performed for the heterogeneous environment.
- We present numerical results to illustrate the impacts of different parameters on the secondary throughput performance and demonstrate the significant throughput gain due to the optimization of different parameters in the proposed framework.

The remaining of this paper is organized as follows. Section 5.3 describes system and sensing models. MAC protocol design, throughput analysis, and optimization are performed in Section 5.4 assuming no reporting errors. Section 5.5 provides further extension for the analysis and optimization considering reporting errors. Section 5.6 presents numerical results followed by concluding remarks in Section 5.7. The summary of key variables in the paper is given in Table 5.1.

5.3 System Model and Spectrum Sensing Design

In this section, we describe the system model and spectrum sensing design for the multi-channel CRNs. Specifically, sensing performances in terms of detection and false alarm probabilities are presented.

5.3.1 System Model

We consider a network setting where N pairs of SUs opportunistically exploit white spaces in M channels for data transmission. For simplicity, we refer to pair i of SUs simply as SU i . We assume that each SU can exploit only one available channel for transmission (i.e., SUs are equipped with narrow-band radios). We will design a synchronized MAC protocol integrating SDCSS for channel access. We assume that each channel is either in the idle or busy state for each predetermined periodic interval, which is referred to as a cycle in this paper.

We further assume that each pair of SUs can overhear transmissions from other pairs of SUs (i.e., collocated networks). There are M PUs each of which may or may not use one corresponding channel for its data transmission in each cycle. In addition, it is assumed that

5.3 System Model and Spectrum Sensing Design

Table 5.1: Summary of Key Variables

Variable	Description
Key variables for no-reporting-error scenario	
$\mathcal{P}_j (\mathcal{H}_0) (\mathcal{P}_j (\mathcal{H}_1))$	probability that channel j is available (or not available)
$\mathcal{P}_d^{ij} (\mathcal{P}_f^{ij})$	probability of detection (false alarm) experienced by SU i for channel j
$\mathcal{P}_d^j (\mathcal{P}_f^j)$	probability of detection (false alarm) for channel j under SDCSS
$\varepsilon^{ij}, \gamma^{ij}$	detection threshold, signal-to-noise ratio of the PU's signal
τ^{ij}, τ	sensing time at SU i on channel j , total sensing time
N_0, f_s	noise power, sampling frequency
a_j, b_j	parameters of a -out-of- b rule for channel j
N, M	total number of SUs, total number of channels
$\mathcal{S}_j^U, \mathcal{S}^U$	set of SUs that sense channel j , set of all N SUs
$\mathcal{S}_i, \mathcal{S}$	set of assigned channels for SU i , set of all M channels
Φ_l^k	particular set k of l SUs
$\Psi_{k_0}^{l_0}$	set l_0 of k_0 actually available channels
$\Theta_{k_1}^{l_1}, \Omega_{k_2}^{l_2}$	set l_1 of k_1 available channels (which are indicated by sensing outcomes), set l_2 of k_2 misdetected channels (which are indicated by sensing outcomes)
$\mathcal{N}\mathcal{J}$	normalized throughput per one channel
$\mathcal{J}_p^{ne}, \mathcal{J}_{j_2}^{ne}$	conditional throughput: for one particular realization of sensing outcomes corresponding to 2 sets $\Theta_{k_1}^{l_1}$ and $\Omega_{k_2}^{l_2}$, for a particular channel j_2
n_j, k_e	number of SUs who select channel j to access, $k_e = \Theta_{k_1}^{l_1} \cup \Omega_{k_2}^{l_2} $
T, T_R	cycle time, total reporting time
T_S, \bar{T}_S	time for transmission of packet, time for successful RTS/CTS transmission
$T_I^{i,j}, \bar{T}_I^j$	i -th duration between 2 consecutive RTS/CTS transmission on channel j (its average value)
T_C, \bar{T}_{cont}	duration of collision, average contention time on channel j
PD	propagation delay
PS, ACK	lengths of packet and acknowledgment, respectively
$SIFS, DIFS$	lengths of short time interframe space and distributed interframe space, respectively
RTS, CTS	lengths of request-to-send and clear-to-send, respectively
p, \mathcal{P}_C^j	transmission probability, probability of a generic slot corresponding to collision
$\mathcal{P}_S^j, \mathcal{P}_I^j$	probabilities of a generic slot corresponding to successful transmission, idle slot
$N_c^j (\bar{N}_c^j)$	number of collisions before the first successful RTS/CTS exchange (its average value)
$f_X^{N_c}, f_X^I$	pmfs of $N_c^j, T_I^{i,j}$
Key variables as considering reporting errors	
$\mathcal{P}_e^{i_1 i_2}$	probability of reporting errors between SUs i_1 and i_2
$\mathcal{P}_d^{i_1 i_2 j} (\mathcal{P}_f^{i_1 i_2 j})$	probabilities of detection (false alarm) experienced by SU i_1 on channel j with the sensing result received from SU i_2
$\Theta_{k_1, j_3}^{l_1}$	l_1 -th set of k_1 SUs whose sensing outcomes indicate that channel j_3 is vacant
$\Omega_{k_2, j_4}^{l_2}$	l_2 -th set of k_2 SUs whose sensing outcomes indicate that channel j_4 is vacant due to misdetection
$\Phi_{k_3, j_3}^{l_3}$	l_3 -th set of k_3 SUs in $\Theta_{k_1, j_3}^{l_1}$ who correctly report their sensing information on channel j_3 to SU i_4
$\Lambda_{k_4, j_3}^{l_4}$	l_4 -th set of k_4 SUs in $\mathcal{S}_{j_3}^U \setminus \Theta_{k_1, j_3}^{l_1}$ who incorrectly report their sensing information on channel j_3 to SU i_4
$\Xi_{k_5, j_4}^{l_5}$	l_5 -th set of k_5 SUs in $\Omega_{k_2, j_4}^{l_2}$ who correctly report their sensing information on channel j_4 to SU i_9
$\Gamma_{k_6, j_4}^{l_6}$	l_6 -th set of k_6 SUs in $\mathcal{S}_{j_4}^U \setminus \Omega_{k_2, j_4}^{l_2}$ who incorrectly report their sensing information on channel j_4 to SU i_9
$\mathcal{S}_{1,i}^a, \mathcal{S}_{2,i}^a$	sets of actually available channels and available due to sensing and/or reporting errors, respectively
$\hat{\mathcal{S}}_1^a, \hat{\mathcal{S}}_2^a$	$\hat{\mathcal{S}}_1^a = \bigcup_{i \in \mathcal{S}^U} \mathcal{S}_{1,i}^a, \hat{\mathcal{S}}_2^a = \bigcup_{i \in \mathcal{S}^U} \mathcal{S}_{2,i}^a$
$\mathcal{S}_i^a, \hat{\mathcal{S}}^a$	$\mathcal{S}_i^a = \mathcal{S}_{1,i}^a \cup \mathcal{S}_{2,i}^a, \hat{\mathcal{S}}^a = \hat{\mathcal{S}}_1^a \cup \hat{\mathcal{S}}_2^a$
k_e^i, k_{max}	$k_e^i = \mathcal{S}_i^a , k_{max} = \hat{\mathcal{S}}^a $
Ψ_j^a, Ψ^a	set of SUs whose SDCSS outcomes indicate that channel j is available, $\Psi^a = \bigcup_{j \in \hat{\mathcal{S}}^a} \Psi_j^a$
N_j, N_{max}	$N_j = \Psi_j^a , N_{max} = \Psi^a $
$\mathcal{J}_p^{re}, \mathcal{J}_{j_2}^{re}$	conditional throughput for one particular realization of sensing outcomes and for a particular channel j_2 , respectively

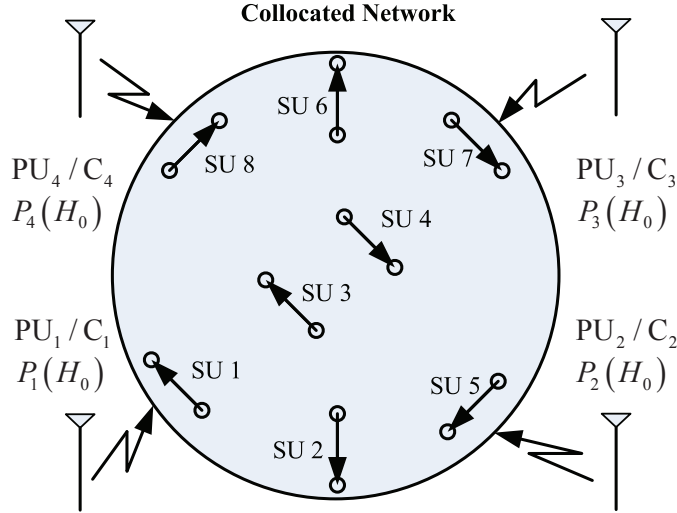


Figure 5.1: Considered network and spectrum sharing model (PU: primary user, SU: secondary user, and C_i is the channel i corresponding to PU_i)

transmission from any pair of SUs on a particular channel will affect the primary receiver which receives data on that channel. The network setting under investigation is shown in Fig. 5.1 where C_i denotes channel i that belongs to PU_i .

5.3.2 Semi-Distributed Cooperative Spectrum Sensing

We assume that each SU i is assigned a set of channels \mathcal{S}_i where it senses all channels in this assigned set at beginning of each cycle in a sequential manner (i.e., sense one-by-one). Optimization of such channel assignment will be considered in the next section. Upon completing the channel sensing, each SU i exchanges the sensing results (i.e., idle/busy status of all channels in \mathcal{S}_i) with other SUs for further processing. Here, the channel status of each channel can be represented by one bit (e.g., 1 for idle and 0 for busy status). Upon collecting sensing results, each SU will decide idle/busy status for all channels. Then, SUs are assumed to employ a distributed MAC protocol to perform access resolution so that only the winning SUs on each channel are allowed to transmit data. The detailed MAC protocol design will be presented later.

Let \mathcal{H}_0 and \mathcal{H}_1 denote the events that a particular PU is idle and active on its corresponding channel in any cycle, respectively. In addition, let $\mathcal{P}_j(\mathcal{H}_0)$ and $\mathcal{P}_j(\mathcal{H}_1) = 1 - \mathcal{P}_j(\mathcal{H}_0)$ be the probabilities that channel j is available and not available for secondary access, respectively. We assume that SUs employ an energy detection sensing scheme and let f_s be

5.3 System Model and Spectrum Sensing Design

the sampling frequency used in the sensing period for all SUs. There are two important performance measures, which are used to quantify the sensing performance, namely detection and false alarm probabilities. In particular, a detection event occurs when a SU successfully senses a busy channel and false alarm represents the situation when a spectrum sensor returns a busy status for an idle channel (i.e., the transmission opportunity is overlooked).

Assume that transmission signals from PUs are complex-valued PSK signals while the noise at the SUs is independent and identically distributed circularly symmetric complex Gaussian $\mathcal{CN}(0, N_0)$ [5]. Then, the detection and false alarm probabilities experienced by SU i for the channel j can be calculated as [5]

$$\mathcal{P}_d^{ij}(\varepsilon^{ij}, \tau^{ij}) = \mathcal{Q} \left(\left(\frac{\varepsilon^{ij}}{N_0} - \gamma^{ij} - 1 \right) \sqrt{\frac{\tau^{ij} f_s}{2\gamma^{ij} + 1}} \right), \quad (5.1)$$

$$\begin{aligned} \mathcal{P}_f^{ij}(\varepsilon^{ij}, \tau^{ij}) &= \mathcal{Q} \left(\left(\frac{\varepsilon^{ij}}{N_0} - 1 \right) \sqrt{\tau^{ij} f_s} \right) \\ &= \mathcal{Q} \left(\sqrt{2\gamma^{ij} + 1} \mathcal{Q}^{-1}(\mathcal{P}_d^{ij}(\varepsilon^{ij}, \tau^{ij})) + \sqrt{\tau^{ij} f_s} \gamma^{ij} \right), \end{aligned} \quad (5.2)$$

where $i \in [1, N]$ is the SU index, $j \in [1, M]$ is the channel index, ε^{ij} is the detection threshold for the energy detector, γ^{ij} is the signal-to-noise ratio (SNR) of the PU's signal at the SU, f_s is the sampling frequency, N_0 is the noise power, τ^{ij} is the sensing time of SU i on channel j , and $\mathcal{Q}(\cdot)$ is defined as $\mathcal{Q}(x) = (1/\sqrt{2\pi}) \int_x^\infty \exp(-t^2/2) dt$.

We assume that a general cooperative sensing scheme, namely a -out-of- b rule, is employed by each SU to determine the idle/busy status of each channel based on reported sensing results from other SUs. Under this scheme, an SU will declare that a channel is busy if a or more messages out of b sensing messages report that the underlying channel is busy. The a -out-of- b rule covers different rules including OR, AND and majority rules as special cases. In particular, $a = 1$ corresponds to the OR rule; if $a = b$ then it is the AND rule; and the majority rule has $a = \lceil b/2 \rceil$.

To illustrate the operations of the a -out-of- b rule, let us consider a simple example shown in Fig. 5.2. Here, we assume that 3 SUs collaborate to sense channel one with $a = 2$ and $b = 3$. After sensing channel one, all SUs exchange their sensing outcomes. SU3 receives the reporting results comprising two "1" and one "0" where "1" means that the channel is busy and "0" means channel is idle. Because the total number of "1s" is two which is larger than or equal to $a = 2$, SU3 outputs the "1" in the final sensing result, namely the channel is busy.

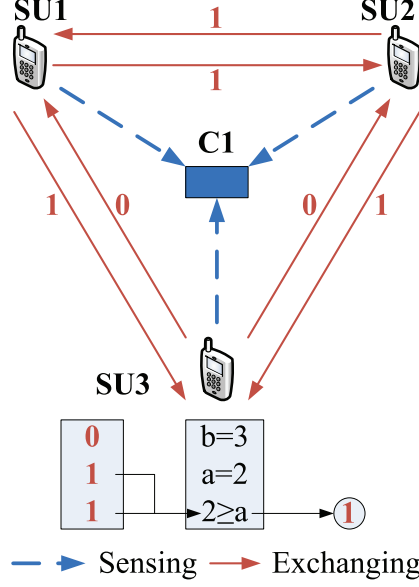


Figure 5.2: Example for SDCSS on 1 channel.

Let us consider a particular channel j . Let \mathcal{S}_j^U denote the set of SUs that sense channel j , $b_j = |\mathcal{S}_j^U|$ be the number of SUs sensing channel j , and a_j be the number of messages indicating that the underlying channel is busy. Then, the final decision on the spectrum status of channel j under the a -out-of- b rule has detection and false alarm probabilities that can be written as [84]

$$\mathcal{P}_u^j(\bar{\varepsilon}^j, \bar{\tau}^j, a_j) = \sum_{l=a_j}^{b_j} \sum_{k=1}^{C_{b_j}^l} \prod_{i_1 \in \Phi_l^k} \mathcal{P}_u^{i_1 j} \prod_{i_2 \in \mathcal{S}_j^U \setminus \Phi_l^k} \bar{\mathcal{P}}_u^{i_2 j}, \quad (5.3)$$

where u represents d or f as we calculate the probability of detection \mathcal{P}_d^j or false alarm \mathcal{P}_f^j , respectively; $\bar{\mathcal{P}}$ is defined as $\bar{\mathcal{P}} = 1 - \mathcal{P}$; Φ_l^k in (5.3) denotes a particular set with l SUs whose sensing outcomes suggest that channel j is busy given that this channel is indeed busy and idle as u represents d and f , respectively. Here, we generate all possible combinations of Φ_l^k where there are indeed $C_{b_j}^l$ combinations. Also, $\bar{\varepsilon}^j = \{\varepsilon^{ij}\}$, $\bar{\tau}^j = \{\tau^{ij}\}$, $i \in \mathcal{S}_j^U$ represent the set of detection thresholds and sensing times, respectively. For brevity, $\mathcal{P}_d^j(\bar{\varepsilon}^j, \bar{\tau}^j, a_j)$ and $\mathcal{P}_f^j(\bar{\varepsilon}^j, \bar{\tau}^j, a_j)$ are sometimes written as \mathcal{P}_d^j and \mathcal{P}_f^j in the following.

Each SU exchanges the sensing results on its assigned channels with other SUs over a control channel, which is assumed to be always available (e.g., it is owned by the secondary network). To avoid collisions among these message exchanges, we assume that there are N reporting time slots for N SUs each of which has length equal to t_r . Hence, the total time

5.3 System Model and Spectrum Sensing Design

Table 5.2: Channel Assignment Example for SUs (x denotes an assignment)

		Channel				
		1	2	3	4	5
SU	1	x		x	x	
	2	x	x			
	3		x	x	x	
	4					
	5	x				x

for exchanging sensing results among SUs is Nt_r . Note that the set of channels assigned to SU i for sensing, namely \mathcal{S}_i , is a subset of all channels and these sets can be different for different SUs. An example of channel assignment (i.e., channel sensing sets) is presented in Table 5.2. In this table, SU 4 is not assigned any channel. Hence, this SU must rely on the sensing results of other SUs to determine the spectrum status.

Remark 1: In practice, the idle/busy status of primary system on a particular channel can be arbitrary and would not be synchronized with the operations of the SUs (i.e., the idle/busy status of any channel can change in the middle of a cycle). Hence, to strictly protect the PUs, SUs should continuously scan the spectrum of interest and evacuate from an exploited channel as soon as the PU changes from an idle to a busy state. However, this continuous spectrum monitoring would be very costly to implement since each SU should be equipped with two half-duplex transceivers to perform spectrum sensing and access at the same time. A more efficient protection method for PUs is to perform periodic spectrum sensing where SUs perform spectrum sensing at the beginning of each fixed-length interval and exploits available frequency bands for data transmission during the remaining time of the interval. In this paper, we assume that the idle/busy status of each channel remains the same in each cycle, which enables us to analyze the system throughput. In general, imposing this assumption would not sacrifice the accuracy of our throughput analysis if PUs maintain their idle/busy status for a sufficiently long time. This is actually the case for many practical scenarios such as in the TV bands, as reported by several recent studies [113]. In addition, our MAC protocol that is developed under this assumption would result in very few collisions with PUs because the cycle time is quite small compared to the typical intervals over which the active/idle statuses of PUs change.

5.4 Performance Analysis and Optimization for Cognitive MAC Protocol

We present the cognitive MAC protocol design, performance analysis, and optimization for the multi-channel CRNs in this section.

5.4.1 Cognitive MAC Protocol Design

We assume that time is divided into fixed-size cycles and it is assumed that SUs can perfectly synchronize with each other (i.e., there is no synchronization error) [62]. We propose a synchronized multi-channel MAC protocol for dynamic spectrum sharing as follows. The MAC protocol has four phases in each cycle as illustrated in Fig. 5.3. The beacon signal is sent on the control channel to achieve synchronization in the first phase [62] which is presented in the simple manner as follows. At the beginning of this phase, each SU senses the beacon signal from the volunteered synchronized SU which is the first SU sending the beacon. If an SU does not receive any beacon, it selects itself as the volunteered SU and sends out the beacon for synchronization. In the second phase, namely the sensing phase of length τ , all SUs simultaneously perform spectrum sensing on their assigned channels. Here, we have $\tau = \max_i \tau^i$, where $\tau^i = \sum_{j \in \mathcal{S}_i} \tau^{ij}$ is total sensing time of SU i , τ^{ij} is the sensing time of SU i on channel j , and \mathcal{S}_i is the set of channels assigned for SU i . We assume that one separate channel is assigned as a control channel which is used to exchange sensing results for reporting as well as broadcast a beacon signal for synchronization. This control channel is assumed to be always available (e.g., it is owned by the secondary network). In the third phase, all SUs exchange their sensing results with each other via the control channel. Based on these received sensing results, each SU employs SDCSS techniques to decide the channel status of all channels and hence has a set of available channels. Then each SU transmitter will choose one available channel randomly (which is used for contention and data transmission) and inform it to the corresponding SU receiver via the control channel.

In the fourth phase, SUs will participate in contention and data transmission on their chosen channels. We assume that the length of each cycle is sufficiently large so that SUs can transmit several packets during this data contention and transmission phase. In particular, we employ the p -persistent CSMA principle [70] to devise our cognitive MAC protocol. In this protocol, each SU attempts to transmit on the chosen channel with a probability of p if it senses an available channel (i.e., no other SUs transmit data on its chosen channel). In case the SU decides not to transmit (with probability of $1 - p$), it will sense the channel and

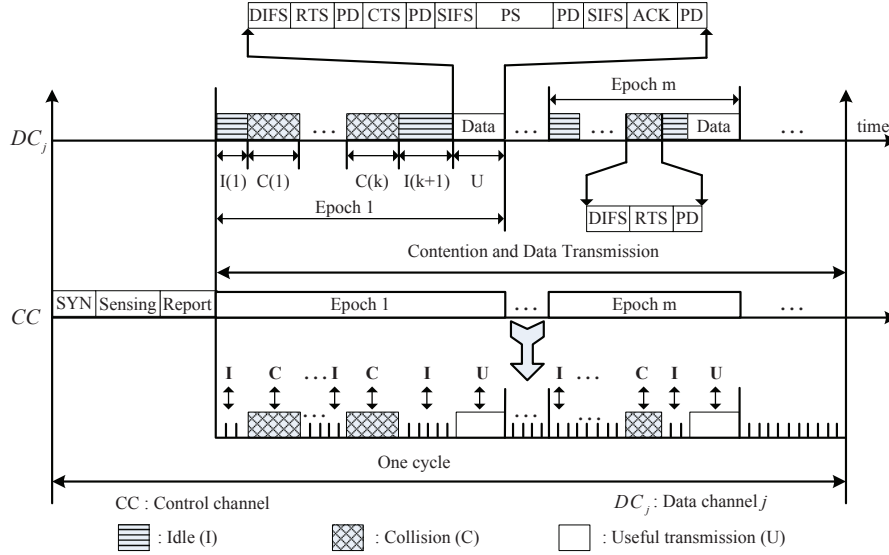


Figure 5.3: Timing diagram of cognitive p -persistent CSMA protocol for one specific channel j .

attempt to transmit again in the next slot with probability p . If there is a collision, the SU will wait until the channel is available and attempt to transmit with probability p as before.

The standard 4-way handshake with RTS/CTS (request-to-send/clear-to-send) [85] will be employed to reserve a channel for data transmission. So the SU choosing to transmit on each available channel exchanges RTS/CTS messages before transmitting its actual data packet. An acknowledgment (ACK) from the receiver is transmitted to the transmitter for successful reception of any packet. The detailed timing diagram of this MAC protocol is presented in Fig. 5.3.

Remark 2: For simplicity, we consider the fixed control channel in our design. However, extensions to consider dynamic control channel selections to avoid the congestion can be adopted in our proposed framework. More information on these designs can be found in [31].

5.4.2 Saturation Throughput Analysis

In this section, we analyze the saturation throughput of the proposed cognitive p -persistent CSMA protocol assuming that there are no reporting errors in exchanging the spectrum sensing results among SUs. Because there are no reporting errors, all SUs acquire the same sensing results for each channel, which implies that they make the same final sensing

5.4 Performance Analysis and Optimization for Cognitive MAC Protocol

decisions since the same a-out-b aggregation rule is employed for each channel. In the analysis, transmission time is counted in terms of contention time slot, which is assumed to be v seconds. Each data packet is assumed to be of fixed size of PS time slots. Detailed timing diagram of the p -persistent CSMA MAC protocol is illustrated in Fig. 5.3.

Any particular channel alternates between idle and busy periods from the viewpoint of the secondary system where each busy period corresponds to either a collision or a successful transmission. We use the term ‘‘epoch’’ to refer to the interval between two consecutive successful transmissions. This means an epoch starts with an idle period followed by some alternating collision periods and idle periods before ending with a successful transmission period. Note that an idle period corresponds to the interval between two consecutive packet transmissions (collisions or successful transmissions).

Recall that each SU chooses one available channel randomly for contention and transmission according to the final cooperative sensing outcome. We assume that upon choosing a channel, an SU keeps contending and accessing this channel until the end of the current cycle. In the case of missed detection (i.e., the PU is using the underlying channel but the sensing outcome suggests that the channel is available), there will be collisions between SUs and the PU. Therefore, RTS and CTS exchanges will not be successful in this case even though SUs cannot differentiate whether they collide with other SUs or the PU. Note that channel accesses of SUs due to missed detections do not contribute to the secondary system throughput.

To calculate the throughput for the secondary network, we have to consider all scenarios of idle/busy statuses of all channels and possible mis-detection and false alarm events for each particular scenario. Specifically, the normalized throughput per one channel achieved by our proposed MAC protocol, $\mathcal{NT}(\{\tau^{ij}\}, \{a_j\}, p, \{\mathcal{S}_i\})$ can be written as

$$\mathcal{NT} = \sum_{k_0=1}^M \sum_{l_0=1}^{C_M^{k_0}} \prod_{j_1 \in \Psi_{k_0}^{l_0}} \mathcal{P}_{j_1}(\mathcal{H}_0) \prod_{j_2 \in \mathcal{S} \setminus \Psi_{k_0}^{l_0}} \mathcal{P}_{j_2}(\mathcal{H}_1) \times \quad (5.4)$$

$$\sum_{k_1=1}^{k_0} \sum_{l_1=1}^{C_{k_0}^{k_1}} \prod_{j_3 \in \Theta_{k_1}^{l_1}} \bar{\mathcal{P}}_f^{j_3} \prod_{j_4 \in \Psi_{k_0}^{l_0} \setminus \Theta_{k_1}^{l_1}} \mathcal{P}_f^{j_4} \times \quad (5.5)$$

$$\sum_{k_2=0}^{M-k_0} \sum_{l_2=1}^{C_{M-k_0}^{k_2}} \prod_{j_5 \in \Omega_{k_2}^{l_2}} \bar{\mathcal{P}}_d^{j_5} \prod_{j_6 \in \mathcal{S} \setminus \Psi_{k_0}^{l_0} \setminus \Omega_{k_2}^{l_2}} \mathcal{P}_d^{j_6} \times \quad (5.6)$$

$$\mathcal{T}_p^{\text{ne}}(\tau, \{a_j\}, p). \quad (5.7)$$

5.4 Performance Analysis and Optimization for Cognitive MAC Protocol

The quantity (5.4) represents the probability that there are k_0 available channels, which may or may not be correctly determined by the SDCSS. Here, $\Psi_{k_0}^{l_0}$ denotes a particular set of k_0 available channels out of M channels whose index is l_0 . In addition, the quantity (5.5) describes the probability that the SDCSS indicates k_1 available channels whereas the remaining available channels are overlooked due to sensing errors where $\Theta_{k_1}^{l_1}$ denotes the l_1 -th set with k_1 available channels. For the quantity in (5.6), k_2 represents the number of channels that are not available but the sensing outcomes indicate that they are available (i.e., due to misdetection) where $\Omega_{k_2}^{l_2}$ denotes the l_2 -th set with k_2 mis-detected channels. The quantity in (5.6) describes the probability that the sensing outcomes due to SUs incorrectly indicates k_2 available channels. Finally, $\mathcal{J}_p^{\text{ne}}(\tau, \{a_j\}, p)$ in (5.7) denotes the conditional throughput for a particular realization of sensing outcomes corresponding to two sets $\Theta_{k_1}^{l_1}$ and $\Omega_{k_2}^{l_2}$.

Therefore, we have to derive the conditional throughput $\mathcal{J}_p^{\text{ne}}(\tau, \{a_j\}, p)$ to complete the throughput analysis, which is pursued in the following. Since each SU randomly chooses one available channel according to the SDCSS for contention and access, the number of SUs actually choosing a particular available channel is a random number. In addition, the SDCSS suggests that channels in $\Theta_{k_1}^{l_1} \cup \Omega_{k_2}^{l_2}$ are available for secondary access but only channels in $\Theta_{k_1}^{l_1}$ are indeed available and can contribute to the secondary throughput (channels in $\Omega_{k_2}^{l_2}$ are misdetected by SUs). Let $\{n_j\} = \{n_1, n_2, \dots, n_{k_e}\}$ be the vector describing how SUs choose channels for access where $k_e = |\Theta_{k_1}^{l_1} \cup \Omega_{k_2}^{l_2}|$ and n_j denotes the number of SUs choosing channel j for access. Therefore, the conditional throughput $\mathcal{J}_p^{\text{ne}}(\tau, \{a_j\}, p)$ can be calculated as follows:

$$\mathcal{J}_p^{\text{ne}}(\tau, \{a_j\}, p) = \sum_{\{n_j\}: \sum_{j \in \Theta_{k_1}^{l_1} \cup \Omega_{k_2}^{l_2}} n_j = N} \mathcal{P}(\{n_j\}) \times \quad (5.8)$$

$$\sum_{j_2 \in \Theta_{k_1}^{l_1}} \frac{1}{M} \mathcal{J}_{j_2}^{\text{ne}}(\tau, \{a_{j_2}\}, p | n = n_{j_2}) \mathcal{J}(n_{j_2} > 0), \quad (5.9)$$

where $\mathcal{P}(\{n_j\})$ in (5.8) represents the probability that the channel access vector $\{n_j\}$ is realized (each channel j where $j \in \Theta_{k_1}^{l_1} \cup \Omega_{k_2}^{l_2}$ is selected by n_j SUs). The sum in (5.9) describes the normalized throughput per channel due to a particular realization of the access vector $\{n_j\}$. Therefore, it is equal to the total throughput achieved by all available channels (in the set $\Theta_{k_1}^{l_1}$) divided by the total number of channels M . Here, $\mathcal{J}_{j_2}^{\text{ne}}(\tau, \{a_{j_2}\}, p | n = n_{j_2})$ denotes the conditional throughput achieved by a particular channel j_2 when there are n_{j_2} contending on this channel and $\mathcal{J}(n_{j_2} > 0)$ represents the indicator function, which is equal to zero if $n_{j_2} = 0$ (i.e., no SU chooses channel j_2) and equal to one, otherwise. Note that the

5.4 Performance Analysis and Optimization for Cognitive MAC Protocol

access of channels in the set $\Omega_{k_2}^{l_2}$ due to missed detection does not contribute to the system throughput, which explains why we do not include these channels in the sum in (5.9).

Therefore, we need to drive $\mathcal{P}(\{n_j\})$ and $\mathcal{J}_{j_2}^{\text{ne}}(\tau, \{a_{j_2}\}, p | n = n_{j_2})$ to determine the normalized throughput. Note that the sensing outcome due to the SDCSS is the same for all SUs and each SU chooses one channel in the set of $k_e = |\Theta_{k_1}^{l_1} \cup \Omega_{k_2}^{l_2}|$ channels randomly. Therefore, the probability $\mathcal{P}(\{n_j\})$ can be calculated as follows:

$$\mathcal{P}(\{n_j\}) = \binom{N}{\{n_j\}} \left(\frac{1}{k_e}\right)^{\sum_{j \in \Theta_{k_1}^{l_1} \cup \Omega_{k_2}^{l_2}} n_j} \quad (5.10)$$

$$= \binom{N}{\{n_j\}} \left(\frac{1}{k_e}\right)^N, \quad (5.11)$$

where $\binom{N}{\{n_j\}}$ is the multinomial coefficient which is defined as $\binom{N}{\{n_j\}} = \binom{N}{n_1, n_2, \dots, n_k} = \frac{N!}{n_1! n_2! \dots n_k!}$.

The calculation of the conditional throughput $\mathcal{J}_{j_2}^{\text{ne}}(\tau, \{a_{j_2}\}, p | n = n_{j_2})$ must account for the overhead due to spectrum sensing and exchanges of sensing results among SUs. Let us define $T_R = N t_r$ where t_r is the report time from each SU to all the other SUs; $\tau = \max_i \tau^i$ is the total the sensing time; $\bar{T}_{\text{cont}}^{j_2}$ is the average total time due to contention, collisions, and RTS/CTS exchanges before a successful packet transmission; T_S is the total time for transmissions of data packet, ACK control packet, and overhead between these data and ACK packets. Then, the conditional throughput $\mathcal{J}_{j_2}^{\text{ne}}(\tau, \{a_{j_2}\}, p | n = n_{j_2})$ can be written as

$$\mathcal{J}_{j_2}^{\text{ne}}(\tau, \{a_{j_2}\}, p | n = n_{j_2}) = \left\lfloor \frac{T - \tau - T_R}{\bar{T}_{\text{cont}}^{j_2} + T_S} \right\rfloor \frac{T_S}{T}, \quad (5.12)$$

where $\lfloor \cdot \rfloor$ denotes the floor function and recall that T is the duration of a cycle. Note that $\left\lfloor \frac{T - \tau - T_R}{\bar{T}_{\text{cont}}^{j_2} + T_S} \right\rfloor$ denotes the average number of successfully transmitted packets in one particular cycle excluding the sensing and reporting phases. Here, we omit the length of the synchronization phase, which is assumed to be negligible.

To calculate $\bar{T}_{\text{cont}}^{j_2}$, we define some further parameters as follows. Let denote T_C as the duration of the collision; \bar{T}_S is the required time for successful RTS/CTS transmission. These

5.4 Performance Analysis and Optimization for Cognitive MAC Protocol

quantities can be calculated under the 4-way handshake mechanism as [70]

$$\begin{cases} T_S = PS + 2SIFS + 2PD + ACK \\ \bar{T}_S = DIFS + RTS + CTS + 2PD \\ T_C = RTS + DIFS + PD \end{cases}, \quad (5.13)$$

where PS is the packet size, ACK is the length of an ACK packet, $SIFS$ is the length of a short interframe space, $DIFS$ is the length of a distributed interframe space, PD is the propagation delay where PD is usually very small compared to the slot size v .

Let T_I^{i,j_2} be the i -th idle duration between two consecutive RTS/CTS transmissions (they can be collisions or successes) on a particular channel j_2 . Then, T_I^{i,j_2} can be calculated based on its probability mass function (pmf), which is derived in the following. Recall that all quantities are defined in terms of number of time slots. Now, suppose there are n_{j_2} SUs choosing channel j_2 , let $\mathcal{P}_S^{j_2}$, $\mathcal{P}_C^{j_2}$ and $\mathcal{P}_I^{j_2}$ be the probabilities of a generic slot corresponding to a successful transmission, a collision and an idle slot, respectively. These quantities are calculated as follows

$$\mathcal{P}_S^{j_2} = n_{j_2} p (1 - p)^{n_{j_2} - 1} \quad (5.14)$$

$$\mathcal{P}_I^{j_2} = (1 - p)^{n_{j_2}} \quad (5.15)$$

$$\mathcal{P}_C^{j_2} = 1 - \mathcal{P}_S^{j_2} - \mathcal{P}_I^{j_2}, \quad (5.16)$$

where p is the transmission probability of an SU in a generic slot. Note that $\bar{T}_{\text{cont}}^{j_2}$ is a random variable (RV) consisting of several intervals corresponding to idle periods, collisions, and one successful RTS/CTS transmission. Hence this quantity for channel j_2 can be written as

$$\bar{T}_{\text{cont}}^{j_2} = \sum_{i=1}^{N_c^{j_2}} (T_C + T_I^{i,j_2}) + T_I^{N_c^{j_2} + 1, j_2} + \bar{T}_S, \quad (5.17)$$

where $N_c^{j_2}$ is the number of collisions before the first successful RTS/CTS exchange. Hence it is a geometric RV with parameter $1 - \mathcal{P}_C^{j_2} / \bar{\mathcal{P}}_I^{j_2}$ (where $\bar{\mathcal{P}}_I^{j_2} = 1 - \mathcal{P}_I^{j_2}$). Its pmf can be expressed as

$$f_X^{N_c}(x) = \left(\frac{\mathcal{P}_C^{j_2}}{\bar{\mathcal{P}}_I^{j_2}} \right)^x \left(1 - \frac{\mathcal{P}_C^{j_2}}{\bar{\mathcal{P}}_I^{j_2}} \right), \quad x = 0, 1, 2, \dots \quad (5.18)$$

5.4 Performance Analysis and Optimization for Cognitive MAC Protocol

Also, T_I^{i,j_2} represents the number of consecutive idle slots, which is also a geometric RV with parameter $1 - \mathcal{P}_I^{j_2}$ with the following pmf

$$f_X^I(x) = (\mathcal{P}_I^{j_2})^x (1 - \mathcal{P}_I^{j_2}), \quad x = 0, 1, 2, \dots \quad (5.19)$$

Therefore, $\bar{T}_{\text{cont}}^{j_2}$ can be written as follows [70]:

$$\bar{T}_{\text{cont}}^{j_2} = \bar{N}_c^{j_2} T_C + \bar{T}_I^{j_2} (\bar{N}_c^{j_2} + 1) + \bar{T}_S, \quad (5.20)$$

where $\bar{T}_I^{j_2}$ and $\bar{N}_c^{j_2}$ can be calculated as

$$\bar{T}_I^{j_2} = \frac{(1-p)^{n_{j_2}}}{1 - (1-p)^{n_{j_2}}} \quad (5.21)$$

$$\bar{N}_c^{j_2} = \frac{1 - (1-p)^{n_{j_2}}}{n_{j_2} p (1-p)^{n_{j_2}-1}} - 1. \quad (5.22)$$

These expressions are obtained by using the pmfs of the corresponding RVs given in (5.18) and (5.19), respectively [70].

5.4.3 Semi-Distributed Cooperative Spectrum Sensing and p -persistent CSMA Access Optimization

We determine optimal sensing and access parameters to maximize the normalized throughput for our proposed SDCSS and p -persistent CSMA protocol. Here, we assume that the sensing sets \mathcal{S}_j^U for different channels j have been given. Optimization of these sensing sets is considered in the next section. Note that the optimization performed in this paper is different from those in [22], [33] because the MAC protocols and sensing algorithms in the current and previous works are different. The normalized throughput optimization problem can be presented as

$$\max_{\{\tau^{ij}\}, \{a_j\}, p} \mathcal{N}\mathcal{T}_p(\{\tau^{ij}\}, \{a_j\}, p, \{\mathcal{S}_i\}) \quad (5.23)$$

$$\text{s.t. } \mathcal{P}_d^j(\bar{\varepsilon}^j, \bar{\tau}^j, a_j) \geq \hat{\mathcal{P}}_d^j, \quad j \in [1, M] \quad (5.24)$$

$$0 < \tau^{ij} \leq T, \quad 0 \leq p \leq 1, \quad (5.25)$$

where \mathcal{P}_d^j is the detection probability for channel j ; $\hat{\mathcal{P}}_d^j$ denotes the target detection probability; $\bar{\varepsilon}^j$ and $\bar{\tau}^j$ represent the vectors of detection thresholds and sensing times on channel j , respectively; a_j describes the parameter of the a_j -out-of- b_j aggregation rule for SDCSS on channel j with $b_j = |\mathcal{S}_j^U|$ where recall that \mathcal{S}_j^U is the set of SUs sensing channel j . The

5.4 Performance Analysis and Optimization for Cognitive MAC Protocol

optimization variables for this problem are sensing times τ^{ij} and parameters a_j of the sensing aggregation rule, and transmission probability p of the MAC protocol.

It was shown in [5] that the constraints on detection probability should be met with equality at optimality under the energy detection scheme and single-user scenario. This is quite intuitive since lower detection probability implies smaller sensing time, which leads to higher throughput. This is still the case for our considered multi-user scenario as can be verified by the conditional throughput formula (5.12). Therefore, we can set $\mathcal{P}_d^j(\bar{\varepsilon}^j, \bar{\tau}^j, a_j) = \widehat{\mathcal{P}}_d^j$ to solve the optimization problem (5.23)-(5.25).

However, $\mathcal{P}_d^j(\bar{\varepsilon}^j, \bar{\tau}^j, a_j)$ is a function of \mathcal{P}_d^{ij} for all SUs $i \in \mathcal{S}_j^U$ since we employ the SDCSS scheme in this paper. Therefore, to simplify the optimization we set $\mathcal{P}_d^{ij} = \mathcal{P}_d^{j*}$ for all SUs $i \in \mathcal{S}_j^U$ (i.e., all SUs are required to achieve the same detection probability for each assigned channel). Then, we can calculate \mathcal{P}_d^{j*} by using (5.3) for a given value of $\widehat{\mathcal{P}}_d^j$. In addition, we can determine \mathcal{P}_f^{ij} with the obtained value of \mathcal{P}_d^{j*} by using (5.2), which is the function of sensing time τ^{ij} .

Even after these steps, the optimization problem (5.23)-(5.25) is still very difficult to solve. In fact, it is the mixed integer non-linear problem since the optimization variables a_j take integer values while other variables take real values. Moreover, even the corresponding optimization problem achieved by relaxing a_j to real variables is a difficult and non-convex problem to solve since the throughput in the objective function (5.23) given in (5.7) is a complicated and non-linear function of optimization variables.

Given this observation, we have devised Alg. 7 to determine the solution for this optimization problem based on the coordinate-descent searching techniques. The idea is that at one time we fix all variables while searching for the optimal value of the single variable. This operation is performed sequentially for all variables until convergence is achieved. Since the normalized throughput given in (5.7) is quite insensitive with respect to p , we attempt to determine the optimized values for $(\{\bar{\tau}^{ij}\}, \{\bar{a}_j\})$ first for different values of p (steps 3–11 in Alg. 7) before searching the optimized value of p in the outer loop (step 12 in Alg. 7). This algorithm converges to the fixed point solution since we improve the objective value over iterations (steps 4–9). This optimization problem is non-convex in general. However, we can obtain its optimal solution easily by using the bisection search technique since the throughput function is quite smooth [127]. For some specific cases such as in homogeneous systems [22, 97, 98], the underlying optimization problem is convex, which can be solved efficiently by using standard convex optimization algorithms.

5.4 Performance Analysis and Optimization for Cognitive MAC Protocol

Algorithm 7 OPTIMIZATION OF SENSING AND ACCESS PARAMETERS

- 1: Assume we have the sets of all SU i , $\{\mathcal{S}_i\}$. Initialize τ^{ij} , $j \in \mathcal{S}_i$, the sets of $\{a_j\}$ for all channel j and p .
 - 2: For each chosen $p \in [0, 1]$, find $\bar{\tau}^{ij}$ and $\{\bar{a}_j\}$ as follows:
 - 3: **for** each possible set $\{a_j\}$ **do**
 - 4: **repeat**
 - 5: **for** $i = 1$ to N **do**
 - 6: Fix all $\tau^{i_1 j}$, $i_1 \neq i$.
 - 7: Find the optimal $\bar{\tau}^{ij}$ as $\bar{\tau}^{ij} = \underset{0 < \tau^{ij} \leq T}{\operatorname{argmax}} \mathcal{NJ}_p(\{\tau^{ij}\}, \{a_j\}, p)$.
 - 8: **end for**
 - 9: **until** convergence
 - 10: **end for**
 - 11: The best $(\{\bar{\tau}^{ij}\}, \{\bar{a}_j\})$ is determined for each value of p as $(\{\bar{\tau}^{ij}\}, \{\bar{a}_j\}) = \underset{\{a_j\}, \{\bar{\tau}^{ij}\}}{\operatorname{argmax}} \mathcal{NJ}(\bar{\tau}^{ij}, \{a_j\}, p)$.
 - 12: The final solution $(\{\bar{\tau}^{ij}\}, \{\bar{a}_j\}, \bar{p})$ is determined as $(\{\bar{\tau}^{ij}\}, \{\bar{a}_j\}, \bar{p}) = \underset{\{\bar{\tau}^{ij}\}, \{\bar{a}_j\}, p}{\operatorname{argmax}} \mathcal{NJ}(\{\bar{\tau}^{ij}\}, \{\bar{a}_j\}, p)$.
-

5.4.4 Optimization of Channel Sensing Sets

For the CRNs considered in the current work, the network throughput strongly depends on the availability of different channels, the spectrum sensing time, and the sensing quality. Specifically, long sensing time τ reduces the communications time on the available channels in each cycle of length T , which, therefore, decreases the network throughput. In addition, poor spectrum sensing performance can also degrade the network throughput since SUs can either overlook available channels (due to false alarm) or access busy channels (due to missed detection). Thus, the total throughput of SUs can be enhanced by optimizing the access parameter p and sensing design, namely optimizing the assignments of channels to SUs (i.e., optimizing the sensing sets for SUs) and the corresponding sensing times.

Recall that we have assumed the channel sensing sets for SUs are fixed to optimize the sensing and access parameters in the previous section. In this section, we attempt to determine an efficient channel assignment solution (i.e., channel sensing sets) by solving the following problem

$$\max_{\{\mathcal{S}_i\}, \{a_j\}} \mathcal{NJ}(\{\bar{\tau}^{ij}\}, \{a_j\}, \bar{p}, \{\mathcal{S}_i\}). \quad (5.26)$$

Note that the optimal values of a_j can only be determined if we have fixed the channel sensing set \mathcal{S}_j^U for each channel j . This is because we aim to optimize the a_j -out-of- b_j aggregation rule of the SDCSS scheme for each channel j where $b_j = |\mathcal{S}_j^U|$. Since a_j takes integer values and optimization of channel sensing sets \mathcal{S}_j^U also involves integer variables where we have to determine the set of SUs \mathcal{S}_j^U assigned to sense each channel j . Therefore, the optimization problem (5.26) is the non-linear integer program, which is NP-hard [125]. In the following,

we present both brute-force search algorithm and low-complexity greedy algorithm to solve this problem.

5.4.4.1 Brute-force Search Algorithm

Due to the non-linear and combinatorial structure of the formulated channel assignment problem, it would be impossible to explicitly determine the optimal closed form solution for problem (5.26). However, we can employ the brute-force search (i.e., the exhaustive search) to determine the best channel assignment. Specifically, we can enumerate all possible channel assignment solutions. Then, for each channel assignment solution (i.e., sets \mathcal{S}_j^U for all channels j), we employ Alg. 7 to determine the best spectrum sensing and accessing parameters $\{\bar{\tau}^{ij}\}, \{a_j\}, p$ and calculate the corresponding total throughput by using the throughput analytical model in 5.4.1. The channel assignment achieving the maximum throughput together with its best spectrum sensing and accessing parameters provides the best solution for the optimization problem (5.26).

5.4.4.2 Low-Complexity Greedy Algorithm

We propose another low-complexity and greedy algorithm to find the solution for this problem, which is described in Alg. 8. In this algorithm, we perform the initial channel assignment in step 1, which works as follows. We first temporarily assign all channels for each SU. Then, we run Alg. 7 to find the optimal sensing times for this temporary assignment, i.e., to determine $\{\bar{\tau}^{ij}\}$, which is used to assign one SU to each channel so that the total sensing time is minimized. In particular, the initial channel assignments are set according to the solution of the optimization problem (5.27)-(5.28) presented in the following.

$$\min_{\{x_{ij}\}} \sum_{i,j} \bar{\tau}^{ij} x_{ij} \tag{5.27}$$

$$\text{s.t. } \sum_i x_{ij} = 1, j \in [1, M]. \tag{5.28}$$

where x_{ij} are binary variables representing the channel assignments where $x_{ij} = 1$ if channel j is allocated for SU i (i.e., $j \in \mathcal{S}_i$) and $x_{ij} = 0$, otherwise. We employ the well-known Hungarian algorithm [128] to solve this problem. Then, we perform further channel assignments in steps 2-18 of Alg. 8. Specifically, to determine one channel assignment in each iteration, we temporarily assign one channel to the sensing set \mathcal{S}_i of each SU i and calculate the increase of throughput for such channel assignment ΔT_{ij} with the optimized channel and

5.4 Performance Analysis and Optimization for Cognitive MAC Protocol

access parameters obtained by using Alg. 7 (step 6). We then search for the best channel assignment $(\bar{i}, \bar{j}) = \operatorname{argmax}_{i,j \in \mathcal{S} \setminus \mathcal{S}_i} \Delta T_{ij}$ and actually perform the corresponding channel assignment if $\Delta T_{\bar{i}\bar{j}} > \delta$ (steps 7–10).

In Alg. 8, $\delta > 0$ is a small number which is used in the stopping condition for this algorithm (step 11). In particular, if the increase of the normalized throughput due to the new channel assignment is negligible in any iteration (i.e., the increase of throughput is less than δ) then the algorithm terminates. Therefore, we can choose δ to efficiently balance the achievable throughput performance with the algorithm running time. In the numerical studies, we will choose δ equal to $10^{-3} \times NT_c$.

The convergence of Alg. 8 can be explained as follows. Over the course of this algorithm, we attempt to increase the throughput by performing additional channel assignments. It can be observed that we can increase the throughput by allowing i) SUs to achieve better sensing performance or ii) SUs to reduce their sensing times. However, these two goals could not be achieved concurrently due to the following reason. If SUs wish to improve the sensing performance via cooperative spectrum sensing, we should assign more channels to each of them. However, SUs would spend longer time sensing the assigned channels with the larger sensing sets, which would ultimately decrease the throughput. Therefore, there would exist a point when we cannot improve the throughput by performing further channel assignments, which implies that Alg. 8 must converge.

There is a key difference in the current work and [33] regarding the sensing sets of SUs. Specifically, the sets of assigned channels are used for spectrum sensing and access in [33]. However, the sets of assigned channels are used for spectrum sensing only in the current work. In addition, the sets of available channels for possible access at SUs are determined based on the reporting results, which may suffer from communications errors. We will investigate the impact of reporting errors on the throughput performance in Section 5.5.

5.4.5 Complexity Analysis

In this section, we analyze the complexity of the proposed brute-force search and low-complexity greedy algorithms.

5.4.5.1 Brute-force Search Algorithm

To determine the complexity of the brute-force search algorithm, we need to calculate the number of possible channel assignments. Since each channel can be either allocated or not

5.4 Performance Analysis and Optimization for Cognitive MAC Protocol

Algorithm 8 GREEDY ALGORITHM

1: Initial channel assignment is obtained as follows:

- Temporarily perform following channel assignments $\tilde{\mathcal{S}}_i = \mathcal{S}$, $i \in [1, N]$. Then, run Alg. 7 to obtain optimal sensing and access parameters $(\{\tilde{\tau}^{ij}\}, \{\tilde{a}_j\}, \tilde{p})$.
- Employ Hungarian algorithm [128] to allocate each channel to exactly one SU to minimize the total cost where the cost of assigning channel j to SU i is $\tilde{\tau}^{ij}$ (i.e., to solve the optimization problem (5.27)-(5.28)).
- The result of this Hungarian algorithm is used to build the initial channel assignment sets $\{\mathcal{S}_i\}$ for different SU i .

2: Set `continue` = 1.

3: **while** `continue` = 1 **do**

4: Optimize sensing and access parameters for current channel assignment solution $\{\mathcal{S}_i\}$ by using Alg. 7.

5: Calculate the normalized throughput $\mathcal{NT}_c = \mathcal{NT}(\{\tilde{\tau}^{ij}\}, \{\tilde{a}_j\}, \tilde{p}, \{\mathcal{S}_i\})$ for the optimized sensing and access parameters.

6: Each SU i calculates the increase of throughput if it is assigned one further potential channel j as $\Delta T_{ij} = \mathcal{NT}(\{\tilde{\tau}^{ij}\}, \{\tilde{a}_j\}, \tilde{p}, \{\tilde{\mathcal{S}}_i\}) - \mathcal{NT}_c$ where $\tilde{\mathcal{S}}_i = \mathcal{S}_i \cup j$, $\tilde{\mathcal{S}}_l = \mathcal{S}_l$, $l \neq i$, and $\{\tilde{\tau}^{ij}\}, \{\tilde{a}_j\}, \tilde{p}$ are determined by using Alg. 7 for the temporary assignment sets $\{\tilde{\mathcal{S}}_i\}$.

7: Find the “best” assignment (\bar{i}, \bar{j}) as $(\bar{i}, \bar{j}) = \operatorname{argmax}_{i, j \in \mathcal{S} \setminus \mathcal{S}_i} \Delta T_{ij}$.

8: **if** $\Delta T_{\bar{i}\bar{j}} > \delta$ **then**

9: Assign channel \bar{j} to SU \bar{i} : $\mathcal{S}_{\bar{i}} = \mathcal{S}_{\bar{i}} \cup \bar{j}$.

10: **else**

11: Set `continue` = 0.

12: **end if**

13: **end while**

14: **if** `continue` = 1 **then**

15: Return to step 2.

16: **else**

17: Terminate the algorithm.

18: **end if**

allocated to any SU, the number of channel assignments is 2^{MN} . Therefore, the complexity of the brute-force search algorithm is $\mathcal{O}(2^{MN})$. Note that to obtain the best channel assignment solution, we must run Alg. 7 to find the best sensing and access parameters for each potential channel assignment, calculate the throughput achieved by such optimized configuration, and compare all the throughput values to determine the best solution.

5.4.5.2 Low-complexity Greedy Algorithm

In step 1, we run Hungarian algorithm to perform the first channel assignment for each SU i . The complexity of this operation can be upper-bounded by $\mathcal{O}(M^2N)$ (see [128] for more details). In each iteration in the assignment loop (i.e., steps 2-18), each SU i needs to calculate the increases of throughput for different potential channel assignments. Then, we select the assignment resulting in maximum increase of throughput. Hence, the complexity involved in these tasks is upper-bounded by MN since there are at most M channels to

assign for each of N SUs. Also, the number of assignments to perform is upper bounded by MN (i.e., iterations of the main loop). Therefore, the complexity of the assignment loop is upper-bounded by M^2N^2 . Therefore, the total worst-case complexity of Alg. 8 is $\mathcal{O}(M^2N + M^2N^2) = \mathcal{O}(M^2N^2)$, which is much lower than that of the brute-force search algorithm. As a result, Table 5.3 in Section 5.6 demonstrates that our proposed greedy algorithms achieve the throughput performance very close to that achieved by the brute-force search algorithms albeit they require much lower computational complexity.

5.4.6 Practical Implementation Issues

In our design, the spectrum sensing and access operation is distributed, however, channel assignment is performed in centralized manner. In fact, one SU is pre-assigned as a cluster head, which conducts channel assignment for SUs (i.e., determine channel sensing sets for SUs). For fairness, we can assign the SU as the cluster head in the round-robin manner. To perform channel assignment, the cluster head is responsible for estimating $\mathcal{P}_j(\mathcal{H}_0)$. Upon determining the channel sensing sets for all SUs, the cluster head will forward the results to the SUs. Then based on these pre-determined sensing sets, SUs will perform spectrum sensing and run the underlying MAC protocol to access the channel distributively in each cycle. It is worth to emphasize that the sensing sets for SUs are only determined once the probabilities $\mathcal{P}_j(\mathcal{H}_0)$ change, which would be quite infrequent in practice (e.g., in the time scale of hours or even days). Therefore, the estimation cost for $\mathcal{P}_j(\mathcal{H}_0)$ and all involved communication overhead due to sensing set optimization operations would be acceptable.

5.5 Consideration of Reporting Errors

In this section, we consider the impact of reporting errors on the performance of the proposed joint SDCSS and access design. Note that each SU relies on the channel sensing results received from other SUs in \mathcal{S}_j^U to determine the sensing outcome for each channel j . If there are reporting errors then different SUs may receive different channel sensing results, which lead to different final channel sensing decisions. The throughput analysis, therefore, must account for all possible error patterns that can occur in reporting channel sensing results. We will present the cooperative sensing model and throughput analysis considering reporting errors in the following.

5.5.1 Cooperative Sensing with Reporting Errors

In the proposed SDCSS scheme, each SU i_1 collects sensing results for each channel j from all SUs $i_2 \in \mathcal{S}_j^U$ who are assigned to sense channel j . In this section, we consider the case where there can be errors in reporting the channel sensing results among SUs. We assume that the channel sensing result for each channel transmitted by one SU to other SUs is represented by a single bit whose 1/0 values indicates that the underlying channel is available and busy, respectively. In general, the error probability of the reporting message between SUs i_1 and i_2 depends on the employed modulation scheme and the signal to noise ratio (SNR) of the communication channel between the two SUs. We denote the bit error probability of transmitting the reporting bit from SU i_2 to SU i_1 as $\mathcal{P}_e^{i_1 i_2}$. In addition, we assume that the error processes of different reporting bits for different SUs are independent. Then, the probability of detection and probability of false alarm experienced by SU i_1 on channel j with the sensing result received from SU i_2 can be written as

$$\mathcal{P}_{u,e}^{i_1 i_2 j} = \begin{cases} \mathcal{P}_u^{i_2 j} (1 - \mathcal{P}_e^{i_1 i_2}) + (1 - \mathcal{P}_u^{i_2 j}) \mathcal{P}_e^{i_1 i_2} & \text{if } i_1 \neq i_2 \\ \mathcal{P}_u^{i_2 j} & \text{if } i_1 = i_2 \end{cases} \quad (5.29)$$

where $u \equiv d$ and $u \equiv f$ represents probabilities of detection and false alarm, respectively. Note that we have $\mathcal{P}_e^{i_1 i_2} = 0$ if $i_1 = i_2 = i$ since there is no sensing result exchange involved in this case. As SU i employs the a_j -out-of- b_j aggregation rule for channel j , the probabilities of detection and false alarm for SU i on channel j can be calculated as

$$\tilde{\mathcal{P}}_u^{ij}(\bar{\varepsilon}^j, \bar{\tau}^j, a_j) = \sum_{l=a_j}^{b_j} \sum_{k=1}^{C_{b_j}^l} \prod_{i_1 \in \Phi_k^l} \mathcal{P}_{u,e}^{i i_1 j} \prod_{i_2 \in \mathcal{S}_j^U \setminus \Phi_k^l} \bar{\mathcal{P}}_{u,e}^{i i_2 j}. \quad (5.30)$$

Again, $u \equiv d$ and $u \equiv f$ represent the corresponding probabilities of detection or false alarm, respectively. Recall that \mathcal{S}_j^U represents the set of SUs who are assigned to sense channel j ; thus, we have $b_j = |\mathcal{S}_j^U|$ and $1 \leq a_j \leq b_j = |\mathcal{S}_j^U|$. For brevity, $\tilde{\mathcal{P}}_u^{ij}(\bar{\varepsilon}^j, \bar{\tau}^j, a_j)$ is written as $\tilde{\mathcal{P}}_u^{ij}$ in the following.

5.5.2 Throughput Analysis Considering Reporting Errors

In order to analyze the saturation throughput for the case there are reporting errors, we have to consider all possible scenarios due to the idle/busy status of all channels, sensing outcomes given by different SUs, and error/success events in the sensing result exchange

5.5 Consideration of Reporting Errors

processes. For one such combined scenario we have to derive the total conditional throughput due to all available channels. Illustration of different involved sets for one combined scenario of following analysis is presented in Fig. 5.4. In particular, the normalized throughput considering reporting errors can be expressed as follows:

$$\mathcal{NT} = \sum_{k_0=1}^M \sum_{l_0=1}^{C_M^{k_0}} \prod_{j_1 \in \Psi_{k_0}^{l_0}} \mathcal{P}_{j_1}(\mathcal{H}_0) \prod_{j_2 \in \mathcal{S} \setminus \Psi_{k_0}^{l_0}} \mathcal{P}_{j_2}(\mathcal{H}_1) \times \quad (5.31)$$

$$\prod_{j_3 \in \Psi_{k_0}^{l_0}} \sum_{k_1=0}^{|\mathcal{S}_{j_3}^U|} \sum_{l_1=1}^{C_{|\mathcal{S}_{j_3}^U|}^{k_1}} \prod_{i_0 \in \Theta_{k_1, j_3}^{l_1}} \bar{\mathcal{P}}_f^{i_0, j_3} \prod_{i_1 \in \mathcal{S}_{j_3}^U \setminus \Theta_{k_1, j_3}^{l_1}} \mathcal{P}_f^{i_1, j_3} \times \quad (5.32)$$

$$\prod_{j_4 \in \mathcal{S} \setminus \Psi_{k_0}^{l_0}} \sum_{k_2=0}^{|\mathcal{S}_{j_4}^U|} \sum_{l_2=1}^{C_{|\mathcal{S}_{j_4}^U|}^{k_2}} \prod_{i_2 \in \Omega_{k_2, j_4}^{l_2}} \bar{\mathcal{P}}_d^{i_2, j_4} \prod_{i_3 \in \mathcal{S}_{j_4}^U \setminus \Omega_{k_2, j_4}^{l_2}} \mathcal{P}_d^{i_3, j_4} \times \quad (5.33)$$

$$\prod_{i_4 \in \mathcal{S}^U} \sum_{k_3=0}^{k_1} \sum_{l_3=1}^{C_{k_1}^{k_3}} \prod_{i_5 \in \Phi_{k_3, j_3}^{l_3}} \bar{\mathcal{P}}_e^{i_4, i_5} \prod_{i_6 \in \Theta_{k_1, j_3}^{l_1} \setminus \Phi_{k_3, j_3}^{l_3}} \mathcal{P}_e^{i_4, i_6} \times \quad (5.34)$$

$$\sum_{k_4=0}^{|\mathcal{S}_{j_3}^U| - k_1} \sum_{l_4=1}^{C_{|\mathcal{S}_{j_3}^U| - k_1}^{k_4}} \prod_{i_7 \in \Lambda_{k_4, j_3}^{l_4}} \mathcal{P}_e^{i_4, i_7} \prod_{i_8 \in \mathcal{S}_{j_3}^U \setminus \Theta_{k_1, j_3}^{l_1} \setminus \Lambda_{k_4, j_3}^{l_4}} \bar{\mathcal{P}}_e^{i_4, i_8} \times \quad (5.35)$$

$$\prod_{i_9 \in \mathcal{S}^U} \sum_{k_5=0}^{k_2} \sum_{l_5=1}^{C_{k_2}^{k_5}} \prod_{i_{10} \in \Xi_{k_5, j_4}^{l_5}} \bar{\mathcal{P}}_e^{i_9, i_{10}} \prod_{i_{11} \in \Omega_{k_2, j_4}^{l_2} \setminus \Xi_{k_5, j_4}^{l_5}} \mathcal{P}_e^{i_9, i_{11}} \times \quad (5.36)$$

$$\sum_{k_6=0}^{|\mathcal{S}_{j_4}^U| - k_2} \sum_{l_6=1}^{C_{|\mathcal{S}_{j_4}^U| - k_2}^{k_6}} \prod_{i_{12} \in \Gamma_{k_6, j_4}^{l_6}} \mathcal{P}_e^{i_9, i_{12}} \prod_{i_{13} \in \mathcal{S}_{j_4}^U \setminus \Omega_{k_2, j_4}^{l_2} \setminus \Gamma_{k_6, j_4}^{l_6}} \bar{\mathcal{P}}_e^{i_9, i_{13}} \times \quad (5.37)$$

$$\mathcal{T}_p^{\text{re}}(\tau, \{a_j\}, p), \quad (5.38)$$

where $\mathcal{T}_p^{\text{re}}(\tau, \{a_j\}, p)$ denotes the conditional throughput for one combined scenario discussed above. In (5.31), we generate all possible sets where k_0 channels are available for secondary access (i.e., they are not used by PUs) while the remaining channels are busy. There are $C_M^{k_0}$ such sets and $\Psi_{k_0}^{l_0}$ represents one particular set of available channels. The first product term in (5.31) denotes the probability that all channels in $\Psi_{k_0}^{l_0}$ are available while the second product term describes the probability that the remaining channels are busy.

5.5 Consideration of Reporting Errors

Then, for one particular channel $j_3 \in \Psi_{k_0}^{l_0}$, we generate all possible sets with k_1 SUs in $\mathcal{S}_{j_3}^U$ ($\mathcal{S}_{j_3}^U$ is the set of SUs who are assigned to sense channel j_3) whose sensing results indicate that channel j_3 is available in (5.32). There are $C_{|\mathcal{S}_{j_3}^U|}^{k_1}$ sets and $\Theta_{k_1, j_3}^{l_1}$ denotes one such typical set. Again, the first product term in (5.32) is the probability that the sensing outcomes of all SUs in $\Theta_{k_1, j_3}^{l_1}$ indicate that channel j_3 is available; and the second term is the probability that the sensing outcomes of all SUs in the remaining set $\mathcal{S}_{j_3}^U \setminus \Theta_{k_1, j_3}^{l_1}$ indicate that channel j_3 is not available.

In (5.33), for one specific channel $j_4 \in \mathcal{S} \setminus \Psi_{k_0}^{l_0}$, we generate all possible sets with k_2 SUs in $\mathcal{S}_{j_4}^U$ whose sensing outcomes indicate that channel j_4 is available due to missed detection. There are $C_{|\mathcal{S}_{j_4}^U|}^{k_2}$ such sets and $\Omega_{k_2, j_4}^{l_2}$ is a typical one. Similarly, the first product term in (5.33) is the probability that the sensing outcomes of all SUs in $\Omega_{k_2, j_4}^{l_2}$ indicate that channel j_4 is available; and the second term is the probability that the sensing outcomes of all SUs in the remaining set $\mathcal{S}_{j_4}^U \setminus \Omega_{k_2, j_4}^{l_2}$ indicate that channel j_4 is not available.

Recall that for any specific channel j , each SU in \mathcal{S}^U (the set of all SUs) receives sensing results from a group of SUs who are assigned to sense the channel j . In (5.34), we consider all possible error events due to message exchanges from SUs in $\Theta_{k_1, j_3}^{l_1}$. The first group denoted as $\Phi_{k_3, j_3}^{l_3}$ includes SUs in $\Theta_{k_1, j_3}^{l_1}$ has its sensing results received at SU $i_4 \in \mathcal{S}^U$ indicating that channel j_3 is available (no reporting error) while the second group of SUs $\Theta_{k_1, j_3}^{l_1} \setminus \Phi_{k_3, j_3}^{l_3}$ has the sensing results received at SU $i_4 \in \mathcal{S}^U$ suggesting that channel j_3 is not available due to reporting errors. For each of these two groups, we generate all possible sets of SUs of different sizes and capture the corresponding probabilities. In particular, we generate all sets with k_3 SUs $i_5 \in \Phi_{k_3, j_3}^{l_3}$ where SU i_4 collects correct sensing information from SUs i_5 (i.e., there is no error on the channel between i_4 and i_5). Similar expression is presented for the second group in which we generate all sets of k_4 SUs $i_6 \in \Theta_{k_1, j_3}^{l_1} \setminus \Phi_{k_3, j_3}^{l_3}$ where SU i_4 collects wrong sensing information from each SU i_6 (i.e., there is an error on the channel between i_4 and i_6). Similarly, we present the possible error events due to exchanges of sensing results from the set of SUs $\mathcal{S}_{j_3}^U \setminus \Theta_{k_1, j_3}^{l_1}$ in (5.35).

In (5.36) and (5.37), we consider all possible error events due to sensing result exchanges for channel $j_4 \in \mathcal{S} \setminus \Psi_{k_0}^{l_0}$. Here, each SU in \mathcal{S}^U collects sensing result information from two sets of SUs in $\Omega_{k_2, j_4}^{l_2}$ and $\mathcal{S}_{j_4}^U \setminus \Omega_{k_2, j_4}^{l_2}$, respectively. The first set includes SUs in $\Omega_{k_2, j_4}^{l_2}$ whose sensing results indicate that channel j_4 is available due to missed detection, while the second set includes SUs in $\mathcal{S}_{j_4}^U \setminus \Omega_{k_2, j_4}^{l_2}$ whose sensing results indicate that channel j_4 is not available. Possible outcomes for the message exchanges due to the first set $\Omega_{k_2, j_4}^{l_2}$ are captured in (5.36) where we present the outcomes for two groups of this first set. For group one, we generate

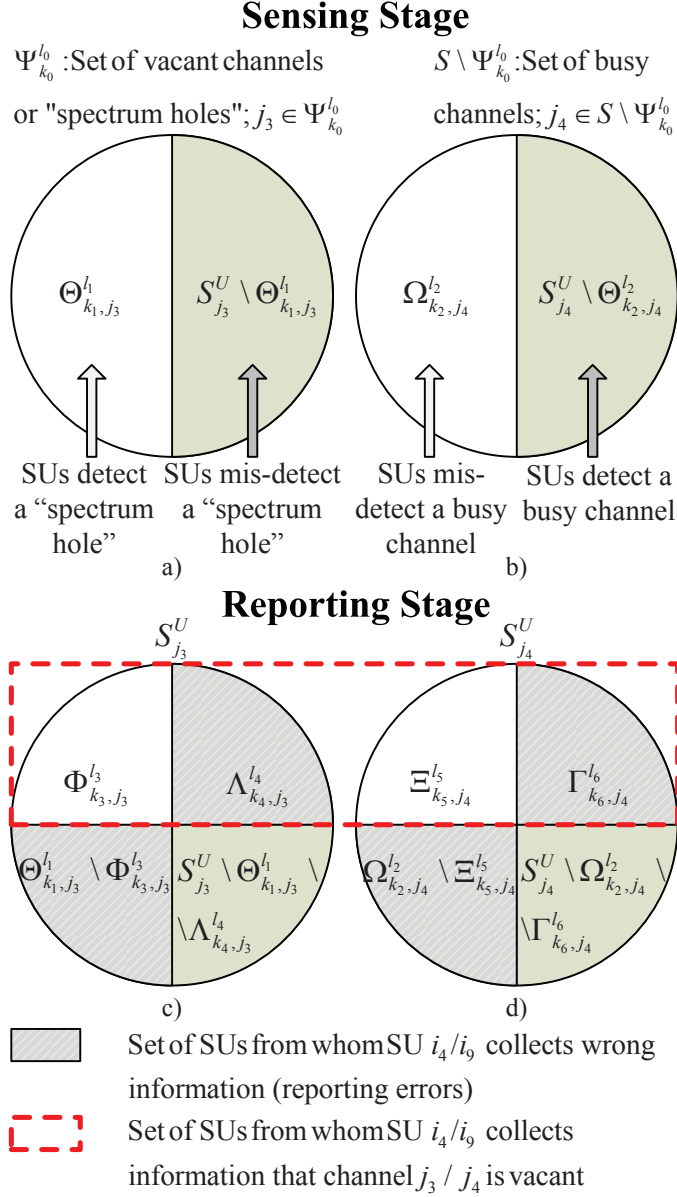


Figure 5.4: Illustration of different sets in one combined scenario.

all sets with k_5 SUs $i_{10} \in \Xi_{k_5, j_4}^{l_5}$ where SU i_9 collects correct sensing information from SUs i_{10} (i.e., there is no error on the channel between i_9 and i_{10}). For group two, we consider the remaining sets of SUs in $\Omega_{k_2, j_4}^{l_2} \setminus \Xi_{k_5, j_4}^{l_5}$ where SU i_9 receives wrong sensing information from each SU i_{11} (i.e., there is an error on the channel between i_9 and i_{11}). Similar partitioning of the set $S_{j_4}^U \setminus \Omega_{k_2, j_4}^{l_2}$ into two groups $\Gamma_{k_6, j_4}^{l_6}$ and $S_{j_4}^U \setminus \Omega_{k_2, j_4}^{l_2} \setminus \Gamma_{k_6, j_4}^{l_6}$ with the corresponding message reporting error patterns is captured in (5.37).

For each combined scenario whose probability is presented above, each SU i has collected

5.5 Consideration of Reporting Errors

sensing result information for each channel, which is the sensing results obtained by itself or received from other SUs. Then, each SU i determines the idle/busy status of each channel j by applying the a_j -out-of- b_j rule on the collected sensing information. Let \mathcal{S}_i^a be set of channels, whose status is “available” as being suggested by the a_j -out-of- b_j rule at SU i . According to our design MAC protocol, SU i will randomly select one channel in the set \mathcal{S}_i^a to perform contention and transmit its data. In order to obtain the conditional throughput $\mathcal{J}_p^{\text{re}}(\tau, \{a_j\}, p)$ for one particular combined scenario, we have to reveal the contention operation on each actually available channel, which is presented in the following.

Let $\mathcal{S}_i^a = \mathcal{S}_{1,i}^a \cup \mathcal{S}_{2,i}^a$ where channels in $\mathcal{S}_{1,i}^a$ are actually available and channels in $\mathcal{S}_{2,i}^a$ are not available but the SDCSS policy suggests the opposite due to sensing and/or reporting errors. Moreover, let $\hat{\mathcal{S}}_1^a = \bigcup_{i \in \mathcal{S}^U} \mathcal{S}_{1,i}^a$ be the set of actually available channels, which are detected by all SUs by using the SDCSS policy. Similarly, we define $\hat{\mathcal{S}}_2^a = \bigcup_{i \in \mathcal{S}^U} \mathcal{S}_{2,i}^a$ as the set of channels indicated as available by some SUs due to errors. Let $k_e^i = |\mathcal{S}_i^a|$ be the number of available channels at SU i ; then SU i chooses one channel in \mathcal{S}_i^a to transmit data with probability $1/k_e^i$. In addition, let $\hat{\mathcal{S}}^a = \hat{\mathcal{S}}_1^a \cup \hat{\mathcal{S}}_2^a$ be set of all “available” channels each of which is determined as being available by at least one SU and let $k_{\max} = |\hat{\mathcal{S}}^a|$ be the size of this set.

To calculate the throughput for each channel j , let Ψ_j^a be the set of SUs whose SDCSS outcomes indicate that channel j is available and let $\Psi^a = \bigcup_{j \in \hat{\mathcal{S}}^a} \Psi_j^a$ be the set of SUs whose SDCSS outcomes indicate that at least one channel in the assigned spectrum sensing set is available. In addition, let us define $N_j = |\Psi_j^a|$ and $N_{\max} = |\Psi^a|$, which describe the sizes of these sets, respectively. It is noted that $N_{\max} \leq N$ due to the following reason. In any specific combination that is generated in Eqs. (5.31)–(5.37), there can be some SUs, denoted as $\{i\}$, whose sensing outcomes indicate that all channels in the assigned spectrum sensing sets are not available (i.e., not available for access). Therefore, we have $\Psi^a = \mathcal{S}^U \setminus \{i\}$, which implies $N_{\max} \leq N$ where $N = |\mathcal{S}^U|$. Moreover, we assume that channels in $\hat{\mathcal{S}}^a$ are indexed by $1, 2, \dots, k_{\max}$. Similar to the throughput analysis without reporting errors, we consider all possible sets $\{n_j\} = \{n_1, n_2, \dots, n_{k_{\max}}\}$ where n_j is the number of SUs choosing channel j for access. Then, we can calculate the conditional throughput as follows:

$$\mathcal{J}_p^{\text{re}}(\tau, \{a_j\}, p) = \sum_{\{n_{j_1}\}: \sum_{j_1 \in \hat{\mathcal{S}}^a} n_{j_1} = N_{\max}} \mathcal{P}(\{N_{j_1}, n_{j_1}\}) \times \quad (5.39)$$

$$\sum_{j_2 \in \hat{\mathcal{S}}_1^a} \frac{1}{M} \mathcal{J}_{j_2}^{\text{re}}(\tau, \{a_{j_2}\}, p | n = n_{j_2}) \mathcal{J}(n_{j_2} > 0). \quad (5.40)$$

Here $\mathcal{P}(\{N_{j_1}, n_{j_1}\})$ is the probability that each channel j_1 ($j_1 \in \hat{\mathcal{S}}^a$) is selected by n_{j_1} SUs for $j_1 = 1, 2, \dots, k_{\max}$. This probability can be calculated as

$$\mathcal{P}(\{N_{j_1}, n_{j_1}\}) = \binom{\{N_{j_1}\}}{\{n_{j_1}\}} \prod_{i \in \Psi^a} \left(\frac{1}{k_e^i} \right), \quad (5.41)$$

where $\binom{\{N_{j_1}\}}{\{n_{j_1}\}}$ describes the number of ways to realize the access vector $\{n_j\}$ for k_{\max} channels, which can be obtained by using the enumeration technique as follows. For a particular way that the specific set of n_1 SUs $\mathcal{S}_1^{n_1}$ choose channel one (there are $C_{N_1}^{n_1}$ such ways), we can express the set of remaining SUs that can choose channel two as $\Psi_2^a = \Psi_2^a \setminus (\mathcal{S}_1^{n_1} \cap \Psi_2^a)$. We then consider all possible ways that n_2 SUs in the set Ψ_2^a choose channel two and we denote this set of SUs as $\mathcal{S}_2^{n_2}$ (there are $C_{\tilde{N}_2}^{n_2}$ such ways where $\tilde{N}_2 = |\Psi_2^a|$). Similarly, we can express the set of SUs that can choose channel three as $\Psi_3^a = \Psi_3^a \setminus ((\cup_{i=1}^2 \mathcal{S}_i^{n_i}) \cap \Psi_3^a)$ and consider all possible ways that n_3 SUs in the set Ψ_3^a can choose channel three, and so on. This process is continued until $n_{k_{\max}}$ SUs choose channel k_{\max} . Therefore, the number of ways to realize the access vector $\{n_j\}$ can be determined by counting all possible cases in the enumeration process.

The product term in (5.41) is due to the fact that each SU i chooses one available with probability $1/k_e^i$. The conditional throughput $\mathcal{T}_{j_2}^{\text{re}}(\tau, \{a_{j_2}\}, p | n = n_{j_2})$ is calculated by using the same expression (5.12) given in Section 5.4. In addition, only actually available channel $j_2 \in \hat{\mathcal{S}}_1^a$ can contribute the total throughput, which explains the throughput sum in (5.40).

5.5.3 Design Optimization with Reporting Errors

The optimization of channel sensing/access parameters as well as channel sensing sets can be conducted in the same manner with that in Section 5.4. However, we have to utilize the new throughput analytical model presented in Section 5.5.2 in this case. Specifically, Algs. 7 and 8 can still be used to determine the optimized sensing/access parameters and channel sensing sets, respectively. Nonetheless, we need to use the new channel sensing model capturing reporting errors in Section 5.5.1 in these algorithms. In particular, from the equality constraint on the detection probability, i.e., $\mathcal{P}_d^j(\bar{\varepsilon}^j, \bar{\tau}^j, a_j) = \hat{\mathcal{P}}_d^j$, we have to use (5.29) and (5.30) to determine P_d^{ij} (and the corresponding P_f^{ij}) assuming that P_d^{ij} are all the same for all pairs $\{i, j\}$ as what we have done in Section 5.4.

Table 5.3: Throughput vs probability of vacant channel (MxN=4x4)

		$\mathcal{P}_j(\mathcal{H}_0)$									
		0.1	0.2	0.3	0.4	0.5	0.6	0.7	0.8	0.9	1
N \mathcal{T}	Greedy	0.0816	0.1524	0.2316	0.2982	0.3612	0.4142	0.4662	0.5058	0.5461	0.5742
	Optimal	0.0817	0.1589	0.2321	0.3007	0.3613	0.4183	0.4681	0.5087	0.5488	0.5796
	Gap (%)	0.12	4.09	0.22	0.83	0.03	0.98	0.40	0.57	0.49	0.93

5.6 Numerical Results

To obtain numerical results in this section, the key parameters for the proposed MAC protocol are chosen as follows: cycle time is $T = 100ms$; the slot size is $v = 20\mu s$, which is the same as in IEEE 802.11p standard; packet size is $PS = 450$ slots (i.e., $450v$); propagation delay $PD = 1\mu s$; $SIFS = 2$ slots; $DIFS = 10$ slots; $ACK = 20$ slots; $CTS = 20$ slots; $RTS = 20$ slots; sampling frequency for spectrum sensing is $f_s = 6MHz$; and $t_r = 80\mu s$. The results presented in all figures except Fig. 5.11 correspond to the case where there is no reporting error.

To investigate the efficacy of our proposed low-complexity channel assignment algorithm (Alg. 8), we compare the throughput performance achieved by the optimal brute-force search and greedy channel assignment algorithm in Table 5.3. In particular, we show normalized throughput $N\mathcal{T}$ versus probabilities $\mathcal{P}_j(\mathcal{H}_0)$ for these two algorithms and the relative gap between them. Here, the probabilities $\mathcal{P}_j(\mathcal{H}_0)$ for different channels j are chosen to be the same and we choose $M = 4$ channels and $N = 4$ SUs. To describe the SNR of different SUs and channels, we use $\{i, j\}$ to denote a combination of channel j and SU i who senses this channel. The SNR setting for different combinations of SUs and channels $\{i, j\}$ is performed for two groups of SUs as $\gamma_1^{ij} = -15dB$: channel 1: $\{1, 1\}, \{2, 1\}, \{3, 1\}$; channel 2: $\{2, 2\}, \{4, 2\}$; channel 3: $\{1, 3\}, \{4, 3\}$; and channel 4: $\{1, 4\}, \{3, 4\}$. The remaining combinations correspond to the SNR value $\gamma_2^{ij} = -20dB$ for group two. The results in this table confirms that the throughput gaps between our greedy algorithm and the brute-force optimal search algorithm are quite small, which are less than 1% for all except the case two presented in this table. These results confirm that our proposed greedy algorithm works well for small systems (i.e., small M and N). In the following, we investigate the performance of our proposed algorithms for larger systems.

To investigate the performance of our proposed algorithm for a typical system, we consider the network setting with $N = 10$ and $M = 4$. We divide SUs into 2 groups where the received SNRs at SUs due to the transmission from PU i is equal to $\gamma_{1,0}^{ij} =$

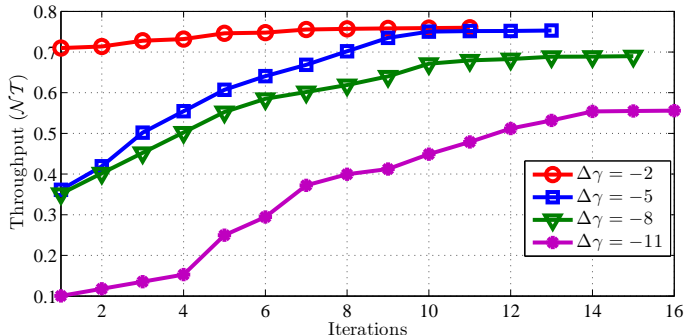


Figure 5.5: Convergence illustration for Alg. 8.

$-15dB$ and $\gamma_{2,0}^{ij} = -10dB$ (or their shifted values described later) for the two groups, respectively. Again, to describe the SNR of different SUs and channels, we use $\{i, j\}$ to denote a combination of channel j and SU i who senses this channel. The combinations of the first group corresponding to $\gamma_{1,0}^{ij} = -10dB$ are chosen as follows: channel 1: $\{1, 1\}, \{2, 1\}, \{3, 1\}$; channel 2: $\{2, 2\}, \{4, 2\}, \{5, 2\}$; channel 3: $\{4, 3\}, \{6, 3\}, \{7, 3\}$; and channel 4: $\{1, 4\}, \{3, 4\}, \{6, 4\}, \{8, 4\}, \{9, 4\}, \{10, 4\}$. The remaining combinations belong to the second group with the SNR equal to $\gamma_{2,0}^{ij} = -15dB$. To obtain results for different values of SNRs, we consider different shifted sets of SNRs where γ_1^{ij} and γ_2^{ij} are shifted by $\Delta\gamma$ around their initial values $\gamma_{1,0}^{ij} = -15dB$ and $\gamma_{2,0}^{ij} = -10dB$ as $\gamma_1^{ij} = \gamma_{1,0}^{ij} + \Delta\gamma$ and $\gamma_2^{ij} = \gamma_{2,0}^{ij} + \Delta\gamma$. For example, as $\Delta\gamma = -10$, the resulting SNR values are $\gamma_1^{ij} = -25dB$ and $\gamma_2^{ij} = -20dB$. These parameter settings are used to obtain the results presented in Figs. 5.5, 5.6, 5.7, 5.8, and 5.9 in the following.

Fig. 5.5 illustrates the convergence of Alg. 2 where we show the normalized throughput NT_p versus the iterations for $\Delta\gamma = -2, -5, -8$ and $-11dB$. For simplicity, we choose δ equals $10^{-3} \times NT_c$ in Alg. 2. This figure confirms that Alg. 8 converges after about 11, 13, 15 and 16 iterations for $\Delta\gamma = -2, -5, -8$, and $-11dB$, respectively. In addition, the normalized throughput increases over the iterations as expected.

Fig. 5.6 presents normalized throughput \mathcal{NT}_p versus transmission probability p and sensing time τ^{11} for the SNR shift equal to $\Delta\gamma = -7$ where the sensing times for other pairs of SUs and channels are optimized as in Alg. 7. This figure shows that channel sensing and access parameters can strongly impact the throughput of the secondary network, which indicates the need to optimize them. This figure shows that the optimal values of p and τ^{11} are around $(\bar{\tau}^{11}, \bar{p}) = (0.0054s, 0.1026)$ to achieve the maximum normalized throughput of $\mathcal{NT}_p = 0.7104$. It can be observed that normalized throughput \mathcal{NT}_p is less sensitive to transmission probability p while it varies more significantly as the sensing time τ^{11} deviates

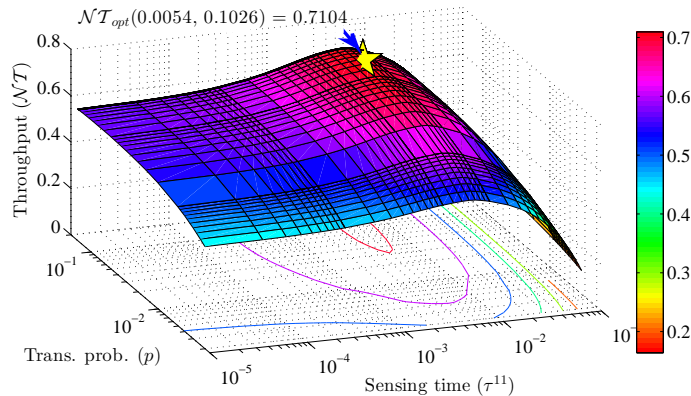


Figure 5.6: Normalized throughput versus transmission probability p and sensing time τ^{11} for $\Delta\gamma = -7$, $N = 10$ and $M = 4$.

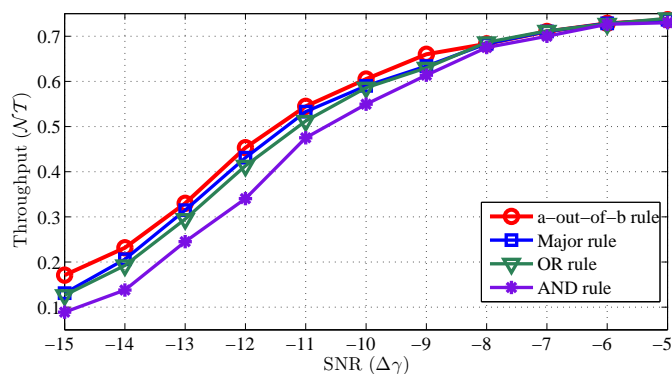


Figure 5.7: Normalized throughput versus SNR shift $\Delta\gamma$ for $N = 10$ and $M = 4$ under 4 aggregation rules.

from the optimal value. In fact, there can be multiple available channels which each SU can choose from. Therefore, the contention level on each available channel would not be very intense for most values of p . This explains why the throughput is not very sensitive to the access parameter p .

In Fig. 5.7, we compare the normalized throughput of the secondary network as each SU employs four different aggregation rules, namely AND, OR, majority, and the optimal a-out-of-b rules. The four throughput curves in this figure represent the optimized normalized throughput values achieved by using Algs. 7 and 8. For the OR, AND, majority rules, we do not need to find optimized a_j parameters for different channels j in Alg. 7. Alternatively, $a_j = 1$, $a_j = b_j$ and $a_j = \lceil b/2 \rceil$ correspond to the OR, AND and majority rules, respectively. It can be seen that the optimal a-out-of-b rule achieves the highest throughput among the considered rules. Moreover, the performance gaps between the optimal a-out-of-b rule and

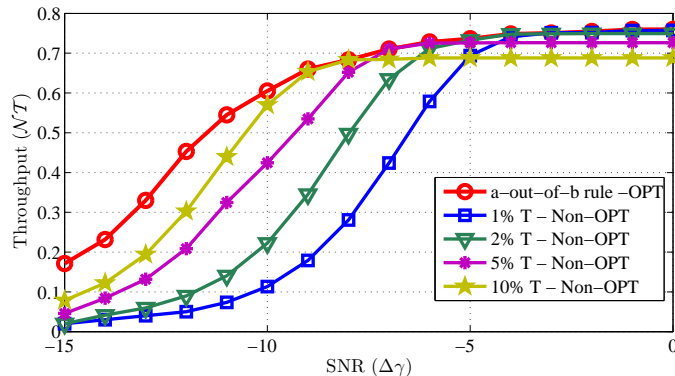


Figure 5.8: Normalized throughput versus SNR shift $\Delta\gamma$ for $N = 10$ and $M = 4$ for optimized and non-optimized scenarios.

other rule tends to be larger for smaller SNR values.

In Fig. 5.8, we compare the throughput performance as the sensing times are optimized by using Alg. 7 and they are fixed at different fractions of the cycle time in Alg. 7. For fair comparison, the optimized a-out-of-b rules are used in both schemes with optimized and non-optimized sensing times. For the non-optimized scheme, we employ Alg. 8 for channel assignment; however, we do not optimize the sensing times in Alg. 7. Alternatively, τ^{ij} is chosen from the following values: $1\%T$, $2\%T$, $5\%T$ and $10\%T$ where T is the cycle time. Furthermore, for this non-optimized scheme, we still find an optimized value of \bar{a}_j for each channel j (corresponding to the sensing phase) and the optimal value of \bar{p} (corresponding to the access phase) in Alg. 7. This figure confirms that the optimized design achieves the largest throughput. Also, small sensing times can achieve good throughput performance at the high-SNR regime but result in poor performance if the SNR values are low. In contrast, too large sensing times (e.g., equal $10\%T$) may become inefficient if the SNR values are sufficiently large. These observations again illustrate the importance of optimizing the channel sensing and access parameters.

We compare the normalized throughput under our optimized design and the round-robin (RR) channel assignment strategies in Fig. 5.9. For RR channel assignment schemes, we first allocate channels for SUs as described in Table 5.4 (i.e., we consider three different RR channel assignments). In the considered round-robin channel assignment schemes, we assign at most 1, 2 and 3 channels for each SU corresponding to cases 1, 2 and 3 as shown in Table 5.4. In particular, we sequentially assign channels with increasing indices for the next SUs until exhausting (we then repeat this procedure for the following SU). Then, we only employ Alg. 7 to optimize the sensing and access parameters for these RR channel

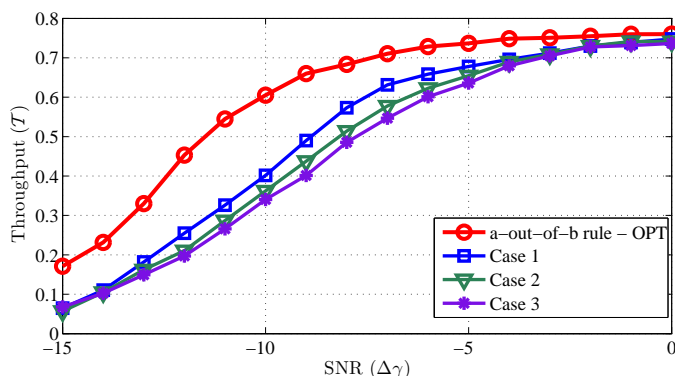


Figure 5.9: Normalized throughput versus SNR shift $\Delta\gamma$ for $N = 10$ and $M = 4$ for optimized and RR channel assignments.

Table 5.4: Round-robin Channel Assignment (x denotes an assignment)

		Channel											
		Case 1				Case 2				Case 3			
		1	2	3	4	1	2	3	4	1	2	3	4
SU	1	x				x	x			x	x	x	
	2		x				x	x			x	x	x
	3			x				x	x			x	x
	4				x				x				x
	5	x				x	x			x	x	x	
	6		x				x	x			x	x	x
	7			x				x	x			x	x
	8				x				x				x
	9	x				x	x			x	x	x	
	10		x				x	x			x	x	x

assignments. Fig. 5.9 shows that the optimized design achieves much higher throughput than those due to RR channel assignments. These results confirm that channel assignments for cognitive radios play a very important role in maximizing the spectrum utilization for CRNs. In particular, it would be sufficient to achieve good sensing and throughput performance if we assign a small number of nearby SUs to sense any particular channel instead of requiring all SUs to sense the channel. This is because “bad SUs” may not contribute to improve the sensing performance but result in more sensing overhead, which ultimately decreases the throughput of the secondary network.

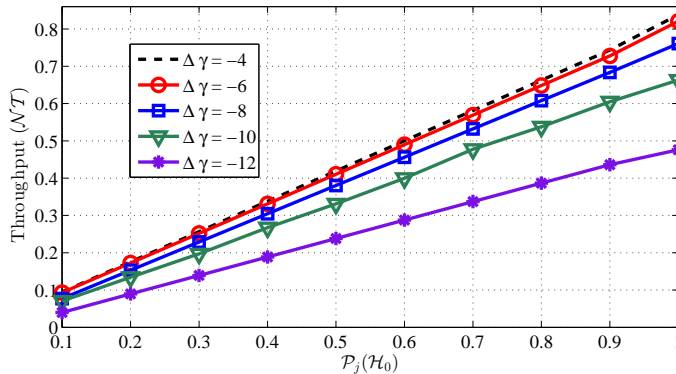


Figure 5.10: Normalized throughput versus probability of having vacant channel $\mathcal{P}_j(\mathcal{H}_0)$ for $N = 10$ and $M = 4$ for optimized channel assignments and a-out-of-b aggregation rule.

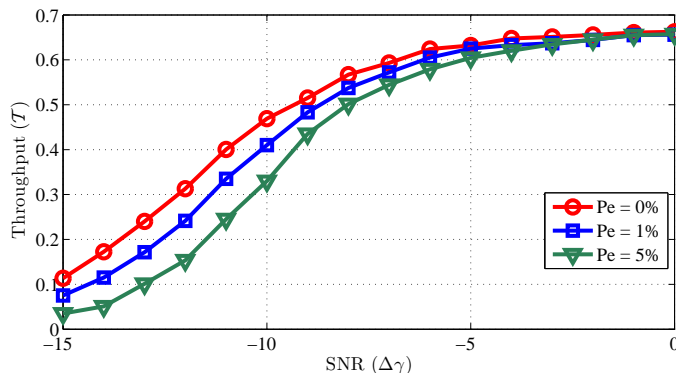


Figure 5.11: Normalized throughput versus SNR shift $\Delta\gamma$ for $N = 4$ and $M = 3$ for optimized channel assignments and a-out-of-b aggregation rules.

In Fig. 5.10, we consider the impact of PUs' activities on throughput performance of the secondary network. In particular, we vary the probabilities of having idle channels for secondary spectrum access ($\mathcal{P}_j(\mathcal{H}_0)$) in the range of $[0.1, 1]$. For larger values of $\mathcal{P}_j(\mathcal{H}_0)$, there are more opportunities for SUs to find spectrum holes to transmit data, which results in higher throughput and vice versa. Moreover, this figure shows that the normalized throughput increases almost linearly with $\mathcal{P}_j(\mathcal{H}_0)$. Also as the $\Delta\gamma$ increases (i.e., higher SNR), the throughput performance can be improved significantly. However, the improvement becomes negligible if the SNR values are sufficiently large (for $\Delta\gamma$ in $[-6, -4]$). This is because for large SNR values, the required sensing time is sufficiently small, therefore, further increase of SNR does not reduce the sensing time much to improve the normalized throughput.

Finally, we study the impact of reporting errors on the throughput performance by using the extended throughput analytical model in Section 5.5. The network setting under in-

investigation has $N = 4$ SUs and $M = 3$ channels. Again, we use notation $\{i, j\}$ to represent a combination of channel j and SU i . The combinations with $\gamma_{10}^{ij} = -10dB$ are chosen as follows: channel 1: $\{1, 1\}, \{2, 1\}, \{3, 1\}$; channel 2: $\{2, 2\}, \{4, 2\}$; channel 3: $\{1, 3\}, \{4, 3\}$. The remaining combinations correspond to $\gamma_{20}^{ij} = -15dB$. We assume that the reporting errors between every pair of 2 SUs are the same, which is denoted as P_e . In Fig. 5.11, we show the achieved throughput as $P_e = 0\%$, $P_e = 1\%$ and $P_e = 5\%$ under optimized design. We can see that when P_e increases, the normalized throughput decreases quite significantly if the SNR is sufficiently low. However, in the high-SNR regime, the throughput performance is less sensitive to the reporting errors.

5.7 Conclusion

We have proposed a general analytical and optimization framework for SDCSS and access design in multi-channel CRNs. In particular, we have proposed the p -persistent CSMA MAC protocol integrating the SDCSS mechanism. Then, we have analyzed the throughput performance of the proposed design and have developed an efficient algorithm to optimize its sensing and access parameters. Moreover, we have presented both optimal brute-force search and low-complexity algorithms to determine efficient channel sensing sets and have analyzed their complexity. We have also extended the framework to consider reporting errors in exchanging sensing results among SUs. Finally, we have evaluated the impacts of different parameters on the throughput performance of the proposed design and illustrated the significant performance gap between the optimized and non-optimized designs. Specifically, it has been confirmed that optimized sensing and access parameters as well as channel assignments can achieve considerably better throughput performance than that due to the non-optimized design. In the future, we will extend SDCSS and MAC protocol design for the multihop CRNs.

Chapter 6

Design and Optimal Configuration of Full-Duplex MAC Protocol for Cognitive Radio Networks Considering Self-Interference

The content of this chapter was submitted in IEEE Access in the following paper:

L. T. Tan, and L. B. Le, “Design and Optimal Configuration of Full-Duplex MAC Protocol for Cognitive Radio Networks Considering Self-Interference,” in *IEEE Access*, 2015 (Under review).

6.1 Abstract

In this paper, we propose an adaptive Medium Access Control (MAC) protocol for full-duplex (FD) cognitive radio networks in which FD secondary users (SUs) perform channel contention followed by concurrent spectrum sensing and transmission, and transmission only with maximum power in two different stages (called the FD sensing and transmission stages, respectively) in each contention and access cycle. The proposed FD cognitive MAC (FDC-MAC) protocol does not require synchronization among SUs and it efficiently utilizes the spectrum and mitigates the self-interference in the FD transceiver. We then develop a mathematical model to analyze the throughput performance of the FDC-MAC protocol where both half-duplex (HD) transmission (HDTx) and FD transmission (FDTx) modes are considered. Then, we study the FDC-MAC configuration optimization through adaptively controlling the

spectrum sensing duration and transmit power level of the FD sensing stage where we prove that there exists optimal sensing time and transmit power to achieve the maximum throughput and we develop an algorithm to configure the proposed FDC-MAC protocol. Extensive numerical results are presented to illustrate the characteristic of the optimal FDC-MAC configuration and the impacts of protocol parameters and the self-interference cancellation quality on the throughput performance. Moreover, we demonstrate the significant throughput gains of the FDC-MAC protocol with respect to existing half-duplex MAC (HD MAC) and single-stage FD MAC protocols.

6.2 Introduction

Engineering MAC protocols for efficient sharing of white spaces is an important research topic in cognitive radio networks (CRNs). One critical requirement for the cognitive MAC design is that transmissions on the licensed frequency band from primary users (PUs) should be satisfactorily protected from the SUs' spectrum access. Therefore, a cognitive MAC protocol for the secondary network must realize both the spectrum sensing and access functions so that timely detection of the PUs' communications and effective spectrum sharing among SUs can be achieved. Most existing research works on cognitive MAC protocols have focused on the design and analysis of HD MAC (e.g., see [47, 48] and the references therein).

Due to the HD constraint, SUs typically employ a two-stage sensing/access procedure where they perform spectrum sensing in the first stage before accessing available spectrum for data transmission in the second stage [2, 5, 16, 22, 33, 115]. This constraint also requires SUs be synchronized during the spectrum sensing stage, which could be difficult to achieve in practice. In fact, spectrum sensing enables SUs to detect white spaces that are not occupied by PUs [5, 22, 33, 48, 71, 72]; therefore, imperfect spectrum sensing can reduce the spectrum utilization due to failure in detecting white spaces and potentially result in collisions with active PUs. Consequently, sophisticated design and parameter configuration of cognitive MAC protocols must be conducted to achieve good performance while appropriately protecting PUs [2, 16, 22, 33, 47, 62, 115]. As a result, traditional MAC protocols [70, 85, 129–131] adapted to the CRN may not provide satisfactory performance.

In general, HD-MAC protocols may not exploit white spaces very efficiently since significant sensing time may be required, which would otherwise be utilized for data transmission. Moreover, SUs may not timely detect the PUs' activity during their transmissions, which

can cause severe interference to active PUs. Thanks to recent advances on FD technologies, a FD radio can transmit and receive data simultaneously on the same frequency band [49–54]. One of the most critical issues of wireless FD communication is the presence of self-interference, which is caused by power leakage from the transmitter to the receiver of a FD transceiver. The self-interference may indeed lead to serious communication performance degradation of FD wireless systems. Despite recent advances on self-interference cancellation (SIC) techniques [50–52] (e.g., propagation SIC, analog-circuit SIC, and digital baseband SIC), self-interference still exists due to various reasons such as the limitation of hardware and channel estimation errors.

6.2.1 Related Works

There are some recent works that propose to exploit the FD communications for MAC-level channel access in multi-user wireless networks [53, 111, 112, 132, 133]. In [53], the authors develop a centralized MAC protocol to support asymmetric data traffic where network nodes may transmit data packets of different lengths, and they propose to mitigate the hidden node problem by employing a busy tone. To overcome this hidden node problem, Duarte et al. propose to adapt the standard 802.11 MAC protocol with the RTS/CTS handshake in [132]. Moreover, Goyal et al. in [133] extend this study to consider interference between two nodes due to their concurrent transmissions. Different from conventional wireless networks, designing MAC protocols in CRNs is more challenging because the spectrum sensing function must be efficiently integrated into the MAC protocol. In addition, the self-interference must be carefully addressed in the simultaneous spectrum sensing and access to mitigate its negative impacts on the sensing and throughput performance.

The FD technology has been employed for more efficient spectrum access design in cognitive radio networks [35, 108, 110, 134] where SUs can perform sensing and transmission simultaneously. In [134], a FD MAC protocol is developed which allows simultaneous spectrum access of the SU and PU networks where both PUs and SUs are assumed to employ the p -persistent MAC protocol for channel contention resolution and access. This design is, therefore, not applicable to the hierarchical spectrum access in the CRNs where PUs should have higher spectrum access priority compared to SUs.

In our previous work [35], we propose the FD MAC protocol by using the standard backoff mechanism as in the 802.11 MAC protocol where we employ concurrent FD sensing and access during data transmission as well as frame fragmentation. Moreover, engineering of a cognitive FD relaying network is considered in [108, 110], where various resource allocation

algorithms to improve the outage probability are proposed. In addition, the authors in [111] develop the joint routing and distributed resource allocation for FD wireless networks. In [112], Choi et al. study the distributed power allocation for a hybrid FD/HD system where all network nodes operate in the HD mode but the access point (AP) communicates by using the FD mode. In practice, it would be desirable to design an adaptable MAC protocol, which can be configured to operate in an optimal fashion depending on specific channel and network conditions. This design will be pursued in our current work.

6.2.2 Our Contributions

In this paper, we make a further bold step in designing, analyzing, and optimizing an adaptive FDC-MAC protocol for CRNs, where the self-interference and imperfect spectrum sensing are explicitly considered. In particular, the contributions of this paper can be summarized as follows.

1. We propose a novel FDC-MAC protocol that can efficiently exploit the FD transceiver for spectrum sensing and access of the white space without requiring synchronization among SUs. In this protocol, after the p -persistent based channel contention phase, the winning SU enters the data phase consisting of two stages, i.e., concurrent sensing and transmission in the first stage (called FD sensing stage) and transmission only in the second stage (called transmission stage). The developed FDC-MAC protocol, therefore, enables the optimized configuration of transmit power level and sensing time during the FD sensing stage to mitigate the self-interference and appropriately protect the active PU. After the FD sensing stage, the SU can transmit with the maximum power to achieve the highest throughput.
2. We develop a mathematical model for throughput performance analysis of the proposed FDC-MAC protocol considering the imperfect sensing, self-interference effects, and the dynamic status changes of the PU. In addition, both one-way and two-way transmission scenarios, which are called HD transmission (HDTx) and FD transmission (FDTx) modes, respectively, are considered in the analysis. Since the PU can change its idle/active status during the FD sensing and transmission stages, different potential status-change scenarios are studied in the analytical model.
3. We study the optimal configuration of FDC-MAC protocol parameters including the SU's sensing duration and transmit power to maximize the achievable throughput

under both FDTx and HDTx modes. We prove that there exists an optimal sensing time to achieve the maximum throughput for a given transmit power value during the FD sensing stage under both FDTx and HDTx modes. Therefore, optimal protocol parameters can be determined through standard numerical search methods.

4. Extensive numerical results are presented to illustrate the impacts of different protocol parameters on the throughput performance and the optimal configurations of the proposed FDC-MAC protocol. Moreover, we show the significant throughput enhancement of the proposed FDC-MAC protocol compared to existing cognitive MAC protocols, namely the HD MAC protocol and a single-stage FD MAC protocol with concurrent sensing and access. Specifically, our FDC-MAC protocol achieves higher throughput with the increasing maximum power while the throughput of the single-stage FD MAC protocols decreases with the maximum power in the high power regime due to the self-interference. Moreover, the proposed FDC-MAC protocol leads to significant higher throughput than that due to the HD MAC protocol.

The remaining of this paper is organized as follows. Section 6.3 describes the system and PU models. FDC-MAC protocol design, and throughput analysis for the proposed FDC-MAC protocol are performed in Section 6.4. Then, Section 6.5 studies the optimal configuration of the proposed FDC-MAC protocol to achieve the maximum secondary throughput. Section 6.6 demonstrates numerical results followed by concluding remarks in Section 6.7.

6.3 System and PU Activity Models

6.3.1 System Model

We consider a cognitive radio network where n_0 pairs of SUs opportunistically exploit white spaces on a frequency band for communications. We assume that each SU is equipped with a FD transceiver, which can perform sensing and transmission simultaneously. However, the sensing performance of each SU is impacted by the self-interference from its transmitter since the transmitted power is leaked into the received signal. We denote $I(P)$ as the average self-interference power, which is modeled as $I(P) = \zeta (P)^\xi$ [49] where P is the SU's transmit power, ζ and ξ ($0 \leq \xi \leq 1$) are predetermined coefficients which represent the quality of self-interference cancellation (QSIC). In this work, we design a asynchronous cognitive MAC protocol where no synchronization is required among SUs and between SUs and PUs.

We assume that different pairs of SUs can overhear transmissions from the others (i.e., a collocated network is assumed). In the following, we refer to pair i of SUs as SU i for brevity.

6.3.2 Primary User Activity

We assume that the PU's idle/active status follows two independent random processes. We say that the channel is available and busy for SUs' access if the PU is in the idle and active (or busy) states, respectively. Let \mathcal{H}_0 and \mathcal{H}_1 denote the events that the PU is idle and active, respectively. To protect the PU, we assume that SUs must stop their transmissions and evacuate from the busy channel within the maximum delay of T_{eva} , which is referred to as channel evacuation time.

Let τ_{ac} and τ_{id} denote the random variables which represent the durations of active and idle channel states, respectively. We denote probability density functions (pdf) of τ_{ac} and τ_{id} as $f_{\tau_{\text{ac}}}(t)$ and $f_{\tau_{\text{id}}}(t)$, respectively. While most results in this paper can be applied to general pdfs $f_{\tau_{\text{ac}}}(t)$ and $f_{\tau_{\text{id}}}(t)$, we mostly consider the exponential pdf in the analysis. In addition, let $\mathcal{P}(\mathcal{H}_0) = \frac{\bar{\tau}_{\text{id}}}{\bar{\tau}_{\text{id}} + \bar{\tau}_{\text{ac}}}$ and $\mathcal{P}(\mathcal{H}_1) = 1 - \mathcal{P}(\mathcal{H}_0)$ present the probabilities that the channel is available and busy, respectively where $\bar{\tau}_{\text{id}}$ and $\bar{\tau}_{\text{ac}}$ denote the average values of τ_{ac} and τ_{id} , respectively. We assume that the probabilities that τ_{ac} and τ_{id} are smaller than T_{eva} are sufficiently small (i.e., the PU changes its status slowly) so that we can ignore events with multiple idle/active status changes in one channel evacuation interval T_{eva} .

6.4 Full-Duplex Cognitive MAC Protocol

In this section, we describe the proposed FDC-MAC protocol and conduct its throughput analysis considering imperfect sensing, self-interference of the FD transceiver, and dynamic status change of the PUs.

6.4.1 FDC-MAC Protocol Design

The proposed FDC-MAC protocol integrates three important elements of cognitive MAC protocol, namely contention resolution, spectrum sensing, and access functions. Specifically, SUs employ the p -persistent CSMA principle [70] for contention resolution where each SU with data to transmit attempts to capture an available channel with a probability p after the channel is sensed to be idle during the standard DIFS interval (DCF Interframe Space). If a particular SU decides not to transmit (with probability of $1 - p$), it will sense the channel

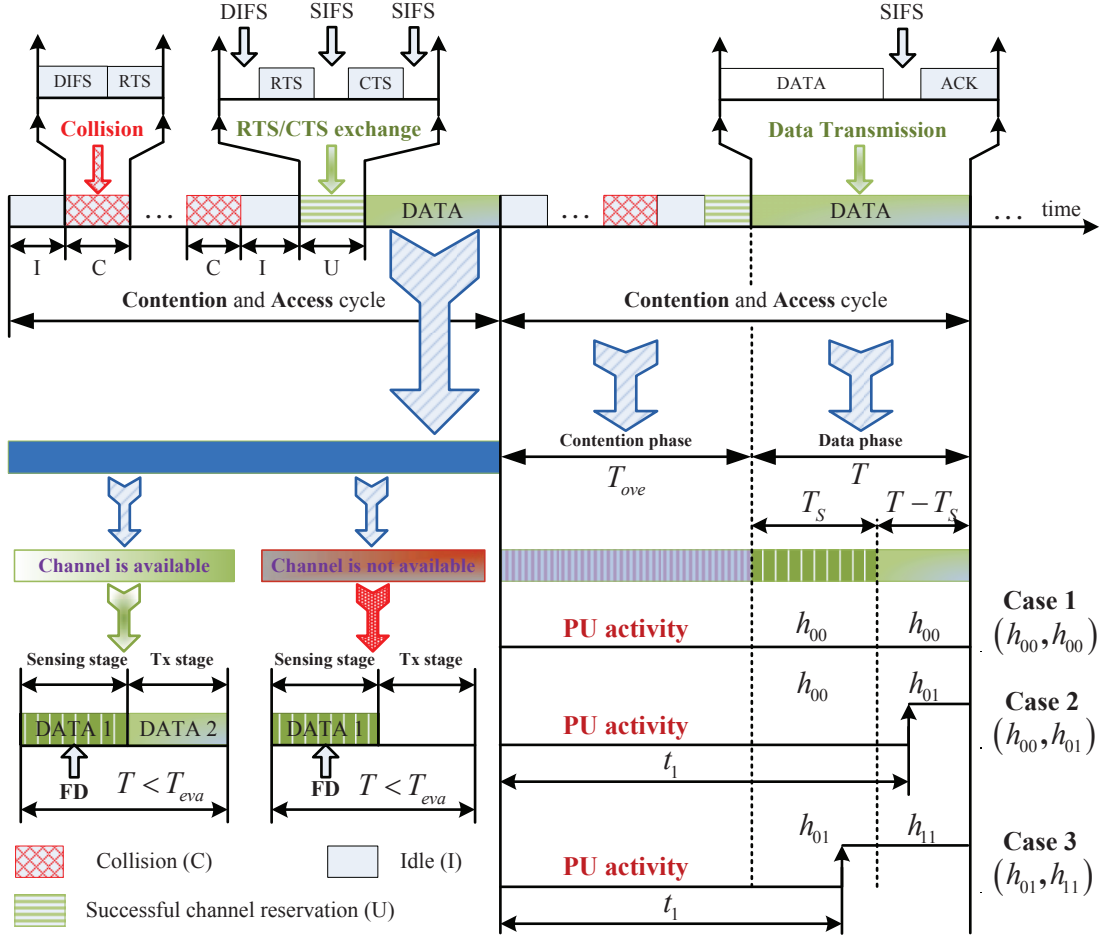


Figure 6.1: Timing diagram of the proposed full-duplex cognitive MAC protocol.

and attempt to transmit again in the next slot of length σ with probability p . To complete the reservation, the four-way handshake with Request-to-Send/Clear-to-Send (RTS/CTS) exchanges [85] is employed to reserve the available channel for transmission. Specifically, the secondary transmitter sends RTS to the secondary receiver and waits until it successfully receives the CTS from the secondary receiver. All other SUs, which hear the RTS and CTS exchange from the winning SU, defer to access the channel for a duration equal to the data transmission time, T . Then, an acknowledgment (ACK) from the SU's receiver is transmitted to its corresponding transmitter to notify the successful reception of a packet. Furthermore, the standard small interval, namely SIFS (Short Interframe Space), is used before the transmissions of CTS, ACK, and data frame as in the standard 802.11 MAC protocol [85].

In our design, the data phase after the channel contention phase comprises two stages

where the SU performs concurrent sensing and transmission in the first stage with duration T_S and transmission only in the second stage with duration $T - T_S$. Here, the SU exploits the FD capability of its transceiver to realize concurrent sensing and transmission the first stage (called FD sensing stage) where the sensing outcome at the end of this stage (i.e., an idle or active channel status) determines its further actions as follows. Specifically, if the sensing outcome indicates an available channel then the SU transmits data in the second stage; otherwise, it remains silent for the remaining time of the data phase with duration $T - T_S$.

We assume that the duration of the SU's data phase T is smaller than the channel evacuation time T_{eva} so timely evacuation from the busy channel can be realized with reliable FD spectrum sensing. Therefore, our design allows to protect the PU with evacuation delay at most T if the MAC carrier sensing during the contention phase and the FD spectrum sensing in the data phase are perfect. Furthermore, we assume that the SU transmits at power levels $P_{\text{sen}} \leq P_{\text{max}}$ and $P_{\text{dat}} = P_{\text{max}}$ during the FD sensing and transmission stages, respectively where P_{max} denotes the maximum power and the transmit power P_{sen} in the FD sensing stage will be optimized to effectively mitigate the self-interference and achieve good sensing-throughput tradeoff. The timing diagram of the proposed FDC-MAC protocol is illustrated in Fig. 6.1.

We allow two possible operation modes in the transmission stage. The first is the HD transmission mode (HDTx mode) where there is only one direction of data transmission from the SU transmitter to the SU receiver. In this mode, there is no self-interference in the transmission stage. The second is the FD transmission mode (FDTx mode) where two-way communications between the pair of SUs are assumed (i.e., there are two data flows between the two SU nodes in opposite directions). In this mode, the achieved throughput can be potentially enhanced (at most doubling the throughput of the HDTx mode) but self-interference must be taken into account in throughput quantification.

Our proposed FDC-MAC protocol design indeed enables flexible and adaptive configuration, which can efficiently exploit the capability of the FD transceiver. Specifically, if the duration of the FD sensing stage is set equal to the duration of the whole data phase (i.e., $T_S = T$), then the SU performs concurrent sensing and transmission for the whole data phase as in our previous design [35]. This configuration may degrade the achievable throughput since the transmit power during the FD sensing stage is typically set smaller P_{max} to mitigate the self-interference and achieve the required sensing performance. We will refer the corresponding MAC protocol with $T_S = T$ as one-stage FD MAC in the sequel.

Moreover, if we set the SU transmit power P_{sen} in the sensing stage equal to zero, i.e., $P_{\text{sen}} = 0$, then we achieve the traditional two-stage HD cognitive MAC protocol where sensing and transmission are performed sequentially in two different stages [22, 33]. Moreover, the proposed FDC-MAC protocol is more flexible than existing designs [35], [22, 33] since different existing designs can be achieved through suitable configuration of the protocol parameters of our FDC-MAC protocol. It will be demonstrated that the proposed FDC-MAC protocol achieves significant better throughput than that of the existing cognitive MAC protocols. In the following, we present the throughput analysis based on which the protocol configuration optimization can be performed.

6.4.2 Throughput Analysis

We now conduct the saturation throughput analysis for the secondary network where all SUs are assumed to always have data to transmit. The resulting throughput can be served as an upper bound for the throughput in the non-saturated scenario [85]. This analysis is performed by studying one specific contention and access cycle (CA cycle) with the contention phase and data phase as shown in Fig. 6.1. Without loss of generality, we will consider the normalized throughput achieved per one unit of system bandwidth (in bits/s/Hz). Specifically, the normalized throughput of the FDC-MAC protocol can be expressed as

$$\mathcal{N}\mathcal{T} = \frac{\mathcal{B}}{T_{\text{ove}} + T}, \quad (6.1)$$

where T_{ove} represents the time overhead required for one successful channel reservation (i.e., successful RTS/CTS exchanges), \mathcal{B} denotes the amount of data (bits) transmitted in one CA cycle per one unit of system bandwidth, which is expressed in bits/Hz. To complete the throughput analysis, we derive the quantities T_{ove} and \mathcal{B} in the remaining of this subsection.

6.4.2.1 Derivation of T_{ove}

The average time overhead for one successful channel reservation can be calculated as

$$T_{\text{ove}} = \bar{T}_{\text{cont}} + 2SIFS + 2PD + ACK, \quad (6.2)$$

where ACK is the length of an ACK message, $SIFS$ is the length of a short interframe space, and PD is the propagation delay where PD is usually small compared to the slot size σ , and \bar{T}_{cont} denotes the average time overhead due to idle periods, collisions, and successful transmissions of RTS/CTS messages in one CA cycle. For better presentation of the paper, the derivation of \bar{T}_{cont} is given in Appendix 6.8.1.

6.4.2.2 Derivation of \mathcal{B}

To calculate \mathcal{B} , we consider all possible cases that capture the activities of SUs and status changes of the PU in the FDC-MAC data phase of duration T . Because the PU's activity is not synchronized with the SU's transmission, the PU can change its idle/active status any time. We assume that there can be at most one transition between the idle and active states of the PU during one data phase interval. This is consistent with the assumption on the slow status changes of the PU as described in Section 6.3.2 since $T < T_{\text{eva}}$. Furthermore, we assume that the carrier sensing of the FDC-MAC protocol is perfect; therefore, the PU is idle at the beginning of the FDC-MAC data phase. Note that the PU may change its status during the SU's FD sensing or transmission stage, which requires us to consider different possible events in the data phase.

We use h_{ij} ($i, j \in \{0, 1\}$) to represent events capturing status changes of the PU in the FD sensing stage and transmission stage where $i = 0$ and $i = 1$ represent the idle and active states of the PU, respectively. For example, if the PU is idle during the FD sensing stage and becomes active during the transmission stage, then we represent this event as (h_{00}, h_{01}) where sub-events h_{00} and h_{01} represent the status changes in the FD sensing and transmission stages, respectively. Moreover, if the PU changes from the idle to the active state during the FD sensing stage and remains active in the remaining of the data phase, then we represent this event as (h_{01}, h_{11})

It can be verified that we must consider the following three cases with the corresponding status changes of the PU during the FDC-MAC data phase to analyze \mathcal{B} .

- **Case 1:** The PU is idle for the whole FDC-MAC data phase (i.e., there is no PU's signal in both FD sensing and transmission stages) and we denote this event as (h_{00}, h_{00}) . The average number of bits (in bits/Hz) transmitted during the data phase in this case is denoted as \mathcal{B}_1 .
- **Case 2:** The PU is idle during the FD sensing stage but the PU changes from the idle to the active status in the transmission stage. We denote the event corresponding to this case as (h_{00}, h_{01}) where h_{00} and h_{01} capture the sub-events in the FD sensing and transmission stages, respectively. The average number of bits (in bits/Hz) transmitted during the data phase in this case is represented by \mathcal{B}_2 .
- **Case 3:** The PU is first idle then becomes active during the FD sensing stage and it remains active during the whole transmission stage. Similarly we denote this event

6.5 FDC–MAC Protocol Configuration for Throughput Maximization

as (h_{01}, h_{11}) and the average number of bits (in bits/Hz) transmitted during the data phase in this case is denoted as \mathcal{B}_3 .

Then, we can calculate \mathcal{B} as follows:

$$\mathcal{B} = \mathcal{B}_1 + \mathcal{B}_2 + \mathcal{B}_3. \quad (6.3)$$

To complete the analysis, we will need to derive \mathcal{B}_1 , \mathcal{B}_2 , and \mathcal{B}_3 , which are given in Appendix 6.8.2.

6.5 FDC–MAC Protocol Configuration for Throughput Maximization

In this section, we study the optimal configuration of the proposed FDC–MAC protocol to achieve the maximum throughput while satisfactorily protecting the PU.

6.5.1 Problem Formulation

Let $\mathcal{N}\mathcal{J}(T_S, p, P_{\text{sen}})$ denote the normalized secondary throughput, which is the function of the sensing time T_S , transmission probability p , and the SU’s transmit power P_{sen} in the FD sensing stage. In the following, we assume a fixed frame length T , which is set smaller than the required evacuation time T_{eva} to achieve timely evacuation from a busy channel for the SUs. We are interested in determining suitable configuration for p , T_S and P_{sen} to maximize the secondary throughput, $\mathcal{N}\mathcal{J}(T_S, p, P_{\text{sen}})$. In general, the optimal transmission probability p should balance between reducing collisions among SUs and limiting the protocol overhead. However, the achieved throughput is less sensitive to the transmission probability p as will be demonstrated later via the numerical study. Therefore, we will seek to optimize the throughput over P_{sen} and T_S for a reasonable and fixed value of p .

For brevity, we express the throughput as a function of P_{sen} and T_S only, i.e., $\mathcal{N}\mathcal{J}(T_S, P_{\text{sen}})$. Suppose that the PU requires that the average detection probability is at least $\bar{\mathcal{P}}_d$. Then, the throughput maximization problem can be stated as follows:

$$\begin{aligned} & \max_{T_S, p, P_{\text{sen}}} \mathcal{N}\mathcal{J}(T_S, P_{\text{sen}}) \\ & \text{s.t. } \hat{\mathcal{P}}_d(\varepsilon, T_S) \geq \bar{\mathcal{P}}_d, \end{aligned} \quad (6.4)$$

$$0 \leq P_{\text{sen}} \leq P_{\text{max}}, \quad 0 \leq T_S \leq T,$$

6.5 FDC–MAC Protocol Configuration for Throughput Maximization

where P_{\max} is the maximum power for SUs, and T_S is upper bounded by T . In fact, the first constraint on $\hat{\mathcal{P}}_d(\varepsilon, T_S)$ implies that the spectrum sensing should be sufficiently reliable to protect the PU which can be achieved with sufficiently large sensing time T_S . Moreover, the SU's transmit power P_{sen} must be appropriately set to achieve good tradeoff between the network throughput and self-interference mitigation.

6.5.2 Parameter Configuration for FDC–MAC Protocol

To gain insights into the parameter configuration of the FDC–MAC protocol, we first study the optimization with respect to the sensing time T_S for a given P_{sen} . For any value of T_S , we would need to set the sensing detection threshold ε so that the detection probability constraint is met with equality, i.e., $\hat{\mathcal{P}}_d(\varepsilon, T_S) = \bar{\mathcal{P}}_d$ as in [5, 22]. Since the detection probability is smaller in **Case 3** (i.e., the PU changes from the idle to active status during the FD sensing stage of duration T_S) compared to that in **Case 1** and **Case 2** (i.e., the PU remains idle during the FD sensing stage) considered in the previous section, we only need to consider **Case 3** to maintain the detection probability constraint. The average probability of detection for the FD sensing in **Case 3** can be expressed as

$$\hat{\mathcal{P}}_d = \int_0^{T_S} \mathcal{P}_d^{01}(t) f_{\tau_{\text{id}}}(t | 0 \leq t \leq T_S) dt, \quad (6.5)$$

where t denotes the duration from the beginning of the FD sensing stage to the instant when the PU changes to the active state, and $f_{\tau_{\text{id}}}(t | \mathcal{A})$ is the pdf of τ_{id} conditioned on event \mathcal{A} capturing the condition $0 \leq t \leq T_S$, which is given as

$$f_{\tau_{\text{id}}}(t | \mathcal{A}) = \frac{f_{\tau_{\text{id}}}(t)}{\Pr\{\mathcal{A}\}} = \frac{\frac{1}{\bar{\tau}_{\text{id}}} \exp(-\frac{t}{\bar{\tau}_{\text{id}}})}{1 - \exp(-\frac{T_S}{\bar{\tau}_{\text{id}}})}. \quad (6.6)$$

Note that $\mathcal{P}_d^{01}(t)$ is derived in Appendix 6.8.3 and $f_{\tau_{\text{id}}}(t)$ is given in (6.18).

We consider the following single-variable optimization problem for a given P_{sen} :

$$\max_{0 < T_S \leq T} \mathcal{NJ}(T_S, P_{\text{sen}}). \quad (6.7)$$

We characterize the properties of function $\mathcal{NJ}(T_S, P_{\text{sen}})$ with respect to T_S for a given P_{sen} in the following theorem whose proof is provided in Appendix 6.8.4. For simplicity, the throughput function is written as $\mathcal{NJ}(T_S)$.

Theorem 1: The objective function $\mathcal{NJ}(T_S)$ of (6.7) satisfies the following properties

1. $\lim_{T_S \rightarrow 0} \frac{\partial \mathcal{N}\mathcal{J}}{\partial T_S} = +\infty$,
2. (a) For HDTx mode with $\forall P_{\text{sen}}$ and FDTx mode with $P_{\text{sen}} < \bar{P}_{\text{sen}}$, we have $\lim_{T_S \rightarrow T} \frac{\partial \mathcal{N}\mathcal{J}}{\partial T_S} < 0$,
 (b) For FDTx mode with $P_{\text{sen}} > \bar{P}_{\text{sen}}$, we have $\lim_{T_S \rightarrow T} \frac{\partial \mathcal{N}\mathcal{J}}{\partial T_S} > 0$,
3. $\frac{\partial^2 \mathcal{N}\mathcal{J}}{\partial T_S^2} < 0, \forall T_S$,
4. The objective function $\mathcal{N}\mathcal{J}(T_S)$ is bounded from above,

where $\bar{P}_{\text{sen}} = N_0 \left[\left(1 + \frac{P_{\text{dat}}}{N_0 + \zeta P_{\text{dat}}^\xi} \right)^2 - 1 \right]$ is the critical value of P_{sen} such that $\lim_{T_S \rightarrow T} \frac{\partial \mathcal{N}\mathcal{J}}{\partial T_S} = 0$.

We would like to discuss the properties stated in Theorem 1. For the HDTx mode with $\forall P_{\text{sen}}$ and FDTx mode with low P_{sen} , then properties 1, 2a, and 4 imply that there must be at least one T_S in $[0, T]$ that maximizes $\mathcal{N}\mathcal{J}(T_S)$. The third property implies that this maximum is indeed unique. Moreover, for the FDTx with high P_{sen} , then properties 1, 2b, 3 and 4 imply that $\mathcal{N}\mathcal{J}(T_S)$ increases in $[0, T]$. Hence, the throughput $\mathcal{N}\mathcal{J}(T_S)$ achieves its maximum with sensing time $T_S = T$. We propose an algorithm to determine optimal (T_S, P_{sen}) , which is summarized in Algorithm 9. Here, we can employ the bisection scheme and other numerical methods to determine the optimal value T_S for a given P_{sen} .

Algorithm 9 FDC-MAC CONFIGURATION ALGORITHM

- 1: **for** each considered value of $P_{\text{sen}} \in [0, P_{\text{max}}]$ **do**
 - 2: Find optimal T_S for problem (6.7) using the bisection method as $\bar{T}_S(P_{\text{sen}}) = \underset{0 \leq T_S \leq T}{\operatorname{argmax}} \mathcal{N}\mathcal{J}(T, P_{\text{sen}})$.
 - 3: **end for**
 - 4: The final solution $(T_S^*, P_{\text{sen}}^*)$ is determined as $(T_S^*, P_{\text{sen}}^*) = \underset{P_{\text{sen}}, \bar{T}_S(P_{\text{sen}})}{\operatorname{argmax}} \mathcal{N}\mathcal{J}(T_S(P_{\text{sen}}), P_{\text{sen}})$.
-

6.6 Numerical Results

For numerical studies, we set the key parameters for the FDC-MAC protocol as follows: mini-slot duration is $\sigma = 20\mu\text{s}$; $PD = 1\mu\text{s}$; $SIFS = 2\sigma \mu\text{s}$; $DIFS = 10\sigma \mu\text{s}$; $ACK = 20\sigma \mu\text{s}$; $CTS = 20\sigma \mu\text{s}$; $RTS = 20\sigma \mu\text{s}$. Other parameters are chosen as follows unless stated otherwise: the sampling frequency $f_s = 6 \text{ MHz}$; bandwidth of PU's signal 6 MHz; $\bar{P}_d = 0.8$; $T = 15 \text{ ms}$; $p = 0.0022$; the SNR of the PU signal at each SU $\gamma_P = \frac{P_P}{N_0} = -20 \text{ dB}$; varying

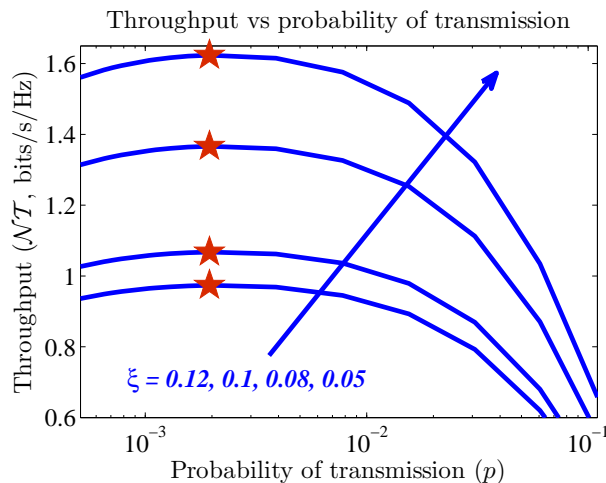


Figure 6.2: Normalized throughput versus transmission probability p for $T = 18$ ms, $\bar{\tau}_{\text{id}} = 1000$ ms, $\bar{\tau}_{\text{ac}} = 100$ ms, and varying ξ .

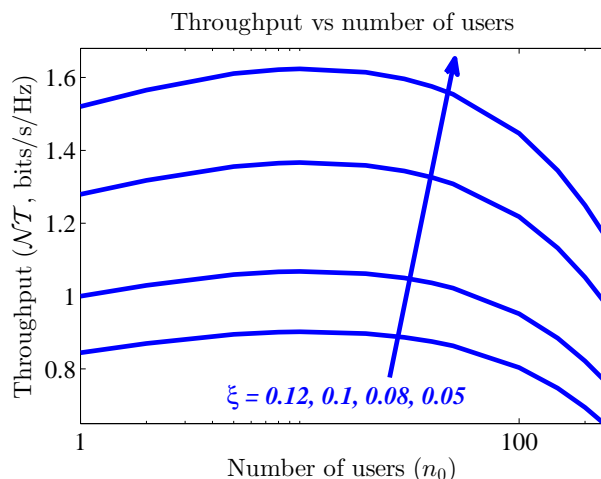


Figure 6.3: Normalized throughput versus the number of SUs n_0 for $T = 18$ ms, $p = 0.0022$, $\bar{\tau}_{\text{id}} = 1000$ ms, $\bar{\tau}_{\text{ac}} = 100$ ms, and varying ξ .

self-interference parameters ζ and ξ . Without loss of generality, the noise power is normalized to one; hence, the SU transmit power P_{sen} becomes $P_{\text{sen}} = \text{SNR}_s$; and we set $P_{\text{max}} = 15\text{dB}$.

We first study the impacts of self-interference parameters on the throughput performance with the following parameter setting: $(\bar{\tau}_{\text{id}}, \bar{\tau}_{\text{ac}}) = (1000, 100)$ ms, $P_{\text{max}} = 25$ dB, $T_{\text{eva}} = 40$ ms, $\zeta = 0.4$, ξ is varied in $\xi = \{0.12, 0.1, 0.08, 0.05\}$, and $P_{\text{dat}} = P_{\text{max}}$. Recall that the self-interference depends on the transmit power P as $I(P) = \zeta (P)^\xi$ where $P = P_{\text{sen}}$ and $P = P_{\text{dat}}$ in the FD sensing and transmission stages, respectively. Fig. 6.2 illustrates the variations of the throughput versus the transmission probability p . It can be observed that when ξ

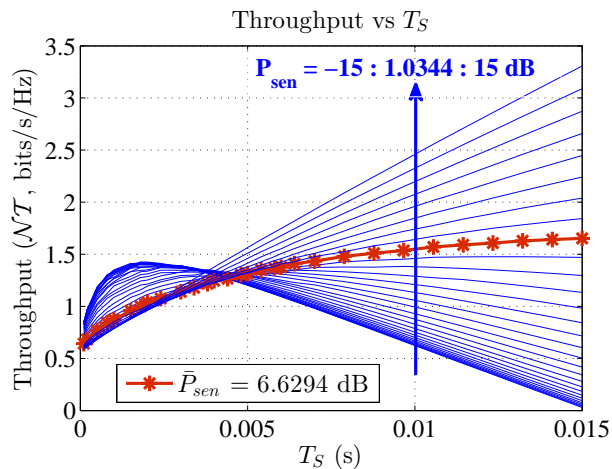


Figure 6.4: Normalized throughput versus SU transmit power P_{sen} and sensing time T_S for $p = 0.0022$, $\bar{\tau}_{\text{id}} = 500$ ms, $\bar{\tau}_{\text{ac}} = 50$ ms, $n_0 = 40$, $\xi = 1$, $\zeta = 0.7$ and FDTx with $P_{\text{dat}} = 15$ dB.

decreases (i.e., the self-interference is smaller), the achieved throughput increases. This is because SUs can transmit with higher power while still maintaining the sensing constraint during the FD sensing stage, which leads to throughput improvement. The optimal P_{sen} corresponding to these values of ξ are $P_{\text{sen}} = SNR_s = \{25.00, 18.01, 14.23, 11.28\}$ dB and the optimal probability of transmission is $p^* = 0.0022$ as indicated by a star symbol. Therefore, to obtain all other results in this section, we set $p^* = 0.0022$.

Fig. 6.3 illustrates the throughput performance versus number of SUs n_0 when we keep the same parameter settings as those for Fig. 6.2 and $p^* = 0.0022$. Again, when ξ decreases (i.e., the self-interference becomes smaller), the achieved throughput increases. In this figure, the optimal SNR_s achieving the maximum throughput corresponding to the considered values of ξ are $P_{\text{sen}} = SNR_s = \{25.00, 18.01, 14.23, 11.28\}$ dB, respectively.

We now verify the results stated in Theorem 1 for the FDTx mode. Specifically, Fig. 6.4 shows the throughput performance for the scenario where the QSIC is very low with large ξ and ζ where we set the network parameters as follows: $p = 0.0022$, $\bar{\tau}_{\text{id}} = 500$ ms, $\bar{\tau}_{\text{ac}} = 50$ ms, $n_0 = 40$, $\xi = 1$, $\zeta = 0.7$, and $P_{\text{dat}} = 15$ dB. Moreover, we can obtain \bar{P}_{sen} as in (6.42) in Appendix 6.8.4, that is $\bar{P}_{\text{sen}} = 6.6294$ dB. In this figure, the curve indicated by asterisks, which corresponds to $P_{\text{sen}} = \bar{P}_{\text{sen}}$, shows the monotonic increase of the throughput with sensing time T_S and other curves corresponding to $P_{\text{sen}} > \bar{P}_{\text{sen}}$ have the same characteristic. In contrast, all remaining curves (corresponding to $P_{\text{sen}} < \bar{P}_{\text{sen}}$) first increase to the maximum values and then decrease as we increase T_S .

Fig. 6.5 illustrates the throughput performance for the very high QSIC with small ξ and

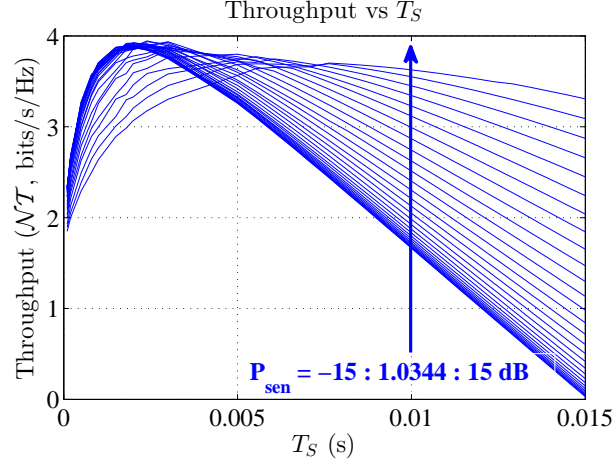


Figure 6.5: Normalized throughput versus SU transmit power P_{sen} and sensing time T_S for $p = 0.0022$, $\bar{\tau}_{\text{id}} = 500$ ms, $\bar{\tau}_{\text{ac}} = 50$ ms, $n_0 = 40$, $\xi = 1$, $\zeta = 0.08$ and FDTx with $P_{\text{dat}} = 15$ dB.

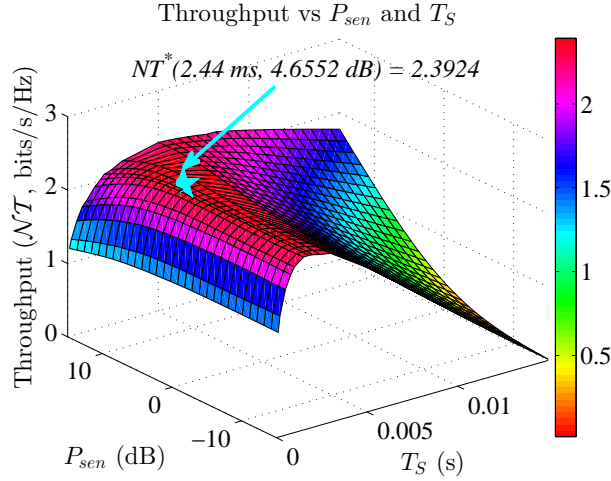


Figure 6.6: Normalized throughput versus SU transmit power P_{sen} and sensing time T_S for $p = 0.0022$, $\bar{\tau}_{\text{id}} = 150$ ms, $\bar{\tau}_{\text{ac}} = 50$ ms, $n_0 = 40$, $\xi = 0.95$, $\zeta = 0.08$ and FDTx with $P_{\text{dat}} = 15$ dB.

ζ where we set the network parameters as follows: $p = 0.0022$, $\bar{\tau}_{\text{id}} = 500$ ms, $\bar{\tau}_{\text{ac}} = 50$ ms, $n_0 = 40$, $\xi = 1$, $\zeta = 0.08$, and $P_{\text{dat}} = 15$ dB. Moreover, we can obtain \bar{P}_{sen} as in (6.42) in Appendix 6.8.4 that is $\bar{P}_{\text{sen}} = 19.9201$ dB. We have $P_{\text{sen}} < P_{\text{max}} = 15\text{dB} < \bar{P}_{\text{sen}}$ in this scenario; hence, all the curves first increases to the maximum throughput and then decreases with the increasing T_S . Therefore, we have correctly validated the properties stated in Theorem 1.

Now we investigate the throughput performance versus SU transmit power P_{sen} and

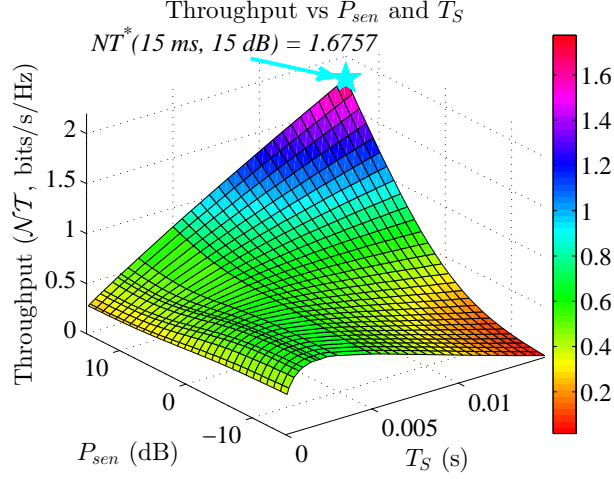


Figure 6.7: Normalized throughput versus SU transmit power P_{sen} and sensing time T_S for $p = 0.0022$, $\bar{\tau}_{\text{id}} = 150$ ms, $\bar{\tau}_{\text{ac}} = 50$ ms, $n_0 = 40$, $\xi = 0.95$, $\zeta = 0.8$ and FDTx with $P_{\text{dat}} = 15$ dB.

sensing time T_S for the case of high QSIC with $\xi = 0.95$ and $\zeta = 0.08$. Fig. 6.6 shows the throughput versus the SU transmit power P_{sen} and sensing time T_S for the FDTx mode with $P_{\text{dat}} = 15$ dB, $p = 0.0022$, $\bar{\tau}_{\text{id}} = 150$ ms, $\bar{\tau}_{\text{ac}} = 50$ ms, and $n_0 = 40$. It can be observed that there exists an optimal configuration of the SU transmit power $P_{\text{sen}}^* = 4.6552$ dB and sensing time $T_S^* = 2.44$ ms to achieve the maximum throughput $\mathcal{N}\mathcal{T}(T_S^*, P_{\text{sen}}^*) = 2.3924$, which is indicated by a star symbol. These results confirm that SUs must set appropriate sensing time and transmit power for the FDC-MAC protocol to achieve the maximize throughput, which cannot be achieved by setting $T_s = T$ as proposed in existing designs such as in [35].

In Fig. 6.7, we present the throughput versus the SU transmit power P_{sen} and sensing time T_S for the low QSIC scenario where $p = 0.0022$, $\bar{\tau}_{\text{id}} = 150$ ms, $\bar{\tau}_{\text{ac}} = 50$ ms, $P_{\text{max}} = 15$ dB, $n_0 = 40$, $\xi = 0.95$, and $\zeta = 0.8$. The optimal configuration of SU transmit power $P_{\text{sen}}^* = 15$ dB and sensing time $T_S^* = 15$ ms to achieve the maximum throughput $\mathcal{N}\mathcal{T}(T_S^*, P_{\text{sen}}^*) = 1.6757$ is again indicated by a star symbol. Under this optimal configuration, the FD sensing is performed during the whole data phase (i.e., there is no transmission stage). In fact, to achieve the maximum throughput, the SU must provide the satisfactory sensing performance and attempt to achieve high transmission rate. Therefore, if the QSIC is low, the data rate achieved during the transmission stage can be lower than that in the FD sensing stage because of the very strong self-interference in the transmission stage. Therefore, setting longer FD sensing time enables to achieve more satisfactory sensing performance and higher transmission rate, which explains that the optimal configuration should set $T_S^* = T$ for the

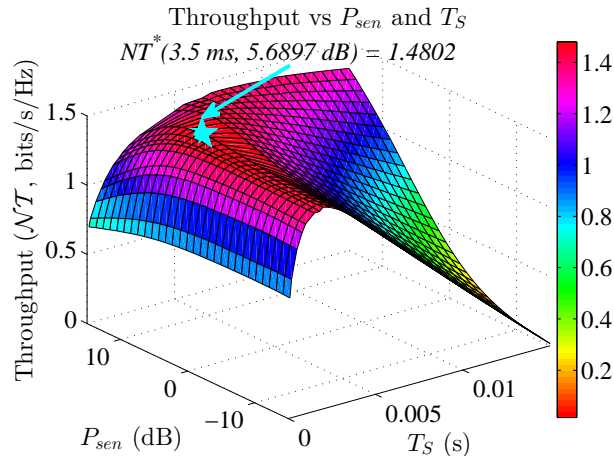


Figure 6.8: Normalized throughput versus SU transmit power P_{sen} and sensing time T_S for $p = 0.0022$, $\bar{\tau}_{id} = 150$ ms, $\bar{\tau}_{ac} = 50$ ms, $n_0 = 40$, $\xi = 0.95$, $\zeta = 0.08$ and HDTx.

low QSIC scenario. This protocol configuration corresponds to existing design in [35], which is a special case of the proposed FDC-MAC protocol.

We now investigate the throughput performance with respect to the SU transmit power P_{sen} and sensing time T_S for the HDTx mode. Fig. 6.8 illustrates the throughput performance for the high QSIC scenario with $\xi = 0.95$ and $\zeta = 0.08$. It can be observed that there exists an optimal configuration of SU transmit power $P_{sen}^* = 5.6897$ dB and sensing time $T_S^* = 3.5$ ms to achieve the maximum throughput $\mathcal{N}\mathcal{T}(T_S^*, P_{sen}^*) = 1.4802$, which is indicated by a star symbol. The maximum achieved throughput of the HDTx mode is lower than that in the FDTx mode presented in Fig. 6.6. This is because with high QSIC, the FDTx mode can transmit more data than the HDTx mode in the transmission stage.

In Fig. 6.9, we show the throughput versus the SU transmit power P_{sen} for $T_S = 2.2$ ms, $p = 0.0022$, $\bar{\tau}_{id} = 1000$ ms, $\bar{\tau}_{ac} = 50$ ms, $n_0 = 40$, $\xi = 0.95$, $\zeta = 0.08$ and various values of T (i.e., the data phase duration) for the FDTx mode with $P_{dat} = 15$ dB. For each value of T , there exists the optimal SU transmit power P_{sen}^* which is indicated by an asterisk. It can be observed that as T increases from 8 ms to 25 ms, the achieved maximum throughput first increases then decreases with T . Also in the case with $T^* = 15$ ms, the SU achieves the largest throughput which is indicated by a star symbol. Furthermore, the achieved throughput significantly decreases when the pair of (T, P_{sen}) deviates from the optimal values, (T^*, P_{sen}^*) .

Finally, we compare the throughput of our proposed FDC-MAC protocol, the single-stage FD MAC protocol where FD sensing is performed during the whole data phase [35]

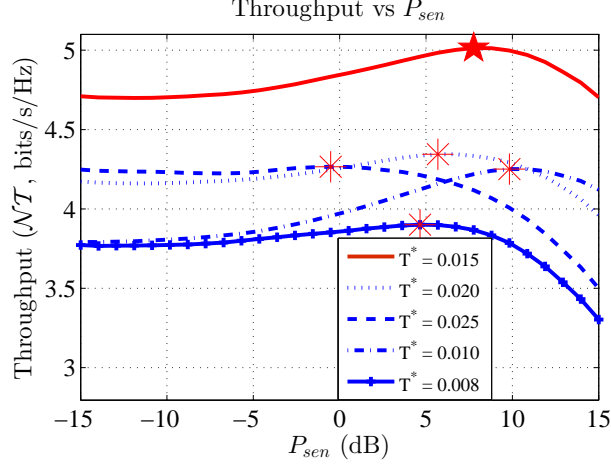


Figure 6.9: Normalized throughput versus SU transmit power P_{sen} for $T_S = 2.2$ ms, $p = 0.0022$, $\bar{\tau}_{\text{id}} = 1000$ ms, $\bar{\tau}_{\text{ac}} = 50$ ms, $n_0 = 40$, $\xi = 0.95$, $\zeta = 0.08$, varying T , and FDTx with $P_{\text{dat}} = 15$ dB.

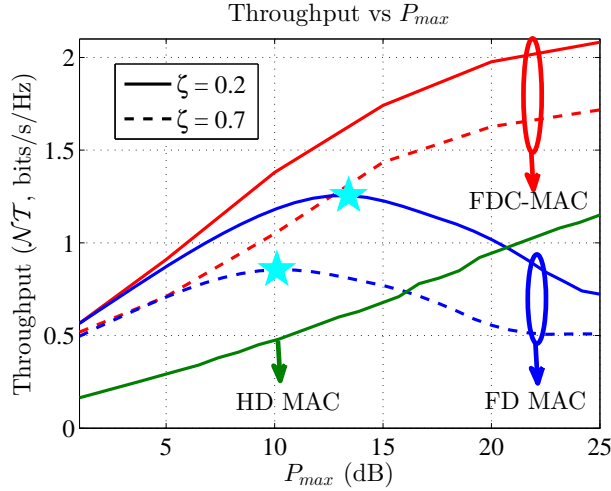


Figure 6.10: Normalized throughput versus P_{max} for $\bar{\tau}_{\text{id}} = 150$ ms, $\bar{\tau}_{\text{ac}} = 75$ ms, $n_0 = 40$, $\xi = 0.85$, $n_0 = 40$, $\zeta = \{0.2, 0.7\}$, and FDTx with $P_{\text{dat}} = P_{\text{max}}$ dB.

and the HD MAC protocol without exploiting concurrent sensing and transmission during the sensing interval in Fig. 6.10. For brevity, the single-stage FD MAC protocol is referred to as FD MAC in this figure. The parameter settings are as follows: $\bar{\tau}_{\text{id}} = 150$ ms, $\bar{\tau}_{\text{ac}} = 75$ ms, $n_0 = 40$, $\xi = 0.85$, $n_0 = 40$, $\zeta = \{0.2, 0.7\}$, and FDTx with $P_{\text{dat}} = P_{\text{max}}$ dB. For fair comparison, we first obtain the optimal configuration of the single-stage FD MAC protocol, i.e., then we use (T^*, p^*) for the HD MAC protocol and FDC-MAC protocol. For the single-stage FD MAC protocol, the transmit power is set to P_{max} because there is only a single stage

where the SU performs sensing and transmission simultaneously during the data phase. In addition, the HD MAC protocol will also transmit with the maximum transmit power P_{\max} to achieve the highest throughput. For both studied cases of $\zeta = \{0.2, 0.7\}$, our proposed FDC-MAC protocol significantly outperforms the other two protocols. Moreover, the single-stage FD MAC protocol [35] with power allocation outperforms the HD MAC protocol at the corresponding optimal power level required by the single-stage FD MAC protocol. However, both single-stage FDC-MAC and HD MAC protocols achieve increasing throughput with higher P_{\max} while the single-stage FD MAC protocol has the throughput first increased then decreased as P_{\max} increases. This demonstrates that the self-interference has the very negative impact on the throughput performance of the single-stage FD MAC protocol, which is efficiently mitigated by our proposed FDC-MAC protocol.

6.7 Conclusion

In this paper, we have proposed the FDC-MAC protocol for cognitive radio networks, analyzed its throughput performance, and studied its optimal parameter configuration. The design and analysis have taken into account the FD communication capability and the self-interference of the FD transceiver. We have shown that there exists an optimal FD sensing time to achieve the maximum throughput. In addition, we have presented extensive numerical results to demonstrate the impacts of self-interference and protocol parameters on the throughput performance. In particular, we have shown that the FDC-MAC protocol achieves significantly higher throughput than the HD MAC protocol, which confirms that the FDC-MAC protocol can efficiently exploit the FD communication capability. Moreover, the FDC-MAC protocol results in higher throughput with the increasing maximum power budget while the throughput of the single-stage FD MAC can decrease in the high power regime. This result validates the importance of adopting the two-stage procedure in the data phase and the optimization of sensing time and transmit power during the FD sensing stage to mitigate the negative self-interference impact.

6.8 Appendices

6.8.1 Derivation of \bar{T}_{cont}

To calculate \bar{T}_{cont} , we define some further parameters as follows. Denote T_{coll} as the duration of the collision and T_{succ} as the required time for successful RTS/CTS transmission. These

quantities can be calculated as follows [70]:

$$\begin{cases} T_{\text{succ}} = DIFS + RTS + SIFS + CTS + 2PD \\ T_{\text{coll}} = DIFS + RTS + PD, \end{cases} \quad (6.8)$$

where $DIFS$ is the length of a DCF (distributed coordination function) interframe space, RTS and CTS denote the lengths of the RTS and CTS messages, respectively.

As being shown in Fig. 6.1, there can be several idle periods and collisions before one successful channel reservation. Let T_{idle}^i denote the i -th idle duration between two consecutive RTS/CTS exchanges, which can be collisions or successful exchanges. Then, T_{idle}^i can be calculated based on its probability mass function (pmf), which is derived as follows. In the following, all relevant quantities are defined in terms of the number of time slots. With n_0 SUs joining the contention resolution, let $\mathcal{P}_{\text{succ}}$, $\mathcal{P}_{\text{coll}}$ and $\mathcal{P}_{\text{idle}}$ denote the probabilities that a particular generic slot corresponds to a successful transmission, a collision, and an idle slot, respectively. These probabilities can be calculated as follows:

$$\mathcal{P}_{\text{succ}} = n_0 p (1 - p)^{n_0 - 1} \quad (6.9)$$

$$\mathcal{P}_{\text{idle}} = (1 - p)^{n_0} \quad (6.10)$$

$$\mathcal{P}_{\text{coll}} = 1 - \mathcal{P}_{\text{succ}} - \mathcal{P}_{\text{idle}}, \quad (6.11)$$

where p is the transmission probability of an SU in a generic slot. In general, the interval T_{cont} , whose average value is \bar{T}_{cont} given in (6.2), consists of several intervals corresponding to idle periods, collisions, and one successful RTS/CTS transmission. Hence, this quantity can be expressed as

$$T_{\text{cont}} = \sum_{i=1}^{N_{\text{coll}}} (T_{\text{coll}} + T_{\text{idle}}^i) + T_{\text{idle}}^{N_{\text{coll}}+1} + T_{\text{succ}}, \quad (6.12)$$

where N_{coll} is the number of collisions before the successful RTS/CTS exchange and N_{coll} is a geometric random variable (RV) with parameter $1 - \mathcal{P}_{\text{coll}}/\bar{\mathcal{P}}_{\text{idle}}$ where $\bar{\mathcal{P}}_{\text{idle}} = 1 - \mathcal{P}_{\text{idle}}$. Therefore, its pmf can be expressed as

$$f_X^{N_{\text{coll}}}(x) = \left(\frac{\mathcal{P}_{\text{coll}}}{\bar{\mathcal{P}}_{\text{idle}}} \right)^x \left(1 - \frac{\mathcal{P}_{\text{coll}}}{\bar{\mathcal{P}}_{\text{idle}}} \right), \quad x = 0, 1, 2, \dots \quad (6.13)$$

Also, T_{idle} represents the number of consecutive idle slots, which is also a geometric RV with parameter $1 - \mathcal{P}_{\text{idle}}$ with the following pmf

$$f_X^{T_{\text{idle}}}(x) = (\mathcal{P}_{\text{idle}})^x (1 - \mathcal{P}_{\text{idle}}), \quad x = 0, 1, 2, \dots \quad (6.14)$$

Therefore, \bar{T}_{cont} (the average value of T_{cont}) can be written as follows [70]:

$$\bar{T}_{\text{cont}} = \bar{N}_{\text{coll}} T_{\text{coll}} + \bar{T}_{\text{idle}} (\bar{N}_{\text{coll}} + 1) + T_{\text{succ}}, \quad (6.15)$$

where \bar{T}_{idle} and \bar{N}_{coll} can be calculated as

$$\bar{T}_{\text{idle}} = \frac{(1-p)^{n_0}}{1-(1-p)^{n_0}} \quad (6.16)$$

$$\bar{N}_{\text{coll}} = \frac{1-(1-p)^{n_0}}{n_0 p (1-p)^{n_0-1}} - 1. \quad (6.17)$$

These expressions are obtained by using the pmfs of the corresponding RVs given in (6.13) and (6.14), respectively [70].

6.8.2 Derivations of \mathcal{B}_1 , \mathcal{B}_2 , \mathcal{B}_3

We will employ a pair of parameters (θ, φ) to represent the HDTX and FDTX modes where $((\theta, \varphi) = (0, 1))$ for HDTx mode and $((\theta, \varphi) = (1, 2))$ for the FDTx mode. Moreover, since the transmit powers in the FD sensing and transmission stages are different, which are equal to P_{sen} and P_{dat} , respectively, we define different SNRs and SINRs in these two stages as follows: $\gamma_{S1} = \frac{P_{\text{sen}}}{N_0}$ and $\gamma_{S2} = \frac{P_{\text{sen}}}{N_0 + P_p}$ are the SNR and SINR achieved by the SU in the FD sensing stage with and without the presence of the PU, respectively; $\gamma_{D1} = \frac{P_{\text{dat}}}{N_0 + \theta I}$ and $\gamma_{D2} = \frac{P_{\text{dat}}}{N_0 + P_p + \theta I}$ for $I = \zeta P_{\text{dat}}^\xi$ are the SNR and SINR achieved by the SU in the transmission stage with and without the presence of the PU, respectively. It can be seen that we have accounted for the self-interference for the FDTx mode during the transmission stage in γ_{D1} by noting that $\theta = 1$ in this case. The parameter φ for the HDTx and FDTx modes will be employed to capture the throughput for one-way and two-way transmissions in these modes, respectively.

The derivations of \mathcal{B}_1 , \mathcal{B}_2 , and \mathcal{B}_3 require us to consider different possible sensing outcomes in the FD sensing stage. In particular, we need to determine the detection probability \mathcal{P}_d^{ij} , which is the probability of correctly detecting the PU given the PU is active, and the false alarm probability \mathcal{P}_f^{ij} , which is the probability of the erroneous sensing of an idle channel, for each event h_{ij} capturing the state changes of the PU. In the following analysis, we assume the exponential distribution for τ_{ac} and τ_{id} where $\bar{\tau}_{\text{ac}}$ and $\bar{\tau}_{\text{id}}$ denote the corresponding average values of these active and idle intervals. Specifically, let $f_{\tau_x}(t)$ denote the pdf of τ_x (x represents ac or id in the pdf of τ_{ac} or τ_{id} , respectively) then

$$f_{\tau_x}(t) = \frac{1}{\bar{\tau}_x} \exp\left(-\frac{t}{\bar{\tau}_x}\right). \quad (6.18)$$

Similarly, we employ T_S^{ij} and T_D^{ij} to denote the number of bits transmitted on one unit of system bandwidth during the FD sensing and transmission stages under the PU's state-changing event h_{ij} , respectively.

We can now calculate \mathcal{B}_1 as follows:

$$\mathcal{B}_1 = \mathcal{P}(\mathcal{H}_0) \int_{t=T_{\text{ove}}+T}^{\infty} T_1^{00} f_{\tau_{\text{id}}}(t) dt = \mathcal{P}(\mathcal{H}_0) T_1^{00} \exp\left(-\frac{T_{\text{ove}}+T}{\bar{\tau}_{\text{id}}}\right), \quad (6.19)$$

where $\mathcal{P}(\mathcal{H}_0)$ denotes the probability of the idle state of the PU, and \mathcal{P}_f^{00} is the false alarm probability for event h_{00} given in Appendix 6.8.3. Moreover, $T_1^{00} = \mathcal{P}_f^{00} T_S^{00} + (1 - \mathcal{P}_f^{00})(T_S^{00} + T_D^{00})$, $T_S^{00} = T_S \log_2(1 + \gamma_{S1})$, $T_D^{00} = \varphi(T - T_S) \log_2(1 + \gamma_{D1})$ where T_S^{00} and T_D^{00} denote the number of bits transmitted (over one Hz of system bandwidth) in the FD sensing and transmission stages of the data phase, respectively. After some manipulations, we achieve

$$\mathcal{B}_1 = \mathcal{K}_e \exp\left(\frac{T}{\Delta\tau}\right) [T_S \log_2(1 + \gamma_{S1}) + \varphi(1 - \mathcal{P}_f^{00})(T - T_S) \log_2(1 + \gamma_{D1})], \quad (6.20)$$

where $\mathcal{K}_e = \mathcal{P}(\mathcal{H}_0) \exp\left(-\left(\frac{T_{\text{ove}}}{\bar{\tau}_{\text{id}}} + \frac{T}{\bar{\tau}_{\text{ac}}}\right)\right)$ and $\frac{1}{\Delta\tau} = \frac{1}{\bar{\tau}_{\text{ac}}} - \frac{1}{\bar{\tau}_{\text{id}}}$.

Moreover, we can calculate \mathcal{B}_2 as

$$\mathcal{B}_2 = \mathcal{P}(\mathcal{H}_0) \int_{t_1=T_{\text{ove}}+T_S}^{T_{\text{ove}}+T} \int_{t_2=T_{\text{ove}}+T-t_1}^{\infty} T_2^{01}(t_1) f_{\tau_{\text{id}}}(t_1) f_{\tau_{\text{ac}}}(t_2) dt_1 dt_2, \quad (6.21)$$

where $T_2^{01}(t_1) = \mathcal{P}_f^{00} T_S^{00} + (1 - \mathcal{P}_f^{00})(T_S^{00} + T_D^{01}(\bar{t}_1))$, $T_D^{01}(t_1) = \varphi(T - T_S - \bar{t}_1) \log_2(1 + \gamma_{D2}) + \varphi \bar{t}_1 \log_2(1 + \gamma_{D1})$, and $\bar{t}_1 = t_1 - (T_{\text{ove}} + T_S)$. In this expression, t_1 denotes the interval from the beginning of the CA cycle to the instant when the PU changes to the active state from an idle state. Again, T_S^{00} and T_D^{01} denote the amount of data transmitted in the FD sensing and transmission stages for this case, respectively. After some manipulations, we achieve

$$\begin{aligned} \mathcal{B}_2 = \mathcal{K}_e \frac{\Delta\tau}{\bar{\tau}_{\text{id}}} \left\{ \left(\exp\left(\frac{T}{\Delta\tau}\right) - \exp\left(\frac{T_S}{\Delta\tau}\right) \right) \left[T_S \log_2(1 + \gamma_{S1}) - \varphi \Delta\tau (1 - \mathcal{P}_f^{00}) \log_2\left(\frac{1 + \gamma_{D1}}{1 + \gamma_{D2}}\right) \right] \right. \\ \left. + \varphi(T - T_S) (1 - \mathcal{P}_f^{00}) \left[\exp\left(\frac{T}{\Delta\tau}\right) \log_2(1 + \gamma_{D1}) - \exp\left(\frac{T_S}{\Delta\tau}\right) \log_2(1 + \gamma_{D2}) \right] \right\}. \quad (6.22) \end{aligned}$$

Finally, we can express \mathcal{B}_3 as follows:

$$\mathcal{B}_3 = \mathcal{P}(\mathcal{H}_0) \int_{t_1=T_{\text{ove}}+T_S}^{T_{\text{ove}}+T} \int_{t_2=T_{\text{ove}}+T-t_1}^{\infty} [\mathcal{P}_d^{01}(\bar{t}_1) T_S^{01}(\bar{t}_1) + (1 - \mathcal{P}_d^{01}(\bar{t}_1))(T_S^{01}(\bar{t}_1) + T_D^{11})] f_{\tau_{\text{id}}}(t_1) f_{\tau_{\text{ac}}}(t_2) dt_1 dt_2 \quad (6.23)$$

where $T_S^{01}(\bar{t}_1) = \bar{t}_1 \log_2(1 + \gamma_{S1}) + (T_S - \bar{t}_1) \log_2(1 + \gamma_{S2})$, $T_D^{11} = \varphi(T - T_S) \log_2(1 + \gamma_{D2})$, $\bar{t}_1 = t_1 - T_{\text{ove}}$, and t_1 is the same as in (6.21). Here, T_S^{01} and T_D^{11} denote the amount of data

delivered in the FD sensing and transmission stages for the underlying case, respectively. After some manipulations, we attain

$$\mathcal{B}_3 = \mathcal{K}_e \int_{t=0}^{T_S} [T_S^{01}(t) + T_D^{11} - \mathcal{P}_d^{01}(t) T_D^{11}] f_{\tau_{\text{id}}}(t) \exp\left(\frac{t}{\bar{\tau}_{\text{ac}}}\right) dt = \mathcal{B}_{31} + \mathcal{B}_{32}, \quad (6.24)$$

where

$$\begin{aligned} \mathcal{B}_{31} &= \mathcal{K}_e \int_{t=0}^{T_S} [T_S^{01}(t) + T_D^{11}] f_{\tau_{\text{id}}}(t) \exp\left(\frac{t}{\bar{\tau}_{\text{ac}}}\right) dt \\ &= \mathcal{K}_e \frac{\Delta\tau}{\bar{\tau}_{\text{id}}} \left\{ \Delta\tau \left[\left(\frac{T_S}{\Delta\tau} - 1 \right) \exp\left(\frac{T_S}{\Delta\tau}\right) + 1 \right] \log_2 \left(\frac{1 + \gamma_{S1}}{1 + \gamma_{S2}} \right) \right. \\ &\quad \left. + \left[\exp\left(\frac{T_S}{\Delta\tau}\right) - 1 \right] [T_D^{11} + T_S \log_2(1 + \gamma_{S2})] \right\}, \end{aligned} \quad (6.25)$$

and

$$\mathcal{B}_{32} = -\mathcal{K}_e T_D^{11} \bar{T}_{32}, \quad (6.26)$$

where $\bar{T}_{32} = \int_{t=0}^{T_S} \mathcal{P}_d^{01}(t) f_{\tau_{\text{id}}}(t) \exp\left(\frac{t}{\bar{\tau}_{\text{ac}}}\right) dt$.

6.8.3 False Alarm and Detection Probabilities

We derive the detection and false alarm probabilities for FD sensing and two PU's state-changing events h_{00} and h_{01} in this appendix. Assume that the transmitted signals from the PU and SU are circularly symmetric complex Gaussian (CSCG) signals while the noise at the secondary receiver is independently and identically distributed CSCG $\mathcal{CN}(0, N_0)$ [5]. Under FD sensing, the false alarm probability for event h_{00} can be derived using the similar method as in [5], which is given as

$$\mathcal{P}_f^{00} = \mathcal{Q} \left[\left(\frac{\epsilon}{N_0 + I(P_{\text{sen}})} - 1 \right) \sqrt{f_s T_S} \right], \quad (6.27)$$

where $\mathcal{Q}(x) = \int_x^{+\infty} \exp(-t^2/2) dt$; f_s , N_0 , ϵ , $I(P_{\text{sen}})$ are the sampling frequency, the noise power, the detection threshold and the self-interference, respectively; T_S is the FD sensing duration.

The detection probability for event h_{01} is given as

$$\mathcal{P}_d^{01} = \mathcal{Q} \left(\frac{\left(\frac{\epsilon}{N_0 + I(P_{\text{sen}})} - \frac{T_S - t}{T_S} \gamma_{PS} - 1 \right) \sqrt{f_s T_S}}{\sqrt{\frac{T_S - t}{T_S} (\gamma_{PS} + 1)^2 + \frac{t}{T_S}}} \right), \quad (6.28)$$

where t is the interval from the beginning of the data phase to the instant when the PU changes its state, $\gamma_{PS} = \frac{P_p}{N_0 + I(P_{\text{sen}})}$ is the signal-to-interference-plus-noise ratio (SINR) of the PU's signal at the SU.

6.8.4 Proof of Proposition 1

The first derivative of $\mathcal{N}\mathcal{T}$ can be written as follows:

$$\frac{\partial \mathcal{N}\mathcal{T}}{\partial T_S} = \frac{1}{T_{\text{ove}} + T} \sum_{i=1}^3 \frac{\partial \mathcal{B}_i}{\partial T_S}. \quad (6.29)$$

We derive the first derivative of \mathcal{B}_i ($i = 1, 2, 3$) in the following. Toward this end, we will employ the approximation of $\exp(x) \approx 1+x$, $x = \frac{T_x}{\tau_x}$, $T_x \in \{T, T_S, T - T_S\}$, $\tau_x \in \{\bar{\tau}_{\text{id}}, \bar{\tau}_{\text{ac}}, \Delta\tau\}$ where recall that $\frac{1}{\Delta\tau} = \frac{1}{\bar{\tau}_{\text{ac}}} - \frac{1}{\bar{\tau}_{\text{id}}}$. This approximation holds under the assumption that $T_x \ll \tau_x$ since we can omit all higher-power terms x^n for $n > 1$ from the Maclaurin series expansion of function $\exp(x)$. Using this approximation, we can express the first derivative of \mathcal{B}_1 as

$$\frac{\partial \mathcal{B}_1}{\partial T_S} = \mathcal{K}_e \exp\left(\frac{T}{\Delta\tau}\right) \left\{ \log_2(1+\gamma_{S1}) - \varphi \left[(T - T_S) \frac{\partial \mathcal{P}_f^{00}}{\partial T_S} + (1 - \mathcal{P}_f^{00}) \right] \log_2(1+\gamma_{D1}) \right\} \quad (6.30)$$

where $\frac{\partial \mathcal{P}_f^{00}}{\partial T_S}$ is the first derivative of \mathcal{P}_f^{00} whose derivation is given in Appendix 6.8.5.

Moreover, the first derivative of \mathcal{B}_2 can be written as

$$\begin{aligned} \frac{\partial \mathcal{B}_2}{\partial T_S} = & \mathcal{K}_e \frac{\Delta\tau}{\bar{\tau}_{\text{id}}} \left\{ \left[\exp\left(\frac{T}{\Delta\tau}\right) - \left(1 + \frac{T}{\Delta\tau}\right) \exp\left(\frac{T_S}{\Delta\tau}\right) \right] \log_2(1 + \gamma_{S1}) \right. \\ & - \varphi \frac{\partial \mathcal{P}_f^{00}}{\partial T_S} \left[\Delta\tau \left(\exp\left(\frac{T_S}{\Delta\tau}\right) - \exp\left(\frac{T}{\Delta\tau}\right) \right) \log_2\left(\frac{1+\gamma_{D1}}{1+\gamma_{D2}}\right) \right. \\ & \left. \left. + (T - T_S) \left(\exp\left(\frac{T}{\Delta\tau}\right) \log_2(1+\gamma_{D1}) - \exp\left(\frac{T_S}{\Delta\tau}\right) \log_2(1+\gamma_{D2}) \right) \right] \right. \\ & \left. + \varphi (1 - \mathcal{P}_f^{00}) \left[-\frac{T - T_S}{\Delta\tau} \exp\left(\frac{T_S}{\Delta\tau}\right) \log_2(1 + \gamma_{D2}) + \exp\left(\frac{T_S}{\Delta\tau}\right) \log_2\left(\frac{1 + \gamma_{D1}}{1 + \gamma_{D2}}\right) \right. \right. \\ & \left. \left. - \left(\exp\left(\frac{T}{\Delta\tau}\right) \log_2(1+\gamma_{D1}) - \exp\left(\frac{T_S}{\Delta\tau}\right) \log_2(1+\gamma_{D2}) \right) \right] \right\}. \quad (6.31) \end{aligned}$$

Finally, the first derivative of \mathcal{B}_3 can be written as

$$\frac{\partial \mathcal{B}_3}{\partial T_S} = \frac{\partial \mathcal{B}_{31}}{\partial T_S} + \frac{\partial \mathcal{B}_{32}}{\partial T_S}, \quad (6.32)$$

where

$$\begin{aligned} \frac{\partial \mathcal{B}_{31}}{\partial T_S} = & \mathcal{K}_e \frac{\Delta\tau}{\bar{\tau}_{\text{id}}} \left\{ \Delta\tau \left[1 + \left(\frac{T_S}{\Delta\tau} - 1\right) \exp\left(\frac{T_S}{\Delta\tau}\right) \right] \log_2\left(\frac{1 + \gamma_{S1}}{1 + \gamma_{S2}}\right) \right. \\ & \left. + \left(\exp\left(\frac{T_S}{\Delta\tau}\right) - 1 \right) [T_S \log_2(1 + \gamma_{S2}) + \varphi (T - T_S) \log_2(1 + \gamma_{D2})] \right\}. \quad (6.33) \end{aligned}$$

To obtain the derivative for \mathcal{B}_{32} , we note that $1 \leq \exp\left(\frac{t}{\bar{\tau}_{ac}}\right) \leq \exp\left(\frac{T_S}{\bar{\tau}_{ac}}\right)$ for $\forall t \in [0, T_S]$. Moreover, from the results in (6.5) and (6.6) and using the definition of \bar{T}_{32} in (6.26), we have $\bar{\mathcal{P}}_d\left(1 - \exp\left(\frac{-T_S}{\bar{\tau}_{id}}\right)\right) \leq \bar{T}_{32} \leq \bar{\mathcal{P}}_d\left(1 - \exp\left(\frac{-T_S}{\bar{\tau}_{id}}\right)\right) \exp\left(\frac{T_S}{\bar{\tau}_{ac}}\right)$. Using these results, the first derivative of \mathcal{B}_{32} can be expressed as

$$\frac{\partial \mathcal{B}_{32}}{\partial T_S} = -\mathcal{K}_e \bar{\mathcal{P}}_d \varphi \frac{T - 2T_S}{\bar{\tau}_{id}} \log_2(1 + \gamma_{D2}). \quad (6.34)$$

Therefore, we have obtained the first derivative of $\mathcal{N}\mathcal{J}$ and we are ready to prove the first statement of Theorem 1. Substitute $T_S = 0$ to the derived $\frac{\partial \mathcal{N}\mathcal{J}}{\partial T_S}$ and use the approximation $\exp(x) \approx 1 + x$, we yield the following result after some manipulations

$$\lim_{T_S \rightarrow 0} \frac{\partial \mathcal{N}\mathcal{J}}{\partial T_S} = -K_0 K_1 \lim_{T_S \rightarrow 0} \frac{\partial \mathcal{P}_f^{00}}{\partial T_S}, \quad (6.35)$$

where $K_0 = \frac{1}{T_{\text{ove}} + T} \mathcal{K}_e$ and

$$K_1 = \varphi \left[T \left(1 + \frac{T}{\Delta\tau} \right) + \frac{T^2}{\bar{\tau}_{id}} \right] \log_2(1 + \gamma_{D1}) + \varphi \frac{T \Delta\tau}{\bar{\tau}_{id}} \log_2(1 + \gamma_{D2}). \quad (6.36)$$

It can be verified that $K_0 > 0$, $K_1 > 0$ and $\lim_{T_S \rightarrow 0} \frac{\partial \mathcal{P}_f^{00}}{\partial T_S} = -\infty$ by using the derivations in Appendix 6.8.5; hence, we have $\lim_{T_S \rightarrow 0} \frac{\partial \mathcal{N}\mathcal{J}}{\partial T_S} = +\infty > 0$. This completes the proof of the first statement of the theorem.

We now present the proof for the second statement of the theorem. Substitute $T_S = T$ to $\frac{\partial \mathcal{N}\mathcal{J}}{\partial T_S}$ and utilize the approximation $\exp(x) \approx 1 + x$, we yield

$$\lim_{T_S \rightarrow T} \frac{\partial \mathcal{N}\mathcal{J}}{\partial T_S} = \frac{1}{T_{\text{ove}} + T} \sum_{i=1}^3 \frac{\partial \mathcal{B}_i}{\partial T_S}(T), \quad (6.37)$$

where we have

$$\frac{\partial \mathcal{B}_1}{\partial T_S}(T) = \mathcal{K}_e \left(1 + \frac{T}{\Delta\tau} \right) \left[\log_2(1 + \gamma_{S1}) - \varphi (1 - \mathcal{P}_f^{00}(T)) \log_2(1 + \gamma_{D1}) \right] \quad (6.38)$$

$$\frac{\partial \mathcal{B}_2}{\partial T_S}(T) = -\mathcal{K}_e \frac{T}{\bar{\tau}_{id}} \log_2(1 + \gamma_{S1}) \quad (6.39)$$

$$\frac{\partial \mathcal{B}_{31}}{\partial T_S}(T) = \mathcal{K}_e \frac{T}{\bar{\tau}_{id}} \left[\log_2(1 + \gamma_{S1}) (1 + \gamma_{S2}) - \varphi \log_2(1 + \gamma_{D2}) \right] \quad (6.40)$$

$$\frac{\partial \mathcal{B}_{32}}{\partial T_S}(T) = \mathcal{K}_e \varphi \frac{T}{\bar{\tau}_{id}} \bar{\mathcal{P}}_d \log_2(1 + \gamma_{D2}).$$

Omit all high-power terms in the expansion of $\exp(x)$ (i.e., x^n with $n > 1$) where $x = \frac{T_x}{\tau_x}$, $T_x \in \{T, T_S, T - T_S\}$, $\tau_x \in \{\bar{\tau}_{id}, \bar{\tau}_{ac}, \Delta\tau\}$, we yield

$$\lim_{T_S \rightarrow T} \frac{\partial \mathcal{N}\mathcal{J}}{\partial T_S} \approx \frac{1}{T_{\text{ove}} + T} \frac{\partial \mathcal{B}_1}{\partial T_S}(T). \quad (6.41)$$

We consider the HDTx and FDTx modes in the following. For the HDTx mode, we have $\varphi = 1$ and $\theta = 0$. Then, it can be verified that $\lim_{T_S \rightarrow T} \frac{\partial \mathcal{N}\mathcal{T}}{\partial T_S} < 0$ by using the results in (6.38) and (6.41). This is because we have $\log_2(1 + \gamma_{S1}) - (1 - \mathcal{P}_f^{00}(T)) \log_2(1 + \gamma_{D1}) \approx \log_2(1 + \gamma_{S1}) - \log_2(1 + \gamma_{D1}) < 0$ (since we have $\mathcal{P}_f^{00}(T) \approx 0$ and $\gamma_{S1} \leq \gamma_{D1}$).

For the FDTx mode, we have $\varphi = 2$, $\theta = 1$, and also $\gamma_{S1} = \frac{P_{\text{sen}}}{N_0}$ and $\gamma_{D1} = \frac{P_{\text{dat}}}{N_0 + I(P_{\text{dat}})} = \frac{P_{\text{dat}}}{N_0 + \zeta P_{\text{dat}}^\xi}$. We would like to define a critical value of P_{sen} which satisfies $\lim_{T_S \rightarrow T} \frac{\partial \mathcal{N}\mathcal{T}}{\partial T_S} = 0$ to proceed further. Using the result in (6.38) and (6.41) as well as the approximation $\mathcal{P}_f^{00}(T) \approx 0$, and by solving $\lim_{T_S \rightarrow T} \frac{\partial \mathcal{N}\mathcal{T}}{\partial T_S} = 0$ we yield

$$\bar{P}_{\text{sen}} = N_0 \left[\left(1 + \frac{P_{\text{dat}}}{N_0 + \zeta P_{\text{dat}}^\xi} \right)^2 - 1 \right]. \quad (6.42)$$

Using (6.38), it can be verified that if $P_{\text{sen}} > \bar{P}_{\text{sen}}$ then $\lim_{T_S \rightarrow T} \frac{\partial \mathcal{N}\mathcal{T}}{\partial T_S} > 0$; otherwise, we have $\lim_{T_S \rightarrow T} \frac{\partial \mathcal{N}\mathcal{T}}{\partial T_S} \leq 0$. So we have completed the proof for the second statement of Theorem 1.

To prove the third statement of the theorem, we derive the second derivative of $\mathcal{N}\mathcal{T}$ as

$$\frac{\partial^2 \mathcal{N}\mathcal{T}}{\partial T_S^2} = \frac{1}{T_{\text{ove}} + T} \sum_{i=1}^3 \frac{\partial^2 \mathcal{B}_i}{\partial T_S^2}, \quad (6.43)$$

where we have

$$\frac{\partial^2 \mathcal{B}_1}{\partial T_S^2} = -\mathcal{K}_e \varphi \exp\left(\frac{T}{\Delta\tau}\right) \log_2(1 + \gamma_{D1}) \left[(T - T_S) \frac{\partial^2 \mathcal{P}_f^{00}}{\partial T_S^2} - 2 \frac{\partial \mathcal{P}_f^{00}}{\partial T_S} \right], \quad (6.44)$$

where $\frac{\partial^2 \mathcal{P}_f^{00}}{\partial T_S^2}$ is the second derivative of \mathcal{P}_f^{00} and according to the derivations in Appendix 6.8.5, we have $\frac{\partial^2 \mathcal{P}_f^{00}}{\partial T_S^2} > 0$, $\frac{\partial \mathcal{P}_f^{00}}{\partial T_S} < 0$, $\forall T_S$. Therefore, we yield $\frac{\partial^2 \mathcal{B}_1}{\partial T_S^2} < 0 \forall T_S$.

Consequently, we have the following upper bound for $\frac{\partial^2 \mathcal{B}_1}{\partial T_S^2}$ by omitting the term $\exp\left(\frac{T}{\Delta\tau}\right) > 1$ in (6.44)

$$\frac{\partial^2 \mathcal{B}_1}{\partial T_S^2} \leq \mathcal{K}_e [h_1(T_S) + h_2(T_S)], \quad (6.45)$$

where

$$\begin{aligned} h_1(T_S) &= -\varphi (T - T_S) \frac{\partial^2 \mathcal{P}_f^{00}}{\partial T_S^2} \log_2(1 + \gamma_{D1}), \\ h_2(T_S) &= 2\varphi \frac{\partial \mathcal{P}_f^{00}}{\partial T_S} \log_2(1 + \gamma_{D1}). \end{aligned}$$

Moreover, we have

$$\begin{aligned}
 \frac{\partial^2 \mathcal{B}_2}{\partial T_S^2} &= \frac{\mathcal{K}_e \Delta \tau}{\bar{\tau}_{\text{id}}} \left\{ -\frac{2 + \frac{T_S}{\Delta \tau}}{\Delta \tau} \exp\left(\frac{T_S}{\Delta \tau}\right) \log_2(1 + \gamma_{S1}) \right. \\
 &\quad - \varphi \frac{\partial^2 \mathcal{P}_f^{00}}{\partial T_S^2} \left[\Delta \tau \left(\exp\left(\frac{T_S}{\Delta \tau}\right) - \exp\left(\frac{T}{\Delta \tau}\right) \right) \log_2\left(\frac{1 + \gamma_{D1}}{1 + \gamma_{D2}}\right) \right. \\
 &\quad \left. \left. + (T - T_S) \left(\exp\left(\frac{T}{\Delta \tau}\right) \log_2(1 + \gamma_{D1}) - \exp\left(\frac{T_S}{\Delta \tau}\right) \log_2(1 + \gamma_{D2}) \right) \right] \right. \\
 &\quad \left. + 2\varphi \frac{\partial \mathcal{P}_f^{00}}{\partial T_S} \left[\left(\exp\left(\frac{T}{\Delta \tau}\right) - \exp\left(\frac{T_S}{\Delta \tau}\right) \right) \log_2(1 + \gamma_{D1}) + \frac{T - T_S}{\Delta \tau} \exp\left(\frac{T_S}{\Delta \tau}\right) \log_2(1 + \gamma_{D2}) \right] \right. \\
 &\quad \left. - \varphi (1 - \mathcal{P}_f^{00}) \frac{T - T_S}{\Delta \tau} \exp\left(\frac{T_S}{\Delta \tau}\right) \log_2(1 + \gamma_{D2}) + \varphi (1 - \mathcal{P}_f^{00}) \frac{1}{\Delta \tau} \exp\left(\frac{T_S}{\Delta \tau}\right) \log_2\left(\frac{1 + \gamma_{D1}}{1 + \gamma_{D2}}\right) \right\} \quad (6.46)
 \end{aligned}$$

Therefore, we can approximate $\frac{\partial^2 \mathcal{B}_2}{\partial T_S^2}$ as follows:

$$\frac{\partial^2 \mathcal{B}_2}{\partial T_S^2} = \mathcal{K}_e [h_3(T_S) + h_4(T_S) + h_5(T_S)], \quad (6.47)$$

where

$$\begin{aligned}
 h_3(T_S) &= -\frac{(2 + \frac{T_S}{\Delta \tau})(1 + \frac{T_S}{\Delta \tau})}{\bar{\tau}_{\text{id}}} \log_2(1 + \gamma_{S1}), \\
 h_4(T_S) &= -\varphi (1 - \mathcal{P}_f^{00}) \frac{T - T_S}{\bar{\tau}_{\text{id}}} \left(1 + \frac{T_S}{\Delta \tau} \right) \log_2(1 + \gamma_{D2}) \\
 &\quad - \varphi \frac{\partial^2 \mathcal{P}_f^{00}}{\partial T_S^2} (T - T_S) \left[\frac{T}{\bar{\tau}_{\text{id}}} \log_2(1 + \gamma_{D1}) - \frac{T_S}{\bar{\tau}_{\text{id}}} \log_2(1 + \gamma_{D2}) \right] \\
 &\quad + 2\varphi \frac{\partial \mathcal{P}_f^{00}}{\partial T_S} \frac{T - T_S}{\bar{\tau}_{\text{id}}} \left[\log_2\left(\frac{1 + \gamma_{D1}}{1 + \gamma_{D2}}\right) + \frac{T_S}{\Delta \tau} \log_2(1 + \gamma_{D2}) \right], \\
 h_5(T_S) &= \varphi (1 - \mathcal{P}_f^{00}) \frac{1}{\bar{\tau}_{\text{id}}} \left(1 + \frac{T_S}{\Delta \tau} \right) \log_2\left(\frac{1 + \gamma_{D1}}{1 + \gamma_{D2}}\right).
 \end{aligned}$$

In addition, we have

$$\begin{aligned}
 \frac{\partial^2 \mathcal{B}_{31}}{\partial T_S^2} &= \frac{\mathcal{K}_e}{\bar{\tau}_{\text{id}}} \exp\left(\frac{T_S}{\Delta \tau}\right) \left\{ \left(1 + \frac{T}{\Delta \tau} \right) \log_2(1 + \gamma_{S1}) \right. \\
 &\quad \left. + \log_2(1 + \gamma_{S2}) + \varphi \left(\frac{T - T_S}{\Delta \tau} - 2 \right) \log_2(1 + \gamma_{D2}) \right\}. \quad (6.48)
 \end{aligned}$$

We can approximate $\frac{\partial^2 \mathcal{B}_{31}}{\partial T_S^2}$ as follows:

$$\frac{\partial^2 \mathcal{B}_{31}}{\partial T_S^2} = \mathcal{K}_e [h_6(T_S) + h_6(T_S)], \quad (6.49)$$

where

$$\begin{aligned} h_6(T_S) &= \frac{1}{\bar{\tau}_{\text{id}}} \log_2(1 + \gamma_{S1})(1 + \gamma_{S2}), \\ h_7(T_S) &= -\frac{2\varphi}{\bar{\tau}_{\text{id}}} \log_2(1 + \gamma_{D2}). \end{aligned} \quad (6.50)$$

Finally, we have

$$\frac{\partial^2 \mathcal{B}_{32}}{\partial T_S^2} = \mathcal{K}_e h_8(T_S), \quad (6.51)$$

where

$$h_8(T_S) = \frac{2\varphi \bar{\mathcal{P}}_d}{\bar{\tau}_{\text{id}}} \log_2(1 + \gamma_{D2}). \quad (6.52)$$

The above analysis yields $\frac{\partial^2 \mathcal{N}\mathcal{I}}{\partial T_S^2} = \mathcal{K}_e \sum_{i=1}^8 h_i(T_S)$. Therefore, to prove that $\frac{\partial^2 \mathcal{N}\mathcal{I}}{\partial T_S^2} < 0$, we should prove that $h(T_S) < 0$ since $\mathcal{K}_e > 0$ where

$$h(T_S) = \sum_{i=1}^8 h_i(T_S). \quad (6.53)$$

It can be verified that $h_1(T_S) < 0$ and $h_4(T_S) < 0, \forall T_S$ because $\frac{\partial^2 \mathcal{P}_f^{00}}{\partial T_S^2} > 0, \frac{\partial \mathcal{P}_f^{00}}{\partial T_S} < 0$ according to Appendix 6.8.5 and $\gamma_{D2} < \gamma_{D1}$. Moreover, we have

$$h_3(T_S) < -\frac{2}{\bar{\tau}_{\text{id}}} \log_2(1 + \gamma_{S1}), \quad (6.54)$$

and because $\gamma_{S1} > \gamma_{S2}$, we have

$$h_3(T_S) < -\frac{1}{\bar{\tau}_{\text{id}}} \log_2(1 + \gamma_{S1})(1 + \gamma_{S2}) = -h_6(T_S). \quad (6.55)$$

Therefore, we have $h_3(T_S) + h_6(T_S) < 0$. Furthermore, we can also obtain the following result $h_7(T_S) + h_8(T_S) \leq 0$ because $\bar{\mathcal{P}}_d \leq 1$. To complete the proof, we must prove that $h_2(T_S) + h_5(T_S) \leq 0$, which is equivalent to

$$-2\bar{\tau}_{\text{id}} \frac{\partial \mathcal{P}_f^{00}}{\partial T_S} \frac{\log_2(1 + \gamma_{D1})}{\log_2\left(\frac{1 + \gamma_{D1}}{1 + \gamma_{D2}}\right)} \geq (1 - \mathcal{P}_f^{00}) \left(1 + \frac{T_S}{\Delta\tau}\right), \quad (6.56)$$

where according to Appendix 6.8.5

$$\frac{\partial \mathcal{P}_f^{00}}{\partial T_S} = -\frac{\bar{\gamma} \sqrt{f_s T_S}}{2\sqrt{2\pi} T_S} \exp\left(-\frac{(\bar{\alpha} + \bar{\gamma} \sqrt{f_s T_S})^2}{2}\right), \quad (6.57)$$

where $\bar{\alpha} = (\bar{\gamma}_1 + 1) \mathcal{Q}^{-1}(\bar{\mathcal{P}}_d)$. It can be verified that (6.56) indeed holds because the LHS of (6.56) is always larger than 2 while the RHS of (6.56) is always less than 2. Hence, we have completed the proof of the third statement of Theorem 1.

Finally, the fourth statement in the theorem obviously holds because \mathcal{B}_i ($i = 1, 2, 3$) are all bounded from above. Hence, we have completed the proof of Theorem 1.

6.8.5 Approximation of \mathcal{P}_f^{00} and Its First and Second Derivatives

We can approximate $\hat{\mathcal{P}}_d$ in (6.5) as follows:

$$\hat{\mathcal{P}}_d = \mathcal{Q} \left[\left(\frac{\epsilon}{N_0 + I} - \bar{\gamma} - 1 \right) \frac{\sqrt{f_s T_S}}{\bar{\gamma}_1 + 1} \right], \quad (6.58)$$

where $\bar{\gamma}$ and $\bar{\gamma}_1$ are evaluated by a numerical method. Hence, \mathcal{P}_f^{00} can be calculated as we set $\hat{\mathcal{P}}_d = \bar{\mathcal{P}}_d$, which is given as follows:

$$\mathcal{P}_f^{00} = \mathcal{Q} \left(\bar{\alpha} + \bar{\gamma} \sqrt{f_s T_S} \right), \quad (6.59)$$

where $\bar{\alpha} = (\bar{\gamma}_1 + 1) \mathcal{Q}^{-1}(\bar{\mathcal{P}}_d)$.

We now derive the first derivative of \mathcal{P}_f^{00} as

$$\frac{\partial \mathcal{P}_f^{00}}{\partial T_S} = -\frac{\bar{\gamma} \sqrt{f_s T_S}}{2\sqrt{2\pi} T_S} \exp \left(-\frac{(\bar{\alpha} + \bar{\gamma} \sqrt{f_s T_S})^2}{2} \right). \quad (6.60)$$

It can be seen that $\frac{\partial \mathcal{P}_f^{00}}{\partial T_S} < 0$ since $\bar{\gamma} > 0$. Moreover, the second derivative of \mathcal{P}_f^{00} is

$$\frac{\partial^2 \mathcal{P}_f^{00}}{\partial T_S^2} = \frac{\bar{\gamma} \sqrt{f_s T_S}}{4\sqrt{2\pi} T_S^2} \left(1 + \frac{1}{2} y \bar{\gamma} \sqrt{f_s T_S} \right) \exp \left(-\frac{y^2}{2} \right), \quad (6.61)$$

where $y = \bar{\alpha} + \bar{\gamma} \sqrt{f_s T_S}$.

We can prove that $\frac{\partial^2 \mathcal{P}_f^{00}}{\partial T_S^2} > 0$ by considering two different cases as follows. For the first case with $\frac{\bar{\alpha}^2}{\bar{\gamma}^2 f_s} \leq T_S \leq T$ ($0 \leq \mathcal{P}_f^{00} \leq 0.5$), this statement holds since $y > 0$. For the second case with $0 \leq T_S \leq \frac{\bar{\alpha}^2}{\bar{\gamma}^2 f_s}$ ($0.5 \leq \mathcal{P}_f^{00} \leq 1$), $y \leq 0$, then we have $0 < y - \bar{\alpha} = \bar{\gamma} \sqrt{f_s T_S} \leq -\bar{\alpha}$ and $0 \leq -y \leq -\bar{\alpha}$. By applying the Cauchy-Schwarz inequality, we obtain $0 \leq -y(y - \bar{\alpha}) \leq \frac{\bar{\gamma}^2}{4} < 1 < 2$; hence $1 + \frac{1}{2} y \bar{\gamma} \sqrt{f_s T_S} > 0$. This result implies that $\frac{\partial^2 \mathcal{P}_f^{00}}{\partial T_S^2} > 0$.

Chapter 7

Conclusions and Further Works

Although cognitive radio technology is an important paradigm shift to solve the spectrum scarcity problem for future wireless networks, many challenges remain to be resolved to achieve the benefits offered by this technology. Our dissertation focuses on the design, analysis, and optimization of joint spectrum sensing and access design for CRNs under different practically relevant network settings. The developed techniques enable a CRN to efficiently exploit idle spectrum over time, frequency, and space for data transmission. In this chapter, we summarize our research contributions and discuss some future research directions.

7.1 Major Research Contributions

We have developed three different CMAC design frameworks addressing different network scenarios for HD CRNs as well as an adaptive FDC-MAC framework for FD CRNs. These research outcomes have been resulted in three journal publications [22, 33], [37] and its corresponding conference publications [35, 38–41] as well as one journal under submission [37].

In the first contribution, we have proposed the MAC protocols for CRNs with parallel sensing that explicitly take into account spectrum-sensing operation and imperfect sensing performance. In addition, we have performed throughput analysis for the proposed MAC protocols and determined their optimal configurations for throughput maximization. These studies have been conducted for both single- and multiple-channel scenarios subject to protection constraints for primary receivers.

In the second contribution, we have investigated the MAC protocol design, analysis, and channel assignment issues for CRNs with sequential sensing. For the channel assignment, we have presented the optimal brute-force and low-complexity algorithms and analyzed their complexity. In particular, we have developed two greedy channel assignment algorithms for throughput maximization, namely non-overlapping and overlapping channel assignment algorithms. In addition, we have proposed an analytical model to quantify the saturation throughput of the overlapping channel assignment algorithm. We have also presented several potential extensions including the design of max-min fair channel assignment algorithms and consideration of imperfect spectrum sensing.

In the third contribution, we study a general SDCSS and access framework for the heterogeneous cognitive environment where channel statistics and spectrum holes on different channels can be arbitrary. Moreover, no central controller is required to collect sensing results and make spectrum sensing decisions. In particular, the design is based on the distributed p -persistent CSMA protocol incorporating SDCSS for multi-channel CRNs. We have performed saturation throughput analysis and optimization of spectrum sensing time and access parameters to achieve the maximum throughput for a given allocation of channel sensing sets. Afterward we have studied the channel sensing set optimization (i.e., channel assignment) for throughput maximization and investigated both exhaustive search and low-complexity greedy algorithms to solve the underlying optimization problem. Then we have extended the design and analysis to consider reporting errors during the exchanges of spectrum sensing results.

In the last contribution, we have proposed the FDC-MAC protocol for FD CRNs, analyzed its throughput performance, and studied its optimal parameter configuration. The design and analysis take into account the FD communication capability and the self-interference of the FD transceiver. In particular, SUs employ the standard p -persistent CSMA mechanism for contention resolution then the winning SU performs simultaneous sensing and transmission during the sensing stage and transmission only in the transmission stage. We have also shown that there exists an optimal FD sensing time to achieve the maximum throughput. Moreover, we have proposed an algorithm to configure different design parameters including SU's transmit power and sensing time to achieve the maximum throughput.

7.2 Further Research Directions

Our research work in this dissertation focuses on the MAC protocol for efficient media sharing and QoS provisioning in CRNs. The following research directions are of importance and deserve further investigation.

7.2.1 Multi-channel MAC protocol design for FD CRNs

The MAC protocol design for FD CRNs was proposed for the single-channel scenario in Chapter 6 where it has been shown to deliver excellent and flexible performance tradeoffs for FD CRNs [35, 36]. This proposed FDC-MAC protocol design is more general and flexible than existing MAC protocols for FD CRNs. However, engineering the multi-channel FD CMAC design is more challenging, which will be pursued in the future. Moreover, we will also consider the channel assignment problem for FD CRNs.

7.2.2 CMAC and routing design for multi-hop HD and FD CRNs

Routing protocol design for HD and FD CRNs presents many interesting open problems to address. In the multi-hop communication environments with spectrum heterogeneity, cross-layer design for CMAC and routing deserves further investigations. In particular, development of suitable coordination and spectrum sensing schemes to manage interference among concurrent SUs' transmissions, efficiently exploit spectrum holes, and protect PUs for HD CRNs and FD CRNs is a good direction for further research. Finally, study of channel assignment is also a promising research direction in multi-hop CRNs.

7.2.3 Applications of cognitive radio networking techniques for smartgrids

We plan to investigate the joint cognitive protocol and data processing design for the smart-grid application. We are particularly interested in exploiting potential sparsity structure of the smartgrid data so that the data can be compressed before being transmitted over the smartgrid communication networks [135, 136]. This is quite expected since many types of smartgrid data can be very correlated over both space and time. Here, existing techniques developed in the compressed sensing field can be applied for processing the smartgrid data [42–44]. Cognitive network protocols employed to deliver smartgrid data can further degrade

the communication performance due to access collisions and the intermittent nature of spectrum holes. Therefore, joint design of cognitive protocols and data processing algorithms is important to ensure the desirable end-to-end QoS performance.

7.3 List of publication

Journals:

[J1] L. T. Tan, and L. B. Le, “Design and Optimal Configuration of Full-Duplex MAC Protocol for Cognitive Radio Networks Considering Self-Interference,” submitted.

[J2] L. T. Tan, and L. B. Le, “Joint Data Compression and MAC Protocol Design for Smartgrids with Renewable Energy,” submitted.

[J3] L. T. Tan, and L. B. Le, “Joint Cooperative Spectrum Sensing and MAC Protocol Design for Multi-channel Cognitive Radio Networks,” *EURASIP Journal on Wireless Communications and Networking*, 2014 (101), June 2014.

[J4] L. T. Tan, and L. B. Le, “Channel Assignment with Access Contention Resolution for Cognitive Radio Networks,” *IEEE Transactions on Vehicular Technology*, vol. 61, no. 6, pp. 2808–2823, July 2012.

[J5] L. T. Tan, and L. B. Le, “Distributed MAC Protocol for Cognitive Radio Networks: Design, Analysis, and Optimization,” *IEEE Transactions on Vehicular Technology*, vol. 60, no. 8, pp. 3990–4003, Oct. 2011

Conferences:

[C1] L. T. Tan and L. B. Le, “Distributed MAC Protocol Design for Full-Duplex Cognitive Radio Networks,” in *2015 IEEE Global Communications Conference (IEEE GLOBECOM 2015)*, San Diego, CA, USA, Dec. 2015.

[C2] L. T. Tan and L. B. Le, “Compressed Sensing Based Data Processing and MAC Protocol Design for Smartgrids,” in *2015 IEEE Wireless Communication and Networking Conference (IEEE WCNC 2015)*, New Orleans, LA USA, pp. 2138 - 2143, March 2015.

[C3] L. T. Tan, and L. B. Le, “General Analytical Framework for Cooperative Sensing and Access Trade-off Optimization,” in *2013 IEEE Wireless Communication and Networking Conference (IEEE WCNC 2013)*, Shanghai, China, pp. 1697 - 1702, April 2013.

[C4] L. T. Tan, and L. B. Le, “Fair Channel Allocation and Access Design for Cognitive Ad Hoc Networks,” in *2012 IEEE Global Communications Conference (IEEE GLOBECOM 2012)*, Anaheim, California, USA, pp. 1162 - 1167, Dec. 2012.

- [C5] L. T. Tan, and L. B. Le, “Channel Assignment for Throughput Maximization in Cognitive Radio Networks,” in *2012 IEEE Wireless Communications and Networking Conference (IEEE WCNC 2012)*, Paris, France, pp. 1427-1431, April 2012.

Chapter 8

Appendix

8.1 Channel Assignment for Throughput Maximization in Cognitive Radio Networks

The content of this appendix was published in *Proc. IEEE WCNC'2012* in the following paper:

L. T. Tan, and L. B. Le, “Channel Assignment for Throughput Maximization in Cognitive Radio Networks,” in *Proc. IEEE WCNC'2012*, Paris, France, pp. 1427–1431, April 2012.

8.2 Fair Channel Allocation and Access Design for Cognitive Ad Hoc Networks

The content of this appendix was published in *Proc. IEEE GLOBECOM'2012* in the following paper:

L. T. Tan, and L. B. Le, “Fair Channel Allocation and Access Design for Cognitive Ad Hoc Networks,” in *Proc. IEEE GLOBECOM'2012*, Anaheim, California, USA, pp. 1162–1167, December 2012.

8.3 General Analytical Framework for Cooperative Sensing and Access Trade-off Optimization

The content of this appendix was published in *Proc. IEEE WCNC'2013* in the following paper:

L. T. Tan, and L. B. Le, “General Analytical Framework for Cooperative Sensing and Access Trade-off Optimization,” in *Proc. IEEE WCNC'2013*, Shanghai, China, pp. 1697–1702, April 2013.

8.4 Distributed MAC Protocol Design for Full-Duplex Cognitive Radio Networks

The content of this appendix was published in *Proc. IEEE GLOBECOM'2015* in the following paper:

L. T. Tan, and L. B. Le, “Distributed MAC Protocol Design for Full-Duplex Cognitive Radio Networks,” in *Proc. IEEE GLOBECOM'2015*, San Diego, CA, USA, December, 2015.

References

- [1] D. DATLA, A. M. WYGLINSKI, AND G. J. MINDEN. **A spectrum surveying framework for dynamic spectrum access networks.** *IEEE Trans. Veh. Tech.*, **58**(8):4158–4168, Oct 2009. 1
- [2] Q. ZHAO AND B. M. SADLER. **A Survey of dynamic spectrum access.** *IEEE Signal Processing Mag.*, **24**(3):79–89, May 2007. xi, 1, 2, 3, 35, 68, 106, 142
- [3] A. GOLDSMITH, S. A. JAFAR, I. MARIC, AND S. SRINIVASA. **Breaking spectrum gridlock with cognitive radios: An information theoretic perspective.** *Proc. IEEE*, **97**(5):894–914, May 2009. xi, 2, 4, 5
- [4] J. M. III. **An integrated agent architecture for software defined radio.** 2000. 1, 3
- [5] Y. C. LIANG, Y. ZENG, E. C. Y. PEH, AND A. T. HOANG. **Sensing-throughput tradeoff for cognitive radio networks.** *IEEE Trans. Wireless Commun.*, **7**(4):1326–1337, April 2008. 1, 10, 14, 15, 30, 35, 37, 39, 68, 70, 82, 106, 112, 122, 142, 152, 164
- [6] D. N. HATFIELD AND P. J. WEISER. **Property rights in spectrum: taking the next step.** In *Proc. IEEE DySPAN'2005*, pages 43–55, Nov 2005. 3
- [7] L. XU, R. TONJES, T. PAILA, W. HANSMANN, M. FRANK, AND M. ALBRECHT. **Drive-ing to the internet: Dynamic radio for IP services in vehicular environments.** In *Proc. IEEE LCN'2000*, pages 281–289, 2000. 3
- [8] W. LEHR AND J. CROWCROFT. **Managing shared access to a spectrum commons.** In *Proc. IEEE DySPAN'2005*, pages 420–444, Nov 2005. 3
- [9] C. RAMAN, R. D. YATES, AND N. B. MANDAYAM. **Scheduling variable rate links via a spectrum server.** In *Proc. IEEE DySPAN'2005*, pages 110–118, Nov 2005. 3
- [10] J. HUANG, R. A. BERRY, AND M. L. HONIG. **Spectrum sharing with distributed interference compensation.** In *Proc. IEEE DySPAN'2005*, pages 88–93, Nov 2005. 3
- [11] L. B. LE AND E. HOSSAIN. **Resource allocation for spectrum underlay in cognitive radio networks.** *IEEE Trans. Wireless Commun.*, **7**(12):5306–5315, Dec. 2008. 4, 30, 35, 36, 68
- [12] D. I. KIM, L. B. LE, AND E. HOSSAIN. **Joint rate and power allocation for cognitive radios in dynamic spectrum access environment.** *IEEE Trans. Wireless Commun.*, **7**(12):5517–5527, Dec. 2008. 4, 30, 35, 36
- [13] A. OZGUR, O. LEVEQUE, AND D. N. C. TSE. **Hierarchical cooperation achieves optimal capacity scaling in ad hoc networks.** *IEEE Trans. Inf. Theory*, **53**(10):3549–3572, Oct 2007. 4
- [14] Y. ZUO, Y. D. YAO, AND B. ZHENG. **Cognitive transmissions with multiple relays in cognitive radio networks.** *IEEE Trans. Wireless Commun.*, **10**(2):648–659, February 2011. 37
- [15] Y. ZUO, Y. D. YAO, AND B. ZHENG. **Outage probability analysis of cognitive transmissions: Impact of spectrum sensing overhead.** *IEEE Trans. Wireless Commun.*, **9**(8):2676–2688, Aug. 2010. 4, 37, 40
- [16] H. KIM AND K. G. SHIN. **Efficient discovery of spectrum opportunities with MAC-layer sensing in cognitive radio networks.** *IEEE Trans. Mobile Comput.*, **7**(5):533–545, May 2008. 4, 5, 7, 31, 32, 36, 70, 106, 142
- [17] H. SU AND X. ZHANG. **Cross-layer based opportunistic MAC protocols for QoS provisionings over cognitive radio wireless networks.** *IEEE J. Sel. Areas Commun.*, **26**(1):118–129, Jan. 2008. 5, 7, 32, 70, 106
- [18] H. SU AND X. ZHANG. **Opportunistic MAC protocols for cognitive radio based wireless networks.** *Proc. CISS'2007*, pages 363–368, 2007. 5, 32, 70, 106
- [19] H. NAN, T. I. HYON, AND S. J. YOO. **Distributed coordinated spectrum sharing MAC protocol for cognitive radio.** *Proc. IEEE DySPAN' 2007*, pages 240–249, 2007. 7, 32, 106
- [20] C. CORDEIRO AND K. CHALLAPALI. **C-MAC: A cognitive MAC protocol for multi-channel wireless networks.** *Proc. IEEE DySPAN'2007*, pages 147–157, 2007.

- [21] A. C. C. HSU, D. S. L. WEIT, AND C. C. J. KUO. **A cognitive MAC protocol using statistical channel allocation for wireless ad-hoc networks.** *Proc. IEEE WCNC'2007*, pages 1525–3511, 2007. 7, 32, 36, 70
- [22] L. T. TAN AND L. B. LE. **Distributed MAC protocol for cognitive radio networks: Design, analysis, and optimization.** *IEEE Trans. Veh. Tech.*, **60**(8):3990–4003, Oct. 2011. 10, 70, 76, 77, 106, 121, 122, 142, 149, 152, 171
- [23] W. WANG, K. G. SHIN, AND W. WANG. **Joint spectrum allocation and power control for multihop cognitive radio networks.** *IEEE Trans. Mobile Comput.*, **10**(7):1042–1055, July 2011. 71, 107
- [24] X. ZHANG AND H. SU. **Opportunistic spectrum sharing schemes for CDMA-based uplink MAC in cognitive radio networks.** *IEEE J. Sel. Areas Commun.*, **29**(4):716–730, April 2011. 71, 107
- [25] Y. J. CHOI AND K. G. SHIN. **Opportunistic access of TV spectrum using cognitive-radio-enabled cellular networks.** *IEEE Trans. Veh. Tech.*, **60**(8):3853–3864, Oct. 2011. 71, 107
- [26] X. ZHANG AND H. SU. **CREAM-MAC: Cognitive radio-enabled multi-channel MAC protocol over dynamic spectrum access networks.** *IEEE J. Sel. Topics Signal Process.*, **5**(1):110–123, Feb. 2011. 6, 8, 32, 71, 107
- [27] M. TIMMERS, S. POLLIN, A. DEJONGHE, L. VAN DER PERRE, AND F. CATTHOOR. **A distributed multi-channel MAC protocol for multihop cognitive radio networks.** *IEEE Trans. Veh. Tech.*, **59**(1):446–459, Jan. 2010. 71
- [28] W. JEON, J. HAN, AND D. JEONG. **A novel MAC scheme for multi-channel cognitive radio ad hoc networks.** *IEEE Trans. Mobile Comput.*, **11**(6):922–934, June 2012. 71
- [29] S. C. JHA, U. PHUYAL, M. M. RASHID, AND V. K. BHARGAVA. **Design of OMC-MAC: An opportunistic multi-channel MAC with QoS provisioning for distributed cognitive radio networks.** *IEEE Trans. Wireless Commun.*, **10**(10):3414–3425, Oct. 2011. 71
- [30] H. SU AND X. ZHANG. **Channel-hopping based single transceiver MAC for cognitive radio networks.** *Proc. IEEE CISS'2008*, pages 197–202, 2008. 5, 71, 95
- [31] J. MO, H. SO, AND J. WALRAND. **Comparison of multichannel MAC protocols.** *IEEE Trans. Mobile Comput.*, **7**(1):50–65, Jan. 2008. xi, 26, 27, 28, 95, 116
- [32] G. KO, A. FRANKLIN, S. J. YOU, J. S. PAK, M. S. SONG, AND C. J. KIM. **Channel management in IEEE 802.22 WRAN systems.** *IEEE Commun. Mag.*, **48**(9):88–94, Sept. 2010. 98
- [33] L. T. TAN AND L. B. LE. **Channel assignment with access contention resolution for cognitive radio networks.** *IEEE Trans. Veh. Tech.*, **61**(6):2808–2823, July 2012. 10, 106, 121, 125, 142, 149, 171
- [34] J. PARK, P. PAWELCZAK, AND D. CABRIC. **Performance of joint spectrum sensing and mac algorithms for multichannel opportunistic spectrum access ad hoc networks.** *IEEE Trans. Mobile Comput.*, **10**(7):1011–1027, July 2011. 5, 8, 31, 32, 107
- [35] L. T. TAN AND L. B. LE. **Distributed MAC protocol design for full-duplex cognitive radio networks.** *Proc. IEEE GLOBECOM'2015*, 2015. 11, 33, 143, 148, 149, 157, 158, 160, 171, 173
- [36] L. T. TAN AND L. B. LE. **Design and optimal configuration of full-duplex MAC protocol for cognitive radio networks considering self-interference.** *submitted*, 2015. 10, 173
- [37] L. T. TAN AND L. B. LE. **Joint cooperative spectrum sensing and MAC protocol design for multi-channel cognitive radio networks.** *EURASIP Journal on Wireless Communications and Networking*, **2014**(1):1–21, 2014. 5, 10, 171
- [38] L. T. TAN AND L. B. LE. **Channel assignment for throughput maximization in cognitive radio networks.** In *Proc. IEEE WCNC'2012*, pages 1427–1431, April 2012. 171
- [39] L. T. TAN AND L. B. LE. **Fair channel allocation and access design for cognitive ad hoc networks.** In *Proc. IEEE GLOBECOM'2012*, pages 1162–1167, Dec 2012. 10
- [40] L. T. TAN AND L. B. LE. **General analytical framework for cooperative sensing and access trade-off optimization.** In *Proc. IEEE WCNC'2013*, pages 1697–1702, April 2013. 10
- [41] L. T. TAN AND L. B. LE. **Compressed sensing based data processing and MAC protocol design for smartgrids.** In *Proc. IEEE WCNC'2015*, pages 2138–2143, March 2015. 171

- [42] L. T. TAN, H. Y. KONG, AND V. N. Q. BAO. **Projected Barzilai-Borwein methods applied to distributed compressive spectrum sensing.** *Proc. IEEE DySPAN 2010*, pages 1–7, April 2010. 15, 173
- [43] L. T. TAN AND H. Y. KONG. **A novel and efficient mixed-signal compressed sensing for wide-band cognitive radio.** *Proc. IFOST 2010*, pages 27–32, Oct. 2010.
- [44] L. T. TAN AND H. Y. KONG. **Using subspace pursuit algorithm to improve performance of the distributed compressive wide-band spectrum sensing.** *Journal of Electromagnetic Engineering And Science*, **11(4)**:250–256, 2011. 15, 173
- [45] T. Q. DUONG, T. T. LE, AND H. ZEPERNICK. **Performance of cognitive radio networks with maximal ratio combining over correlated rayleigh fading.** In *Proc. IEEE ICCE'2010*, pages 65–69, Aug 2010. 15, 18
- [46] L. T. TAN, J. H. LEE, AND H. Y. KONG. **Primary user detection using a generalized selection combining over rayleigh fading channel.** *International Journal of Internet, Broadcasting and Communication*, **2(2)**:1–3, 2010. 4, 5, 15, 18
- [47] C. CORMIOB AND K. R. CHOWDHURYA. **A survey on MAC protocols for cognitive radio networks.** *Elsevier Ad Hoc Networks*, **7(7)**:1315–1329, Sept. 2009. 5, 6, 29, 31, 36, 70, 106, 142
- [48] T. YUCEK AND H. ARSLAN. **A survey of spectrum sensing algorithms for cognitive radio applications.** *IEEE Commun. Surveys Tuts.*, **11(1)**:116–130, First Quarter 2009. 5, 12, 31, 36, 68, 82, 142
- [49] M. DUARTE, C. DICK, AND A. SABHARWAL. **Experiment-driven characterization of full-duplex wireless systems.** *IEEE Trans. Wireless Commun.*, **11(12)**:4296–4307, December 2012. 5, 8, 33, 143, 145
- [50] E. EVERETT, A. SAHAI, AND A. SABHARWAL. **Passive self-interference suppression for full-duplex infrastructure nodes.** *IEEE Trans. Wireless Commun.*, **13(2)**:680–694, February 2014. 143
- [51] A. SABHARWAL, P. SCHNITER, D. GUO, D. W. BLISS, S. RANGARAJAN, AND R. WICHMAN. **In-band full-duplex wireless: challenges and opportunities.** *IEEE J. Sel. Areas Commun.*, **32(9)**:1637–1652, Sept 2014. 8, 33
- [52] D. KORPI, L. ANTTILA, V. SYRJALA, AND M. VALKAMA. **Widely linear digital self-interference cancellation in direct-conversion full-duplex transceiver.** *IEEE J. Sel. Areas Commun.*, **32(9)**:1674–1687, Sept 2014. 143
- [53] M. JAIN, J. I. CHOI, T. KIM, D. BHARADIA, S. SETH, K. SRINIVASAN, P. LEVIS, S. KATTI, AND P. SINHA. **Practical, real-time, full duplex wireless.** In *Proc. ACM MobiCom'2011*, MobiCom'11, pages 301–312, New York, NY, USA, 2011. ACM. 143
- [54] J. I. CHOI, M. JAIN, K. SRINIVASAN, P. LEVIS, AND S. KATTI. **Achieving single channel, full duplex wireless communication.** In *Proc. ACM MobiCom'2010*, pages 1–12. ACM, 2010. 5, 143
- [55] W. AFIFI AND M. KRUNZ. **Incorporating self-interference suppression for full-duplex operation in opportunistic spectrum access systems.** *IEEE Trans. Wireless Commun.*, **14(4)**:2180–2191, April 2015. 5, 8, 33
- [56] W. CHENG, X. ZHANG, AND H. ZHANG. **Full-duplex spectrum-sensing and MAC-protocol for multichannel nontime-slotted cognitive radio networks.** *IEEE J. Sel. Areas Commun.*, **33(5)**:820–831, May 2015. 5, 9, 33
- [57] S. HAYKIN. **Cognitive radio: brain-empowered wireless communications.** *IEEE J. Sel. Areas Commun.*, **23(2)**:201–220, Feb 2005. 6, 15
- [58] D. CABRIC, S. M. MISHRA, AND R. W. BRODERSEN. **Implementation issues in spectrum sensing for cognitive radios.** In *Proc. Asilomar Conf. on Signals, Systems and Computers 2004*, **1**, pages 772–776 Vol.1, Nov 2004. 15
- [59] L. GAVRILOVSKA, D. DENKOVSKI, V. RAKOVIC, AND M. ANGJELICHINOSKI. **Medium access control protocols in cognitive radio networks: Overview and general classification.** *IEEE Commun. Surveys Tuts.*, **16(4)**:2092–2124, Fourthquarter 2014. xi, 29, 30, 31
- [60] E. AHMED, A. GANI, S. ABOLFAZLI, L. J. YAO, AND S. U. KHAN. **Channel assignment algorithms in cognitive radio networks: Taxonomy, open issues, and challenges.** *IEEE Commun. Surveys Tuts.*, **PP(99)**:1–1, 2014. 6, 31
- [61] L. MA, X. HAN, AND C. C. SHEN. **Dynamic open spectrum sharing MAC protocol for wireless ad hoc networks.** In *Proc. IEEE DySPAN 2005*, pages 203–213, Nov 2005. 6

- [62] Y. R. KONDAREDDY AND P. AGRAWAL. **Synchronized MAC protocol for multi-hop cognitive radio networks.** *Proc. IEEE ICC'2008*, pages 3198–3202, 2008. 6, 31, 36, 39, 70, 106, 115, 142
- [63] L. LE AND E. HOSSAIN. **OSA-MAC: A MAC protocol for opportunistic spectrum access in cognitive radio networks.** *Proc. IEEE WCNC'2008*, pages 1426–1430, 2008. 7, 31, 32, 70, 106
- [64] G. GANESAN AND Y. LI. **Cooperative spectrum sensing in cognitive radio. Part I: Two user networks.** *IEEE Trans. Wireless Commun.*, **6**(6):2204–2213, Jun. 2007. 7, 31, 107
- [65] G. GANESAN AND Y. LI. **Cooperative spectrum sensing in cognitive radio, part II: Multiuser networks.** *IEEE Trans. Wireless Commun.*, **6**(6):2214–2222, June 2007. 7
- [66] S. CHAUDHARI, J. LUNDEN, V. KOIVUNEN, AND H. V. POOR. **Cooperative sensing with imperfect reporting channels: Hard decisions or soft decisions?** *IEEE Trans. Signal Process.*, **60**(1):18–28, Jan 2012. 7, 15, 31, 107
- [67] J. W. LEE. **Cooperative spectrum sensing scheme over imperfect feedback channels.** *IEEE Commun. Lett.*, **17**(6):1192–1195, June 2013. 7, 31, 107
- [68] H. B. SALAMEH, M. KRUNZ, AND O. YOUNIS. **Cooperative adaptive spectrum sharing in cognitive radio networks.** *IEEE/ACM Trans. Netw.*, **18**(4):1181–1194, Aug. 2010. 8, 31, 32, 71, 106
- [69] S. J. KIM AND G. B. GIANNAKIS. **Sequential and cooperative sensing for multi-channel cognitive radios.** *IEEE Trans. Signal Process.*, **58**(8):4239–4253, Aug. 2010. 8, 31, 107
- [70] F. CALI, M. CONTI, AND E. GREGORI. **Dynamic tuning of the IEEE 802.11 protocol to achieve a theoretical throughput limit.** *IEEE/ACM Trans. Networking*, **8**(6):785–799, Dec. 2000. xi, 8, 18, 22, 23, 25, 26, 106, 108, 115, 120, 121, 142, 146, 161, 162
- [71] S. HAYKIN, D. J. THOMSON, AND J. H. REED. **Spectrum sensing for cognitive radio.** *Proc. IEEE*, **97**(5):849–877, May 2009. 12, 15, 142
- [72] E. AXELL, G. LEUS, E. G. LARSSON, AND H. V. POOR. **Spectrum sensing for cognitive radio : State-of-the-art and recent advances.** *IEEE Signal Process. Mag.*, **29**(3):101–116, May 2012. 142
- [73] I. F. AKYILDIZ, B. F. LO, AND R. BALAKRISHNAN. **Cooperative spectrum sensing in cognitive radio networks: A survey.** *Phys. Commun.*, **4**(1):40–62, March 2011. 12
- [74] H. URKOWITZ. **Energy detection of unknown deterministic signals.** *Proc. IEEE*, **55**(4):523–531, April 1967. 14
- [75] F. F. DIGHAM, M. S. ALOUINI, AND M. K. SIMON. **On the energy detection of unknown signals over fading channels.** In *Proc. IEEE ICC'2003*, **5**, pages 3575–3579 vol.5, May 2003. 15, 18
- [76] F. F. DIGHAM, M. S. ALOUINI, AND M. K. SIMON. **On the energy detection of unknown signals over fading channels.** *IEEE Trans. Commun.*, **55**(1):21–24, Jan 2007. 15, 18
- [77] H. TANG. **Some physical layer issues of wideband cognitive radio systems.** In *Proc. IEEE DySPAN'2005*, pages 151–159, Nov 2005. 15
- [78] S. M. MISHRA, S. TEN BRINK, R. MAHADEVAPPA, AND R. W. BRODERSEN. **Cognitive technology for ultra-wideband/wimax coexistence.** In *Proc. IEEE DySPAN'2005*, pages 179–186, April 2007.
- [79] S. GEIRHOFER, L. TONG, AND B. M. SADLER. **A measurement-based model for dynamic spectrum access in wlan channels.** In *Proc. IEEE MILCOM'2006*, pages 1–7, Oct 2006. 15
- [80] N. S. SHANKAR, C. CORDEIRO, AND K. CHALLAPALI. **Spectrum agile radios: utilization and sensing architectures.** In *Proc. IEEE DySPAN'2005*, pages 160–169, Nov 2005. 15
- [81] Z. TIAN AND G. B. GIANNAKIS. **A wavelet approach to wideband spectrum sensing for cognitive radios.** In *Proc. IEEE CROWNCOM'2006*, pages 1–5, June 2006. 15
- [82] Z. TIAN AND G. B. GIANNAKIS. **Compressed sensing for wideband cognitive radios.** In *Proc. IEEE ICASSP'2007*, **4**, pages IV–1357–IV–1360, April 2007. 15
- [83] Z. FANZI, C. LI, AND Z. TIAN. **Distributed compressive spectrum sensing in cooperative multihop cognitive networks.** *IEEE J. Sel. Areas Signal Processing*, **5**(1):37–48, Feb 2011. 15
- [84] Y. WEI, H. LEUNG, C. WENQING, AND C. SIYUE. **Optimizing voting rule for cooperative spectrum sensing through learning automata.** *IEEE Trans.*

- Veh. Tech.*, **60**(7):3253–3264, Sept. 2011. 17, 31, 107, 113
- [85] G. BIANCHI. **Performance analysis of the IEEE 802.11 distributed coordination function.** *IEEE J. Sel. Areas Commun.*, **18**(3):535–547, Mar. 2000. xi, 18, 19, 20, 21, 22, 23, 31, 41, 42, 44, 45, 52, 97, 116, 142, 147, 149
- [86] N. ABRAMSON. **The ALOHA System: another alternative for computer communications.** In *Proc. AFIPS*, pages 281–285. ACM, 1970. 25
- [87] F. BACCELLI, B. BLASZCZYSHYN, AND P. MUELHALER. **An Aloha protocol for multihop mobile wireless networks.** *IEEE Trans. Info. Theory*, **52**(2):421–436, 2006. 25
- [88] R. E. KAHN, S. A. GRONEMEYER, J. BURCHFIELD, AND R. C. KUNZELMAN. **Advances in packet radio technology.** *Proc. IEEE*, **66**(11):1468–1496, 1978. 25
- [89] I. DEMIRKOL, C. ERSOY, AND F. ALAGOZ. **MAC protocols for wireless sensor networks: a survey.** *IEEE Commun. Mag.*, **44**(4):115–121, 2006. 26
- [90] Y. C. TAY, K. JAMIESON, AND H. BALAKRISHNAN. **Collision-minimizing CSMA and its applications to wireless sensor networks.** *IEEE J. Sel. Areas Commun.*, **22**(6):1048–1057, Aug 2004. 26
- [91] A. TZAMALOUKAS AND J. J. GARCIA-LUNA-ACEVES. **Channel-hopping multiple access.** In *Proc. IEEE ICC’2000*, **1**, pages 415–419 vol.1, 2000. 28
- [92] P. BAHL, R. CHANDRA, AND J. DUNAGAN. **SSCH: slotted seeded channel hopping for capacity improvement in IEEE 802.11 ad-hoc wireless networks.** In *Proc. ACM MobiCom’2004*, pages 216–230. ACM, 2004. 29
- [93] H. S. W. SO, J. WALRAND, AND J. MO. **McMAC: A multi-channel MAC proposal for ad hoc wireless networks.** In *Proc. IEEE WCNC’2007*, pages 334–339. Citeseer, 2007. 29
- [94] Y. C. LIANG, K. C. CHEN, G. Y. LI, AND P. MAHONEN. **Cognitive radio networking and communications: An overview.** *IEEE Trans. Veh. Tech.*, **60**(7):3386–3407, 2011. 29, 31
- [95] J. UNNIKRISHNAN AND V. V. VEERAVALLI. **Cooperative sensing for primary detection in cognitive radio.** *IEEE J. Sel. Topics Signal Process.*, **2**(1):18–27, Feb. 2008. 31, 36
- [96] Z. QUAN, S. CUI, AND A. H. SAYED. **Optimal linear cooperation for spectrum sensing in cognitive radio networks.** *IEEE J. Sel. Topics Signal Process.*, **2**(1):28–40, Feb. 2008. 31, 107
- [97] E. C. Y. PEH, Y. C. LIANG, AND Y. L. GUAN. **Optimization of cooperative sensing in cognitive radio networks: A sensing-throughput tradeoff view.** *Proc. IEEE ICC’2009*, pages 3521–3525, 2009. 31, 35, 107, 122
- [98] Z. WEI, R. K. MALLIK, AND K. LETAIEF. **Optimization of cooperative spectrum sensing with energy detection in cognitive radio networks.** *IEEE Trans. Wireless Commun.*, **8**(12):5761–5766, Dec. 2009. 31, 122
- [99] T. CUI, F. GAO, AND A. NALLANATHAN. **Optimization of cooperative spectrum sensing in cognitive radio.** *IEEE Trans. Veh. Tech.*, **60**(4):1578–1589, May 2011. 31, 107
- [100] S. MALEKI, S. P. CHEPURI, AND G. LEUS. **Optimal hard fusion strategies for cognitive radio networks.** In *Proc. IEEE WCNC’2011*, pages 1926–1931, March 2011. 31, 107
- [101] S. MALEKI, S. P. CHEPURI, AND G. LEUS. **Optimization of hard fusion based spectrum sensing for energy-constrained cognitive radio networks.** *Physical Communication*, **9**(0):193–198, 2013. 31, 107
- [102] C. DOERR, M. NEUFELD, J. FIFIELD, T. WEINGART, D. C. SICKER, AND D. GRUNWALD. **MultiMAC: An adaptive MAC framework for dynamic radio networking.** *Proc. IEEE DySPAN’2005*, pages 548–555, 2005. 31, 70, 106
- [103] J. SHI, E. ARYAFAR, T. SALONIDIS, AND E. W. KNIGHTLY. **Synchronized CSMA contention: Model, implementation and evaluation.** *Proc. IEEE INFOCOM*, pages 2052–2060, 2009. 39, 42, 75
- [104] J. SO AND N. H. VAIDYA. **Multi-channel mac for ad hoc networks: handling multi-channel hidden terminals using a single transceiver.** *Proc. ACM MobiHoc*, pages 222–233, 2004. 68
- [105] J. JIA, Q. ZHANG, AND X. SHEN. **HC-MAC: A hardware-constrained cognitive MAC for efficient spectrum management.** *IEEE J. Sel. Areas Commun.*, **26**(1):106–117, Jan. 2008. 32, 71, 106

- [106] T. SHU AND M. KRUNZ. **Exploiting microscopic spectrum opportunities in cognitive radio networks via coordinated channel access.** *IEEE Trans. Mobile Comput.*, **9**(11):1522–1534, Nov. 2010. 71, 107
- [107] L. TASSIULAS AND S. SARKAR. **Maxmin fair scheduling in wireless ad hoc networks.** *IEEE J. Sel. Areas Commun.*, **23**(1):163–173, Jan. 2005. 31, 87
- [108] H. KIM, S. LIM, H. WANG, AND D. HONG. **Optimal power allocation and outage analysis for cognitive full duplex relay systems.** *IEEE Trans. Wireless Commun.*, **11**(10):3754–3765, October 2012. 33, 143
- [109] G. ZHENG, I. KRIKIDIS, AND B. OTTERSTEN. **Full-duplex cooperative cognitive radio with transmit imperfections.** *IEEE Trans. Wireless Commun.*, **12**(5):2498–2511, May 2013.
- [110] J. BANG, J. LEE, S. KIM, AND D. HONG. **An efficient relay selection strategy for random cognitive relay networks.** *IEEE Trans. Wireless Commun.*, **14**(3):1555–1566, March 2015. 33, 143
- [111] D. RAMIREZ AND B. AAZHANG. **Optimal routing and power allocation for wireless networks with imperfect full-duplex nodes.** *IEEE Trans. Wireless Commun.*, **12**(9):4692–4704, September 2013. 33, 143, 144
- [112] W. CHOI, H. LIM, AND A. SABHARWAL. **Power-controlled medium access control protocol for full-duplex wifi networks.** *IEEE Trans. Wireless Commun.*, **14**(7):3601–3613, July 2015. 33, 143, 144
- [113] C. STEVENSON, G. CHOUINARD, L. ZHONGDING, H. WENDONG, S. J. SHELLHAMMER, AND W. CALDWELL. **IEEE 802.22: The first cognitive radio wireless regional area network standard.** *IEEE Commun. Mag.*, **47**(1):130–138, Jan. 2009. 35, 38, 114
- [114] N. DEVROYE, P. MITRAN, AND V. TAROKH. **Achievable rates in cognitive radio channels.** *IEEE Trans. Inform. Theory*, **52**(5):1813–1827, May 2006. 36
- [115] F. WANG, M. KRUNZ, AND S. CUI. **Price-based spectrum management in cognitive radio networks.** *IEEE J. Sel. Topics Signal Process.*, **2**(1):74–87, Feb 2008. 36, 142
- [116] D. NIYATO AND E. HOSSAIN. **Competitive pricing for spectrum sharing in cognitive radio networks: Dynamic game, inefficiency of Nash equilibrium, and collusion.** *IEEE J. Sel. Areas Commun.*, **26**(1):192–202, Jan 2008. 36
- [117] Y. ZUO, Y. D. YAO, AND B. ZHENG. **A selective-relay based cooperative spectrum sensing scheme without dedicated reporting channels in cognitive radio networks.** *IEEE Trans. Wireless Commun.*, **10**(4):1188–1198, April 2011. 37
- [118] S. P. BOYD AND L. VANDENBERGHE. *Convex optimization.* Cambridge University Press, 2004. 46
- [119] S. KAMESHWARAN AND Y. NARAHARI. **Nonconvex piecewise linear knapsack problems.** *European J. Operational Research*, **192**(1):56–68, Jan. 2009. 46
- [120] V. KRISHNAN. *Probability and Random Processes.* Wiley-Interscience, 3rd edition edition, 2006. 58, 64
- [121] G. K. KARAGIANNIDIS AND A. S. LIOUMPAS. **An improved approximation for the Gaussian Q-function.** *IEEE Commun. Let.*, **11**(8):644–646, Aug. 2007. 61
- [122] H. SALAMEH, M. M. KRUNZ, AND O. YOUNIS. **MAC protocol for opportunistic cognitive radio networks with soft guarantees.** *IEEE Trans. Mobile Comput.*, **8**(10):1339–1352, Oct 2009. 70
- [123] T. SHU, S. CUI, AND M. KRUNZ. **WLC05-3: Medium access control for multi-channel parallel transmission in cognitive radio networks.** In *Proc. IEEE GLOBECOM*2006*, pages 1–5, Nov 2006. 70
- [124] T. CHEN, H. ZHANG, G. M. MAGGIO, AND I. CHLAMTAC. **CogMesh: A cluster-based cognitive radio network.** In *Proc. IEEE DySPAN*2007*, pages 168–178, April 2007. 70, 71
- [125] J. LEE AND S. EDS. LEYFFER. *Mixed integer nonlinear programming.* The IMA Volumes in Mathematics and its Applications, Springer, 154 edition, 2012. 72, 123
- [126] **802.11 standard.** *Online:* <http://www.ieee802.org/11>. 97
- [127] R. FAN AND H. JIANG. **Optimal multi-channel cooperative sensing in cognitive radio networks.** *IEEE Trans. Wireless Commun.*, **9**(3):1128–1138, March 2010. 122
- [128] H. W. KUHN. **The Hungarian method for the assignment problem.** *Naval Res. Logist. Quart.*, **1955**(2):83–97, 1955. 124, 126

REFERENCES

- [129] C. THORPE AND L. MURPHY. **A survey of adaptive carrier sensing mechanisms for IEEE 802.11 wireless networks.** *IEEE Commun. Surveys Tuts.*, **16**(3):1266–1293, Third 2014. 142
- [130] H. S. CHHAYA AND S. GUPTA. **Performance modeling of asynchronous data transfer methods of IEEE 802.11 MAC protocol.** *Wireless networks*, **3**(3):217–234, 1997.
- [131] I. F. AKYILDIZ, J. MCNAIR, L. C. MARTORELL, R. PUIGJANER, AND Y. YESHA. **Medium access control protocols for multimedia traffic in wireless networks.** *IEEE Network*, **13**(4):39–47, Jul 1999. 142
- [132] M. DUARTE, A. SABHARWAL, V. AGGARWAL, R. JANA, K. K. RAMAKRISHNAN, C. W. RICE, AND N. K. SHANKARANARAYANAN. **Design and characterization of a full-duplex multiantenna system for wifi networks.** *IEEE Trans. Veh. Tech.*, **63**(3):1160–1177, March 2014. 143
- [133] S. GOYAL, P. LIU, O. GURBUZ, E. ERKIP, AND S. PANWAR. **A distributed MAC protocol for full duplex radio.** In *Proc. Asilomar Conf. Signals, Syst. Comput.*, pages 788–792, Nov 2013. 143
- [134] W. CHENG, X. ZHANG, AND H. ZHANG. **Full-duplex spectrum-sensing and MAC-protocol for multichannel nontime-slotted cognitive radio networks.** *IEEE J. Sel. Areas Commun.*, **33**(5):820–831, May 2015. 143
- [135] Y. C. ELДАР, P. KUPPINGER, AND H. BOLCSKEI. **Block-sparse signals: Uncertainty relations and efficient recovery.** *IEEE Trans. Signal Process.*, **58**(6):3042–3054, June 2010. 173
- [136] R. G. BARANIUK, V. CEVHER, M. F. DUARTE, AND C. HEGDE. **Model-based compressive sensing.** *IEEE Trans. Inform. Theory*, **56**(4):1982–2001, April 2010. 173